The oncofetal RNA-binding protein IGF2BP1 is a miRNA- and m⁶A-dependent enhancer of gene expression in cancer

Dissertation

zur Erlangung des

Doktorgrades der Naturwissenschaften (Dr. rer. nat.)

Der

Naturwissenschaftlichen Fakultät I – Biowissenschaften –

der Martin-Luther-Universität Halle-Wittenberg,

vorgelegt

von Herrn Simon Müller

geboren am 21.08.1989 in Hannover

The greatest ideas are literally worthless if you keep them to yourself.
If you don't publish your discoveries, you didn't make them!

TABLE OF CONTENTS

I   ABSTRACT

RNA-binding proteins (RBPs) are critical regulators of post-transcriptional gene expression. RBPs regulate all aspects of the complex life of RNA. They are capable of recognizing hundreds of transcripts and forming large regulatory networks to maintain cell homeostasis. Dysregulations of numerous RBPs have been implicated in a variety of malignancies and cancer, respectively.

The human IGF2 mRNA-binding protein (IGF2BP) family is composed of three highly conserved RBPs: IGF2BP1, IGF2BP2, and IGF2BP3. All three IGF2BP paralogues are similar in size and share the same modular domain structure, including six classical RNA-binding domains. At the post-transcriptional level, IGF2BPs control the fate of target mRNAs, including their localization, translation, and stability. Adult organisms express IGF2BP2 on a widespread basis. In contrast, IGF2BP1 and IGF2BP3 exhibit an oncofetal expression pattern, with high levels of expression during embryogenesis and significant upregulation or even *de novo* synthesis in a variety of cancers. However, overexpression of all three paralogues is associated with poor patient prognosis and clinical outcomes in several cancers. Their paralogue-specific molecular determinants and affected phenotypes in certain tumor cells remain largely unknown.

In the context of this doctoral thesis, a side-by-side comparative analysis of all IGF2BP paralogues established that IGF2BP1 possesses the most extensively conserved oncogenic potential and promotes an 'aggressive' phenotype in a broad panel of cancer cells, including a) cell proliferation, b) cell migration, c) spheroid proliferation, d) spheroid invasion, and e) anoikis resistance / self-renewal. Notably, IGF2BP1 also accelerated tumor growth and metastasis in nude mice. These cellular phenotypes were mainly facilitated by impairing miRNA-directed degradation of several novel target mRNAs encoding oncogenic effector proteins. Further studies discovered that IGF2BP1 promotes the expression of the transcription factor SRF in a conserved 3'UTR- and N^6-methyladenosine (m⁶A)-dependent manner by inhibiting the miRNA-directed mRNA decay pathway. Our studies unraveled that IGF2BP1 promotes the expression of several SRF-driven transcripts. Through this and other post-transcriptional enhancer functions, IGF2BP1 promotes tumor spheroid growth and invasion. Intrigued by these findings, we identified another IGF2BP1-enhanced transcription factor driven program, the E2F hallmark pathway, promoting G1/S cell cycle transition via miRNA- and m⁶A-dependent stabilization of mRNAs encoding positive checkpoint regulators and downstream effectors. The small molecule BTYNB impaired this enhancer function by inhibiting IGF2BP1-RNA interactions. At low micromolar concentrations, BTYNB-exposed cancer cells showed reduced cell proliferation *in vitro*, and subcutaneous tumor growth or peritoneal spread in nude mice. Thus, the preserved roles of IGF2BP1 and the inhibitory potency of the small molecule lead inhibitor, BTYNB, indicate IGF2BP1's broad therapeutic target potential in the treatment of solid tumors.

II INTRODUCTION

The complex life of messenger RNAs

In 1958 Francis Crick formulated the central dogma of molecular cell biology dealing with the sequence-specific sequential transfer of cellular genetic information into protein synthesis (Crick, 1970; Crick, 1958). Briefly, genetic information is encoded by double-stranded deoxyribonucleic acid (DNA) in the cellular genome. DNA is transcribed into single-stranded ribonucleic acid (RNA) that serves as a template for the synthesis of proteins. Therefore, protein-encoding RNA, so-called messenger RNA (mRNA), is the essential temporary intermediate in the transfer of genetic information from DNA to proteins. Notably, this information cannot be reverted from proteins to either other proteins or ribonucleic acids, respectively. Next to the essential class of mRNAs, the cellular genome also contains many genes of non-coding RNAs (ncRNAs) that are transcribed from DNA but not translated into proteins, e.g., ribosomal RNAs (rRNAs), transfer RNAs (tRNAs), small RNAs like microRNAs (miRNAs) and long non-coding RNAs (lncRNAs). In multicellular organisms, each somatic cell contains the same DNA-encoded genetic information. However, phenotypical and functional diversity of different cell types arise from the specific expression of distinct gene sets. While some genes are ubiquitously expressed in every cell, the expression of other genes from the same genome may vary in a cell-type-specific manner. Over 60 years of research upon Crick's formulation of the central dogma, many regulatory mechanisms of gene expression during cellular differentiation and homeostasis have been identified. The expression of a particular gene underlies multiple control mechanisms on different stages, including epigenetic, transcriptional, post-transcriptional, translational, and post-translational regulation steps. Scientific interest in gene regulation increased with the identification of misregulations associated with several malignancies and cancer, respectively.

Post-transcriptional and translational gene regulation mechanisms comprise several complex maturation, modification, and further RNA regulatory processes. A plethora of cellular RNA-binding factors, RNA-binding proteins (RBPs) and ncRNAs, associate to mRNAs forming dynamic ribonucleoprotein complexes (RNPs) that are principally involved in the regulation of gene expression (Dreyfuss et al., 2002) and constantly underly compositional changes in a context-dependent manner. Conventional RBPs are able to bind target RNAs (mRNAs or ncRNAs) via one or several modular and structurally-defined RNA-binding domains (RBDs), like an RNA recognition motif (RRM, (Clery et al., 2008)), an hnRNP K homology domain (KH, (Valverde et al., 2008)), a DEAD-box helicase domain (Linder and Jankowsky, 2011), a double-stranded RNA-binding motif (Chang and Ramos, 2005), a zinc-finger domain (Font and Mackay, 2010) or other, less abundant domains such as a YT521-B homology domain (YTH) that specifically binds chemically modified RNAs (reviewed in (Gerstberger et al., 2014)). Unconventional RBPs, lacking specific globular RBDs, feature alternative modes of RNA-binding by intrinsically disordered regions, protein-protein interfaces or enzymatic cores (Hentze et al., 2018). For instance, recent advances in identifying the structures of major RNP machineries like the ribosome and

spliceosome have shown the presence of complicated protein–RNA interactions that are not facilitated by classical RBDs (Behrmann et al., 2015; Plaschka et al., 2017). These discoveries implied that unconventional RNA-binding is a more widespread phenomenon than previously thought (Hentze et al., 2018). The development of different next-generation sequencing and modern protein mass spectrometry approaches enabled the genome-wide identification and characterization of RNA-binding proteins at a systems-biology level. These encompass RNA interactome captures (RIC) for the discovery (Castello et al., 2013), or several modified versions of cross-linking immunoprecipitations (CLIP) of RBPs to identify binding footprints, such as PAR-CLIP (photoactivatable-ribonucleoside-enhanced CLIP, (Hafner et al., 2010)), iCLIP (individual-nucleotide resolution CLIP, (Konig et al., 2011)), and eCLIP (enhanced CLIP, (Van Nostrand et al., 2016). In RIC protocols, the UV light irradiation of cultivated cells or organisms covalently links proteins to RNA. Upon denaturing cell lysis, complexes are then captured on oligo(dT) beads and RBPs identified by mass spectrometry. In CLIP protocols, RBPs are also covalently crosslinked to associated RNAs by UV light irradiation of cultured cells. Protein–RNA complexes are immunoprecipitated using an RBP-specific antibody and RBP-bound areas are identified by high-throughput sequencing.

The first census of human RBPs, established in 2014, comprised in total 1542 proteins (Gerstberger et al., 2014) including a specific subset of 692 mRNA-binding proteins (mRBPs). The latter were recently described as "mRNA clothes" (Singh et al., 2015) and principally involved in all steps of the mRNA life cycle. Comprehensive evaluations from several unbiased large-scale RNA interactome studies increased the integrated number of candidate RBPs from different human cell types to a number of 1914 RBPs (Hentze et al., 2018) and nowadays 4257 RBPs (Gebauer et al., 2021), summarized in an available online database (RBPbase, https://rbpbase.shiny.embl.de). This vast and further increasing number of cellular RBPs already indicates the complex endeavor a newly synthesized mRNA faces before translation into a polypeptide. However, the concept that RBPs regulate the fate of the target RNA is widely applicable but not universal. Not every cellular RNA-protein interaction should be assumed to be physiologically relevant for the regulation of gene expression (Hentze et al., 2018). While RBPs can bind hundreds of mRNA targets, they may control only a fraction of them (Gebauer et al., 2021). Conversely, any individual mRNA can be bound by several RBPs that bind simultaneously, sequentially, or mutually exclusive, indicating dynamic changes throughout the mRNA life cycle (Mitchell and Parker, 2014).

The fascinating life of an mRNA starts in the nucleus with the transcription, the 'birth', of a protein-coding gene by RNA polymerase II, resulting in precursor mRNAs (pre-mRNAs) with exonic and intronic regions. The transformation of a pre-mRNA into a mature mRNA by nuclear RBPs requires the attachment of a 7-methylguanosine cap structure (m^7G) at the 5' end (*capping,* reviewed in (Shuman, 2002)), the removal of intronic and conjunction of exonic regions (*splicing and alternative splicing*, reviewed in (Jurica and Moore, 2003)), the addition of a poly(A)-tail to the 3' end (*polyadenylation,* reviewed in (Proudfoot, 2011)), and/or the specific introduction of chemical modifications (reviewed in (Roundtree et al., 2017)). Upon the nuclear export of mature mRNAs to the cytoplasm, two major classes of associated RNA-binding factors coordinate post-

transcriptional gene regulation and influence the alternative polyadenylation, stability, subcellular localization and/or translation efficacy (**Figure 1**). These include *a)* cytoplasmic RBPs and *b)* ncRNAs – e.g., miRNAs and lncRNAs. Cytoplasmic RBPs recruit mRNAs in messenger RNPs (mRNPs) that influence the stability and degradation or translation of the mRNA in a composition-dependent manner. While RBPs can act in both directions, promoting or inhibiting mRNA degradation or translation, miRNAs negatively modulate the mRNA fate by destabilizing targeted transcripts and/or reducing their translation efficacy.
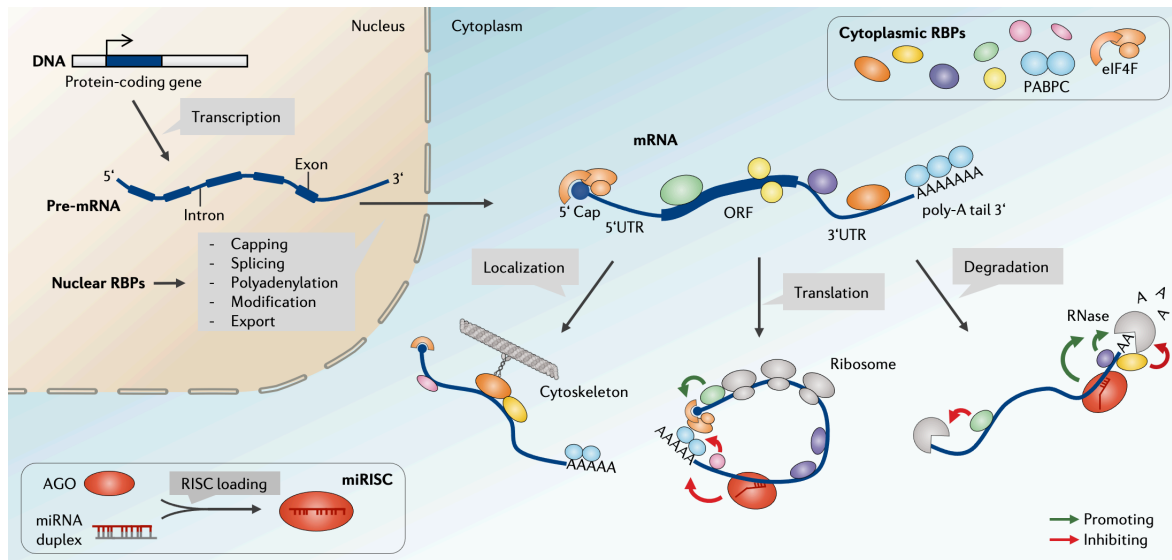

Figure 1 | **Post-transcriptional gene regulation in the cytoplasm.** A protein-coding gene is transcribed from DNA in precursor messenger RNA (pre-mRNA). In the nucleus, this pre-mRNA is processed by RNA-binding proteins (RBPs) during the capping, polyadenylation, splicing and modification into mature mRNA with a 5' m^{7}G-CAP-structure, an open reading frame (ORF) flanked by 5' or 3' untranslated regions (UTRs) and a 3' poly(A)-tail. Upon the export of the mRNA cytoplasmic RBPs and ncRNAs, miRNAs and lncRNAs (not shown), modulate the stability/degradation, localization, and translation into a protein. The guide strand of a miRNA duplex is incorporated (RISC loading) into an Argonaute protein (AGO) forming the miRNA-induced silencing complex (miRISC). The recruitment of the miRISC to responsive elements in mRNAs leads to either elevated mRNA degradation or translational inhibition. While miRNAs are generally negative regulators, cytoplasmic RBPs modulate the mRNA fate in a diverse manner. They associate to certain cis-elements and can either promote or inhibit the mRNA degradation and the translation efficacy.

The biogenesis and mechanisms of microRNAs

MicroRNAs are a class of broadly conserved small non-coding RNAs of 20-25 nucleotides (nt) in length. In 1993, the first small RNA, *lin-4*, that can act as an endogenous regulator of complementary target genes, was found in *C. elegans* (Proudfoot, 2011; Wightman et al., 1993). Almost ten years later the laboratory of Thomas Tuschl identified the first mammalian miRNAs (Lagos-Quintana et al., 2001). At that moment, miRNA-related research conquered both nucleic acid-focused journals, e.g., *RNA* or *Nucleic Acids Research*, and broad life-science journals like *Nature*, *Cell* and *Science*. MiRNAs are encoded *a)* as separate genes that are transcribed in primary monocistronic transcripts or *b)* as a cluster that consists of a set of several miRNAs, which are

transcribed in one primary polycistronic transcript from nearby-located miRNA genes (Bartel, 2004), e.g. the miR-17-92 cluster that encode for a total of 15 miRNAs (Concepcion et al., 2012). Often these genes are located in intronic regions of protein-coding genes. Primary transcripts, pri-miRNAs, are generated by RNA polymerase II and contain, like mRNAs, a 5' cap structure and a 3'-located poly(A)-tail (Kim, 2005). The sequence of the mature miRNA is located in the stem of the hairpin-structured pri-miRNA with 5' and 3' single-stranded RNA tails. In the canonical pathway of miRNA biogenesis pri-miRNAs are first processed by the microprocessor complex (**Figure 2**, reviewed in (Kim, 2005)). This complex of the RNase III-type endonuclease DROSHA and a dimer of the double-stranded RNA-binding protein DGCR8 (DiGeorge Critical Region 8) cleaves pri-miRNAs in single hairpin-structured precursor miRNAs (pre-miRNAs). Following the microprocessor-cleavage, pre-miRNAs are exported into the cytoplasm by GTP-dependent interactions with EXP5 (Exportin 5). In the cytoplasm, the other RNase III-type endonuclease DICER in association with the trans-activation-repsonsive RNA-binding protein (TRBP) cleaves the pre-miRNA near the loop-region generating a 20-25 nt long miRNA duplex. This miRNA duplex, that consists of guide and passenger strands, is loaded onto an Argonaute (AGO) protein forming the precursor RNA-induced silencing complex (pre-RISC). The pre-RISC releases the passenger strand and associates with TNRC6 proteins to generate the mature miRNA-induced silencing complex (miRISC). Determinants for the strand choice are a) the thermodynamic stability of the 5'- and 3' ends of the duplex and b) the nucleotide at nucleotide position 1. Usually, the guide strand is in relation unstable at the 5' side and contains a uridine at nucleotide position 1 (Kim, 2005).
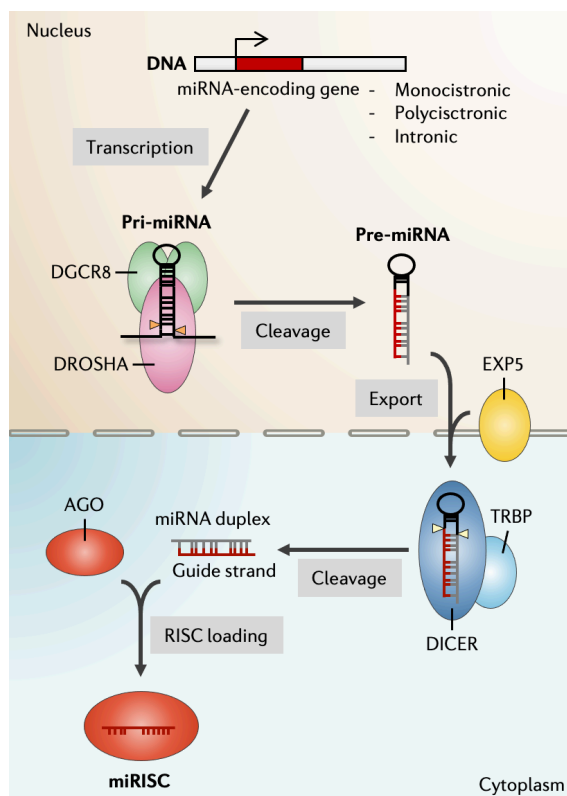
Figure 2 | **The canonical biogenesis of miRNAs.** MiRNA genes are located in individual, clustered or intronic and become transcribed into mono- or polycistronic primary transcripts (pri-miRNAs). The microprocessor-complex of RNAse III-type enzyme DROSHA and DGCR8 cleaves pri-miRNAs generating pre-miRNAs. Pre-miRNAs are exported by exportin 5 (EXP5) in the cytoplasm. The cytoplasmic RNAse III-type enzyme DICER cleaves pre-miRNAs in concert with TRBP (also known as TARBP2) in 20-25 nt long miRNA duplexes with a guide and passenger strand. These duplexes are loaded onto Argonaute proteins forming pre- and after release of the passenger strand mature miRNA-induced silencing complexes (miRISCs). Illustration modified from (Treiber et al., 2018)

In recent studies, the side-by-side genomic deletion of DROSHA, EXP5 or DICER re-evaluated a substantial decrease in miRNA abundance. However, some miRNAs were still produced in processing- or exporting-factor-deleted cells (Kim et al., 2016). Several mature miRNAs can be produced by microprocessor-independent non-canonical pathways, e.g. by pre-miRNAs that are generated from short introns (mirtrons) by the splicosome (Berezikov et al., 2007) or by other endogenous hairpin RNAs like small nucleolar RNAs (snoRNAs) (Ender et al., 2008) or tRNAs, respectively. Apart from these microprocessor-independent pathways, there is only one miRNA, miR-451, known that escapes DICER-processing during maturation. The pre-miR-451 is directly incorporated in the AGO2 protein. Upon slicing by AGO2 the cleaved pre-miR-451 is further trimmed by PARN (3'-5' exonuclease poly(A)-specific ribonuclease) resulting in a mature miR-451. However, the vast majority of conserved miRNAs, about 99%, follow the canonical biogenesis pathway and only a few are processed in a DROSHA- or DICER-independent manner (Ha and Kim, 2014).
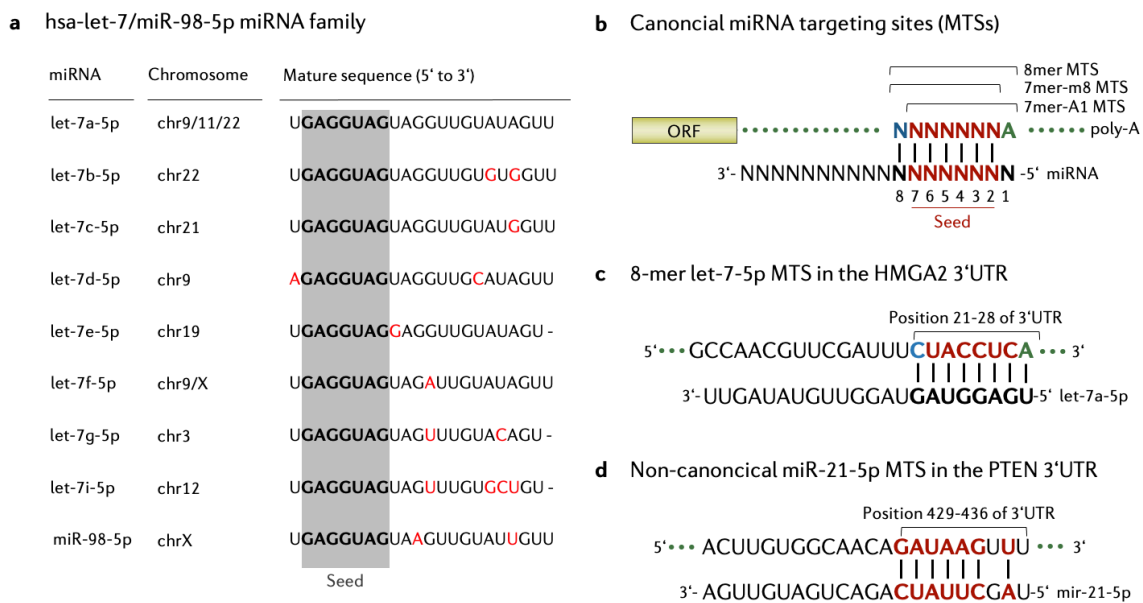
Figure 3 | **MicroRNA families and targeting sites. a,** Categorization of let-7p/miR-98-5p miRNAs into a miRNA family according to conserved seed regions at position 2-8 (grey, non-conserved bases in red). **b,** Canonical miRNA targeting sites (MTSs) including 8mer (complementarity at position 1-8), 7mer-m8 (complementarity at position 2-8) and 7mer-A1 (complementarity at position 2-7 and A-U pairing at position 1). **c,** Predicted and verified canonical 8mer let-7-5p site in the HMGA2 3'UTR. **d,** Non-canonical verified miR-21-5p MTS in the PTEN 3'UTR.

Deep sequencing enabled the mapping of 1917 hairpin miRNA precursors and 2654 mature miRNA sequences in the human genome that are deposited in the miRNA database, miRBase (www.mirbase.org, (Kozomara et al., 2019)). Based on mature sequences, miRNAs from different miRNA-encoding genes are categorized into specific groups, so-called miRNA families, that contain conserved seed sequences at positions 2-8 in the guide strand (Mathelier and Carbone, 2013). For example, the let-7/miR-98-5p family comprises nine mature miRNAs from 12

distinct annotated loci with a conserved 5'-GAGGUAG-3' seed region (**Figure 3a**). Seed regions mainly define canonical miRNA targeting sites (MTSs) in mRNAs, that are often located in 3' untranslated regions and recruit the miRISC to specific transcripts. There are different types of MTSs, including two types of 7mers (7mer-m8 and 7mer-A1) and 8mers, according to complementary bases of the miRNA and mRNA that define the targeting specificity (**Figure 3b**, (Grimson et al., 2007; Lewis et al., 2005)). In order to identify direct miRNA-target interactions, several online prediction tools have been developed, e.g., TargetScan (www.targetscan.org, (Agarwal et al., 2015)) or miRWalk (www.mirwalk.umm.uni-heidelberg.de, (Dweep et al., 2011)). These tools solidly predict canonical MTSs according to seed complementarities, target secondary structure and thermodynamic properties, e.g., the experimentally validated let-7-5p 8mer in the HMGA2 3'UTR (**Figure 3c**, (Lee and Dutta, 2007)). However, these seed regions are not always sufficient for regulation indicating other characteristics for the miRNA specificity. Non-canonical miRNA-target interactions defined by (partially) disrupted seed pairing with extensive 3' complementarities, e.g., the functional miR-21-5p MTS in the PTEN 3'UTR (**Figure 3d**, (Meng et al., 2007)), cannot be identified by prediction tools relying on standard algorithms. Most importantly, however, not every predicted MTS is functionally relevant. Hence, nearly every miRNA-target interaction needs to be experimentally verified in a certain cellular context. Computational predictions estimate that each individual miRNA can associate to hundreds of different target mRNAs while 3'UTRs of distinct mRNAs harbor MTSs of a plethora of miRNAs indicating the complexity and diversity of miRNA-mediated gene regulation.

Currently, the broadly accepted consensus is that miRNAs inhibit the cap-dependent translation during the initiation and predominantly destabilize targeted transcripts in mammalian cells (**Figure 4**, reviewed in (Jonas and Izaurralde, 2015)). While the molecular mechanisms of the translational repression remain to be unraveled in detail, the degradation of miRNA targets depends on several multi-protein complexes. As mentioned before, miRNAs are associated with AGO proteins forming the fundamental core of the miRISC. The human genome encodes four AGO (AGO1-4) proteins. AGO2 has been shown to be the only catalytically active paralogue that directly cleaves perfectly complementary targets (Ipsaro and Joshua-Tor, 2015; Jo et al., 2015). However, the mainly occurring partial complementarity of miRNAs and mRNAs usually prevents the direct endonucleolytic cleavage by AGO2, indicating additional cellular factors to mediate the gene silencing. Accordingly, AGO proteins directly interact with members of the TNRC6 protein family that comprises three paralogues: TNRC6A-C. TNRC6 proteins function as docking scaffolds for the cytoplasmic poly(A) binding protein (PABPC) and effectors of the cellular RNA decay machinery, such as the deadenylase complexes PAN2-PAN3 and CCR4-NOT (Behm-Ansmant et al., 2006). The PAN2-PAN3 complex catalyzes the initial phase of the poly(A) shortening, which is continued by the CCR4-NOT complex (Yamashita et al., 2005). In consecutive steps, the CCR4-NOT complex lead via DDX6 to the recruitment of the multi-protein catalytic decapping complex consisting of DCP1/2 and EDC3/4. Upon the deadenylation and decapping of the mRNA, the cytoplasmic exoribonuclease 1 (XRN1) finally facilitates the 5'-3'-directed degradation. These consecutive destabilization events occur to be the main cause for the

miRNA-mediated gene silencing while miRNAs only modestly inhibit the translation efficacy (Huntzinger and Izaurralde, 2011). Ribosome profiling experiments show that the reduced protein synthesis is caused up to 84% by steady-state mRNA degradation with slightly less efficient translation of undegraded target mRNAs (Eichhorn et al., 2014; Guo et al., 2010). Interestingly, the 3'UTRs of about 60% of human mRNAs are considered miRNA targets of 90 broadly conserved miRNA families (Friedman et al., 2009). With this broad target spectrum, multiple expressed miRNAs, referred to as the cellular miRNome, cooperate to maintain a certain homeostasis between fundamental biological processes like cell death and proliferation or differentiation. Dysregulations in miRNA biogenesis, expression and in miRNA-mediated gene regulation are frequently observed in all kind of human malignancies including cardiovascular diseases, hepatitis, diabetes, atherosclerosis and cancer, respectively (reviewed in (Esquela-Kerscher and Slack, 2006; Kasinski and Slack, 2011; Lin and Gregory, 2015; Rupaimoole and Slack, 2017)).
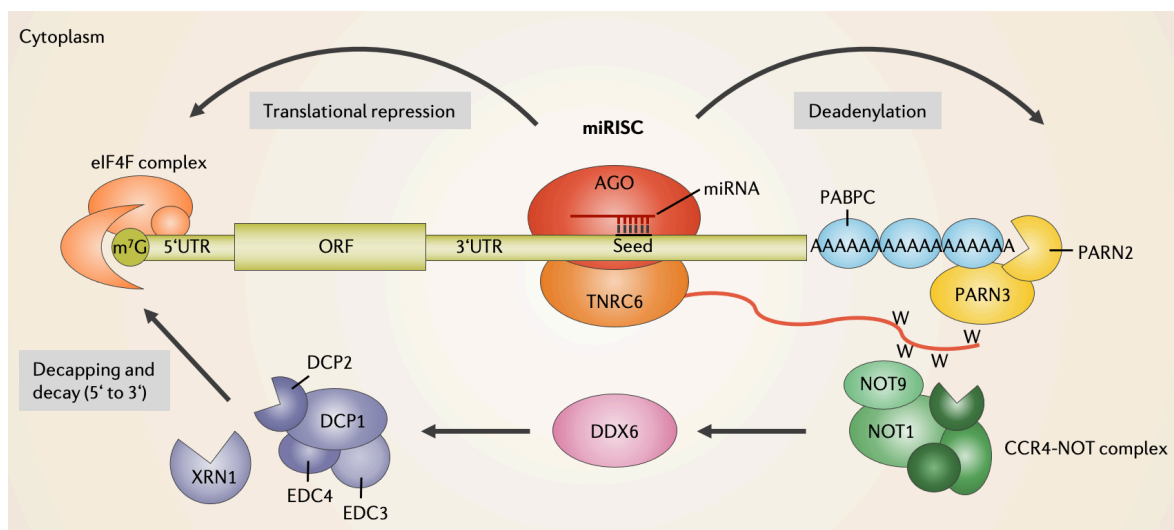

Figure 4 | **Mechanisms of the miRISC-mediated gene silencing in humans.** Mature miRNAs and AGO proteins form the core miRISC complex. Guided to sequence-elements in target mRNAs, recognized by the specific miRNA seed-region, miRISC induces translational repression or degradation of target mRNAs. For gene silencing, AGO proteins interact with TNRC6 proteins that consecutively interact with PAPBC and the deadenylase complexes PAN2-PAN3 and CCR4-NOT. Upon deadenylation, CCR4-NOT recruits the decapping complex via DDX6. Decapping is facilitated by DCP2 that interacts with other proteins in a complex: DCP1, EDC3/4. Finally, the exoribonuclease 1 (XRN1) catalyzes the 5'-3' degradation of the mRNA.

The role of miRNAs and RNA-binding proteins in human cancer

Cancer is the generic name for a collection of similar genetic diseases and the second cause of worldwide death, respectively. The origin of cancer can almost be anywhere in the human body. Cancers are classified by the tissue type the tumor originates from. The most common type of cancer, about 80-85 %, are carcinomas that arise from epithelial cells or tissue, respectively. There are also sarcomas emerging from connective tissue or muscle cells. The broad class of

hematological tumors, like leukemias and lymphomas, are derived from the bone marrow or the lymphatic system.

But how does cancer arise? - There is a principal balance between cell growth and death to maintain homeostasis and function in normal tissue. During cancer development, this tissue homeostasis breaks down, and abnormal cells grow in an uncontrolled way resulting in the formation of primary tumors. There are two types of tumors with different progressions: Benign and malignant tumors. While benign tumors consist of neoplastic cells that are not invasive, cells of aggressive and malignant tumors acquire the ability to invade surrounding or spread to peripheral tissue leading to the formation of secondary tumors, metastases.

In 2000 Hanahan and Weinberg formulated six acquired biological capabilities of cancer cells during the development of human tumors, the hallmarks of cancer: 1) Sustaining proliferative signals, 2) Evading growth suppressors, 3) Resisting cell death, 4) Enabling replicative immortality, 5) Inducing angiogenesis and 6) Activating tissue invasion and metastasis (Hanahan and Weinberg, 2000). However, continuous conceptual research has added significant updates to the originally proposed hallmarks, including two emerging hallmarks, 7) Deregulating cellular energetics and 8) Avoiding immune destruction, and two enabling characteristics of cancer cells, 9) Genome instability & mutation, and 10) Tumor-promoting inflammation (Hanahan and Weinberg, 2011). On a molecular basis, genes that control cancer hallmarks are classified into two categories: a) oncogenes and b) tumor-suppressor genes. Together, the overexpression of oncogenes and the loss of tumor-suppressors principally drive tumorigenesis.

The Cancer Genome Atlas (TCGA, https://www.cancer.gov/tcga), a broad cancer genomics initiative, has molecularly described approximately 20,000 primary cancer and matched normal samples representing 33 different cancer types by investigating respective genomics, transcriptomics, and proteomics. There is no wonder that next-generation sequencing data of poly-A enriched or small RNAs revealed a plethora of dysregulated mRNAs and ncRNAs, such as miRNAs, implying that post-transcriptional alterations can have severe impacts on cancer progression. For instance, the deregulation of miRNA functions is observed across all cancer types and during different stages of progression (Esquela-Kerscher and Slack, 2006; Nicoloso et al., 2009). Tumor-promoting miRNAs, so-called oncomiRs, are characterized by mainly targeting tumor-suppressor-encoding mRNAs, while tumor-suppressive miRNAs by targeting mRNAs that encode oncogenic factors. The expression of these miRNAs is altered due to epigenetic events (e.g., DNA hypo/hypermethylation or aberrant histone modification patterns), genomic events, such as deletions or amplifications, transcriptional changes by key transcription factors (e.g., c-Myc and p53), or general defects in biogenesis, maturation and functionality (Rupaimoole and Slack, 2017). The major biogenesis enzymes, DICER and DROSHA, are frequently downregulated in several cancers and associated with poor patient outcomes, e.g., in lung cancer (Karube et al., 2005), in ovarian cancer (Merritt et al., 2008), in endometrial cancer (Torres et al., 2011) and in specific subtypes of breast cancer (Dedes et al., 2011). Mutations in biogenesis pathway-related genes occur in numerous tumors (Lin and Gregory, 2015), such as DICER mutations in ovarian cancers impairing miRNA processing (Heravi-Moussavi et al., 2012) or genetic defects in EXP5

impairing the export of miRNA duplexes to the cytoplasm (Melo et al., 2010). In response to tumor hypoxia, the effective functions of miRNAs can be further inhibited by the epidermal growth factor receptor (EGFR)-dependent phosphorylation of AGO2, resulting in decreased binding to DICER and impaired RISC-loading (Shen et al., 2013).

In summary, tumors show a plethora of dysregulations in the synthesis, biogenesis, and functionality of miRNAs, generally resulting in the reprogramming of the individual cancer miRNome with elevated expression of oncomiRs and reduced expression of tumor-suppressive miRNAs. Among the latter's, the earliest evidence of miRNA involvement in human cancer was reported in 2002 when the Croce group identified the genomic deletion of the miR-15a and miR-16-1 genes in B-cell chronic lymphocytic leukemia cells (Calin et al., 2002). These miRNAs act as tumor-suppressors by repressing Bcl-2 expression resulting in the induction of apoptosis (Cimmino et al., 2005). Further, members of the miR-34, miR-200 and let-7 families present very prominent and well-studied tumor-suppressive miRNAs. The miR-34 family consists of three members (miR-34a, b, c), which are encoded in two distinct genomic loci (miR-34a and miR-34b/34c) and frequently downregulated in cancers (Li et al., 2013; Liu et al., 2011; Rokavec et al., 2014). During the DNA damage response, all miR-34 members are transcriptionally activated by the "master" tumor-suppressor p53 (Yamakuchi and Lowenstein, 2009) and directly target the anti-apoptotic factors sirtuin 1 (SIRT1, (Li et al., 2013)) or BCL2 (Di Martino et al., 2012). Further, the p53-miR-34 axis deregulates the expression of cell cycle-promoting kinases, such as cyclin-dependent kinase 4 and 6 (CDK4, CDK6) required for the G1/S transition, inducing a proliferation arrest (Misso et al., 2014). In addition to the regulation of the two major hallmark pathways, proliferation and apoptosis, recent studies showed the role of miR-34 impairing the immune evasion of cancer cells, one of the emerging hallmarks. Increased interactions of programmed cell death protein 1 (PD1), which is upregulated in cytotoxic T cells upon activation, and elevated PD1 ligand 1 (PDL1) on tumor cells elicits an immunosuppressive response (Bardhan et al., 2016; Pardoll, 2012). However, miR-34 directly targets the PDL1 mRNA resulting in a reduced expression and thereby inhibition of the immune evasion in acute myeloid leukemia (AML) and lung cancer, respectively (Cortez et al., 2016; Wang et al., 2015c).

The let-7 miRNA family functions as a keeper of differentiation and downregulation in cancer is associated with initiation and progression of the malignancy (Bussing et al., 2008). Levels of let-7 miRNAs gradually increase during embryogenesis and remain high in adult tissues (Sempere et al., 2004). The expression of individual let-7 members or the whole family are reduced in many types of cancer compared to corresponding normal tissues, such as breast (Sempere et al., 2007), ovarian (Nam et al., 2008) or lung cancer (Yanaihara et al., 2006). This repression is most often associated with poor patient prognosis (Balzeau et al., 2017). Pleiotropic effects on post-transcriptional gene regulation by let-7 miRNAs influence nearly all hallmarks of cancer including proliferation, cell cycle progression, metabolism, apoptosis, migration, and invasion (Boyerinas et al., 2010; Wang et al., 2012). As previously introduced, the family comprises ten mature miRNAs sharing overlapping functions with the characteristic seed region and high 3' homology (**Figure 3a**). A plethora of oncogene-encoding mRNAs are directly targeted by let-7

(Roush and Slack, 2008). These targets include major oncogenes like MYC (Sampson et al., 2007), KRAS (Johnson et al., 2005) or the high-mobility group AT-hook protein 2 (HMGA2, (Yu et al., 2007)). The latter is a chromatin-associated nonhistone protein and architectural transcription factor with an oncofetal expression pattern. HMGA2 is widely expressed in undifferentiated embryonal cells, barely or non-detectable in normal adult tissues, and re-expressed in nearly all types of cancer and thereby negatively correlated to let-7 levels (Shell et al., 2007). In total, the HMGA2 3'UTR harbors seven let-7 MREs (Park et al., 2007). Comparative bioinformatics revealed twelve oncofetal proteins that are targeted by let-7 miRNAs in late embryogenesis, such as the RNA-binding proteins insulin-like growth factor 2 mRNA-binding protein 1 (IGF2BP1, five let-7 MREs) and Lin-28 homolog B (LIN28B, four let-7 MREs), respectively (Boyerinas et al., 2008). Interestingly, in early embryogenesis and carcinogenesis pri-miRNAs of the let-7 member accumulate while mature miRNAs are downregulated indicating post-transcriptional regulatory changes. Indeed, the two RNA-binding proteins LIN28A/B associate to loop regions in pri- or pre-let-7 via N-terminal cold shock domains (CSD) inhibiting DROSHA- and DICER-dependent processing in a negative feedback-loop. Upon binding to pre-let-7, LIN28A/B further recruit terminal uridylyl transferases (TUTases, mainly TUT4/7). These mediate the 3'-oligouridylation of the precursor RNAs resulting in resistance to DICER recognition and induction of the 3' to 5'-directed degradation by exonucleases (Wang et al., 2015b). In conclusion, the upregulation of LIN28 proteins prevents the maturation of tumor-suppressive let-7 miRNAs and results in a downregulation of this tumor-suppressive miRNA family across various cancers.

On the other side, oncomiRs frequently show an increased expression and function in tumors compared to normal tissues. Prominent examples include miRNAs like miR-21, miR-221/2, miR-155 and miRNAs encoded in the miR-17-92 cluster (Rupaimoole and Slack, 2017). This genetic cluster encodes six mature miRNAs (miR-17, miR-18a, miR-19a/b, miR-20a and miR-92a) of four distinct seed families and is very often transcriptionally dysregulated in hematopoietic and solid cancers in a MYC-dependent manner (Mogilyansky and Rigoutsos, 2013). In embryonic cells the miR-17-92 cluster is highly expressed and has important functions during development (Ventura et al., 2008). An elevated expression in cancer promotes several hallmark pathways by directly targeting a variety of transcripts. These include the pro-apoptotic protein BIM or anti-angiogenic factors, such as thrombospondin 1 (TSP1) and connective tissue growth factor (CTGF), resulting in reduced apoptosis and induced angiogenesis (Dews et al., 2006; Koralov et al., 2008).

However, one of the earliest identified and most upregulated miRNAs in solid and hematological malignancies remains miR-21 (Feng and Tsao, 2016), e.g., in colorectal cancer (Asangani et al., 2008) or breast cancer (Frankel et al., 2008). Over 3000 PubMed-indexed articles reveal the tumor-promoting role of miR-21 during all stages across human carcinogenesis. The high miR-21 expression occurs due to genomic amplifications of the chromosomal 17q region (Krichevsky and Gabriely, 2009), harboring the miRNA-encoding gene, or due to transcription factors that are frequently upregulated in cancer, such as the activation protein AP-1 (Fujita et al., 2008). One of the most prominent miR-21 target mRNAs is programmed cell death protein 4 (PDCD4, (Asangani et al., 2008; Ferraro et al., 2014; Yang et al., 2015)). PDCD4 is a well-known

tumor-suppressor involved in apoptosis and metastasis and is frequently downregulated in a variety of cancers. By targeting tumor-suppressor-encoding mRNAs like PDCD4 or phosphatase and tensin homolog (PTEN, (Xu et al., 2014; Xue et al., 2016)), miR-21 directly modulates cancer hallmark pathways such as resisting cell death, proliferative signaling and invasion/metastasis. The role as an oncomiR has also been supported by *in vivo* mouse models of lung cancer where the loss-of-function of miR-21 in a *K-ras^{LA2}* mouse model resulted in decreased and the gain-of-function of miR-21 in increased tumorigenesis (Hatley et al., 2010).

In summary, the discoveries of dysregulations in miRNA expression and transcriptome-wide profiling studies demonstrate that miRNA expression signatures are associated with different tumor types, tumor grades and clinical outcomes indicating miRNAs as potential therapeutic targets (Peng and Croce, 2016).

Next to the broad class of miRNAs, RNA-binding proteins have a central role in post-transcriptional gene regulation. Dysregulated RBP functions influence the expression of associated RNAs related to cancer phenotypes (Gebauer et al., 2021; Lukong et al., 2008; Pereira et al., 2017). Most recently, a comprehensive pan-cancer characterization suggests many RNA-binding proteins as potential drivers of tumor progression (Wang et al., 2018b). Aberrantly expressed RBPs can modulate the expression of oncogenes, tumor-suppressors, or genes that are crucial for genome stability (Kang et al., 2020). At this point, the mechanistic roles of RBPs are not restricted to determine the fate of associated mRNAs. RBPs can also regulate miRNA processing and activity, highlighting complex layers of post-transcriptional regulation in cancer progression (van Kouwenhove et al., 2011). For instance, LIN28 proteins (LIN28A and LIN28B) contain a conserved combination of three RBDs (an N-terminal cold-shock domain and two C-terminal zinc-finger domains) that facilitate the selective binding to terminal loops of let-7 precursor miRNAs. LIN28A is predominantly expressed in the cytoplasm and recruits terminal uridylyl transferases (TUT4/7) to polyuridylate pre-let-7, thereby blocking DICER-dependent processing and finally leading to degradation by exoribonuclease DIS3L2 (Hagan et al., 2009; Heo et al., 2009; Ustianenko et al., 2013). LIN28B, mainly localized in the nucleus, also binds to pre-let-7 and blocks the processing by the microprocessor (Piskounova et al., 2008). However, the detailed mechanism of the LIN28B-mediated repression of let-7 members remains unclear (Balzeau et al., 2017). In cancer, elevated expression of LIN28 proteins leads to the general downregulation of let-7 miRNAs. This repression functionally results in the upregulation of many let-7 target mRNAs encoding oncogenic factors, as mentioned before (e.g., KRAS, MYC, and HMGA2). The activated LIN28/let-7 pathway promotes many cancer hallmarks (sustained proliferation, enhanced invasion/metastasis, and angiogenesis) and is associated with poor clinical prognosis in different cancer types (Balzeau et al., 2017; Viswanathan et al., 2009).

Furthermore, RBPs substantially regulate the expression of protein-coding genes by modulating the mRNA processing like RNA modification, alternative splicing or alternative polyadenylation, and the cytoplasmic mRNA fate, such as subcellular localization, stability, or translation. The chemical modification of RNA regulates temporal and spatial gene expression patterns. Alterations in RNA modification are associated with developmental disorders and

cancer, respectively (Delaunay and Frye, 2019). The most common internal mRNA modification is N^6-methyladenosine (m6A, (Zaccara et al., 2019)). In 2012, the first next-generation sequencing approaches revealed the topography of m6A in the transcriptome, the so-called epitranscriptome (Meyer et al., 2012). Around one-third of mammalian mRNAs include m6A modifications, with an average of three to five m6A modifications per mRNA (Huang et al., 2020a). This reversible modification plays a central role in mRNA metabolism (**Figure 5**). RNA, like DNA and protein, may be methylated and demethylated by specialized methyltransferases ("writers") and demethylases ("erasers"). The multicomponent m6A writer complex, which includes the core N6-adenosine-methyltransferase 3 (METTL3) and its adaptors, or the N6-adenosine-methyltransferase 16 (METTL16) write m6A modification predominantly in the nucleus. Further writer complex components include the essential co-factor N6-adenosine-methyltransferase 14 (METTL14), the adaptor WT1 associated protein (WTAP), and several WTAP-interactors (Zaccara et al., 2019). Contrary, the erasers AlkB homolog 5 (ALKBH5) and Fat-mass and obesity-associated protein (FTO) remove written m6A modifications.
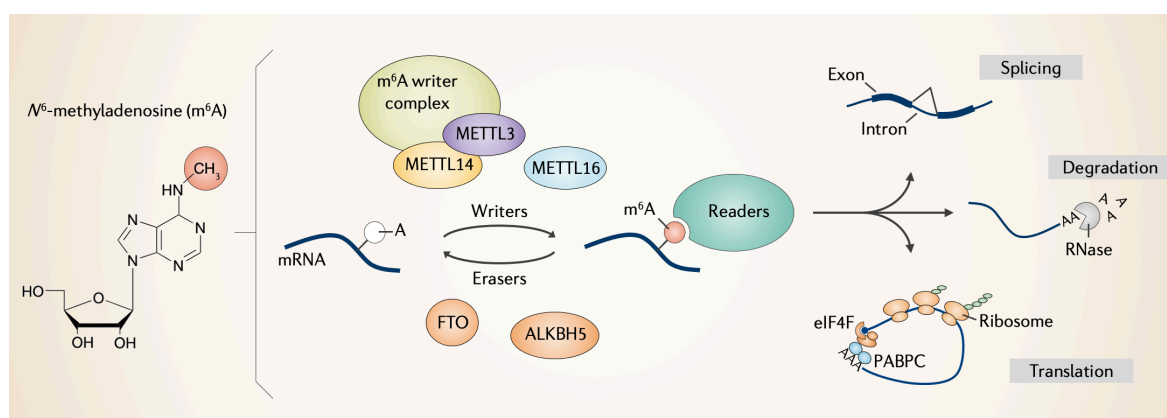

Figure 5 | **The role of m^{6}A and its associated machinery in RNA metabolism.** The m^{6}A RNA methylation landscape in mRNA is mediated by writers, including METTL3, METTL14, and the m^{6}A-writer complex (principal components: WTAP, VIRMA, CBLL1, and ZC3H13), and METTL16, by erasers FTO and ALKBH5, and by reader proteins with indicated primary functions in mRNA metabolism, including splicing, degradation, and translation. m^{6}A – N^6-methyladeonsine

Notably, nearly all components of the m6A machinery (writers and erasers) have been linked to cancer and proposed as possible therapeutic targets (Barbieri and Kouzarides, 2020). In many cancers, the m6A writer complex appears to have an oncogenic or tumor suppressive role, indicating puzzling mechanisms and strict context-dependencies. For instance, several studies show that METTL3 promotes the progression of lung (Lin et al., 2016) or liver (Chen et al., 2018) cancer, while others claim tumor-suppressive functions of the METTL3-14 complex, such as in endometrial cancer (Liu et al., 2018). It appears even more controversial in AML. On the one side, high METTL3 levels increase the translation of oncogenic factors, such as MYC (Vu et al., 2017), required to maintain the undifferentiated phenotype of AML cells (Barbieri et al., 2017). However, the eraser FTO can also serve as an oncogene in acute myeloid leukemia (Li et al., 2017) , implying that maintaining the equilibrium of cellular m6A levels is critical for cancer cells and functions may

vary in a complex m⁶A reader composition-dependent manner. Most of the functions and processes of m⁶A writers and erasers are mediated by the different m⁶A binders, so-called "readers" (Barbieri and Kouzarides, 2020). As a result, several reader proteins have been identified as prospective therapeutic targets due to their distinct and significant roles in cancer (Huang et al., 2020a). For instance, the YTH domain-containing protein 2 (YTHDF2) is overexpressed in AML and reduces the amounts of numerous proapoptotic transcripts via promoting an m⁶A-dependent RNA decay mechanism. In summary, all m⁶A epitranscriptomic machinery components are implicated in cancer. Although their mode of action seems partly controverse, m⁶A modification influence the fate of target RNAs in a diverse manner. or Cytoplasmic readers, like YTHDF2, influence the stability and degradation or translation efficacy of associated transcripts, whereas nuclear reader proteins preferentially bind m⁶A-modified mRNAs, which affect alternative mRNA splicing (Zaccara et al., 2019). For instance, the nuclear m⁶A-binding protein YTHDC1 controls alternative mRNA splicing by recruiting pre-mRNA splicing factors to specific binding sites, promoting exon inclusions (Xiao et al., 2016).

Alternative splicing is a core mechanism to generate different mRNA variants from a single pre-mRNA to expand cellular protein diversity (Nilsen and Graveley, 2010). Several RBPs bind to cis-regulatory elements, located in exons or introns of the RNA, serving as enhancers or silencers to regulate the exon usage positively or negatively during the mRNA maturation. Alternative cleavage and polyadenylation (APA) is a 3'-end regulatory process to generate mature mRNA variants with a diverse coding sequence or 3'UTR length (Elkon et al., 2013). Like alternative splicing, RBP-mediated APA enables multiple transcript variants with different stability and translation efficacy properties from a single origin RNA. Hence, it is not surprising that dysregulated alternative splicing or polyadenylation events frequently occur in transformed cancer cells (Dvinge et al., 2016; Gruber and Zavolan, 2019). The proto-oncogenic Serine/Arginine-rich (SR) family proteins have multiple functions in constitutive and alternative splicing and aberrant expression in cancer causes unusual splicing events (Zheng et al., 2020). Increased expression of SRSF1, SRSF2 and SRSF3 correlates with progression, as observed in ovarian cancer (Fischer et al., 2004). SRSF1 is additionally upregulated in a variety of tumor types, including colon, liver, lung, and breast cancer (Anczukow et al., 2015; de Miguel et al., 2014; Karni et al., 2007). In Glioblastoma, SRSF1 regulates the alternative splicing of anti- to pro-angiogenic of the Vascular Endothelial Growth Factor A (VEGFA) isoforms (Barbagallo et al., 2019). Antagonists of SR-proteins belong to the hnRNP a/B family that have also been linked to cancer progression. In hepatocellular carcinoma, overexpression of HNRNPA1 increases the ratio of the alternatively spliced oncogenic CD44 isoforms (mainly CD44v6), which promote cellular invasiveness and correlate with poor clinical outcomes in patients (Zhou et al., 2013). Further, RBPs with reported oncogenic functions in alternative splicing include Polypyrimidine tract-binding protein (PTB, (Izaguirre et al., 2012)), Epithelial splicing regulatory protein 1 and 2 (ESRP1 and ESRP2, (Warzecha et al., 2009; Yae et al., 2012) and Src-associated in mitosis of 68 kDa (SAM68, (Paronetto et al., 2010)). On the other side, alternative splicing-related RBPs with tumor-suppressive functions include Quaking (QKI, (Conn et al., 2015)) promoting the internal junction of EMT-related

circRNAs by back-splicing of precursor RNAs or multiple members of the splicing regulatory RNA-binding motif protein family (RBM4, RBM10 and RBM47) that inhibit cancer hallmarks, such as sustained proliferation, evading apoptosis and invasion (Hernandez et al., 2016; Vanharanta et al., 2014; Wang et al., 2014). Alterations in the 3'UTR length of mRNAs can change stability and translation efficacy. The proto-oncogenic Cytoplasmic polyadenylation element proteins (CPEB1-4) are aberrantly expressed in cancer and coordinate the alternative 3'-end processing machinery inducing APA of several target mRNAs (D'Ambrogio et al., 2013). For instance, CPEB1-mediated alternative polyadenylation and 3'UTR shortening correlates with cell proliferation and tumor progression (Bava et al., 2013). In melanoma, upregulated CPEB4 induces APA of drivers, such as MITF and RAB72A, and promotes their translation (Perez-Guijarro et al., 2016).

Proto-oncogenic or tumor-suppressive RNA-binding proteins also act through a wider range of mechanisms including modulations of mRNA stability and translation. The stability and integrity of an mRNA is mainly determined by the 5' cap and 3' poly A-tail that are co-transcriptionally incorporated. These determinants interact with cytoplasmic proteins, eIF4E and PABP, to prevent the conventional degradation by exonucleases including classical pathways like deadenylation/3'→5' decay and decapping/5'→3'-decay (Garneau et al., 2007). However, mRNA decay can also be accomplished by unusual routes through cleavage by endonucleases (e.g., AGO2, PMR1, IRE1 and RNase MRP). RBPs can promote (destabilization) or inhibit (stabilization) the degradation of target mRNAs. Well-studied mRNA stability elements are mainly located in 3'UTRs and comprise miRNA-binding sites and AU-rich elements (AREs), often found in many transcripts that encode tightly-regulated genes involved in transient biological processes like proto-oncogenes or transcription factors (Khabar, 2005). There is no wonder that RBPs associate to these regulatory elements and thereby interfere with the stability of the bound mRNA. For instance, AU-rich element binding protein 1 (AUF1) or a member of the HU family of RNA-binding protein family (ELAVL1, also known as HuR) bind to the AREs of target mRNAs and are frequently deregulated in cancer, as observed for ELAVL1 in colon (Denkert et al., 2006), lung (Mrena et al., 2005; Wang et al., 2011), breast (Denkert et al., 2004b) and ovarian cancer (Denkert et al., 2004a). The tumor-suppressing AUF1 primarily promotes the ARE-dependent decay of transcripts that encode cell cycle regulatory proteins (CCND1, CDKN2A), apoptosis regulators (BAX, BCL2), metastasis regulators (FGF9, MMP9) or even lncRNAs, such as NEAT1 (Zucconi and Wilson, 2011). Moreover, butyrate response factor 1 (BRF1), KH-type splicing regulatory protein (KSRP), and tristetraprolin (TTP) enhance ARE-mRNA decay trough the recruitment into cytoplasmic RNP granules and degradation sites (Xiao and Wang, 2011), such as processing bodies (P-bodies (Luo et al., 2018)). The proto-oncogenic ELAVL1 contains a combination of three classical RRMs and governs mRNA stability in a contrary but ARE-dependent manner. ELAVL1 stabilizes several mRNAs associated to the proliferative cell cycle (CCNA, CCNB1 and CCND1), to metastasis (MMP9), to angiogenesis (VEGFA) or to epithelial-to-mesenchymal transition (SNAI1) (Wang et al., 2013). Clinical data also show that high ELAVL1 level are related to advanced tumor stages and poor survival in cancer patients (Wang et al., 2013).

RNA-binding proteins are also involved in consecutive translational regulation steps during initiation, elongation, or termination. Many RBPs associate to mRNAs' regulatory 5' and 3'UTRs leading to altered translation efficacies (Truitt and Ruggero, 2016). ELAVL1 directly interacts with the 3'UTR of musashi 1(MSI1) and thereby increases both stability and translation in glioblastoma (Vo et al., 2012) or enhances topoisomerase IIα (TOP2A) translation by competing with repressive miRNAs (Srikantan et al., 2011). Musashi proteins (MSI1 and MSI2) belong to the A/B hnRNP family class and harbor two RRMs facilitating the RNA-binding. Both musashi proteins repress the translation of tumor-suppressors like p21 and NUMB in cancer cells (Fox et al., 2016; Niu et al., 2017). However, both musashi proteins facilitate the effective translation of oncogenes, like MYC, BRD4 and HMGA2 (Fox et al., 2016; Park et al., 2015). In conclusion, the loss of either MSI1 or MSI2 impairs pancreatic cancer progression in patient-derived xenograft mouse models. Nowadays, many research articles focus on aberrantly expressed and functionally altered RBPs associated to malignancies and cancer, respectively.

In the context of this dissertation, members of the insulin-like growth factor 2 mRNA binding protein (IGF2BP) family were of particular interest. The following chapters will focus on their specific roles in post-transcriptional gene regulation, expression patterns, and implications for development, and cancer, respectively.

The Insulin-like Growth Factor 2 mRNA binding Protein family – IGF2BPs

The human IGF2 mRNA binding protein family consists of three canonical RNA-binding proteins: IGF2BP1, IGF2BP2, and IGF2BP3 (Bell et al., 2013). Over the past years and decades, IGF2BP-related research increasingly documented the contribution of these RBPs in central biological processes, especially in the context of development and cancer progression. Of note, other literature-used synonyms encompass IMPs, CRD-BPs, ZBPs, KOCs, Vg1RBPs, and VICKZs. The "older" family name VICKZ is derived from the first letters of the synonyms Vg1-RBP/Vera in *Xenopus laevis*, human IMP1-3 (insulin-like growth factor 2 mRNA binding protein / IGF2BP1-3), KOC (KH domain-containing protein overexpressed in cancer), murine CRD-BP (Coding Region instability Determinant Binding Protein) and chicken orthologue ZBP1 (Zipcode Binding Protein 1) already indicating the evolution from various research fields (Yisraeli, 2005).

In 1997, the laboratory of Robert Singer identified ZBP1 as an RNA-binding protein that functions within in a complex to subcellular localize the β-actin (ACTB) mRNA by binding to a 54-nt sequence element, termed zipcode and located in the 3'UTR, in fibroblasts derived from chicken embryos (Ross et al., 1997). At the same time, a screen designed to unravel overexpressed proteins in human pancreatic carcinomas identified KOC (now known as IGF2BP3) without further functional studies (Mueller-Pillasch et al., 1997). One year later, the murine and human IGF2BP1 orthologues, named CRD-BP, were shown first to promote MYC mRNA stability by binding to the coding region instability determinant (CRD), published in *Nucleic Acids Research* (Doyle et al., 1998). In the following, these proteins are defined as IGF2BPs according to the official gene symbols to avoid confusion in nomenclature.
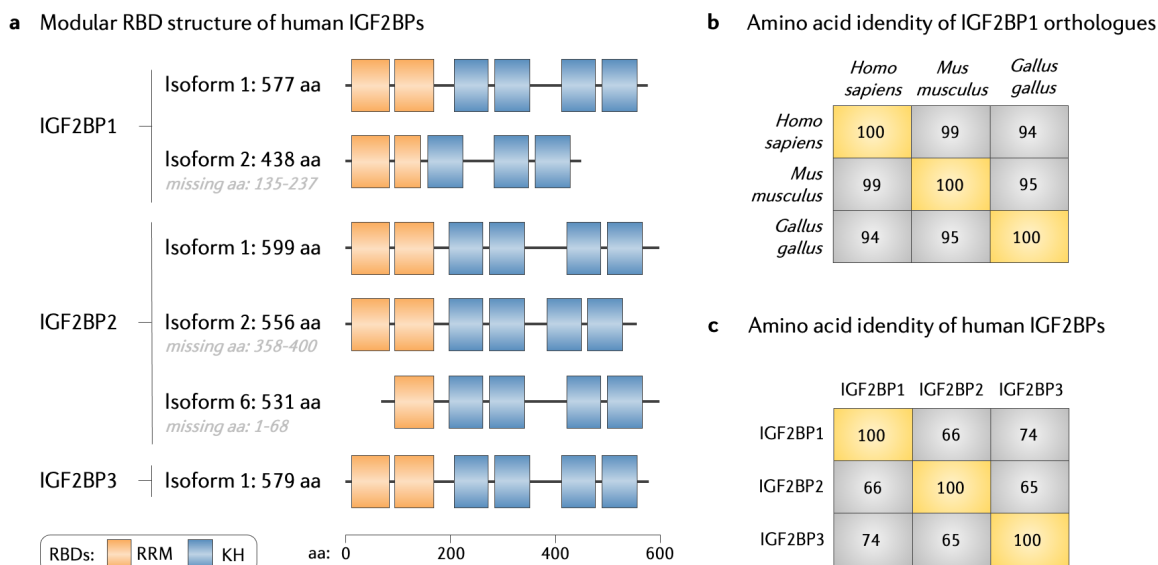
a Modular RBD structure of human IGF2BPs

b Amino acid idendity of IGF2BP1 orthologues

	Homo sapiens	Mus musculus	Gallus gallus
Homo sapiens	100	99	94
Mus musculus	99	100	95
Gallus gallus	94	95	100

c Amino acid idendity of human IGF2BPs

	IGF2BP1	IGF2BP2	IGF2BP3
IGF2BP1	100	66	74
IGF2BP2	66	100	65
IGF2BP3	74	65	100

Figure 6 | **The structure and identity of the IGF2BP family. a,** Canonical RNA-binding domain (RBD) structure of human IGF2BP isoforms. The following UniProt-derived (www.uniprot.org) human isoforms are presented: IGF2BP1 (Isoform 1: Q9NZI8-1, Isoform 2: Q9NZI8-2), IGF2BP2 (Isoform 1: Q9Y6M1-2, Isoform 2: Q9Y6M1-1, Isoform 6: Q9Y6M1-6), IGF2BP3 (Isoform 1: O00425-1). IGF2BP1 isoform 2 and IGF2BP2 isoform 2-6 are generated by alternative splicing (IGF2BP2 Isoforms 2, 3 and 4 differ in N-terminal amino acids of Isoform 1, IGF2BP2 isoform 5 differs in N-terminal amino acids of isoform 6). RRM – RNA recognition motiv, KH – hnRNP K homology domain. **b,** Percentage of amino acid identity of IGF2BP1 orthologues from human (Homo sapiens), mouse (Mus musculus) and chicken (Gallus gallus). **c,** Percentage of amino acid identity of human IGF2BP paralogues (predominant isoforms 1).

All three IGF2BP paralogues share the characteristic modular RBD structure with two N-terminal RRMs and four C-terminal KH domains (Bell et al., 2013), leading to predominantly expressed protein isoforms of similar molecular weight (**Figure 6a**, IGF2BP1-Isoform 1: 63.48 kDa, IGF2BP2-Isoform 1: 66.12 kDa, IGF2BP3-Isoform 1: 63.71 kDa). The amino acid identity of IGF2BP1 orthologues shows high conservation across humans, mouse, and chicken variants (**Figure 6b**). Human IGF2BPs share substantial amino acid homology ranging from 66-74% (**Figure 6c**) with higher degree of resemblance in the structured RBDs (Bell et al., 2013). The six conserved RBDs are arranged in di-domains (RRM1-2, KH1-2, and KH3-4), that are closely spaced by distinct linker regions in the protein sequence (Yisraeli, 2005). All members of the IGF2BP family bind RNA, regardless of orthologue or paralogue (Bell et al., 2013). Early binding studies indicate that the KH domains mainly bind the ACTB zipcode, whereas the RRMs are not involved in direct RNA-binding but are crucial for the proper subcellular sorting of the ACTB mRNA (Farina et al., 2003) and may contribute to the stability of Protein-RNA association (Nielsen et al., 2004). Further mutation analyzes of the internal GXXG loop of all KH domains in glycine-glutamate-glutamate-glycine (GEEG) show that the RNA-binding of IGF2BP1 and IGF2BP2 is essentially mediated by these four domains (Wachter et al., 2013). However, the contribution of the KH di-domains to RNA-binding appears target-dependent (Dagil et al., 2019). For instance, the recognition of CD44 and MYC mRNAs needs all four KH domains of IGF2BP1 (Nielsen et al., 2002; Vikesaa et al., 2006), whereas recognition of the ACTB and a variety of other neuronal mRNAs requires only the C-terminal KH3-

4 di-domain (Patel et al., 2012). The KH3-4 di-domain is also critical for the re-modelling of the target RNA structure. For-instance, the KH3-4 domains bind to a bipartite RNA fragment within the first 28 nucleotides of the ACTB zipcode forming an intramolecular anti-parallel pseudodimer with the RNA-binding surfaces at opposite ends. By binding of both KH domains at the same time, the RNA backbone is looped and rotated around 180 degrees (Chao et al., 2010). Furthermore, IGF2BPs have also been discovered as m⁶A-binding proteins using pulldown studies with m⁶A RNA probes and mass spectrometry (Huang et al., 2018a). Mutation studies show that the KH3–4 domains are also essentially required for this m⁶A recognition and binding, although the KH1–2 domains may play a supporting function. These findings together indicate the necessity to determine whether the RNA-binding di-domains have intrinsically diverse RNA-binding characteristics that facilitate a distinct target spectrum of IGF2BPs. Recent efforts showed that all four KH domains of IGF2BP1 have significantly different nucleobase specificities and binding kinetics. While KH1-2 binds to a target RNA an order of magnitude faster than KH3-4, the KH3-4– RNA complex has a 14-fold longer lifespan (Dagil et al., 2019). However, the low specificity and rapid kinetics of KH2 in comparison to KH4 (very specific binding to a GGAC motif) for the RNA suggest that this domain may participate in the early stages of IGF2BP1 binding by facilitating relatively dynamic and non-specific interactions with the RNA. The role of the KH di-domains appears less pronounced in IGF2BP3, where mutations in the KH domains modestly affect binding (Wachter et al., 2013), and all RBDs, including the N-terminal RRMs, contribute to direct RNA interactions (Schneider et al., 2019). Taken together, all findings underly the complexity and plasticity of the RNA-binding properties of IGF2BPs and indicate a broad paraloque-specific target spectrum with different contributions of the RBDs.

IGF2BPs predominantly localize in cytoplasmic granular-like RNA-protein complexes. However, there is evidence that IGF2BPs already bind target mRNAs in the nucleus at the transcription site, as shown for the ACTB mRNA using high-speed imaging (Oleynikov and Singer, 2003) or recently for MYC mRNA fragments using IGF2BP-pulldowns from nuclear extracts (Huang et al., 2018a). Moreover, IGF2BP1-containing granules embrace the nuclear cap-binding protein (NCPB1) and components of the nuclear exon junction complex (Jonson et al., 2007). These granules also lack the 60 S ribosomal subunits, and the translation initiation factors eIF4E and eIF4G suggesting that IGF2BP-associated transcripts are translationally inactive (Jonson et al., 2007; Weidensdorfer et al., 2009). Hence, IGF2BPs associate to virgin-like target mRNAs caging them with other proteins into cytoplasmic mRNPs, such as Y-box binding protein 1 (YBX1) or ELAVL1 (Jonson et al., 2007; Wachter et al., 2013; Weidensdorfer et al., 2009). The fate of the specific target mRNA can then be modulated by the respective IGF2BP paralogue in terms of localization, stability/degradation, or translation (as shown for IGF2BP1 in **Figure 7**). IGF2BPs directly interact with a plethora of mRNAs suggesting RNA-binding in a pleiotropic manner with over 8.000 bound transcripts, as revealed by several independent CLIP studies using different modified protocols and cell types of overexpressed and endogenous IGF2BP paralogues (Conway et al., 2016; Hafner et al., 2010; Van Nostrand et al., 2016). In addition, IGF2BP1 also binds ncRNAs, such as the short non-coding RNA Y3 (Kohn et al., 2010), the lncRNAs H19, HULC, and THOR

(Hammerle et al., 2013; Hosono et al., 2017; Runge et al., 2000) or the circular RNAs circXPO1 and circPTPRA (Huang et al., 2020b; Xie et al., 2021), forming non-coding ribonucleoprotein complexes (ncRNPs). These ncRNAs serve as temporary scaffolds (e.g., Y3, THOR), presumably modulating IGF2BP1 function or as expression-regulated target RNAs (e.g., HULC).
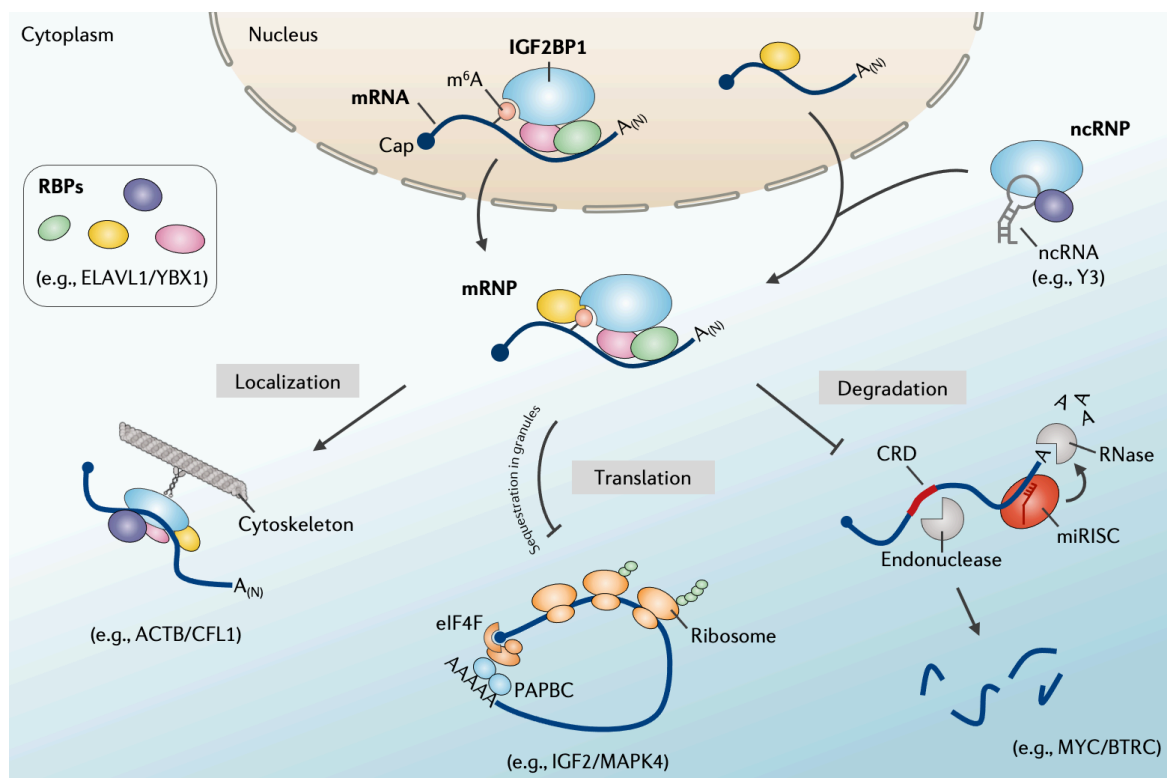

Figure 7 | Post-transcriptional gene regulation by IGF2BP1. IGF2BP1 associates with other proteins and specific preferentially m6A-modified mRNAs or ncRNAs to form granule-like mRNPs / ncRNPs. The main IGF2BP1 functions are to localize the mRNA to distant subcellular compartments, stabilize mRNAs by preventing the CRD-dependent endonuclease- or miRISC-mediated degradation, or sequester mRNAs leading to spatially and temporally repressed translation.

Depending on the specific target RNA, IGF2BPs regulate RNA localization, turnover, or translation, leading to elevated or decreased protein synthesis. A well-studied example is the before-mentioned ACTB mRNA. IGF2BP1 spatially and temporally represses the translation of the ACTB mRNA by sequestration in cytoplasmic granules. Via the direct association of IGF2BP1 with the motor protein KIF11, the translationally silent mRNP is transported along the microtubule cytoskeleton to the leading edge of fibroblasts supporting cell migration or to the exploratory growth cones of developing and dendritic arbors in hippocampal neurons (Huttelmaier et al., 2005; Oleynikov and Singer, 2003; Perycz et al., 2011; Song et al., 2015). Furthermore, IGF2BP1 localizes the cofilin-1 (CFL1) mRNA in a 3'UTR-dependent manner to the cell periphery of lung carcinoma cells elevating cell motility (Maizels et al., 2015). Initial studies focusing on the name-giving IGF2 mRNA show that IGF2BP1 binds to the 5'UTR leading to the translational repression during late mammalian development (Nielsen et al., 1999). Another example is the IGF2BP1-facilitated inhibition of the mitogen-activated protein kinase 4 (MAPK4) mRNA translation.

Reduced MAPK4 protein levels boost the cell migration velocity by antagonizing MAPK activated protein kinase 5 (MK5) activation, finally resulting in elevated cellular acting dynamics (Stohr et al., 2012). The most reported IGF2BP1 function relies on the RNA stability control by preventing mRNA from degradation. As mentioned before, IGF2BP1 binds CRD regions located in coding sequences. During translational pausing caused by an inefficient usage of rare codons, IGF2BP1 protects CRDs of the multi-drug-resistance-factor 1 (MDR1) and MYC transcripts from endonuclease-mediated degradation (Doyle et al., 1998; Lemm and Ross, 2002; Sparanese and Lee, 2007; Weidensdorfer et al., 2009). Surprisingly, IGF2BP1 also extends the half-life of the proto-oncogene encoding F-box/WD repeat-containing protein 1A (BTRC, also known as βTrCP1) in a CRD-independent manner but also by binding to the coding sequence (Noubissi et al., 2006). This mRNA contains a different cis-acting destabilizing element that determines the rate of mRNA turnover: a miRNA-binding site. In 2009, a study from the Spiegelmann group reported for the first that IGF2BP1 prevents an mRNA from degradation by the miRNA-induced silencing complex. IGF2BP1 recruits the BTRC mRNA in protective mRNPs inhibiting the miR-183-mediated gene silencing (Elcheva et al., 2009). Further studies by the same group showed that the miR-340-mediated decay of the Microphthalmia-associated transcription factor (MITF) mRNA is impaired by binding of IGF2BP1 to the respective site located in the 3'UTR (Goswami et al., 2015). In addition, IGF2BP1 maintains LIN28B and HMGA2 expression by binding these let-7 target mRNAs in protective mRNPs, essentially lacking miRISC-components, such as let-7 miRNAs or AGO2 (Busch et al., 2016).

Similar mechanisms have been reported for the other IGF2BP paralogues. For instance, IGF2BP3 sequesters the oncogene-encoding HMGA2 transcripts in RNP safe houses to protect them from let-7-mediated silencing (Jonson et al., 2014). By binding to the appropriate miRNA-binding sites, IGF2BP2 protects mRNAs from let-7-dependent silence, as shown for HMGA1, HMGA2 and CCND1 mRNAs (Degrauwe et al., 2016a). It is commonly accepted that IGF2BPs are important for RNA localization, promote RNA stability or lower the translation efficacy. However, there are no rules without exceptions. To name a few, IGF2BP1 destabilizes the lncRNA HULC by recruiting the CCR4-Not-complex to the transcript leading to deadenylation and decay (Hammerle et al., 2013), or IGF2BP2 and IGF2BP3 promote the translation of the IGF2 mRNA by binding to the highly structured IGF2 5'UTR stimulating the translation initiation through an internal ribosome entry (Dai et al., 2011; Liao et al., 2005). Another contrary study indicated that IGF2BP3 recruits the miRNA-induced silencing complex to specific target mRNAs instead of protecting them (Ennajdaoui et al., 2016).

Taken together, IGF2BPs belong to a family of highly conserved RNA-binding proteins that regulate the fate of associated transcripts at several levels, including localization, stability, and translation rate. Although the proteins of the IGF2BP family are very similar in size, structure, and function, they show paralogue-specific expression patterns during development and carcinogenesis (Bell et al., 2013).

The role of IGF2BPs during development and carcinogenesis

The whole IGF2BP family has a high level of expression throughout embryonic development. Mammalian IGF2BPs already appear in the zygote and peak on mouse embryonic day E10.5 to E12.5, especially in neuronal cells of the forebrain and hindbrain (Nielsen et al., 1999; Runge et al., 2000). The expression levels rapidly decrease with the ongoing murine development to post-natal stages. IGF2BP1 transcripts have little or no expression in differentiated cells, with some persisting expression levels in the intestine of adult mice (Hansen et al., 2004). IGF2BP3 also shows negligible expression in adult murine tissues. IGF2BP2 principally follows the pattern of the other paralogues, with decreasing expression during embryogenesis. However, IGF2BP2 transcripts are detectable in adult mouse tissues, including brain, heart, lung, liver, and kidney, to name a few (Bell et al., 2013). Interestingly, a comprehensive analysis of 1542 RBPs also identified a similar expression pattern across the human fetal hippocampus development (**Figure 8**, (Gerstberger et al., 2014)).
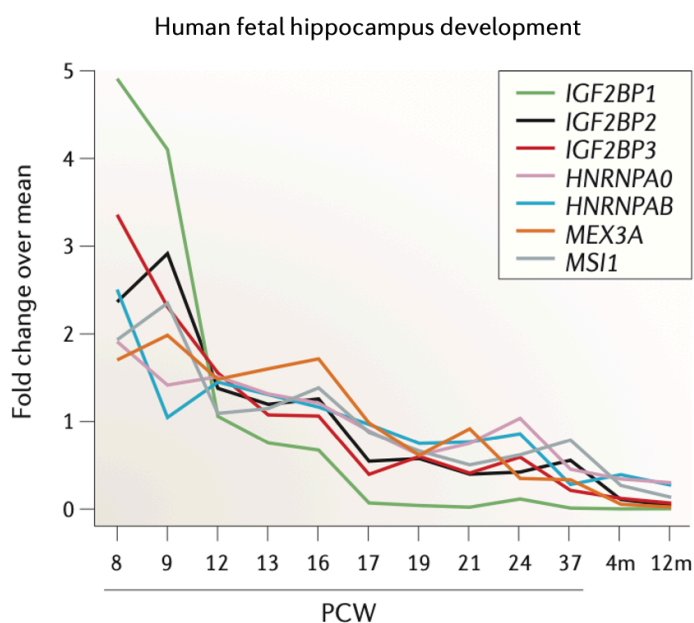
Figure 8 | **Expression of differentially expressed RBPs across human fetal hippocampus development.** The fold change over mean expression is shown for the indicated most-differentially RBPs across 12 stages of the human fetal hippocamps development ranging from post-conception week (PCW) 8 to 12 months (12m) after birth. Expression was profiled by RNA-sequencing and data were deposited in the BrainSpan database (www.brainspan.org). Taken from (Gerstberger et al., 2014), Figure 7Ca

This analysis revealed the most differentially expressed RBPs showing high expression during early development with a rapid decrease in expression at later stages. These include all IGF2BPs, two members of the HNRNP family (HNRNPA0 and HNRNPAB), the Mex-3 RNA binding family member A (MEX3A), and MSI1, mainly confirming the observed expression pattern of the murine IGF2BP orthologues. The evaluation of the specific gene expression in human adult tissues using data from the Genotype-Tissue Expression Project (GTEx, www.gtexportal.org) further supports, that IGF2BP1 and IGF2BP3 are virtually absent upon birth (except from testis, where the expression is detectable) and have median TPMs (transcripts per million) lower than 0.05 determined by RNA-sequencing. In contrary, IGF2BP2 is detectable in noticeable amounts across human tissues (around 10 TPM in median) and seems to be only member involved in controlling the mRNA fate in adult tissues. For instance, genome-wide association studies showed that a

single nucleotide polymorphism (SNP) in the second intron of the IGF2BP2 gene correlates with an increased risk of type 2 diabetes (Christiansen et al., 2009), or a study that showed the role of IGF2BP2 in muscle cells, where the depletion of IGF2BP2 results in changes of muscle cell shapes and a decrease in motility (Boudoukha et al., 2010). IGF2BP2 also regulates nutrient and energy metabolism. In accordance, IGF2BP2-knockout mice show several phenotypes, including modestly smaller size but substantially longer lifespan in a high fat diet mediated by increased resistance to obesity (Dai et al., 2015). The physiological role in embryonic development has so far only been analyzed for IGF2BP1 using IGF2BP1-deficient mice harboring a gene-trap insertion (Hansen et al., 2004). These mice have significantly increased perinatal mortality with a survival of 50% three days after birth and are on average about 40% smaller than wild-type mice indicating a dwarfism phenotype. A key determinant of the neuronal development is the control of localized translation. As before mentioned, the ATCB mRNA is transported via translational silent IGF2BP1-containing mRNPs to developing axons or dendrites. ACTB protein synthesis is forced by the SRC-dependent phosphorylation of IGF2BP1 that releases the RNA for spatial translation to promote the formation of growth cones (Huttelmaier et al., 2005). Further, IGF2BP1 also promotes the self-renewal of fetal neural stem/progenitor cells, thereby representing an essential factor for maintaining stem cell properties required for the cellular expansion and brain development (Nishino et al., 2013). In support, IGF2BP1 also promotes the survival and adhesion of human pluripotent stem cells (Conway et al., 2016).

Despite being mainly absent in adult tissues, many studies indicate a re-expression of IGF2BP1 and IGF2BP3 in various cancer types. Due to the high expression during development and *de novo* synthesis in cancer, the expression of these two IGF2BP paralogues is characterized as oncofetal (Bell et al., 2013). However, high expression of all IGF2BP family members has been extensively linked to nearly all types of cancer by identifying the respective RNAs using methods like RT-qPCR, microarray analyses or RNA-sequencing, or the individual proteins using immunohistochemistry staining (reviewed in detail: (Bell et al., 2013; Degrauwe et al., 2016b; Huang et al., 2018b; Lederer et al., 2014; Mancarella and Scotlandi, 2019)). To name just a few examples, IGF2BP1 is significantly overexpressed and correlates with disease progression or patient prognosis in ovarian (Kobel et al., 2007), lung (Kato et al., 2007; Shi et al., 2017), liver (Gutschner et al., 2014; Zhou et al., 2015), cervical (Su et al., 2016; Wang et al., 2018a), gastrointestinal (Chen et al., 2021; Mongroo et al., 2011), thyroid (Haase et al., 2021), and central nervous systems cancers, such as neuroblastoma (Bell et al., 2015), and glioblastoma (Wang et al., 2015a). There is no wonder that many papers try to partly answer necessary open questions, like *a)* Why is IGF2BP1 upregulated in the certain type of cancer, *b)* What phenotypes are affected by IGF2BP1 in the used cell model and *c)* What are the underlying mechanistic details and the direct target mRNAs.

Interestingly, the expression of IGF2BP1 is virtually controlled at every level described before, including epigenetic control by TET1/2 DNA demethylases (Mahaira et al., 2014), gene amplification in neuroblastoma (Bell et al., 2015), transcriptional regulation driven by the proto-oncogenes β-catenin (CTNNB1) or MYC (Noubissi et al., 2006; Noubissi et al., 2010), and post-

transcriptional repression by a myriad of (partly exotic sounding) miRNAs, including let-7 (Boyerinas et al., 2008), miR-491 (Gong et al., 2016), miR-98 (Jiang et al., 2017), miR-625 (Zhou et al., 2015), miR-9 (Zhang et al., 2015), miR-1275 (Fawzy et al., 2015), miR-196b (Rebucci et al., 2015), miR-708 (Qin et al., 2017), miR-150 (Qu et al., 2016), miR-873 (Wang et al., 2015a), miR-140 (Su et al., 2016), and miR-124 (Wang et al., 2018a). All listed miRNAs are downregulated in the respective cancer samples and serve as tumor-suppressive miRNAs by targeting the pro-oncogenic functions of IGF2BP1. The latter have been extensively studied *in cellulo* as well as *in vivo* using mouse models and linked to several target mRNAs. IGF2BP1 influences various cellular properties, such as proliferation, apoptosis, chemoresistance, migration, and invasion, by stabilizing cancer-related transcripts like MYC (Gutschner et al., 2014; Huang et al., 2018a; Xu et al., 2017b), MKI67 (Gutschner et al., 2014), GLI1 (Noubissi et al., 2009), PTEN (Stohr et al., 2012), MDR1 (Sparanese and Lee, 2007), CD44 (Vikesaa et al., 2006), BTRC (Elcheva et al., 2009; Noubissi et al., 2006), LEF1 (Zirkel et al., 2013), and KRAS (Mongroo et al., 2011). In a transgenic mouse model, the forced overexpression of murine Igf2bp1, driven by whey acidic protein (WAP) promoter, in mammary epithelial cells results in the formation of mammary tumors with an incidence of 95% in high (average age 53 weeks) and 65% in low (average age 60 weeks) expressing mice, indicating dose-dependency (Tessier et al., 2004). Accordingly, murine xenograft studies reveal that the depletion of IGF2BP1 in human liver cancer cells substantially impaired tumor growth (Gutschner et al., 2014). Colon cancer cell-derived xenograft studies with IGF2BP1 deficiency demonstrate decreased number of tumor cells entering blood vessels, implying that IGF2BP1 supports early steps in metastasis directly. In conclusion, overexpression of IGF2BP1 in the same model results in increased tumor development and cancer cell spread into the blood circulation (Hamilton et al., 2013), providing further *in vivo* evidence that IGF2BP1 is pro-oncogenic post-transcriptional regulator.

The oncofetal expression and pro-tumorigenic function emphasize IGF2BP1 as a therapeutic target in the treatment of cancer. A recent study describes the identification of a small molecule that precisely targets IGF2BP1's RNA-binding activity – BTYNB (Mahapatra et al., 2017). In this study, 160.000 small molecules were screened for inhibiting IGF2BP1 binding to a fluorescein-labeled MYC RNA fragment using a fluorescence anisotropy-based assay. By inhibiting the expression of MYC in ovarian cancer- and melanoma-derived cells, this compound dramatically decreased cancer cell proliferation *in vitro*, suggesting that IGF2BP1 is principally druggable and a promising target for cancer treatment.

The aims of the thesis

IGF2BPs are highly conserved oncofetal RNA-binding proteins (RBPs) that orchestrate the fate of target RNAs at the post-transcriptional level, including localization, translation, and stability. Three mammalian IGF2BP paralogues (IGF2BP1–3) have been discovered. IGF2BP2 is ubiquitously expressed in adult organisms. In contrast, IGF2BP1 and IGF2BP3 show an oncofetal expression pattern with high expression during embryogenesis and severe upregulation or even *de novo* synthesis in various cancers. However, all three paralogues may be overexpressed upon malignant transformation and are detectable on RNA and protein levels in a wide variety of cancer types, where their presence frequently correlates with poor patient prognosis. This doctoral study focused on the following primary aims:

Although IGF2BPs are overexpressed in several of these cancers, their paralogue-specific functions in certain tumor cells remain largely unknown. *Accordingly, the first main objective of this work was to evaluate the role of individual IGF2BP members in a panel of cancer cell lines to identify paralogue-dependent cellular phenotypes and underlying molecular determinants.*

IGF2BPs preferentially bind m^6A-modified mRNAs and recruit target transcripts in protective mRNPs, inhibiting their miRNA-directed degradation. *Thus, the second major aim was to explore the interdependency of m^6A-modifcation and miRNA-dependent control of novel as well as conserved IGF2BP1 target mRNAs.*

Furthermore, IGF2BP1 is known to promote the stability of mRNAs encoding proto-oncogenic transcriptional regulators such as MYC and HMGA2. IGF2BP1, on the other hand, associates with thousands of mRNAs in a pleiotropic manner. *Therefore, a further objective of this study was to determine whether IGF2BP1 enhances the transcription factor-driven gene expression at the post-transcriptional level in a conserved manner across cancer cells.*

So far, conserved effector pathways, as well as the possibility of targeting IGF2BP1 in cancer, have remained mainly elusive. Although only demonstrated *in vitro*, the small molecule BTYNB showed promising IGF2BP1 inhibition. *In accordance, the final aim was to discover these conserved oncogenic pathways and utilize the data to assess the target potential druggability of IGF2BP1 by BTYNB in cancer treatment.*

III SUMMARY AND DISCUSSION

The oncofetal, non-catalytical IGF2 mRNA binding protein 1 (IGF2BP1) is a central modulator of post-transcriptional gene regulation diversely orchestrating the fate of associated mRNAs and thereby affecting various cellular properties that are particularly important during development and carcinogenesis, respectively.

This doctoral dissertation examined the molecular determinants and underlying mechanisms for IGF2BP1-dependent phenotypes using *in vitro* and *in vivo* models. Several findings suggest that IGF2BP1 possesses a highly conserved oncogenic potential and promotes an aggressive tumor cell phenotype via antagonizing miRNA-mediated gene expression impairment (Muller et al., 2018). Further results demonstrate that IGF2BP1 promotes SRF expression in a conserved and N^6-methyladenosine (m⁶A)-dependent manner by impairing the SRF mRNA's miRNA-directed decay, resulting in elevated SRF transcriptional activity. In addition, IGF2BP1 enhances SRF's transcriptional output by fostering SRF-driven transcripts at the post-transcriptional level resulting in elevated tumor cell growth and invasion (Muller et al., 2019). Finally, we demonstrate that IGF2BP1 is a post-transcriptional enhancer of the E2F-driven hallmark pathway in cancer cells, promoting G1/S cell cycle transition via miRNA- and m⁶A-dependent stabilization of mRNAs encoding positive regulators of this checkpoint. The small molecule IGF2BP1 inhibitor BTYNB disrupts this function in preclinical models by impairing IGF2BP1's RNA-binding capacity (Muller et al., 2020).

IGF2BP1 promotes aggressive cell phenotypes by interfering with the downregulation of oncogenic factors by microRNAs (Müller et al., 2018)

The IGF2 mRNA binding protein family is composed of three canonical RNA-binding proteins: IGF2BP1, IGF2BP2, and IGF2BP3. While the IGF2BP family proteins are highly homologous in terms of size, structure, and function, they exhibit paralogue-specific expression patterns and functions during carcinogenesis. We examined the phenotypic roles of IGF2BPs in five tumor cell lines derived from distinct solid cancers, starting with ovarian cancer, where increased expression of all three IGF2BPs has been shown to promote tumorigenesis and correlate with adverse patient prognosis (Davidson et al., 2014; Hsu et al., 2015; Kobel et al., 2007; Kobel et al., 2009). Independent Kaplan-Meier analyses were used to re-evaluate the correlation with patient prognosis of IGF2BPs in 1232 serous ovarian carcinomas. Only high IGF2BP1 mRNA expression showed conserved association with significantly reduced overall survival (OS), corroborating previous findings (Kobel et al., 2007). Moreover, elevated IGF2BP1 abundance was associated with progression-free survival (PFS), in particular in the vast majority of p53-mutated serous ovarian cancers (Supplementary Figure S1A in (Muller et al., 2018)). To determine whether IGF2BP paralogues play distinct roles in ovarian cancer-derived ES-2 cells, oncogenic tumor cell properties were assessed following IGF2BP paralogue-specific side-by-side depletions using small interfering RNA (siRNA) pools (Figure 1A and B in (Muller et al., 2018)). One of the primary

drawbacks of siRNA experiments is the presence of sequence-specific off-target effects. By achieving low concentrations of individual non-overlapping siRNAs, siRNA pools reduce off-target bias and increase knockdown efficiency as well as specificity (Hannus et al., 2014). Among IGF2BP depletion studies, only the knockdown of IGF2BP1 resulted in the conserved and significant reduction of all investigated phenotypes in cancer cells. Phenotypes evaluated included: a) cell proliferation, b) cell migration, c) spheroid proliferation, d) anoikis resistance / self-renewal, and e) spheroid invasion (Figure 1C-G in (Muller et al., 2018)). The Class 2 Clustered Regularly Interspaced Short Palindromic Repeat (CRISPR) allows the genome editing, in particular gene silencing, at high precision and efficiency (Cong et al., 2013; Hsu et al., 2013; Ran et al., 2013). This system settles on genome-targeting single guide RNAs (sgRNAs) guiding the CRISPR-associated programmable endonuclease (Cas9) to specific sites in the genome. The sgRNA contains a Cas9-binding scaffold sequence and a 20-nucleotide spacer that defines the genomic target region. At the targeting site, the Cas9 nuclease breaks both DNA strands. Cells repair the break using the non-homologous end joining repair (NHEJ) pathway leading, in most cases, to gene knockouts due to inserted or deleted bases. Aiming to rule out potential bias of siRNA depletion due to remaining off-target effects, investigated phenotypes were re-analyzed in ovarian cancer-derived ES-2 cells following CRISPR/Cas9-mediated deletion of IGF2BP1 or 3. Confirming siRNA-directed knockdown studies, only IGF2BP1 deficiency significantly impaired tumor cell phenotypes (Figure 1H-J in (Muller et al., 2018)). This was further supported by gain-of-function studies settling on forced overexpression of GFP-tagged (green fluorescent protein) IGF2BP1. This significantly enhanced the analyzed phenotypes in ES-2 cells (Supplementary Figure 2 in (Muller et al., 2018)). To determine whether IGF2BP1 deletion also impairs tumorigenesis *in vivo*, iRFP-labeled (near-infrared fluorescent protein) IGF2BP1-knockout and control ES-2 cells were used to monitor the growth and metastasis of subcutaneous xenografts. This analysis confirmed that IGF2BP1 deletion significantly decreased tumor growth, as observed in previous studies using liver (Gutschner et al., 2014) and colon cancer cells (Hamilton et al., 2013), and provided strong evidence that IGF2BP1 is important for the metastasis of tumors in nude mice (Figure 2 in (Muller et al., 2018)), as suggested by analyses in melanoma (Craig et al., 2012) and colon cancer models (Hamilton et al., 2013). Notably, in a recent study, we further supported the pro-metastatic role of IGF2BP1 by demonstrating that IGF2BP1-overexpression accelerates the spread of ovarian cancer cells in the peritoneum of nude mice upon intraperitoneal application of cancer cells (Bley et al., 2021).

In a wide range of cancer types, all three IGF2BP paralogues are overexpressed during malignant transformation. To assess their paralogue-specific phenotypic conservation in cancer cells, we analyzed phenotypes in four additional cancer-derived cell lines: OVCAR-3 (ovarian carcinoma), MV-3 (melanoma), A549 (lung adenocarcinoma), and HepG2 (hepatocellular carcinoma). Only the depletion of IGF2BP1 resulted in the conserved and significant reduction of both investigated cell properties, spheroid growth and anoikis resistance (Figure 3 in (Muller et al., 2018)). In sharp contrast, the knockdowns of the two other IGF2BP paralogues, IGF2BP2 and 3, showed overall milder and strongly cancer cell context-dependent phenotypic roles. For

instance, the loss of IGF2BP2 only decreased spheroid proliferation in lung adenocarcinoma- and liver cancer-derived (A549 and HepG2) cells. This confirms recent findings that IGF2BP2 promotes tumor cell proliferation and maintains cancer stem cell characteristics (Dai et al., 2017; Degrauwe et al., 2016a; Huang et al., 2018a; Li et al., 2019; Pu et al., 2020). IGF2BP3 depletions preserved phenotypic effects only moderately, despite claims that IGF2BP3 plays proto-oncogenic roles in tumor cells from numerous cancers (Lederer et al., 2014; Mancarella and Scotlandi, 2019). However, among the five tumor-derived cell lines studied here, IGF2BP3 showed the most severe phenotypic influence of the three IGF2BPs in lung cancer-derived cells. This backs up recent research showing that IGF2BP3 induces an aggressive phenotype in lung cancer cells (Shi et al., 2017; Zhao et al., 2017). Further research is required to investigate IGF2BP-dependent regulation of other characteristics such as the influence on cancer cell metabolism and immune evasion. Additionally, it is unknown if IGF2BP2 and IGF2BP3 promote tumor growth *in vivo* since cell analyses are constrained by a variety of factors, most notably the absence of tumor-stroma or tumor-immune communications. Thus, our findings may underestimate the oncogenic potential of IGF2BP2 and IGF2BP3 at this point.

Previous research has established that one of the major functions of IGF2BPs is to regulate mRNA turnover (Bell et al., 2013). Initial PAR-CLIP studies showed that the three IGF2BPs recognized a plethora of partially overlapping target RNAs (mapping to approx. 8.400 protein-coding genes) with a strong preference for 3'UTR-binding (Hafner et al., 2010). However, the partly distinct phenotypic roles observed for IGF2BP paralogues in cancer-derived cells suggested that IGF2BPs modulate partially distinct (m)RNA targets. To investigate this further, RNA-sequencing was used to monitor gene expression in ES-2 cells after side-by-side depletions of IGF2BP paralogues. The loss of IGF2BPs had varying and modestly overlapping effects on mRNA abundance, but not on miRNA or lncRNA abundance (Figure 3C and Supplementary Figure S3 in (Muller et al., 2018)). IGF2BP1's phenotypic roles are conserved among tumor-derived cells, suggesting that functionally relevant protein-RNA associations are conserved as well. Accordingly, the conservation of CLIP sites reported for IGF2BP1 in HEK293 (PAR-CLIP; (Hafner et al., 2010)), human pluripotent stem cells (eCLIP; (Conway et al., 2016)), leukemia-derived K562 and liver cancer-derived HepG2 cells (eCLIP and iCLIP; (Van Nostrand et al., 2016)) was determined for the 5'UTR, the coding sequence (CDS) and the 3'UTR regions of protein-coding genes. This resulted in a so-called CLIP score indicating the number of experiments demonstrating direct IGF2BP1 binding. The 5'UTRs, CDSs, and 3'UTRs of downregulated mRNAs (DN, n=272) upon IGF2BP1 depletion had significantly higher CLIP scores than upregulated (UP, n=288) or control (C, n=280; randomly selected) transcripts (Figure 4E–G in (Muller et al., 2018)). Consistent with preferred 3'UTR association (Hafner et al., 2010), the highest CLIP score was identified for this cis-element in DN mRNAs. Moreover, DN transcripts showed substantially elevated 3'UTR length. This provided further evidence that IGF2BP1 mainly acts via target mRNA 3'UTRs, a *bona fide* landscape for post-transcriptional gene regulation and RNA turnover control.

IGF2BP1 has been shown to impair the miRNA-directed degradation of some target mRNAs, such as BTRC, MITF, HMGA2 and LIN28B (Busch et al., 2016; Elcheva et al., 2009; Goswami

et al., 2015). Interestingly, the DN mRNAs exhibit increased AGO binding, as revealed by CLIP, and vulnerability to regulation by microRNAs expressed in tumor-derived cells compared to non-DN mRNAs by harboring an increased number of miRNA-binding sites (Figure 5A-C in (Muller et al., 2018). Aiming to test this experimentally, we co-depleted the miRNA-biogenesis enzymes DROSHA and DICER. This reduced the expression of mature miRNAs and elevated the RNA and protein level of several investigated DN mRNAs (Figure 5E in (Muller et al., 2018)). In view of these findings, we hypothesized that IGF2BP1 protects target mRNAs from downregulation by the miRNA-induced silencing complex. To investigate this hypothesis, we expected that the respective IGF2BP1-dependent regulation is abolished by the depletion of antagonizing destabilizing effectors, here endogenous miRNAs – in other words "Who needs a protective shield when nobody is attacking". In order, we investigated whether IGF2BP1 impairs miRNA-directed downregulation of these miR-prone target mRNAs by comparing mRNA levels upon IGF2BP1 depletion versus transcript abundance upon the co-depletion of IGF2BP1, DICER, and DROSHA. The knockdown of IGF2BP1 alone confirmed significant reductions of miR-prone target mRNAs. In contrast, the triple depletion resulted in significantly increased target mRNA abundance (Figure 5D-F in (Muller et al., 2018)) providing supportive evidence for the hypothesized shielding-mechanism by IGF2BP1. This was further reinforced by complementary studies indicating elevated AGO2-association to target mRNAs in IGF2BP1 deficient cells (Figure 5H in (Muller et al., 2018)). Aiming to determine whether the observed impairment of miRNA-dependent regulation is primarily due to IGF2BP1's direct coverage of miRNA binding sites (MBSs), we examined the regulation of the newly identified target mRNA SIRT1 mRNA in further detail. Luciferase reporter studies demonstrated that (a) IGF2BP1 promotes SIRT1 mRNA stability in a 3'UTR-dependent manner (Figure 6A and B in (Muller et al., 2018) and that (b) multiple MBSs overlap with IGF2BP1-binding sites identified by CLIP, such as miR-22 and miR-155 targeting sites (Figure 6C and D in (Muller et al., 2018)). Notably, IGF2BP2 inhibits miRNA-directed gene silencing in a similar manner, for instance by directly covering let-7 targeting sites of several mRNAs. (Degrauwe et al., 2016a).

At reduced miRNA levels, the IGF2BP1-dependent stabilization of target mRNAs was abolished, suggesting that the IGF2BP1-dependent regulation of target mRNAs is strictly miRNome-dependent. In order, the effects on target mRNAs LIN28B, sirtuin 1 (SIRT1), and mitogen-activated protein kinase 6 (MAPK6, also known as ERK3) were evaluated in let-7 expressing ovarian cancer-derived ES-2 and liver cancer-derived Huh-7 cells largely lacking let-7 miRNA expression, as revealed by small RNA sequencing. The target mRNAs were chosen because the let-7 miRNA family regulates LIN28B and MAPK6, but not SIRT1 (Boyerinas et al., 2008; Elkhadragy et al., 2017), which we confirmed in miTRAP analyses. MiTRAP (miRNA trapping by RNA *in vitro* affinity purification) enables the fast identification of miRNAs co-purifying with *in vitro* transcribed RNA in cell lysates (Braun et al., 2014). Interestingly, IGF2BP1 depletion reduced LIN28B and MAPK6 mRNA as well as protein exclusively in ES-2 cells. In contrast, SIRT1 expression was downregulated in both, ES-2 and Huh-7 cells (Figure 7 in (Muller et al., 2018)), indicating the strict miRNome-dependency for IGF2BP1-regulated target transcripts.

Finally, we evaluated if these newly identified target mRNAs, including MAPK6 and methaderin (MTDH) encode crucial downstream effectors of IGF2BP1-driven oncogenic phenotypes (Figure 8 and Supplementary Figure S8 in (Muller et al., 2018)). MTDH is a reported pro-oncogenic factor that has a variety of roles in the development of cancer and metastasis, respectively (Dhiman et al., 2019). *In vivo*, the deletion of MAPK6 inhibits KRAS G12C-driven NSCLC tumor development, while *in vitro*, MAPK6 kinase activity is necessary for the anchorage-independent growth of lung cancer cells (Bogucka et al., 2021). Several downstream effectors (particularly MTDH and MAPK6) substantially reduced all three oncogenic cell characteristics, including anoikis-resistance, spheroid growth, and invasion (Figure 8A-c in (Muller et al., 2018)). Most notably, none of the depletions of newly identified target mRNAs substantially improved any of the phenotypic outcomes studied. Furthermore, we showed the conserved co-expression of IGF2BP1 with target mRNAs in correlation analyses using TCGA expression data available for melanoma, ovarian, liver, and lung cancer (Figure 8D in (Muller et al., 2018)). This establishes a connection between conserved targets discovered *in cellulo* and primary malignancies, which may be relevant for evaluating treatment options targeting IGF2BP1-dependent effector networks in cancer.

Taken together, this study provides evidence that the oncogenic potential of IGF2BP1 is conserved across cancer cells and is largely facilitated by impairing miRISC-directed degradation of molecular determinants encoding oncogenic downstream effectors (**Figure 9**).
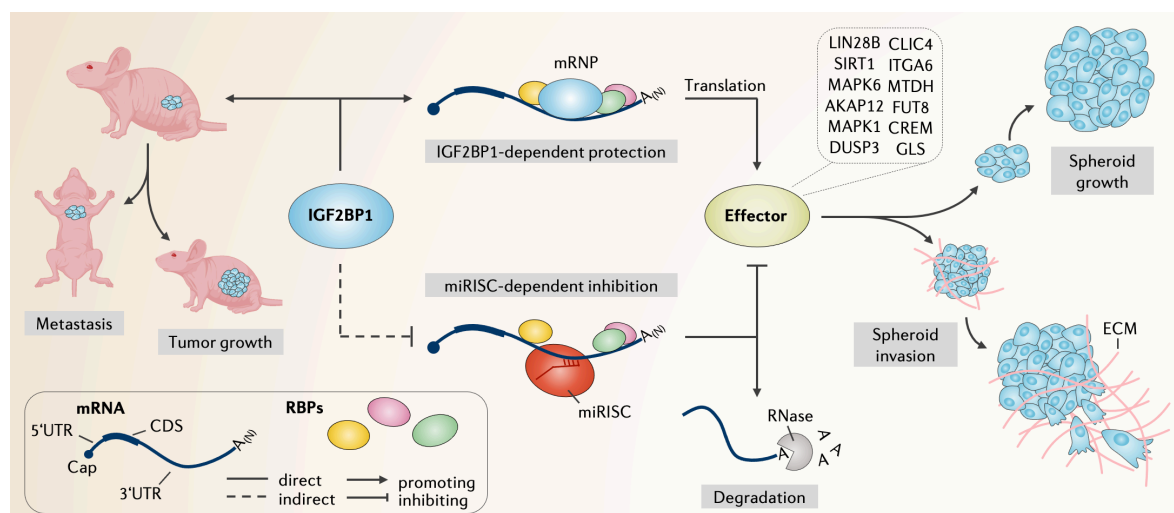

Figure 9 | **IGF2BP1 enhances an aggressive tumor cell phenotype by impairing miRNA-directed downregulation of oncogenic factors.** IGF2BP1 promotes tumor growth and metastasis of xenograft tumors by recruiting target mRNAs in protective mRNPs and inhibiting miRISC-dependent inhibition and degradation. Upon translation of indicated novel target mRNAs, effectors promote oncogenic cell properties, including spheroid growth and invasion. ECM – extracellular matrix

SRF and IGF2BP1 synergize in promoting gene expression in cancer (Müller et al., 2019)

The consistent phenotypic role of IGF2BP1 in tumor-derived cells implies that the protein exclusively promotes the expression of other oncogenic pathways, which are not or only weakly regulated by the other IGF2BP paralogues (Muller et al., 2018). Intrigued by the identified miRNome-dependent regulation, we aimed to discover common IGF2BP1 effector networks in cancer cells. Therefore, the IGF2BP1-dependent gene expression in Huh-7 (derived from liver cancer) and ES-2 (derived from ovarian cancer) cells was determined by RNA-sequencing following siRNA-mediated depletion. Among the many transcripts downregulated in both cancer cell lines (242) was the serum response factor (SRF) mRNA, which encodes a transcriptional regulator with a conserved role in controlling proliferative and invasive tumor cell properties (Miano, 2010). We validated the conserved control of SRF expression by IGF2BP1 in four other tumor cell lines originated from different primary cancers, including MV-3 (derived from melanoma) and A549 (derived from lung cancer). The reduction of IGF2BP1 reduced SRF mRNA and protein levels in all cell types using siRNA-mediated depletions or CRISPR/Cas9-mediated deletions, which have been restored in independent rescue experiments (Figure 1 and Supplementary Figure 2 in (Muller et al., 2019)). In the 3'UTR of the SRF mRNA, several IGF2BP1-CLIP hits were found, suggesting that this cis-element is involved in the conserved regulation, as observed previously for many IGF2BP1 targets (Busch et al., 2016; Muller et al., 2018). To confirm the regulation via the endogenous 3'UTR, the corresponding region in the SRF locus was genetically deleted in A549 cells using two sgRNAs to guide Cas9 nuclease to proximal and distal regions of the 3'UTR without impairing the native polyadenylation signal in the distal 3'UTR (Figure 2B and C in (Muller et al., 2019)). While the SRF expression was dramatically decreased in parental cells following IGF2BP1 depletion, the abundance of SRF mRNA and protein remained unchanged in SRF-Δ3'UTR cells depleted for IGF2BP1, indicating the strictly 3'UTR-dependent regulation of SRF by IGF2BP1 (Figure 2D and E in (Muller et al., 2019)).

In recent research, IGF2BPs have been identified as a distinct family of reader proteins that specifically recognize the RNA N^6-methyladenosine (m⁶A) modification, as shown for the MYC mRNA (Huang et al., 2018a). Huang et al. demonstrated that the m⁶A-modification increases IGF2BP1's RNA-binding affinity, reducing MYC transcript degradation, and consequently resulting in elevated MYC protein abundance in cancer cells. Intrigued by these findings, we hypothesized that IGF2BP1 increases the expression of SRF in an m⁶A-dependent way. This was supported by available m⁶A-RIP-seq data indicating modification of the SRF mRNA, especially in the proximal 3'UTR and distal regions of the coding sequence (Figure 2F and I in (Muller et al., 2019)). N^6-methyladenosine is the most common internal mRNA modification and is added to mRNAs by a multicomponent writer complex, primarily formed by the catalytic METTL3-METTL14 heterodimer (Zaccara et al., 2019). To determine if SRF expression is regulated by m⁶A-modifications, we co-depleted the methyltransferases METTL3 and METTL14 in parental and SRF-Δ3'UTR cells using an siRNA pool targeting both of them. In parental cells, the co-depletion of

METTL3/14 resulted in a substantial downregulation of the SRF protein. In contrast, SRF protein levels were unchanged in SRF-Δ3'UTR A549 cells upon the METTL3/14 co-depletion (Figure 2G and H in (Muller et al., 2019)). Notably, m⁶A-modified nucleotides coincide significantly with previously identified IGF2BP1-CLIP sites in HepG2 cells, and the METTL3/14 co-depletion substantially decreased the SRF mRNA's interaction with IGF2BP1, confirming an m⁶A-reader function as observed for MYC (Huang et al., 2018a). However, it remains controversial whether IGF2BP1 binds m⁶A directly (Zaccara et al., 2019). In pulldown experiments, IGF2BP proteins interact with YTHDF proteins, therefore suggesting a potentially indirect interaction with m⁶A-modified RNAs or an enhancement/stabilization of direct mRNA binding by additional, indirect m⁶A-dependent association (Youn et al., 2018). According to another study, IGF2BPs bind m⁶A-modified mRNAs due to an m⁶A-directed structural transition (Sun et al., 2019). IGF2BPs may bind to an alternatively folded RNA caused by the modification. Nonetheless, IGF2BPs may play essential roles in m⁶A RNA metabolism, but it will be necessary to determine whether they act as YTHDF protein binding partners or as direct modification readers.

As previously demonstrated, IGF2BPs primarily regulate mRNA turnover by preventing target mRNAs from miRNA-directed degradation. Interestingly, several studies identified SRF to be regulated by several miRNAs, including miR-22 (Xu et al., 2017a), miR-125b (Wang et al., 2021), and miR-214 (Li et al., 2020). In line with this, the reduction of IGF2BP1 resulted in an increased SRF mRNA degradation, which was attributed to enhanced miRNA-directed AGO2 interactions (Figure 3 in (Muller et al., 2019)). Small RNA-seq studies of miRNA expression indicated a conserved expression of miRNAs predicted to target the SRF-3'UTR exhibited in the four tumor cell lines where IGF2BP1-dependent regulation of SRF expression was identified. In conclusion, our data show that IGF2BP1 inhibits the downregulation of SRF expression by antagonizing miRNAs in an m⁶A-dependent manner conserved across cancer cells derived from different primary cancers (**Figure 10a**).

Of note, CLIP hits in the 3'UTR of the SRF mRNA have been identified for all three IGF2BPs. However, we demonstrated that only IGF2BP1 depletion impairs SRF expression, showing a tight paralogue-specificity (Supplementary Figure 4A-C in (Muller et al., 2019)), and supporting our previous findings that IGF2BPs serve distinct function in cancer cells (Muller et al., 2018). Furthermore, IGF2BP1 associates with other RBPs, such as ELAVL1, and recruits target mRNAs in cytoplasmic mRNPs (Wachter et al., 2013). ELAVL1 is a known regulator of mRNA turnover and serves pro-oncogenic roles in a variety of cancers (Wang et al., 2013). So, it was tempting to hypothesize that both proteins work together to regulate SRF expression via antagonizing miRNAs. In A549 cells, IGF2BP1 and ELAVL1 were side-by-side depleted using siRNA pools (Supplementary Figure 5A in (Muller et al., 2019)). While the loss of IGF2BP1 lowered SRF protein levels, ELAVL1 depletion had little effect, suggesting that IGF2BP1 regulates SRF expression independently of ELAVL1 or the other IGF2BP paralogues.

SRF regulates gene expression in conjunction with cofactors, such as TCFs (ELK1, 3, and 4) and MRTFs (MRTFA and MRTFB). This transcriptional regulation regulates cell proliferation, contractility, and pro-invasive behavior (Gualdrini et al., 2016). In cancer cells, IGF2BP1 depletion

impairs SRF/TCF- and SRF/MRTF-dependent transcriptional control by decreasing cellular SRF abundance, but not of the cofactors. The activity of SRF/TCF- and SRF/MRTF-dependent luciferase reports was assessed by depleting IGF2BP1 or SRF. Both reporters' activities have been significantly reduced, implying a disturbed SRF transcriptional activity due to the lower expression. In accordance with the reported cellular functions, the depletion of both factors significantly inhibited the growth and invasion of ES-2-derived spheroids suggesting a putative synergy in promoting oncogenic cell properties (Figure 4 in (Muller et al., 2019).

In view of IGF2BP1's pleotropic RNA-binding properties (Conway et al., 2016; Hafner et al., 2010; Muller et al., 2018), we speculated that IGF2BP1 increases not only transcriptional activity by elevating SRF abundance, but further amplifies SRF's transcriptional output by inhibiting the degradation of SRF-driven mRNAs. The study of IGF2BP1-overexpressing cells depleted for SRF revealed increased spheroid proliferation in an RNA-binding dependent manner, as revealed by exploring an RNA-binding deficient mutant (Wachter et al., 2013). Thus, IGF2BP1 partially rescued reduced transcriptional output by SRF, by stabilizing the respective mRNAs. Knocking down either IGF2BP1 or SRF resulted in many overlapping up- (489) or down-regulated (539) genes. Candidates for co-regulation by IGF2BP1 and SRF in cancer were further evaluated by investigating the correlation of the respective mRNAs with IGF2BP1 and SRF transcript abundance across the four primary cancers linked to the analyzed cancer cell lines: Ovarian, liver, lung cancer, and melanoma. We identified a subset of 35 SRF/IGF2BP1-dependent transcripts (Figure 5C-F in (Muller et al., 2019)), that show a) reduced expression upon IGF2BP1 and SRF depletion, b) positive correlation with IGF2BP1 and SRF expression across four primary cancers and c) IGF2BP1-binding to the respective 3'UTR (revealed by CLIP) and SRF-binding to the respective promoter region (revealed by ChIP – chromatin immunopreciptation). Strikingly, the expression of these transcripts is correlated with a poor overall survival probability in several cancers (Figure 6g in (Muller et al., 2019)). Collectively, this provides strong evidence that SRF/IGF2BP1-enhanced gene expression serves as a conserved driver of carcinogenesis (**Figure 10b**). Exemplary, we demonstrated this for two genes FOXK1 and PDLIM7, which are driven by SRF at the transcriptional level and enhanced by IGF2BP1 post-transcriptionally due to impaired mRNA decay (Figures 5,6 and Supplementary Figure 7 in (Muller et al., 2019). Both factors promoted the spheroid growth of ES-2 cells and were correlated with the poor clinical outcome of cancer patients.

In conclusion, these data imply that SRF/IGF2BP1-dependent gene expression may serve as a potential therapeutic target in cancer treatment, especially in the view that either IGF2BP1 as well as SRF have been shown to drive metastasis (Hamilton et al., 2013; Medjkane et al., 2009; Muller et al., 2018). While inhibiting the ubiquitously expressed SRF is expected to have a wide range of unfavorable side effects, inhibiting IGF2BP1, which has an oncofetal expression pattern, may be beneficial. This provides a novel strategy for inhibiting oncogenic gene expression, including genes whose expression is increased by SRF/IGF2BP1 co-regulation (summarized in **Figure 10a, b**).
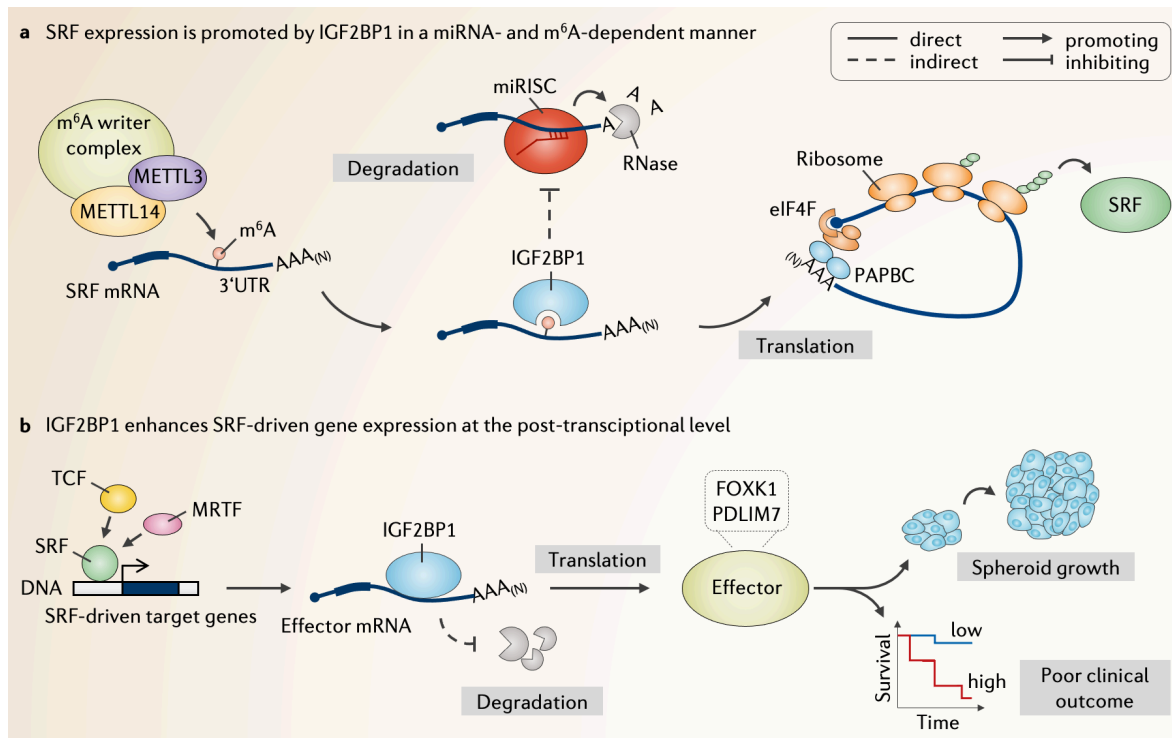
Figure 10 | **IGF2BP1 promotes SRF-dependent transcription in cancer. a,** SRF expression is promoted by IGF2BP1 in a miRNA and m^{6}A-dependent manner. The m^{6}A writer complex, which comprises core methyltransferases METTL3 and METTL14, adds m^{6}A modification in the 3'UTR of the SRF mRNA. The RNA-binding of IGF2BP1 is stimulated by m^{6}A-modification fostering the inhibition of miRISC-directed degradation and promoting mRNA translation. **b,** IGF2BP1 enhances SRF-driven gene expression at the post-transcriptional level. SRF drives the transcription of target genes via interactions with cofactors, including TCFs and MRTFs. IGF2BP1 binds SRF-driven effector-encoding mRNAs, preventing degradation, and promoting translation into proteins. Effectors, including FOXK1 and PDLIM7, enhance spheroid growth and correlate with poor clinical outcome of cancer patients.

IGF2BP1 is a druggable post-transcriptional enhancer of E2F and E2F-driven genes (Müller et al., 2020)

Among the IGF2BPs, only IGF2BP1 exhibits a high degree of conservation of oncogenic potential in cancer cell lines (Muller et al., 2018; Muller et al., 2019). This oncogenic role was largely led back to the stabilization of the MYC mRNA (Gutschner et al., 2014; Huang et al., 2018a). However, in most cancers, IGF2BP1 and MYC mRNA levels appear to be only moderately correlated, indicating the presence of additional underlying effector pathways, such as the previously described SRF-IGF2BP1-axis (Muller et al., 2019).

In accordance with tumor-promoting functions of IGF2BP1, a meta-analysis of all 33 TCGA-provided cancer transcriptome data sets, which included 9282 tumor samples, revealed that elevated IGF2BP1 expression is significantly linked with a decreased overall survival probability but not correlated with MYC expression (Figure 1A und Supplementary Figure S1A, C, D in (Muller et al., 2020)). The synthesis of IGF2BP1 was found to be significantly increased in the great majority of cancers, including liver, lung, ovarian, and pancreatic cancer, as well as melanoma

compared to respective normal tissues. This analysis corroborates prior reports of oncofetal expression (Bell et al., 2013). Accordingly, we hypothesized that IGF2BP1 potentially acts via highly conserved tumor-promoting pathways next to stimulating MYC- and/or SRF-driven gene expression. To this end, the IGF2BP1-associated expression of protein-coding genes was examined in the five malignancies mentioned above to identify major potential effectors and associated pathways. Gene set enrichment analyses (GSEA) of genes ordered by their median correlation with IGF2BP1 expression revealed a remarkable and conserved enrichment of positively correlated genes in the E2F Targets cancer hallmark and KEGG (Kyoto Encyclopedia of Genes and Genomes) Cell Cycle pathway (Figure 1C and E in (Muller et al., 2020)), which has been confirmed in a recent meta-analysis (Glass et al., 2021). Regulating the rate of cell division and cycle is important for development, stem cell maintenance, tissue homeostasis, and cancer, respectively (Weber et al., 2014). The eukaryotic cell cycle includes four phases: gap 1 (G1), DNA synthesis (S), gap 2 (G2), and mitosis (M), which are controlled by intracellular checkpoints. During G1 phase, cells either start a cell division program or enter a dormant G0 state (Liu et al., 2019). For instance, human embryonic stem cells rapidly proliferate and display a short G1 phase and fast transition to S phase (Neganova et al., 2009). The primary transcriptional mechanism controlling G1/S cell cycle progression and proliferation is the CDK-RB-E2F axis (Kent and Leone, 2019). In a typical cell cycle model, cyclin D 4 or 6 (CDK4/6) complexes phosphorylate and functionally inactivate the retinoblastoma protein (RB1). This activates or deactivates E2F transcription factors, which transactivate genes essential for S phase entrance and progression (Liu et al., 2019). The E2F transcription factor family consists of eight members from distinct genes encoding transcriptional activators (E2F1-3) and repressors (E2F4-8). Alterations in one or more members occur in almost all cancers, resulting in increased oncogenic E2F activity and uncontrolled cell cycle transition and proliferation (Kent and Leone, 2019). Cell cycle progression studies revealed that IGF2BP1 knockdown as well as knockout increased the proportion of cells in the G1 phase resulting in reduced cell and spheroid proliferation in a panel of five tumor cell lines, derived from the five aforementioned primary cancers (PANC-1, ES-2, HepG2, MV-3 and A549). Furthermore, the knockout of IGF2BP1 also impaired tumor growth of A549-derived xenografts in nude mice (Figure 2 in (Muller et al., 2020)). Intrigued by the high proportion of cells in G1, we hypothesized that IGF2BP1 also affects the general length of this phase and endorses a proliferative stem-cell like phenotype. Therefore, we used the fluorescent ubiquitination-based cell cycle indicator (FUCCI) system to analyze the duration of cell cycle phases. The FUCCI system uses two components of the eukaryotic DNA replication control system, chromatin licensing and DNA replication factor 1 (Cdt1) and geminin (Zielke and Edgar, 2015). Cdt1 protein peaks in G1 phase immediately before DNA replication begins and rapidly decreases in S phase. On the other hand, geminin levels are high in S and G2, but low in late mitosis and G1. In the respective phase, the E3 ubiquitin ligases APC/C^{Cdh1} (targeting geminin in G1) and SCF^{Skp2} (targeting Cdt1 in S and G2) reduce sequentially Cdt1 and Geminin expression. The FUCCI method uses fluorescent proteins fused to Cdt1 and geminin degrons to monitor the cell cycle phase. Of note, a time-resolved study using the FUCCI system showed that the depletion of IGF2BP1 prolonged the G1 phase about 2-

fold (Figure 2E and F in (Muller et al., 2020)). Taken together, we identified IGF2BP1 as a conserved G1/S-transition regulator in cancer cells, shortening G1 phase, promoting tumor cell proliferation *in vitro* and tumor development *in vivo*.

The IGF2BP1-dependent G1/S-transition control was further investigated in all five tumor cell lines using RNA-sequencing to discover conserved mRNAs that encode underlying downstream effectors. We ranked all protein-coding genes by their median or cell-specific expression fold change and performed GSEA. This analysis revealed a significant downregulation of the hallmark pathway E2F Targets and the KEGG Cell Cycle pathway. Surprisingly, substantial reductions of MYC mRNA expression were only found in HepG2 and MV3 cells. However, these findings pointed to IGF2BP1 playing a critical role in regulating E2F-driven transcription. In agreement, IGF2BP1 depletion and deletion substantially reduced E2F1-3 mRNA and protein expressions in almost all cancer cells studied (Figure 3 and Supplementary Figure S3 in (Muller et al., 2020)).

The primary and conserved role of IGF2BP1 is based on the 3'UTR-, miRNA-, and m6A-dependent control of mRNA turnover, as indicated before. So far, the only reported RBPs shown to control E2F expression were pumilio proteins (PUM1 and PUM2). These were suggested to promote the miRNA-directed downregulation of E2F3 (Kent and Leone, 2019; Miles et al., 2012). Therefore, we investigated the regulation of the E2F1 mRNA in detail. Reminiscent of findings reported for IGF2BP1 controlling SRF expression, we could demonstrate that the depletion of IGF2BP1 resulted in: 1) a decreased E2F1 mRNA half-life; 2) a downregulation of E2F1-3'UTR containing luciferase reporters; 3) an increased AGO2-association of the E2F1 mRNA; 4) these regulatory roles of IGF2BP1 were abolished when deleting the bulk E2F1 3'UTR-encoding region by CRSPR/Cas9 genome engineering (Figure 4 in (Muller et al., 2020)). Furthermore, the co-depletion of METTL3 and 14 reduced the association of IGF2BP1 with the E2F1 mRNA leading to decreased expressions of mRNA and protein. In line with these findings, METTL3/14-co-depletion led to an accumulation of cells in the G1, resulting in impaired cell proliferation and spheroid growth (Figure 5 in (Muller et al., 2020)).

In view of the many parallels of IGF2BP1-directed control of E2F1 and SRF, we speculated that IGF2BP1 also stabilizes many E2F-downstream mRNAs, and found that IGF2BP1 directly stabilized E2F-driven transcripts that encode oncogenic effectors like MKI67, DSCC1, BUB1B, and GINS1, to name a few candidates of the IGF2BP1/E2F-dependent network (Figure 6 in (Muller et al., 2020)). Most notably, these results unraveled, IGF2BP1 is the first RNA-binding protein serving as a conserved, post-transcriptional super-enhancer of E2F1-3 as well as E2F-driven effector mRNAs. With the IGF2BP1-inhibitor BTYNB available, we aimed to 1) test E2F-IGF2BP-driven gene expression and 2) evaluate the therapeutic target potential of IGF2BP1. BTYNB is a small molecule inhibitor (Molecular weight: 309.18 Da) of the protein, was recently discovered in a high-throughput screen (Mahapatra et al., 2017). *In vitro*, BTYNB inhibited the IGF2BP1 interaction with MYC RNA fragments and reduced the proliferation of different tumor cells, suggesting for the first time the druggability of IGF2BP1 in principle (Mahapatra et al., 2017). Accordingly, we speculated that this lead compound also interferes with E2F/IGF2BP1-driven gene expression.

BTYNB exposure inhibited the cell proliferation of all five investigated cell lines at low μM concentrations and interfered with IGF2BP1-E2F1 mRNA association in cells (Figure 7A, B and Supplementary Figure S8 in (Muller et al., 2020)). Furthermore, BTYNB consistently reduced the activity of E2F1 3'UTR luciferase reporters and lowered E2F1 expression at the protein and mRNA levels in a conserved manner across cancer cell lines. Of note, BTYNB also interfered with the IGF2BP1/E2F downstream effector transcripts (DSCC1, BUB1B, MKI67, and GINS1) that showed significantly reduced associations to IGF2BP1 and strongly decreased steady-state mRNA levels (Figure 7F and Supplementary Figure S8 in (Muller et al., 2020)). However, BTYNB also reduced the association of IGF2BP1 with the MYC mRNA but had negligible effects on MYC expression in the cells tested. This provides strong evidence that that MYC represents a context-dependent IGF2BP1 effector, whereas E2F1 most appears highly conserved. Aiming to test the therapeutic target potential of IGF2BP1 and therapeutic suitability of the lead compound BTYNB, we demonstrated substantial suppression of subcutaneous tumor growth and peritoneal spread of iRFP-labeled ovarian cancer ES-2 cells by BTYNB (Figure 7G, H, and Supplementary Figure S8 in (Muller et al., 2020)). Of note, our studies also provide evidence that a combination therapy with IGF2BP1-directed inhibition may be beneficial for cancer treatment. Palbociclib is a potent FDA-approved cell cycle inhibitor that targets essential E2F-activating kinases, highly selective to CDK4 and CDK6 and used for the treatment of hormone-receptor (HR)-positive breast cancers (Laderian and Fojo, 2017). By targeting E2F-activating kinases, Palbociclib inhibited cell proliferation in synergy with BTYNB at low doses (Figure 7I in (Muller et al., 2020)).
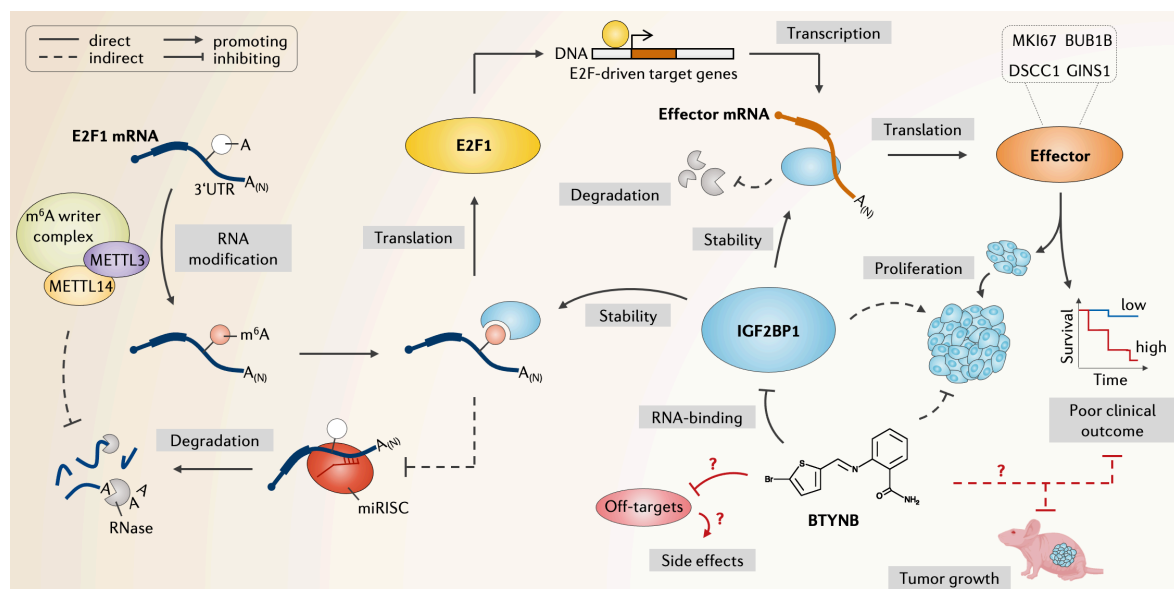

Figure 11 | **IGF2BP1 is a druggable, post-transcriptional enhancer of E2F-driven gene expression in cancer.** The m^{6}A writer complex adds m^{6}A modification to the 3'UTR of the E2F1 mRNA. IGF2BP1 binds to the modified mRNA, preventing miRISC degradation and increasing protein translation. Upon E2F-driven transcription of effector-encoding mRNAs, IGF2BP1 protects the respective mRNAs from degradation, promoting translation into proteins. Effectors such as MKI67, DSCC1, BUB1B, and GINS1 promote spheroid growth and correlate with the prognosis of cancer patients. The small molecule BTYNB inhibits the binding capacity of IGF2BP1, thereby indirectly reducing cell proliferation. If and how BTYNB directly interferes with off-targets, that cause side-effects, or the potential benefit for cancer treatment is indicated in red lines.

In summary, our studies demonstrated that IGF2BP1 is a druggable, m⁶A- and miRNA-dependent post-transcriptional super-enhancer of E2F transcription factors and the E2F-driven hallmark pathway, promoting the G1/S transition, shortening G1 length and resulting in severely increased proliferation and stem-cell like phenotype of cancer cells (**Figure 11**).

Future Perspectives – IGF2BP1-directed inhibition in cancer treatment

As stated in detail above, RBPs can influence the overall progression of various cancer types by controlling the expression of target mRNAs at the post-transcriptional level. This includes characteristics such as cancer cell proliferation, apoptosis, invasion, and metastasis, respectively. Alterations in RNA metabolism caused by dysregulated RBPs can result in transcriptome-wide changes. Due to the broad range of cancer pathways that RBPs affect, they become fascinating targets for cancer therapy. Recent years have seen an increase in studies targeting formerly 'undruggable' non-catalytic RBPs using a variety of approaches and classes of inhibitory molecules, such as inhibitory peptides, anti-sense oligonucleotides (ASO), siRNAs, or small molecule compounds (Mohibi et al., 2019).

Small molecules are by far the most often utilized type of inhibitors to target the function of pro-oncogenic factors in cancer treatment. Early drug discovery principles include initial target identification and validation, high throughput screening and lead identification, lead optimization, and finally the selection of a candidate compound for clinical development (Hughes et al., 2011). Several RBPs emerged as primary therapeutic targets during the initial target selection and validation process, including the aberrantly expressed or localized ELAVL1. Small molecule compounds, such as MS-444, okicenone, dehydromutactin, dihydrotanshinone-I, azaphilone-9 (Aza-9), CMLD-2 and KH-3 have been identified as potent ELAVL1 inhibitors that decrease its RNA-binding activity. These inhibitors also show anti-cancer effects in both in vitro and in vivo models without systemic toxicity (Allegri et al., 2019; Filippova et al., 2017; Kaur et al., 2017; Lal et al., 2017; Lang et al., 2017; Meisner et al., 2007; Wu et al., 2020). However, oncofetal RBPs, which are distinguished by their high abundance during embryonic development and *de novo* synthesis in cancer but are not expressed in adult healthy tissue, serve as biomarkers and *bona fide* therapeutic targets. The expression of these RBPs often correlates with poor clinical outcome of patients. While targeting ubiquitously expressed RBPs likely poses various and undesired side-effects in healthy tissue, the targeting of oncofetal RBPs using specific small molecule inhibitors may be advantageous. For instance, oncofetal RBPs with reported oncogenic roles in cancer include MSI1, LIN28B, and IGF2BP1, respectively.

The oncogenic potential of IGF2BP1 is conserved across solid cancers, according to clinical data as well as studies in cancer cell and xenograft models. As shown in detail, IGF2BP1 regulates mRNA turnover in a 3'UTR-, miRNA- and m⁶A-dependent manner, promoting cancer hallmarks, such as proliferation and metastasis. We revealed that IGF2BP1 is a post-transcriptional enhancer of SRF- and E2F-driven effector pathways. IGF2BP1-directed inhibition, essentially by

the small molecule compound BTYNB, has shown promise in both cellular and mouse cancer models, respectively. The conserved functions of IGF2BP1 and the inhibitory potency of BTYNB demonstrated here suggest that IGF2BP1 has a broad therapeutic potential in the treatment of solid cancers. Our findings emphasize BTYNB as a suitable lead compound for the therapeutic inhibition of IGF2BP1's tumor-promoting and RNA-binding-dependent functions. However, several issues and open questions remain unresolved (also indicated in **Figure 11**) and warrant additional research: 1) What are direct BTYNB off-targets, 2) What are potential BTYNB side effects, 3) Is BTYNB an effective inhibitor *in vivo*, 4) Which other combination therapies synergize with BTYNB and 5) What are potential BTYNB lead optimizations to improve the potency and selectivity? – The present data clearly recommends that further preclinical and presumably clinical assessment and optimization of IGF2BP1-directed inhibitors in cancer treatment should be expedited in exciting following studies.

IV PUBLICATIONS

Article: IGF2BP1 enhances an aggressive tumor cell phenotype by impairing miRNA-mediated downregulation of oncogenic factors

IGF2BP1 enhances an aggressive tumor cell phenotype by impairing miRNA-directed downregulation of oncogenic factors

Simon Müller[†], Nadine Bley[†], Markus Glaß[†], Bianca Busch, Vanessa Rousseau, Danny Misiak, Tommy Fuchs, Marcell Lederer and Stefan Hüttelmaier[*]

Institute of Molecular Medicine, Section for Molecular Cell Biology, Faculty of Medicine, Martin Luther University Halle-Wittenberg, Kurt-Mothes-Str. 3a, 06120 Halle, Germany

ABSTRACT

The oncofetal IGF2 mRNA binding proteins (IGF2BPs) are upregulated in most cancers but their paralogue-specific roles in tumor cells remain poorly understood. In a panel of five cancer-derived cell lines, IGF2BP1 shows highly conserved oncogenic potential. Consistently, the deletion of IGF2BP1 impairs the growth and metastasis of ovarian cancer-derived cells in nude mice. Gene expression analyses in ovarian cancer-derived cells reveal that the knockdown of IGF2BPs is associated with the downregulation of mRNAs that are prone to miRNA regulation. All three IGF2BPs preferentially associate upstream of miRNA binding sites (MBSs) in the 3′UTR of mRNAs. The downregulation of mRNAs co-regulated by miRNAs and IGF2BP1 is abrogated at low miRNA abundance or when miRNAs are depleted. IGF2BP1 associates with these target mRNAs in RISC-free complexes and its deletion enhances their association with AGO2. The knockdown of most miRNA-regulated target mRNAs of IGF2BP1 impairs tumor cell properties. In four primary cancers, elevated synthesis of these target mRNAs is largely associated with upregulated IGF2BP1 mRNA levels. In ovarian cancer, the enhanced expression of IGF2BP1 and most of its miRNA-controlled target mRNAs is associated with poor prognosis. In conclusion, these findings indicate that IGF2BP1 enhances an aggressive tumor cell phenotype by antagonizing miRNA-impaired gene expression.

INTRODUCTION

MicroRNAs (miRNAs, miRs) are highly conserved and abundant small non-coding RNAs inhibiting gene expression by inducing target mRNA degradation and/or the inhibition of translation (1). They influence virtually all cell functions and play vital roles in controlling development and differentiation. Deregulated miRNA expression and/or function has been reported in essentially all human diseases including cancer where miRNAs serve oncogenic as well as tumor suppressive roles (2,3). One prominent example is the let-7 miRNA family. This miRNA family is highly conserved and acts in a tumor suppressive manner by interfering with the synthesis of oncogenic factors including H/KRAS, MYC/N, HMGA2 and LIN28A/B to name a few (4–8). However, although downregulated in most cancers including ovarian carcinomas (9), let-7 miR-NAs still sum up to one of the most abundant miRNA families in most cancer-derived cells. This strongly suggests mechanisms impairing miRNA action in cancer. One obvious way of escaping miRNA-directed regulation is the 'deletion' of miRNA binding sites (MBSs) by shortening 3′UTRs via alternative polyadenylation. This has been reported for upregulated HMGA2 and IGF2BP1 expression in aggressive cancers (10,11). However, the longest and thus 'miRNA-prone' 3′UTRs of mRNAs like IGF2BP1 are maintained in some aggressive cancers (12). Alternatively, miRNAs may be 'sponged' and thus sequestered by the upregulated expression of mRNAs comprising MBSs for tumor-suppressive miRNAs. This was proposed for neuroblastoma where the amplification of the MYCN gene was suggested to impair let-7 activity (13). However, how the miRNA-sequestering transcripts escape miRNA-directed degradation allowing the sustained synthesis of oncogenic factors like HMGA2 or MYCs remains controversial. Finally, some RNA-binding proteins (RBPs) have been reported to either promote or impair the miRNA-directed degradation of target mRNAs (14).

[*]To whom correspondence should be addressed. Tel: +49 345 5573959; Fax: +49 345 557126; Email: stefan.huettelmaier@medizin.uni-halle.de
[†]The authors wish it to be known that, in their opinion, the first three authors should be regarded as Joint First Authors.

The oncofetal IGF2 mRNA binding proteins (IGF2BPs; alias: VICKZ, CRD-BP, IMPs or ZBPs) present an oncogenic family of RBPs reported to control mRNA transport, translation and turnover during development and in cancer cells (15). IGF2BP1 and 3 are *bona fide* oncofetal proteins with high expression during embryogenesis and *de novo* synthesis or significant upregulation in various tumors (15,16). IGF2BP2 is the only family member with ubiquitous expression in the adult organism (15). All three IGF2BPs were shown to promote an 'aggressive' tumor cell phenotype. IGF2BP1 and 3 enhance the viability, growth, migration, invasion and/or metastatic potential of tumor-derived cells *in vitro* and *in vivo* (17–22). Both these IGF2BPs are frequently co-upregulated in cancer suggesting shared upstream effectors, presumably including the oncogene MYC, promoting their expression (23). Elevated expression of IGF2BPs has also been reported in progenitor cells and all three IGF2BPs were suggested to sustain stem-cell properties in non-transformed as well as cancer cells (24–26).

Recent reports indicate that the loss of DICER induces a partially irreversible epigenetic shift inducing a pan-cancer gene expression signature including all three IGF2BPs (27). In the respective study, the loss of all three IGF2BPs substantially interfered with the 'oncogenic potential' of DICER-deleted and re-expressing cells. This suggests that IGF2BPs are key modulators of miRNA-controlled gene expression in cancer. Consistently, IGF2BP1 antagonizes the tumor suppressive action of the let-7 family in ovarian cancer-derived cells via a self-sustaining oncogenic triangle comprising IGF2BP1, HMGA2 and LIN28B (12). IGF2BP2 was proposed to support glioblastoma stem cell maintenance by impairing the inhibition of gene expression by let-7 miRNAs, and IGF2BP3 was shown to interfere with the downregulation of HMGA2 by let-7 miRNAs (24,28). These studies suggested that all three IGF2BPs promote tumorigenesis by interfering with the miRNA-directed degradation of oncogene-encoding mRNAs in cancer cells.

Starting from ovarian cancer in which elevated expression of all three IGF2BPs was reported to promote tumorigenesis (17,29,30), we analyzed the phenotypic roles of IGF2BPs in five tumor cell lines derived from distinct solid cancers. These studies revealed that IGF2BP1 has the most conserved 'oncogenic potential' of all three IGF2BPs. The protein enhances an 'aggressive' tumor cell phenotype largely by impairing the miRNA-directed downregulation of mRNAs.

MATERIALS AND METHODS

Plasmids and cloning

Cloning strategies including vectors, oligonucleotides used for PCR and restrictions sites are summarized in Supplementary Table T5. All constructs were validated by sequencing.

RIP, RNA isolation and RT-qPCR

For RNA co-immunoprecipitations (RIP) ES-2 cell extracts (1×10^7 per condition) were prepared on ice using RIP buffer (10 mM Hepes, 150 mM KCl, 5 mM MgCl$_2$, 0.5% NP40, pH 7.0). Cleared extracts were incubated with anti-GFP antibodies and Protein G Dynabeads (Life Technologies) for 30 min at room temperature (RT). After 3 washing steps with RIP buffer, protein-RNA complexes were eluted by SDS. Protein isolation was analyzed by Western blotting. Co-purified RNA was extracted using TRIZOL and analyzed by RT-qPCR analyses as described previously (12). Primers are summarized in Supplementary Table T5.

miTRAP experiments

miTRAP experiments using 3′UTRs of LIN28B, SIRT1 and MAPK6 or MS2 control RNA were essentially performed as described recently (31).

Northern and Western blotting

Northern blotting of small RNAs and semi-quantitative infrared Western blotting were performed as recently described (12). Probes and antibodies are summarized in Supplementary Tables T5 and T7, respectively.

Luciferase reporter assays

Luciferase reporter analyses were performed essentially as previously described (12). Luciferase activity was determined 48 h post-transfection of reporters. Reporters containing a minimal vector-encoded 3′UTR (MCS) served as normalization controls.

RNA sequencing and differential gene expression

Libraries for RNA-sequencing (RNA-seq) were essentially prepared as recently described (31,32). Sequencing was performed on an Illumina HighScan-SQ (IZKF, Leipzig, Germany). Low quality read ends as well as remaining parts of sequencing adapters were clipped off using Cutadapt (V 1.6). For total and small RNA-seq analyses reads were aligned to the human genome (UCSC GRCh37/hg19) using TopHat2 (V 2.0.13; (33)) or Bowtie2 (V 2.2.4; (34)), respectively. FeatureCounts (V 1.4.6; (35)) was used for summarizing gene-mapped reads. Ensembl (GRCh37.75; (36)) or miRBase (V 20; (37)) were used for annotations (see Supplementary Table T1A). Differential gene expression (DE) was determined by edgeR (V 3.12; (38)) using TMM normalization, essentially as described previously ((32); see Supplementary Table T1B).

MicroRNA–target predictions

MultiMiR (V 2.1.1; (39)) was used for the analysis of transcript-specific miRNA-targeting (Supplementary Table T3).

CLIP data analysis and CLIP scores

Publically available data of significantly enriched CLIP peaks for the listed proteins were derived from indicated studies: a) IGF2BP1-3 (40–42); AGO2 (43–45); c) AGO1-4 (40). Data were obtained from ENCODE, NCBI GEO, CLIPdb and doRiNA. Peak coordinates were mapped to

mRNAs as well as intronic regions of all annotated genes (RefSeq, hg19). To generate the cis-element (5′UTR, CDS or 3′UTR) sorted CLIP score, the number of datasets reporting CLIP hits in the respective element of a mRNA were summed up. For IGF2BP1 (CLIP score range: 0–8) the following data were considered: 1 PAR-CLIP (HEK293), 2 eCLIP (hESCs), 2 eCLIP (HepG2), 2 eCLIP (K562) and 1 iCLIP (K562). For IGF2BP2 (CLIP score range: 0–7) the following data were considered: 2 eCLIP (hESCs), 2 eCLIP (K562), 2 iCLIP (K562) and 1 PAR-CLIP (HEK293). For IGF2BP3 (CLIP score range: 0–6) the following data were considered: 1 PAR-CLIP (HEK293), 1 eCLIP (hESCs), 2 eCLIP (HepG2) and 2 iCLIP (K562). For determining AGO (1–4) CLIP scores in the 3′UTR of indicated mRNAs (CLIP score range: 0–6) the following PAR-CLIP data were considered: HEK293 (3), BC-1 (2) and LCL-35 (1) cells.

Kaplan-Meier and gene expression correlation analyses

Hazardous ratios (HR) for indicated genes and tumor cohorts of serous ovarian carcinoma were determined by the Kaplan-Meier (KM) plotter online tool using 'best cutoff analyses' (www.kmplot.com). Gene expression correlations were analyzed via the R2 platform (http://hgserver1.amc.nl/cgi-bin/r2/main.cgi) using the indicated TCGA-provided datasets.

GAEA and GSEA analyses

Gene annotation enrichment analyses (GAEA) of differentially up- or downregulated transcripts (Supplementary Table T1B) were performed using the DAVID functional annotation chart 6.8 (https://david.ncifcrf.gov/home.jsp) to identify enriched GO-terms for biological processes (Supplementary Table T1D). Only GO terms containing 10 or more genes were considered. Gene set enrichment analyses (GSEA) were performed with the GSEA-Software (46) using a list of all protein coding genes ranked according to fold changes upon knockdown of the respective IGF2BP.

Cell culture and transfection

Cells were cultured and transfected essentially as described recently (12). SiRNAs used are summarized in Supplementary Table T6. For the depletion of DICER1/DROSHA cells were re-transfected after 3 days and harvested 6 days after the initial transfection.

Spheroid growth, invasion and self-renewal assay

The analyses of 3D spheroid growth and anoikis-resistance were performed as recently described (12). For spheroid invasion assays, 1×10^3 cells (in a 96-well) were used in a Cultrex spheroid invasion assay (Trevigen) according to manufacturer's protocol using DMEM (10% FBS), as previously described (47). Invasion was monitored by bright-field microscopy (Nikon TE-2000-E). The invasion index was determined by the perimeter of the invasive front normalized to sphere body perimeters.

3D-Migration and microscopy

Analysis of single cell 3D migration and microscopy was performed as previously described (12). ES-2 cells were embedded in 1.8 mg/ml or 4 mg/ml Collagen I (Merck Millipore) gel as indicated to generate matrices with varying 'stiffness'.

Animal handling and xenograft assay

Animals were handled according to the guidelines of the Martin Luther University. Permission was granted by a local ethical review committee. For subcutaneous xenograft assays 1×10^5 iRFP-labeled ES-2 cells (stably transduced using iRFP encoding lentiviruses; (22)) were harvested in media supplemented with 50% (v/v) matrigel (Sigma) and injected into the left flank of six week old female immunodeficient athymic FOXN1$^{nu/nu}$ nude mice (Charles River). Mice were held with access to chlorophyll-free food to avoid background noise in iRFP image acquisition. Tumor growth and volume were monitored and measured as recently described (22). For monitoring metastasis, subcutaneous tumors of ketamine/xylazine-anaesthetized mice were removed by surgery 16 days post-injection before the tumor burden exceeded the termination criterion (tumor diameter of 1.5 cm). Primary tumors were imaged and the weight was measured. Resection of primary tumors was validated by iRFP imaging post-surgery. Metastasis formation was monitored by iRFP imaging. Mice were sacrificed when termination criteria were reached or 10 weeks post-surgery without metastasis formation according to ethical guidelines.

RESULTS

IGF2BP paralogues serve distinct roles in ovarian cancer-derived cells

Independent studies reported that the elevated expression of all three human IGF2BP paralogues (IGF2BP1-3) is associated with poor prognosis in ovarian cancer. This was re-evaluated by Kaplan-Meier analyses in 1232 serous ovarian carcinomas using KM plotter combining available datasets to a multi-centric study (48). Elevated IGF2BP1 and 3 mRNA expression was significantly associated with reduced overall survival (OS) supporting previous findings (Supplementary Figure S1A (17,29)). Significant association of upregulated mRNA expression with reduced progression free survival (PFS) probability was only observed for IGF2BP1. Surprisingly, the expression of IGF2BP3 was significantly associated with a better PFS prognosis. This trend was even enhanced when analyzing p53-mutated serous ovarian carcinomas. For ovarian cancer, these observations suggested that: (a) IGF2BPs are associated with partially distinct patient prognosis; (b) IGF2BP1 and 3 synthesis is associated with a poor prognosis irrespective of disease progression (OS); c) IGF2BP1 synthesis is associated with a higher risk of disease progression (PFS), in particular in p53-mutated tumors.

To test if IGF2BP paralogues also serve distinct roles in ovarian cancer-derived cells, five tumor cell properties collectively referred to as 'oncogenic tumor cell properties' were monitored upon the paralogue-specific depletion

of IGF2BPs using siRNA pools (Figure 1A and B). ES-2 cells were used for these studies since they are considered suitable models for studying serous ovarian cancer *in cellulo* (49), express all three IGF2BPs (Figure 1A and B; Supplementary Figure S1B) and harbor p53 mutations. Moreover, independent studies used these cells for analyzing the role of IGF2BP paralogues (12,17,30). Only the depletion of IGF2BP1 significantly reduced the viability of 2D-cultured ES-2 cells (Figure 1C). The viability and size (quantification not shown) of ES-2 spheroids was significantly decreased by the knockdown of IGF2BP1 (Figure 1D), as previously demonstrated (12). In contrast, spheroid viability remained unaffected by IGF2BP2 depletion and was even significantly enhanced at reduced IGF2BP3 levels. Anoikis-resistance, analyzed at reduced FBS concentration (1%) and low adhesion conditions, was significantly impaired by the knockdown of IGF2BP1 and 2 but remained largely unaffected by the depletion of IGF2BP3 (Figure 1E). In elastic 3D-collagen matrices, only the knockdown of IGF2BP1 severely impaired the speed and distance of single cell migration supporting previous reports indicating that IGF2BP1 promotes tumor cell migration (Figure 1F; Supplementary Movie M1; (12,19)). Consistent with impaired migration, the knockdown of IGF2BP1 essentially abolished the invasion of ES-2 spheroids in 3D-matrigel matrices (Figure 1G). Spheroid invasion was modestly reduced by IGF2BP2 depletion and slightly enhanced by the knockdown of IGF2BP3. To exclude potential bias by siRNA-dependent off-target effects, three of the investigated phenotypes were analyzed upon the CRISPR/CAS9-directed deletion of IGF2BP1 or 3 in ES-2 cells (Supplementary Figure S1C). The loss of IGF2BP1 severely impaired the viability of spheroids, anoikis resistance and spheroid invasion (Figure 1H–J). The deletion of IGF2BP3 modestly enhanced spheroid viability whereas anoikis resistance and spheroid invasion remained largely unaffected. To test if the re-expression of IGF2BP1 restores oncogenic tumor cell properties, spheroid invasion was analyzed in IGF2BP1-deleted ES-2 cells that stably express GFP, GFP-IGF2BP1 or a RNA-binding deficient GFP-IGF2BP1 (GFP-I1mut) mutant (12,50). In comparison to GFP or GFP-I1mut expressing cells, invasion was significantly increased by GFP-IGF2BP1 indicating that the phenotypic effects observed by depletion or deletion unlikely result from off-target effects (Supplementary Figure S2A). To determine if the forced expression of IGF2BPs promotes tumor cell phenotypes, the migration speed of ES-2 cells in stiff 3D-collagen I matrices (4mg/ml) was monitored upon IGF2BP overexpression (Supplementary Figure S2B; Supplementary movie M2). In contrast to the forced expression of IGF2BP2 or 3, GFP-IGF2BP1 significantly enhanced 3D-migration speed. This increase was severely reduced by the depletion of exogenous (siRNA: GFP) as well as total IGF2BP1 (siRNA: I1). Intrigued by these findings spheroid growth, anoikis resistance and invasion were analyzed by the overexpression of GFP-IGF2BP1 (Supplementary Figure S2C–E). All three phenotypes were significantly enhanced by the forced expression of IGF2BP1 indicating that the protein enhances an 'aggressive' ES-2 tumor cell phenotype.

IGF2BP1 deletion impairs tumor growth in nude mice

Aiming to test if the deletion of IGF2BP1 also impairs tumorigenesis *in vivo*, control (parental) and IGF2BP1-deleted ES-2 cells were transduced with lentiviral vectors encoding iRFP (near-infrared fluorescent protein). This allows monitoring the growth of *Xenografts* by non-invasive near-infrared imaging, as previously described (22).

To determine how IGF2BP1 deletion affects tumor growth, 1×10^5 ES-2 cells were injected subcutaneously (*sc*) in the left flank of female *Foxn1^{nu}* mice. The analysis of tumor size demonstrated that tumor growth was significantly delayed for ES-2 cells lacking IGF2BP1 (Figure 2A and B). All tumors were isolated when the first tumors reached a tumor diameter of ~1.5 cm (termination criterion). This endpoint analysis confirmed that tumor volume and mass were substantially reduced by IGF2BP1 deletion indicating that the loss of IGF2BP1 interferes with tumor growth *in vivo* (Figure 2C–E).

IGF2BP1's phenotypic roles *in cellulo*, in particular enhanced migration and invasion, suggested that the protein also promotes metastasis. Even though metastasis of *sc* tumors derived from ovarian cancer cells appeared unlikely, metastasis was monitored after the resection of primary tumors (Figure 2F). Complete resection of primary *sc* tumors was confirmed by infrared imaging after surgery. Starting ~2 weeks after surgery, metastases were observed in two of five control mice (ES-2 parental cells) that survived surgery. Metastases were found at the *pleura* (data not shown) and/or at the residual thymus. In contrast, up to 10 weeks after surgery no metastases were observed in four surviving animals that were injected with IGF2BP1-deleted ES-2 cells (sgI1) initially. Although remaining preliminary, these findings provide strong evidence that the deletion of IGF2BP1 interferes with the 'metastatic potential' of ES-2 cells in nude mice. This is consistent with the observation that IGF2BP1 promotes the migratory and invasive potential of ES-2 cells *in vitro* and that IGF2BP1 expression is associated with poor overall and progression free survival in ovarian cancer.

Conservation of oncogenic roles of the IGF2BP family in cancer-derived cells

All three IGF2BPs were reported to promote 'oncogenic' properties of tumor cells derived from distinct solid cancers. To investigate the phenotypic conservation of IGF2BP paralogues in cancer cells, two phenotypes (spheroid growth and anoikis resistance) were analyzed in four additional cancer-derived cell lines: OVCAR-3 (ovarian carcinoma), MV-3 (melanoma), A549 (lung adenocarcinoma) and HepG2 (Hepatocellular carcinoma, HCC). Only the depletion of IGF2BP1 impaired both cell properties, in all analyzed tumor-derived cells (Figure 3A–C, blue). The knockdown of IGF2BP2 significantly interfered with spheroid growth and anoikis resistance in HepG2 cells and anoikis resistance in A549 cells (Figure 3A–C, light gray). Spheroid growth and anoikis resistance were impaired by IGF2BP3 depletion only in A549 cells (Figure 3A–C, dark gray), supporting a recently reported role of this paralogue in lung cancer (51). In melanoma-derived MV-3 cells, the knockdown of IGF2BP3 led to enhanced spheroid growth.
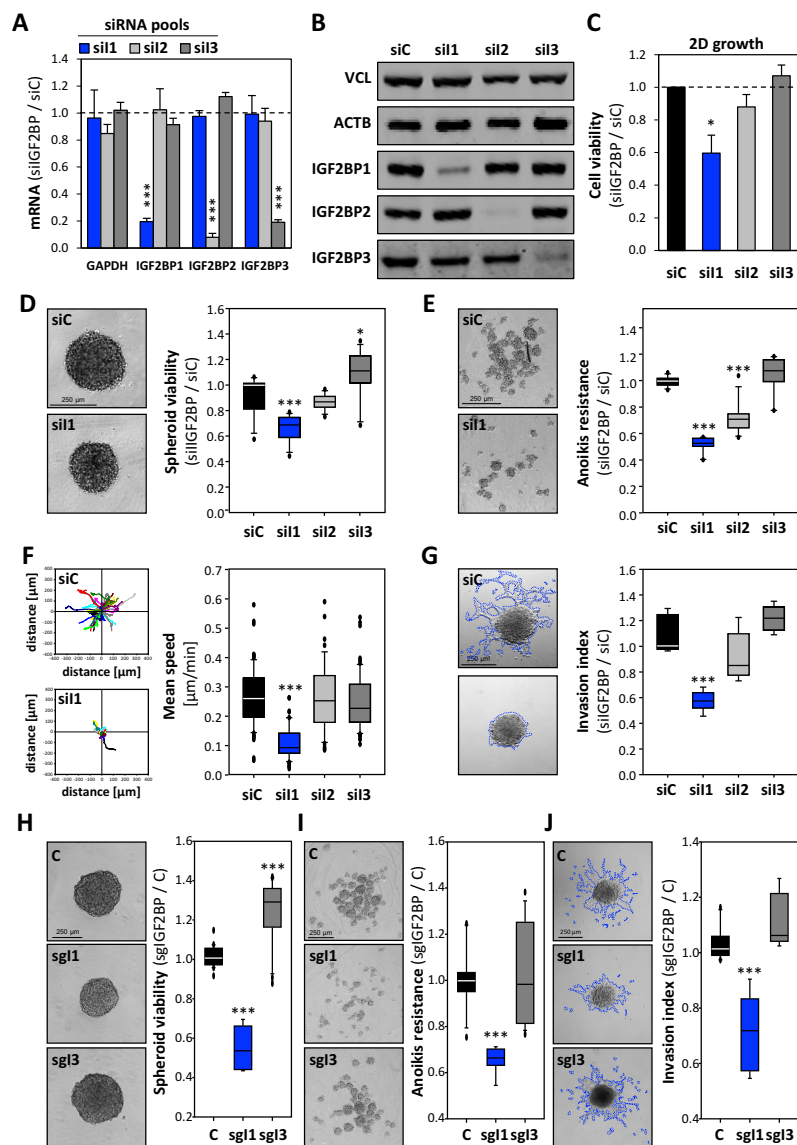
Figure 1. Phenotypic roles of IGF2BPs in ovarian cancer-derived cells. (**A**) RT-qPCR analysis of paralogue-specific IGF2BP depletion (72 h) using siRNA pools in ES-2 cells. ACTB mRNA levels served as normalization control. (**B**) Representative Western blot analysis of knockdown analyses shown in (A). VCL and ACTB served as loading controls. (**C, D**) The viability of ES-2 cells in a 2D cell culture system (C) or ES-2 derived spheroids cultured at 10% FBS in concave ultra-low attachment plates (D) was determined by Cell-titer GLO (Promega) 72h post-transfection with indicated siRNA pools. Cells transfected with control siRNA (siC) served as control and the median viability was set to one. (**E**) Anoikis-resistance and self-renewal potential of ES-2 cells was determined relative to controls (median set to one) by Cell-titer GLO 6 days post-transfection with siRNA pools. Cells were cultured in planar ultra-low attachment plates at 1% FBS. (**F**) Single cell migration of ES-2 cells in 3D collagen matrix (1.8 mg/ml) was determined over 10h starting ∼60 h post-transfection of indicated siRNA pools. The distance (left panel) and mean speed (right panel) of single cell migration was analyzed in total projections of acquired z-stack image series. Data for at least 40 single cell tracks per condition are shown. (**G**) The invasive potential of ES-2 spheroids in 3D matrigel matrix was analyzed 72 h post-transfection of indicated siRNA pools. The relative invasion index (median of controls set to one) was determined by the perimeters of the invasive front (traced by blue dashed line) normalized to spheroid body perimeter. (**H–J**) The spheroid viability (H), anoikis-resistance (I) and spheroid invasion (J) of IGF2BP1- (sgI1) or IGF2BP3-deleted (sgI3) ES-2 cells were determined (average of two clones) as described in D, E and G, respectively. Parental ES-2 cells served as control. Representative images (D, E, G, H–J) or cell trajectories (F) of controls (siC, knockdown; C, parental ES-2), siI1-transfected, IGF2BP1- (sgI1) or IGF2BP3-deleted (sgI3) ES-2 cells are shown in left panels. Statistical significance was determined by Student's *t*-test; *P < 0.05; ***P < 0.001.
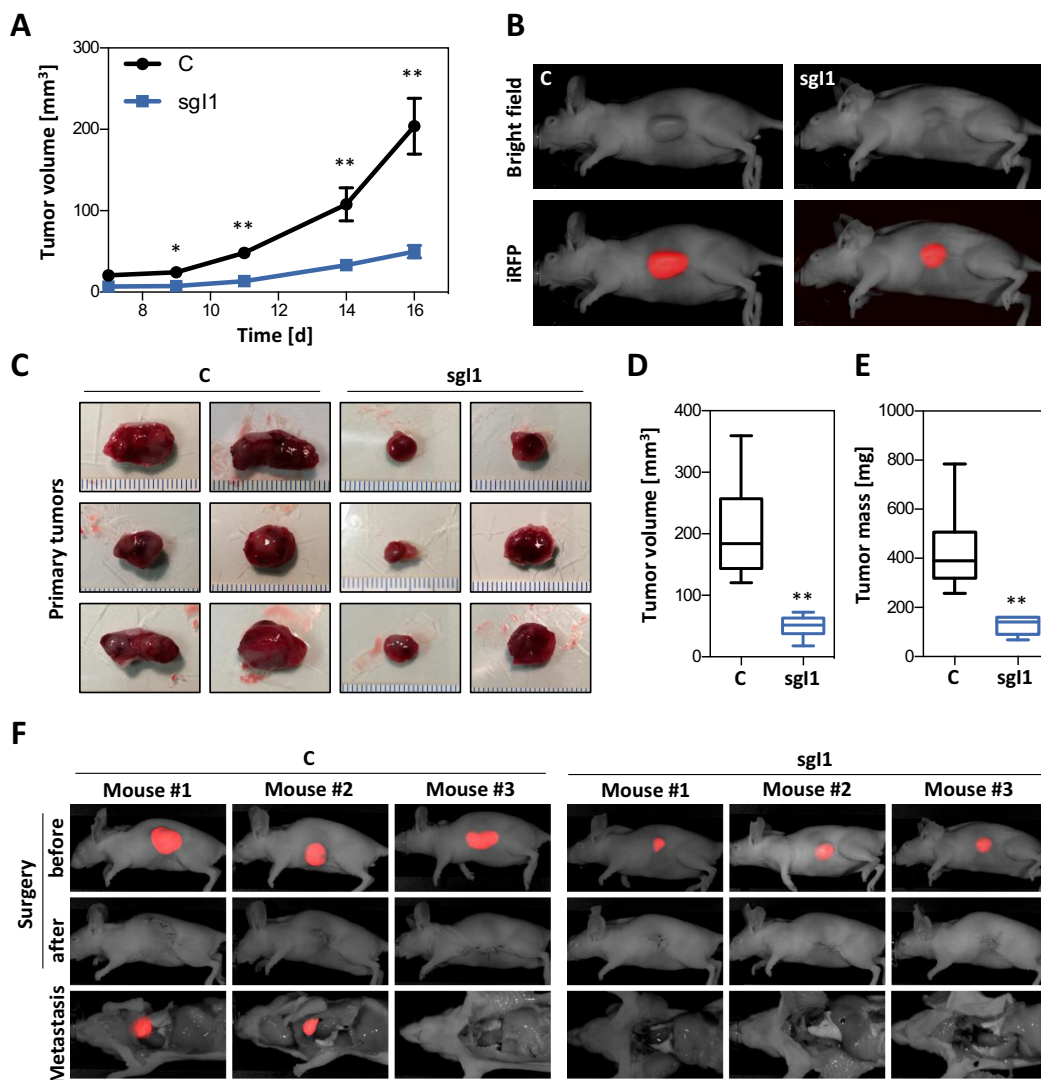
Figure 2. The deletion of IGF2BP1 in ES-2 cells impairs tumor growth and metastasis formation *in vivo*. Control (C) or IGF2BP1-deleted (sgI1) ES-2 cells were stably transduced with iRFP-encoding lentiviral vectors and injected into the left flank of female nude mice (n = 6 for each condition) to induce the formation of heterologous *Xenograft* tumors. (**A**) The tumor volume was measured at indicated time points post-injection by a caliper. Error bars indicate standard error of mean (SEM). (**B**) Representative images of macroscopic tumors acquired by bright field (upper panel) or non-invasive infrared imaging (lower panel) are shown 16d post-injection. (**C**) Images of primary tumors removed by surgery when the first tumors reached the termination criterion. (**D**, **E**) The volume (D) and weight (E) of removed primary tumors were determined and depicted by boxplots. (**F**) Representative images of three mice are shown before (upper panel) and after (middle panel) surgery. Distant metastases observed in control animals (injected with parental ES-2 cells) are shown in the lower panel using invasive infrared imaging. The standard error of mean (SEM) is shown in (A). Statistical significance was determined by Mann–Whitney's test; *$P < 0.05$; **$P < 0.01$.
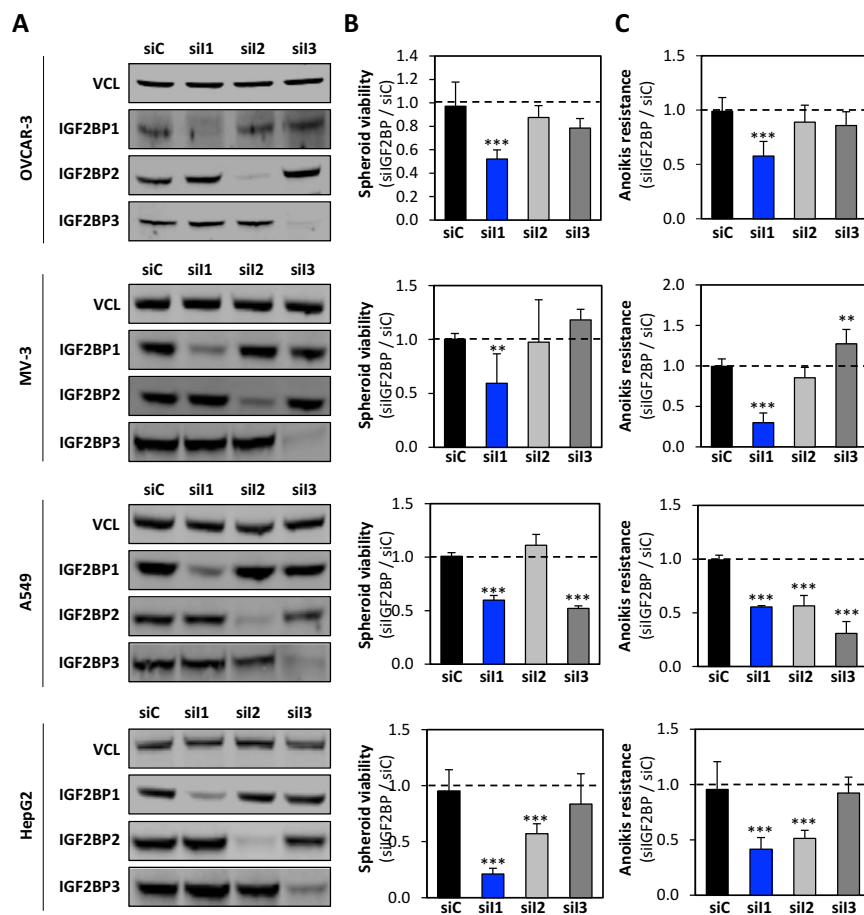
Figure 3. Conservation of IGF2BPs' phenotypic roles in cancer-derived cells. (**A**) Representative Western blot analysis of paralogue-specific IGF2BP depletion (72 h) using siRNA pools in ovarian cancer-derived OVCAR-3 cells, melanoma-derived MV3 cells, lung cancer-derived A549 cells and HCC-derived HepG2 cells. VCL served as loading control. (**B**, **C**) The viability of spheroids and Anoikis resistance of indicated cell lines transfected with control (siC) or siRNA pools targeting indicated IGF2BP paralogues was determined as described in Figure 1B, C. Statistical significance was determined by Student's t-test; $**P < 0.01$; $***P < 0.001$.

In summary, these findings indicate that IGF2BP1's phenotypic role in cancer-derived cells is largely conserved whereas the role of IGF2BP2 and 3 varies in a cancer cell-dependent manner.

IGF2BP depletion impairs the expression of partially distinct mRNA panels

Previous studies largely agree that one major role of IGF2BPs is the control of mRNA turnover (15,16). The partially diverse phenotypic roles of IGF2BP paralogues observed in cancer-derived cells, however, suggested that IGF2BPs modulate partially distinct (m)RNA targets. This was addressed by monitoring gene expression upon the paralogue-specific depletion of IGF2BPs in ES-2 cells using RNA-sequencing.

The knockdown of IGF2BPs affected the abundance of mRNAs to varying extend whereas miRNA and lncRNA abundance were only modestly changed (Supplementary Figure S3A–I; Supplementary Table T1A and B). This indicated that IGF2BPs mainly regulate the abundance of mRNAs. To reveal gene sets or pathways regulated by the IGF2BP-dependent control of mRNA abundance gene set enrichment analyses (GSEA) were performed. These identified partially overlapping 'pathway gene sets' for all three IGF2BPs including MYC target genes, epithelial-to-mesenchymal transition (EMT) and KRAS signaling (Figure 4A; Supplementary Table T1C). The identification of these pathways is supported by previously reported roles of IGF2BPs. For instance, IGF2BP1 was shown to promote MYC expression, promotes a mesenchymal tumor cell phenotype and shows cross-talk with KRAS signal-
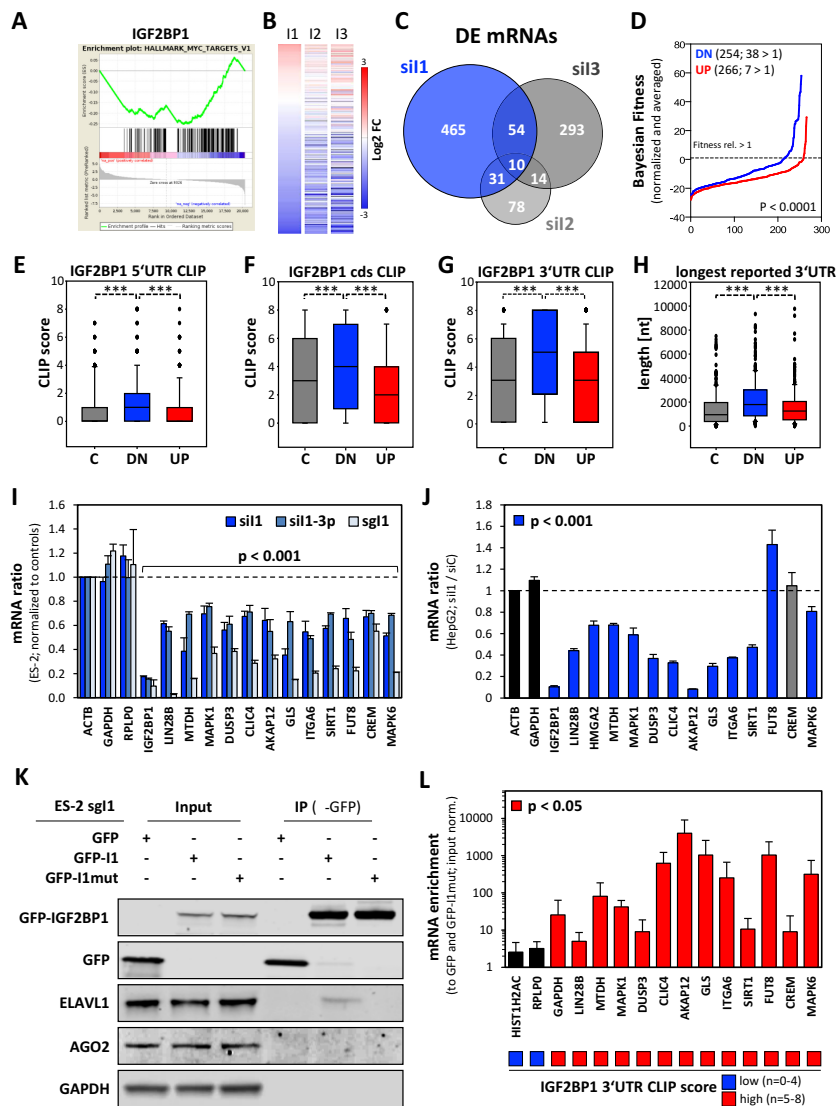
Figure 4. Control of mRNA expression by IGF2BPs in ES-2 cells. (**A**) Enrichment plot for the pathway gene set 'MYC_TARGETS_V1' determined by gene set enrichment analysis (GSEA) of mRNA expression changes observed upon IGF2BP1 depletion (72 h) in ES-2 cells. (**B**) Heatmap indicating the $\log_2$ fold change in expression (FPKM) observed for the 'MYC_TARGETS_V1' gene set upon the depletion of IGF2BP1 (I1), IGF2BP2 (I2) or IGF2BP3 (I3) in ES-2 cells. (**C**) Venn diagram showing the number and overlap of mRNAs with significant (FDR <0.1) differential expression (DE) upon the paralogue-specific depletion of IGF2BPs. (**E–G**) The IGF2BP1 CLIP scores determined in the 5′UTR (E), CDS (F) or 3′UTR (G) of mRNAs significantly down- (DN, blue; 272), upregulated (UP, red; 288) or unchanged (C, 280, gray) are depicted by box plots. (**H**) The length of the longest reported 3′UTR of mRNAs shown in (E–G) are shown by box plots. (**I**) Differential expression of indicated mRNAs was determined relative to controls (siC for depletion; parental ES-2 cells for deletion) by: a) RT-qPCR upon IGF2BP1 depletion using siRNA pools (siI1); b) RT-qPCR upon IGF2BP1 depletion using a 3′UTR-directed siRNA (siI1-3p) not included in the pool (a); c) RT-qPCR in response to IGF2BP1-deletion (sgI1) in ES-2 cells. GAPDH and RPLP0 mRNAs served as negative controls. (**J**) Differential expression of indicated mRNAs upon IGF2BP1 depletion (siRNA pool) in HepG2 cells was determined by RT-qPCR. GAPDH served as negative control. ACTB served as normalization control in both (I, J) RT-qPCR analyses. (**K, L**) The co-purification of proteins (K) and mRNAs (L) was determined in IGF2BP1-deleted cells expressing GFP, GFP-IGF2BP1 (GFP-I1) or an RNA-binding deficient IGF2BP1 (GFP-I1mut) using immunopurification (IP) by anti-GFP antibodies. Indicated proteins were analyzed by Western blotting (K) in Inputs and upon IP. GAPDH served as negative control. The co-purification of mRNAs was determined by RT-qPCR analyses (L). The enrichment of indicated mRNAs with GFP-IGF2BP1 was determined relative to the co-purification of mRNAs with GFP and GFP-I1mut upon input normalization. RPLP0 and HISTH2AC served as negative controls. The IGF2BP1 3′UTR CLIP score of indicated mRNAs is shown by a heatmap (lower panel). Statistical significance was determined by Student's *t*-test; ***$P < 0.001$.

ing (17,52,53). Closer inspection of the mRNAs denoted as leading edge subset by the GSEA application revealed a substantial overlap of transcripts deregulated upon the depletion of IGF2BP paralogues (Supplementary Figure S4A, D and G). Pearson correlation analyses revealed that the fold change of mRNA abundance determined for transcripts comprised in the respective gene sets was significantly correlated upon the depletion of IGF2BP paralogues (Supplementary Figure S4B, E and H). The strongest association with correlation coefficients between 0.76–0.8 was observed for the 'MYC_TARGETS_V1' gene set. Transcripts comprised in this gene set were mostly downregulated by the depletion of IGF2BPs supporting a role of IGF2BPs in promoting MYC expression. However, in ES-2 cells only the depletion of IGF2BP1 and 2 reduced MYC protein levels (Supplementary Figure S4J). In contrast, MYC protein abundance was modestly increased by the depletion of IGF2BP3 suggesting distinct regulation of MYC target gene expression by this paralogue. Like observed for MYC, IGF2BP paralogues regulated KRAS mRNA levels to varying extend (Supplementary Figure S4K). These findings suggested that IGF2BPs control similar 'pathway gene sets' but regulate mRNA abundance in a largely paralogue-dependent manner. This was supported by four observations: (i) IGF2BPs controlled the abundance of mRNAs comprised in the evaluated 'pathway gene sets' in a distinct manner (Figure 4B; Supplementary Figure S4C, F and I); (ii) The number of mRNAs showing significantly (FDR < 0.1) changed expression upon the depletion of every single IGF2BP was rather small (Figure 4C); (iii) The knockdown of IGF2BP1 had the most prominent effect on the differential expression (DE) of mRNAs supporting its comparatively 'strong' phenotypic role in ES-2 cells (Figure 4C); (iv) Gene annotation enrichment analyses (GAEA) of mRNAs showing significant DE indicated a substantial paralogue-dependent diversity (Supplementary Figure S5A and Table T1D). For IGF2BP1, GAEA showed a significant enrichment of cell migration-associated genes among downregulated (DN) transcripts. In contrast, cell death-associated mRNAs were significantly enriched among DN transcripts upon IGF2BP3 knockdown. This was in good agreement with phenotypic effects observed in ES-2 cells and suggested that prime effector mRNAs of IGF2BPs are comprised among DN transcripts. This hypothesis was evaluated further by analyzing the tumor cell fitness relevance of DE transcripts (54). Cell fitness relevance, indicated by a Bayesian factor greater one or elevated fitness scores, was significantly higher for DN transcripts when compared to mRNAs upregulated (UP) upon IGF2BP1 depletion (Figure 4D; Supplementary Figure S5B and C). Although less prominent, this trend was also observed for the other two IGF2BP paralogues.

Aiming to identify target mRNAs regulated directly by IGF2BP1, the conservation of CLIP (cross-linking immunoprecipitation) sites reported for DE transcripts in HEK293 (PAR-CLIP; (40)), human pluripotent stem cells (eCLIP; (42)), leukemia-derived K562 and HCC-derived HepG2 cells (eCLIP and iCLIP; (41)) was determined (Supplementary Table T2). This strategy settled on the observation that IGF2BP1's phenotypic roles were largely conserved among tumor-derived cells suggesting that func-

tionally relevant protein-RNA associations are conserved as well. To allow for a rapid and comprehensive genome wide view of IGF2BP1-CLIP data derived by distinct techniques and analysis strategies, identical CLIP-site positions in 5′UTRs, coding sequences (CDS) and 3′UTRs were determined by considering eight data sets (40–42). The overlay of CLIP sites revealed candidate hot spots of IGF2BP1-association in target mRNAs, for instance the LIN28B 3′UTR (Supplementary Figure S6A; (12)). To rate CLIP-reported mRNA-binding, the CLIP score (CS) indicating the number of experiments demonstrating binding of IGF2BP1 in the 5′UTR, CDS and 3′UTR of specific mRNAs was determined. For the LIN28B 3′UTR, IGF2BP1-binding was reported in all of the eight considered analyses indicating the maximum CS of eight and thus a high conservation of this protein-mRNA association. The genome wide analysis of IGF2BP1's CLIP scores confirmed preferential binding to mRNAs and identified the 3′UTR as the preferentially bound cis-element, as previously reported (Supplementary Figure S6B, C; (40)).

The analysis of transcripts differentially expressed upon IGF2BP1 depletion in ES-2 cells revealed significantly elevated CLIP scores for the 5′UTRs, CDSs as well as 3′UTRs of DN (272) mRNAs when compared to UP (288) or control (C, 280; randomly selected) transcripts (Figure 4E–G). The largest median CS was determined for 3′UTRs and the median length of the longest reported 3′UTR of mRNAs was significantly elevated among DN mRNAs (Figure 4H). Based on PAR-CLIP (40) and RNA Bind-n-Seq (42) analyses, AC-rich RNA-binding motifs were suggested for IGF2BP1. All of these were significantly increased in the 3′UTRs (normalized to 3′UTR length) of DN transcripts (Supplementary Figure S6D–H). This was not observed for a GU-rich control motif providing further evidence that IGF2BP1 preferentially associates at the 3′UTR of its DN target mRNAs. Significantly increased CLIP scores were also observed for mRNAs significantly downregulated upon IGF2BP2 or 3 depletion suggesting that all three IGF2BPs promote the abundance of target mRNAs in a preferentially 3′UTR-dependent manner (Supplementary Figure S7A–C).

To validate regulation by IGF2BP1 and test if the conservation of CLIP sites is a valid indicator for mRNA association, 11 DN transcripts with an IGF2BP1 3′UTR CS greater than four were selected for further analyses. In ES-2 cells, all these mRNAs and the recently reported target mRNA LIN28B, serving as positive control, were downregulated upon IGF2BP1 deletion (sgI1) and its depletion using a 3′UTR-directed siRNA (siI1-3p) not comprised in the siRNA pool (Figure 4I). With the exception of two mRNAs (FUT8 and CREM), all selected DN mRNAs were also decreased by the depletion of IGF2BP1 in HCC-derived HepG2 cells (Figure 4J). This indicated that the conservation of IGF2BP1's phenotypic roles is associated with substantially conserved regulation of mRNA fate. Next, the association of proteins and mRNAs was analyzed in ES-2 cells using RIP. To this end, co-purification was determined in IGF2BP1-deleted ES-2 cells expressing GFP-IGF2BP1 (GFP-I1), RNA-binding deficient IGF2BP1 (GFP-I1mut; (50)) or GFP. The RNA-binding protein HuR (ELAVL1) was only co-purified with wild type IGF2BP1 confirm-

ing the RNA-dependent association of both proteins (Figure 4K; (50)). No association was observed for GAPDH (negative control) or AGO2 suggesting that IGF2BP1 does neither associate with RISC factors nor RISC-associated mRNAs. The analysis of input-normalized mRNA enrichment revealed that all 11 DN mRNAs and LIN28B were selectively enriched with GFP-IGF2BP1 when compared to GFP or GFP-I1mut (Figure 4L). Two transcripts with low CLIP scores (HIST1H2AC and RPLP0) served as negative controls. Finally, the abundance of DN mRNAs in IGF2BP1-deleted ES-2 cells re-expressing GFP-IGF2BP1 was compared to cells expressing GFP or GFP-I1mut (Supplementary Figure S7D). In contrast to largely unaffected controls (HIST1H2AC and RPLP0), the abundance of all (except CREM) DN transcripts was significantly increased by wild type IGF2BP1. This showed that IGF2BP1 re-expression restored target mRNA levels in a RNA-binding dependent manner and thus largely excluded bias by off-target effects. In summary, these findings indicate that IGF2BP1 promotes the abundance of target mRNAs by associating with these transcripts and other RBPs, e.g. HuR, in AGO2 and thus RISC-free mRNPs, as previously proposed (12).

Candidate target mRNAs of IGF2BP1 are preferred miRNA targets

IGF2BP1 impairs the miRNA-directed degradation of some target mRNAs, for instance BTRC1 or LIN28B (12,55). If mRNAs deregulated upon IGF2BP1 depletion or deletion in ES-2 cells are prone to miRNA-dependent regulation was first analyzed by predicting miRNA-targeting of DN, UP as well as control transcripts using multiMiR (39). The number of miRNAs showing at least 100 CPM (counts per million mapped transcripts) in ES-2 cells and predicted by at least two of eight databases was significantly increased for DN transcripts (Figure 5A; Supplementary Tables T3 and T4). This was also observed for the abundance of targeting miRNAs in ES-2 cells (Figure 5B). Finally, transcripts deregulated upon IGF2BP1 depletion as well as randomly selected unaffected control mRNAs were analyzed for AGO CLIP sites in their 3′UTR. Assuming that miRNA- and thus RISC-targeting is conserved, as determined for IGF2BP1-binding, five AGO2 and one AGO1-4 CLIP study were investigated (40,43–45). Consistent with increased miR-targeting, AGO-CLIP scores were significantly increased among DN transcripts (Figure 5C). Notably, this was also observed for the other IGF2BP paralogues suggesting that all three IGF2BPs preferentially promote the expression of miRNA-regulated target mRNAs (Supplementary Figure S7A–C). For LIN28B and the 11 selected DN target mRNAs of IGF2BP1 miR-dependent regulation was further on confirmed by elevated mRNA levels determined upon the co-depletion of DICER and DROSHA in ES-2 cells (Figure 5D and E). This was associated with severely reduced miRNA levels, as demonstrated by Northern blotting for let-7a, miR-22 and miR-21, the most abundant miRNA in ES-2 cells (Figure 5D). If IGF2BP1 impairs miRNA-directed downregulation of miR-prone target mRNAs was investigated by comparing mRNA levels upon IGF2BP1 depletion alone and the triple

knockdown of IGF2BP1, DICER and DROSHA (Figure 5D and F). In contrast to controls (ACTB, GAPDH and RPLP0), all analyzed IGF2BP1 target mRNAs were significantly reduced by the knockdown of IGF2BP1 and upregulated by the triple depletion. This was further supported by analyzing LIN28B protein levels (Figure 5D). These were decreased upon the depletion of IGF2BP1 and enhanced by the triple knockdown. Together, this indicated that the IGF2BP1-dependent regulation of miRNA-controlled target mRNAs is strictly miRNA-dependent. Finally, this was evaluated by analyzing the association of mRNAs with AGO2 in control (parental ES-2 cells) and IGF2BP1-deleted ES-2 cells, as previously shown for IGF2BP3 (21). The analysis of proteins co-purified with AGO2 confirmed that IGF2BP1 and AGO2 are not associated in ES-2 cells, as previously shown by IGF2BP1-RIP (Figure 5G; compare to Figure 4K). The analysis of input-normalized mRNA enrichment showed that the AGO2-association of all 12 IGF2BP1 target transcripts was significantly enhanced in cells deleted for IGF2BP1 (Figure 5H). In conclusion, these findings indicate that IGF2BP1 interferes with the miRNA-dependent downregulation of its miR-prone target mRNAs by preventing miRNA/RISC-association.

IGF2BP1 interferes with miRNA-directed decay of the SIRT1 mRNA

Aiming to evaluate if the observed impairment of miRNA-dependent regulation solely relies on the direct coverage of miRNA binding sites (MBS) by IGF2BP1, regulation of the SIRT1 mRNA, one of the novel miR-prone target mRNAs, was analyzed in further detail. The SIRT1 mRNA decayed more rapidly upon the depletion of IGF2BP1 indicating that the protein interfered with SIRT1 mRNA turnover (Figure 6A). The activity of a luciferase reporter comprising the SIRT1 3′UTR was significantly reduced in ES-2 cells deleted for IGF2BP1 (Figure 6B). This was not observed for a control reporter comprising a vector-encoded 3′UTR (MCS) suggesting that IGF2BP1 controls SIRT1 mRNA turnover largely via the 3′UTR. In silico predictions of miRNAs targeting the SIRT1 3′UTR and expressed in ES-2 cells with a CPM greater than 100 by multiMiR identified six different miRNAs (Figure 6C). Additionally, seven MBSs for this cis-element were proposed by TargetScan 7.1 (www.targetscan.org). Three (miRs: 155, 22, 140-I) of the seven predicted MBSs overlap with nucleotides (nt) for which CLIP sites were reported by at least two of the eight considered IGF2BP1-CLIP studies. To test the activity and IGF2BP1-dependent regulation of SIRT1-derived MBSs, luciferase reporters comprising the respective MBSs and 20 nt up and downstream of the SIRT1 3′UTR were fused 3′ to a luciferase CDS. Compared to a control reporter (MCS), the activity of all seven reporters comprising SIRT1-derived MBSs was significantly reduced in parental ES-2 control cells suggesting miRNA-targeting of all MBSs (Figure 6D, gray). Compared to parental ES-2 cells, the deletion of IGF2BP1 significantly reduced the activity of reporters comprising the SIRT1-derived MBSs with reported IGF2BP1 CLIP sites suggesting coverage of these MBSs (Figure 6D, blue). Finally, the distribution of IGF2BP1-3 as well as AGO2 CLIP sites in the 3′UTR of human
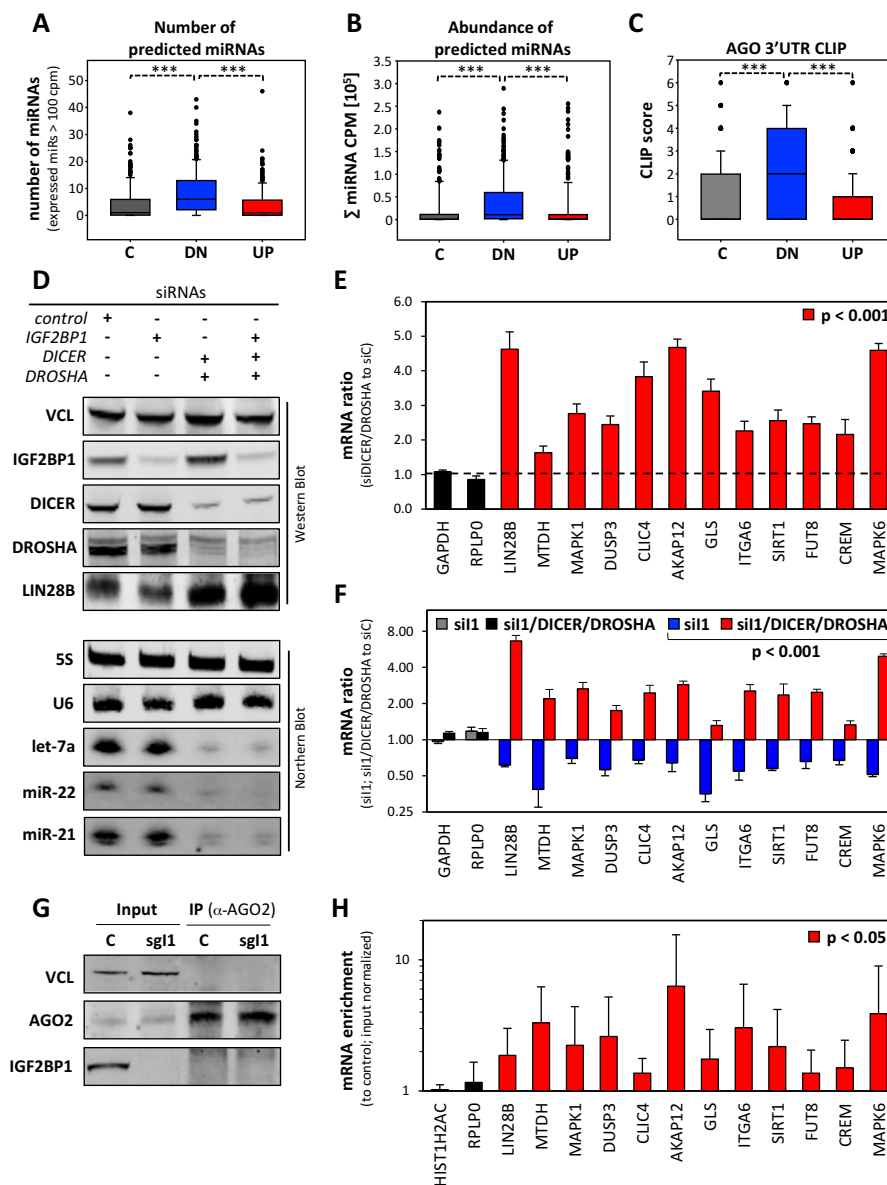
Figure 5. IGF2BP1 target mRNAs are prone to miRNA-dependent regulation. (**A**, **B**) The number (A) and summed abundance (B) of miRNAs expressed in ES-2 cells and predicted to target the transcripts analyzed in Figure 4E–H is depicted by box plots. Only miRNAs expressed with a CPM>100 and predicted (multiMiR) by at least 2 out of 8 databases were considered. (**C**) The AGO CLIP scores determined for the 3′UTRs of mRNAs analyzed in (A, B) are depicted by box plots. (**D**) Representative Western blot analysis (upper panel) of indicated proteins upon the depletion of IGF2BP1, DICER and DROSHA co-depletion or triple depletion in ES-2 cells 6d post-transfection (re-transfection after 3d). VCL served as loading control. Representative Northern blot analysis of indicated ncRNAs upon the indicated depletions are shown in the lower panel. 5S and U6 ncRNAs served as loading controls. (**E**, **F**) The differential expression of indicated mRNAs upon DICER/DROSHA (E), IGF2BP1 (F, siI1) or triple knockdown (F, siI1/DICER/DROSHA) was determined by RT-qPCR using ACTB for normalization. GAPDH and RPLP0 served as negative controls. Color coding indicates significance determined by Student's *t*-test. (**G**, **H**) The co-purification of proteins (G) and mRNAs (H) with AGO2 in parental (C, control) or IGF2BP1-deleted (sgI1) ES-2 cells was determined by immunopurification (IP) using anti-AGO2 antibodies. Indicated proteins were analyzed by Western blotting (G) in Inputs and upon IP. VCL served as loading and negative control. The co-purification of mRNAs was determined by RT-qPCR analyses (H). The enrichment of indicated mRNAs with AGO2 in IGF2BP1-deleted cells was determined relative to parental cells upon input normalization. RPLP0 and HISTH2AC served as negative controls. Statistical significance was determined by Student's *t*-test; ***$P < 0.001$.
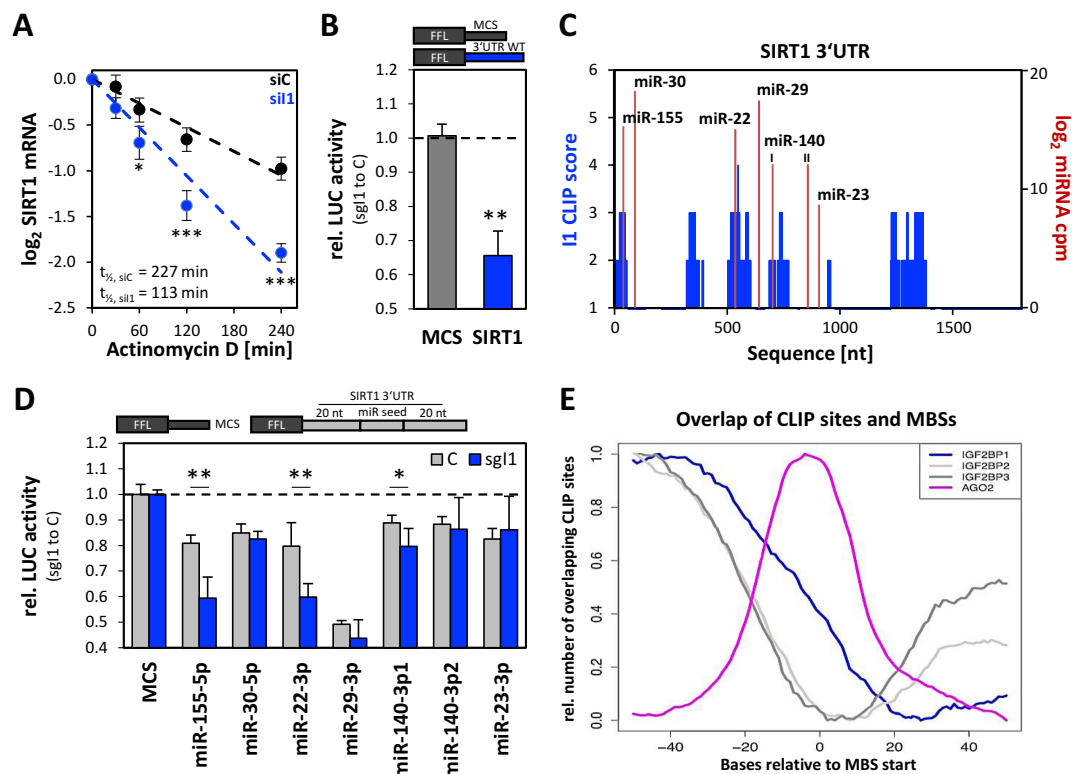
Figure 6. IGF2BP1 interferes with the miRNA-directed decay of the SIRT1 mRNA. (**A**) The decay of SIRT1 mRNA was monitored by RT-qPCR in IGF2BP1-depleted (siI1) or control-transfected (siC) ES-2 cells by blocking mRNA synthesis using actinomycin D (5 μM) for indicated time points upon normalization to RNA input levels. (**B**) The activities of a control luciferase-reporter (MCS) and a reporter comprising the 3′UTR of SIRT1 was determined in IGF2BP1-deleted ES-2 cells (sgI1) and control cells (C, parental ES-2 cells). Relative (sgI1 to C) reporter activity is shown. (**C**) The number of CLIP studies showing CLIP sites for IGF2BP1 in the SIRT1 3′UTR (left axis, blue) and targeting sites of miRNAs (right axis, red) are shown for the SIRT1 3′UTR at nucleotide-resolution. MiRNA abundance is indicated as $\log_2$ CPM. (**D**) The activity of luciferase reporters comprising fragments of the 3′UTR of SIRT1 with 20 nt 5′ or 3′ of MBSs shown in (C) were determined relative to control reporter activity (MCS) in IGF2BP1-deleted cells (sgI1, blue) and parental ES-2 cells (C, gray). (**E**) The relative number of overlapping CLIP sites determined for IGF2BP1-3 or AGO2 in the proximity of MBSs are shown relative to the MBS start sites predicted by TargetScan for human mRNAs (hg19). Statistical significance was determined by Student's *t*-test; *$P < 0.05$; **$P < 0.01$; ***$P < 0.001$.

mRNAs was compared to predicted MBS positions (Figure 6E). AGO2 CLIP sites tended to overlap with MBS start sites suggesting that the protein preferentially associates in the 5′-vicinity of MBSs. In contrast, IGF2BP CLIP sites were enriched ~40 nucleotides upstream of MBS start sites but showed variable overlap with AGO2-binding regions. Among IGF2BP paralogues, IGF2BP1 CLIP sites showed the most prominent overlap with AGO2 CLIP sites in the 5′-vicinity of MBSs. In contrast to IGF2BP1 and AGO2, binding of IGF2BP2 and 3 was modestly enhanced in the 3′-vicinity of MBSs suggesting similar but distinct binding properties of IGF2BPs in proximity to MBSs. In summary, this suggests that IGF2BPs do not preferentially cover MBSs but partially overlap with AGO2-binding sites.

IGF2BP1 modulates mRNA fate in a miRNome-dependent manner

The IGF2BP1-dependent stabilization of miR-prone target mRNAs was abrogated when miRNAs were depleted implying that IGF2BP1-dependent regulation is miRNome-dependent. This was tested for the validated miR-prone target mRNAs LIN28B, SIRT1 and MAPK6 in ovarian cancer-derived ES-2 and HCC-derived Huh-7 cells. These target mRNAs were chosen since LIN28B and MAPK6 are prone to regulation by the let-7 miRNA family whereas this was neither reported nor predicted for the SIRT1 mRNA (12,56). The latter, however, is regulated by miR-22 (57). This was validated by miTRAP (miRNA trapping by RNA affinity purification) in ES-2 cells (31). The affinity purification of the MS2-tagged *in vitro* transcribed LIN28B, SIRT1 and MAPK6 3′UTRs from ES-2 cell lysates revealed co-purification of AGO2

and IGF2BP1 proteins indicating miRNA-dependent regulation and IGF2BP1-association (Figure 7A). The analysis of miRNAs co-purified with the respective 3′UTRs by RT-qPCR showed substantial enrichment of the let-7a miRNA only for the LIN28B and MAPK6 3′UTRs (Figure 7B–D). In contrast, miR-22 was co-purified only with the SIRT1 3′UTR. The most abundant miRNA in ES-2 cells, miR-21, was barely enriched with any of the three 3′UTRs. MiRNA-sequencing revealed that both, ES-2 and Huh-7 cells, express miR-22 whereas in contrast to ES-2, Huh-7 cells barely contain let-7 miRNAs (Supplementary Table T4). This was validated by Northern blotting (Figure 7E). In agreement with miRNA levels, the activity of let-7a antisense (as) luciferase reporters remained unchanged in Huh-7 cells whereas their activity was substantially reduced in ES-2 cells (Figure 7F). Compared to control reporters (MCS), the activity of miR-22 as-reporters was severely reduced in both cells and repression was slightly enforced in Huh-7 cells expressing miR-22 at slightly higher levels. In ES-2 cells, the depletion of IGF2BP1 severely reduced the abundance of all three mRNAs whereas the expression of control transcripts (ACTB and GAPDH) remained unchanged (Figure 7G). In Huh-7 cells, the knockdown of IGF2BP1 only reduced SIRT1 mRNA abundance. This was further supported by analyzing protein levels (Figure 7H–K). The abundance of LIN28B, SIRT1 and MAPK6 proteins was reduced upon IGF2BP1 depletion only in ES-2 cells whereas SIRT1 protein was downregulated also in Huh-7 cells. In summary, these findings indicate that the IGF2BP1-dependent regulation of miR-prone target mRNAs is strictly miRNome-dependent and thus can vary in a cell context-dependent manner.

IGF2BP1 controls tumor cell properties by promoting the expression of miRNA-regulated target mRNAs

The presented analyses indicated that IGF2BP1 promotes oncogenic tumor cell properties and that this is associated with the impairment of miRNA-dependent downregulation of its miRNA-controlled target mRNAs. To evaluate if the 12 (including LIN28B) validated 'miRNA-prone' target mRNAs of IGF2BP1 could serve as downstream effectors in promoting an 'aggressive' tumor cell phenotype anoikis resistance, spheroid growth and spheroid invasion were monitored upon their depletion in ES-2 cells using siRNA pools (Figure 8A–C; Supplementary Figure S8A–D). The knockdown of IGF2BP1 served as positive control.

All three tumor cell phenotypes were significantly impaired by the depletion of IGF2BP1 whereas the knockdown of LIN28B only interfered with spheroid invasion. With the exception of one downstream effector, GLS, the knockdown of all analyzed IGF2BP1-target mRNAs impaired at least one of the investigated phenotypes. Notably, we observed variable association of phenotypic effects. For instance, although SIRT1 depletion impaired anoikis-resistance, invasive potential and spheroid viability remained essentially unchanged. Likewise, although the knockdown of AKAP12 interfered with spheroid invasion, anoikis resistance and spheroid viability were essentially unaffected. Intriguingly, invasive potential was influenced by most of the validated downstream effectors support-

ing the view that IGF2BP1 is a post-transcriptional driver of invasive potential and thus likely of metastasis as supported by *in vivo* studies (see Figure 2). Five of the effectors (ITGA6, MAPK1, FUT8, MTDH and MAPK6) significantly modulated all three phenotypes suggesting a pivotal role in 'IGF2BP1-driven' cancers. Most importantly, none of the depletions significantly enhanced any of the analyzed phenotypic effects. In summary, this indicates that the impairment of miRNA-directed downregulation of its target mRNAs is a major role of IGF2BP1 in cancer-derived cells. Moreover, IGF2BP1 obviously acts via pleiotropic downstream effectors indicating that specific phenotypic roles are interfered by more than one effector.

If IGF2BP1 expression is associated with effector expression also in primary cancers was tested by Pearson correlation in primary ovarian cancer (EOC), hepatocellular cancer (HCC), lung adenocarcinoma (LUAD) and skin cutaneous melanoma (SKM) samples (Figure 8D). Data were derived from TCGA-provided RNA-sequencing data. With the exception of DUSP3 all analyzed IGF2BP1 effectors showed co-expression, indicated by positive correlation coefficients (Pearson R), in at least three of the analyzed cancer data sets. The average Pearson correlation coefficient (Figure 8D, trend) confirmed that effector expression is overall positively associated with IGF2BP1 abundance in all four cancers. Finally, the prognostic relevance of effector expression on progression free (PFS) and overall survival (OS) was analyzed by Kaplan Meier studies in serous ovarian carcinomas (SOC) by KM plotter (Figure 8E). IGF2BP1 and LIN28B were identified as the most prominent indicators of a poor prognosis. This is indicated by hazardous ratios (HR) greater than one determined for all analyzed conditions. The highest HR was retrieved for IGF2BP1 in PFS analysis (HR: 2.35; $P = 8.6 \times 10^{-5}$) of p53-mutated SOC. With the exception of MAPK1 and FUT8, elevated expression of all effectors was associated with poor PFS-prognosis in p53-mutated SOC. Consistently, the highest average HR (Figure 8E, trend) was observed for PFS-prognosis in p53-mutated SOC. This was expected since effectors were identified in p53-mutated ovarian cancer-derived ES-2 cells.

DISCUSSION

The depletion of IGF2BPs in five tumor cell lines derived from distinct cancers indicates that IGF2BP paralogues serve partially distinct phenotypic roles. IGF2BPs show similar RNA-binding properties and control partially overlapping pathways. However, the sets of significantly deregulated transcripts upon IGF2BP depletion are mainly divergent. AGO2 as well as IGF2BPs preferentially associate with mRNAs downregulated upon IGF2BP depletion suggesting that IGF2BPs mainly impair the decay of their miRNA-controlled target mRNAs. This is confirmed by the analysis of 12 miRNA-regulated target mRNAs of IGF2BP1. Notably, the vast majority of these mRNAs encode factors promoting the anoikis resistance, spheroid viability and/or spheroid invasion of ovarian cancer-derived cells. In primary cancer, enhanced IGF2BP1 synthesis is associated with the elevated expression of these transcripts. Like IGF2BP1, most of its miRNA-controlled target tran-
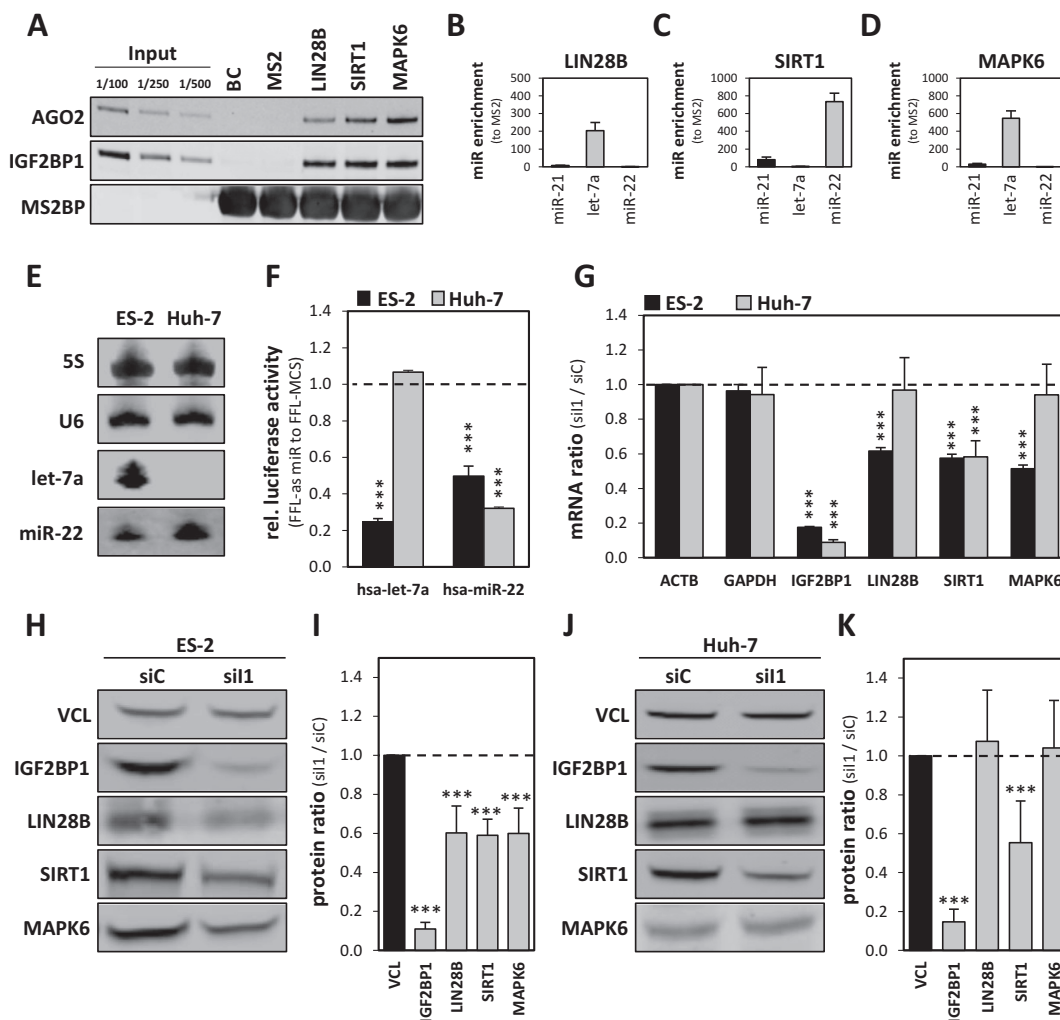
Figure 7. IGF2BP1 modulates target mRNA fate in a miRNome-dependent manner. (**A**) Representative Western blot analysis of indicated proteins associated with the *in vitro* transcribed 3′UTRs of indicated mRNAs in miTRAP studies (ES-2 cells). MS2BP-coated and MS2/MS2BP-coated amylose resins served as negative controls. Dilutions of protein inputs are shown on the left. (**B–D**) The association of indicated miRNAs with the 3′UTRs of LIN28B (B), SIRT1 (C) and MAPK6 (D) was determined by miTRAP using RT-qPCR. The enrichment of miRNAs co-purified with 3′UTRs was analyzed relative to MS2 controls. (**E**) Representative Northern blot analysis of indicated ncRNAs in ES-2 and Huh-7 cells. U6 and 5S RNAs served as loading controls. (**F**) The activity of let-7 and miR-22 miRNAs in ES-2 and Huh-7 cells was analyzed by miRNA antisense luciferase reporters. The activity of antisense reporters (FFL-as) was normalized to control reporters comprising a vector-encoded 3′UTR (FFL-MCS). (**G**) RT-qPCR analysis of indicated transcripts upon the depletion of IGF2BP1 in ES-2 and Huh-7 cells. ACTB mRNA levels were used for normalization. GAPDH served as negative control. (**H–K**) Western blot analysis of IGF2BP1 depletion by siRNA pools (72 h) in ES-2 cells (H, I) and HCC-derived Huh-7 cells (J, K). VCL served as loading and normalization control for determining relative protein ratios in (I, K). Statistical significance was determined by Student's *t*-test; ****P* < 0.001.

scripts indicate poor prognosis in ovarian cancer. Together this indicates that IGF2BP1 enhances an 'aggressive' tumor cell phenotype largely by impairing the downregulation of its miRNA-regulated target mRNAs.

Paralogue-specific roles of IGF2BPs in cancer-derived cells

The analysis of tumor cell phenotypes in a panel of five tumor cells derived from distinct solid cancers indicates that IGF2BP1 has the most conserved 'oncogenic potential' of the IGF2BP family *in cellulo* (Figures 1 and 3; Supplementary Figure S2). This is supported by *Xenograft* studies revealing that the deletion of IGF2BP1 interferes with tumor
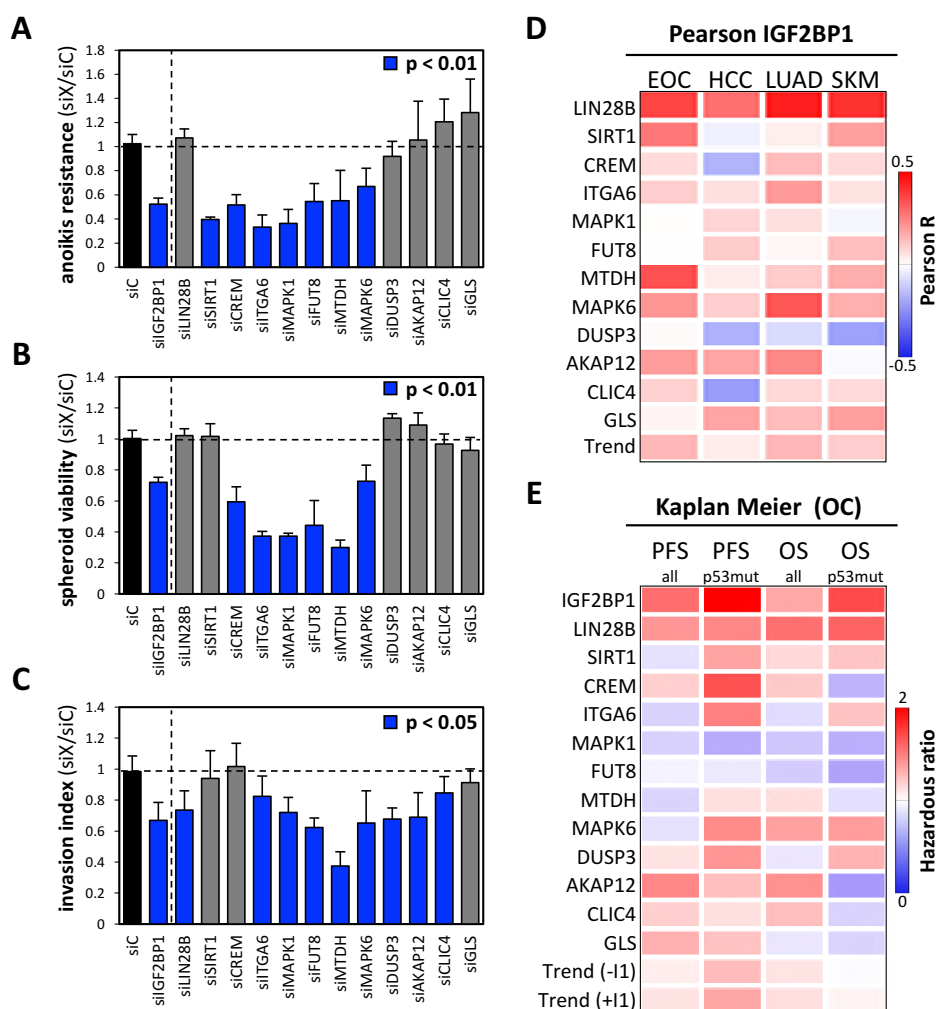
Figure 8. The majority of IGF2BP1's downstream effectors promote 'oncogenic' tumor cell properties. (**A–C**) The indicated tumor cell properties were monitored in 3D-cultured ES-2 cells 72h post-transfection of siRNA pools directed against indicated target mRNAs, as described in Figure 1. Cells transfected with control siRNA (siC) served as control. The anoikis resistance, spheroid viability and invasion index upon the depletion of indicated factors were determined relative to controls (siC; indicated by dashed line). Statistical significance was determined by Student's *t*-test and is indicated by color-coding. (**D**) The co-expression of indicated mRNAs with IGF2BP1 was analyzed by Pearson correlation in TCGA cohorts of ovarian cancer samples (EOC, 304), hepatocellular carcinoma (HCC, 371), lung adenocarcinoma (LUAD, 515) and melanoma (SKM, 470). Pearson correlation coefficients (R) are indicated by a heat map. (**E**) The hazardous ratio (HR) determined by KM plotter for indicated mRNAs using the best cutoff for indicated conditions in ovarian cancer samples is shown by a heat map. Scale bars for correlations (D) and hazardous ratios (E) are indicated in the right panels.

growth (Figure 2), as previously shown for the depletion of IGF2BP1 in HCC-derived HepG2 cells (22). Upon the resection of primary tumors, metastases were only observed when cells expressed IGF2BP1 (Figure 2). These observations provide strong evidence that the protein promotes metastasis as supported by studies in other cancer models (18,20). The depletion of IGF2BP2 as well as 3 interfered with selected tumor cell phenotypes in some of the analyzed cancer-derived cells indicating that their 'onco-

genic potential' varies in a cancer cell-dependent manner. In lung adenocarcinoma- as well as HCC-derived tumor cells (A549 and HepG2), the knockdown of IGF2BP2 impaired spheroid growth and/or anoikis resistance (Figure 3). This supports recent findings indicating that IGF2BP2 enhances the proliferation of tumor cells by promoting the expression of IGF2 and HMGA1 and preserves cancer stem cell phenotypes (24,58). The comparatively moderate conservation of phenotypic effects observed upon IGF2BP3 deple-

tion are surprising in view of the various reports suggesting IGF2BP3 to serve 'oncogenic' roles in tumor cells derived from distinct cancers (16). Notably, however, analyses in the five tumor-derived cell lines analyzed here indicate that IGF2BP3 had the most pronounced phenotypic effect of all three IGF2BPs in lung cancer-derived cells (Figure 3). This supports recent studies reporting that IGF2BP3 promotes an 'aggressive' phenotype of lung cancer-derived cells by attenuating p53 protein stability (51). This potentially indicates that IGF2BP3 has a partially p53-dependent role in some cancer cells. Except A549 and HepG2 cells all of the tumor cells analyzed here were reported to harbor p53 mutations and/or impaired activity. However, the depletion of IGF2BP3 did not impair the analyzed phenotypes in HepG2 cells suggesting that IGF2BP3-dependent regulation of an 'aggressive' tumor cell phenotypes depends on additional yet to determine preconditions. In addition to distinct mutational burden, the observed phenotypic variation is likely associated with substantially distinct IGF2BP paralogue-dependent regulation of mRNA fate. GSEAs that considered differences in transcript abundancies regardless of statistical significance identified mainly the same effector pathways for all three IGF2BPs. However, differential expression of effector transcripts comprised in these pathways varies in a significantly IGF2BP paralogue-dependent manner (Figure 4A and B; Supplementary Figure S4). This suggests that IGF2BPs control partially distinct effector mRNAs, regulate the fate of the same mRNA with varying efficiency and/or control the same mRNA in an opposing manner. Evidence for all these options was observed by comparing differential expression of mRNAs comprised in the GSEA-identified pathways controlled by all three IGF2BPs (Figure 4B; Supplementary Figure S4). Moreover, GAEAs of mRNAs showing significant deregulation upon the paralogue-specific depletion of IGF2BPs suggest partially distinct functions of IGF2BP paralogues based on substantially distinct and paralogue-dependent regulation of mRNA abundance (Supplementary Figure S5A). Despite this variation, all three IGF2BPs preferentially associate with miRNA-targeted mRNAs downregulated upon their depletion suggesting that their main role is the stabilization of target mRNAs (Figure 4E-H; Supplementary Figure S7A–C), as validated here for IGF2BP1 (Figures 4, 5 and 6). Future studies have to characterize the previously proposed variation of RNA-binding properties among IGF2BPs by determining the role of the six RNA-binding domains, two RNA recognition motifs (RRMs) and four HNRNK homology (KH) domains, comprised in all three IGF2BPs (50). Moreover, it needs to be addressed how the relative abundance of IGF2BP paralogues influences their RNA-binding properties and how these are modulated by posttranslational modifications. Together, suchlike studies will likely reveal complex and paralogue-dependent RNA-binding motifs expected in view of up to six partially varying RNA-binding motifs to be considered in IGF2BPs. At the cellular level, future studies need to reveal the conservation of IGF2BP effector transcripts in cancer-derived cells and have to test IGF2BP-dependent regulation of additional phenotypes like metabolic control. This will likely reveal which tumor cell properties are primarily regulated by IGF2BP2 and 3 and which effector

pathways are affected preferentially by these paralogues. Moreover, it remains to be determined if an oncogenic role of IGF2BP2 and 3 is enhanced *in vivo*. *In cellulo* analyses are limited by various means, in particular the lack of tumor-stroma cross-talk. Thus, our studies potentially underestimate the oncogenic potential of IGF2BP2 and 3. With regard of these limitations, the here presented analyses demonstrate that IGF2BP1 has highly conserved oncogenic potential in cancer cells and *in vivo*. These findings indicate that this paralogue is a prime candidate target for therapeutic intervention in distinct solid cancers.

IGF2BP1 promotes an aggressive tumor cell phenotype by 'safe-guarding' miRNA-controlled mRNAs

IGF2BPs were reported to control the transport, translation and turnover of mRNAs in the cytoplasm (15). These regulatory roles are partially interconnected, for instance the regulation of ACTB mRNA localization and its spatially restricted translation in developing neurons (59). However, the most frequently reported IGF2BP-dependent regulation in cancer-derived or transformed cells is the stabilization of mRNAs (40), more precisely the impairment of miRNA-directed degradation of IGF2BP target mRNAs (12,21,28,60). An enhancement of (m)RNA decay by IGF2BPs was only suggested for the lncRNA HULC and the IGF2BP3-dependent stimulation of miRNA-targeting of some IGF2BP3-target mRNAs (21,61). The here presented studies indicate that mRNAs downregulated (DN) upon decreased or lost IGF2BP expression are preferentially bound by these RBPs (Supplementary Figure S7A–C). This supports the view that IGF2BPs mainly impair the degradation of mRNAs. Moreover, DN mRNAs show increased AGO-binding and susceptibility to the regulation by microRNAs expressed in tumor-derived cells (Figure 5A–C). The depletion of microRNAs or the lack of miRNA expression, e.g. let-7a in Huh-7 cells, abolished stabilization by IGF2BP1 target mRNAs (Figures 5D–E and 7). This indicates that IGF2BP1 preferentially impairs the miRNA-directed downregulation of effector mRNAs and thus controls the fate of miR-prone mRNAs in a strictly miRNome-dependent manner. In contrast to other studies favoring a direct coverage of miRNA binding sites (MBS) by IGF2BPs (21,24,28), we show here that IGF2BPs barely cover MBSs directly (Figure 6E). Instead they seem to preferentially associate approximately 40 nucleotides upstream of MBSs. Nonetheless, some MBSs are impaired by the binding of IGF2BP1 at or in proximity to the MBS as demonstrated for the IGF2BP1-dependent regulation of SIRT1 expression (Figure 6A–D). Both, direct coverage as well as regulation without MBS-coverage, is also observed for HuR (62). Moreover, this mode of regulation is compatible with the previously proposed 'safe-guard' hypothesis (12,28). This does not essentially rely on a direct coverage of MBSs but is also consistent with binding-induced conformational changes at MBSs or the sequestering of target mRNAs in protective mRNPs preventing RISC/miRNA-targeting. The latter appears most plausible since the association of IGF2BP1 with RISC/miRNA-bound mRNAs was neither observed by the immunopurification of IGF2BP1 nor AGO2 (Figures 4K and 5G). Fur-

thermore, previous studies indicated that miRNA-regulated target mRNAs of IGF2BP1 are enriched in RISC/miRNA-free mRNPs (12). At least for IGF2BP1, these observations also argue against an enhancement of miRNA-directed targeting of mRNAs upon IGF2BP1-binding, as proposed for some target mRNAs of IGF2BP3 (21). If this would be observed for at least some mRNAs, it would be expected that IGF2BP1-associated mRNA-protein complexes also comprise RISC components like AGO proteins and miRNAs. This, however, was not observed in this or previous studies (12). Finally, AGO CLIP scores in the 3′UTR of mRNAs upregulated upon IGF2BP1 depletion were significantly smaller than observed for transcripts downregulated at reduced IGF2BP1 levels (Figure 4E–G). Although this was also observed for candidate target mRNAs of IGF2BP2 and 3 (Supplementary Figure S7A-C), future studies are required to clarify if and how these paralogues unlike IGF2BP1 potentially promote RISC/miRNA-association of their miRNA-controlled target mRNA. Conceivable are mechanisms by which IGF2BPs promote RISC/miRNA-association upon binding to target transcripts or indirectly by modulating the abundance of regulators of miRNA-dependent regulation, e.g. other RBPs.

The analysis of selected miRNA-controlled effector mRNAs of IGF2BP1 revealed that their depletion impaired at least one of three analyzed tumor cell phenotypes, with one exception (GLS). Consistently, mRNAs downregulated upon IGF2BP1 depletion were enriched for factors with conserved tumor cell fitness relevance (Figure 4D; (54)). Together this indicates that IGF2BP1 promotes an aggressive tumor cell phenotype largely by impairing the miRNA-dependent downregulation of its effector mRNAs. Although these findings need further investigation, this also appears to be the main role of IGF2BP2 and 3 since tumor cell fitness relevance was likewise increased among mRNAs downregulated by the depletion of these paralogues (Supplementary Figure S5B andC). For IGF2BP1, a role in 'safe-guarding' its miRNA-controlled target mRNAs in primary cancer is further on supported by the conserved positive correlation of upregulated expression observed in four primary cancers (Figure 8D). Notably, the cancer cells studied here were derived from the four primary cancer types analyzed in these correlation studies. Thus, the conservation of IGF2BP1's phenotypic roles *in cellulo* is well associated with the co-expression of target mRNAs in the same primary cancer. Finally, elevated expression of IGF2BP1 and its miRNA-regulated effector mRNAs was largely associated with an unfavorable prognosis in p53-mutated serous ovarian carcinomas (Figure 8E). Together this provides strong evidence that the 'safe-guarding' of miRNA-controlled target mRNAs is a major role of IGF2BP1 in tumor cells. Future studies now have to reveal the conservation of this regulation across cancers to develop and evaluate therapeutic strategies aiming at interfering with IGF2BP1-dependent effector networks in cancer.

DATA AVAILABILITY

Total RNA- as well as small RNA-Seq data were deposited at NCBI GEO (GSE109605).

SUPPLEMENTARY DATA

Supplementary Data are available at NAR Online.

REFERENCES

1. Baek,D., Villen,J., Shin,C., Camargo,F.D., Gygi,S.P. and Bartel,D.P. (2008) The impact of microRNAs on protein output. *Nature*, **455**, 64–71.
2. Lin,S. and Gregory,R.I. (2015) MicroRNA biogenesis pathways in cancer. *Nat. Rev. Cancer*, **15**, 321–333.
3. Hayes,J., Peruzzi,P.P. and Lawler,S. (2014) MicroRNAs in cancer: biomarkers, functions and therapy. *Trends Mol. Med.*, **20**, 460–469.
4. Yu,F., Yao,H., Zhu,P., Zhang,X., Pan,Q., Gong,C., Huang,Y., Hu,X., Su,F., Lieberman,J. *et al.* (2007) let-7 regulates self renewal and tumorigenicity of breast cancer cells. *Cell*, **131**, 1109–1123.
5. Lee,Y.S. and Dutta,A. (2007) The tumor suppressor microRNA let-7 represses the HMGA2 oncogene. *Genes Dev.*, **21**, 1025–1030.
6. Boyerinas,B., Park,S.M., Shomron,N., Hedegaard,M.M., Vinther,J., Andersen,J.S., Feig,C., Xu,J., Burge,C.B. and Peter,M.E. (2008) Identification of let-7-regulated oncofetal genes. *Cancer Res.*, **68**, 2587–2591.
7. Sampson,V.B., Rong,N.H., Han,J., Yang,Q., Aris,V., Soteropoulos,P., Petrelli,N.J., Dunn,S.P. and Krueger,L.J. (2007) MicroRNA let-7a down-regulates MYC and reverts MYC-induced growth in Burkitt lymphoma cells. *Cancer Res.*, **67**, 9762–9770.
8. Balzeau,J., Menezes,M.R., Cao,S. and Hagan,J.P. (2017) The LIN28/let-7 Pathway in Cancer. *Front. Genet.*, **8**, 31.
9. van Jaarsveld,M.T., Helleman,J., Berns,E.M. and Wiemer,E.A. (2010) MicroRNAs in ovarian cancer biology and therapy resistance. *Int. J. Biochem. Cell Biol.*, **42**, 1282–1290.
10. Mayr,C. and Bartel,D.P. (2009) Widespread shortening of 3′UTRs by alternative cleavage and polyadenylation activates oncogenes in cancer cells. *Cell*, **138**, 673–684.
11. Mayr,C., Hemann,M.T. and Bartel,D.P. (2007) Disrupting the pairing between let-7 and Hmga2 enhances oncogenic transformation. *Science*, **315**, 1576–1579.
12. Busch,B., Bley,N., Muller,S., Glass,M., Misiak,D., Lederer,M., Vetter,M., Strauss,H.G., Thomssen,C. and Huttelmaier,S. (2016) The oncogenic triangle of HMGA2, LIN28B and IGF2BP1 antagonizes tumor-suppressive actions of the let-7 family. *Nucleic Acids Res.*, **44**, 3845–3864.
13. Powers,J.T., Tsanov,K.M., Pearson,D.S., Roels,F., Spina,C.S., Ebright,R., Seligson,M., de Soysa,Y., Cahan,P., Theissen,J. *et al.* (2016) Multiple mechanisms disrupt the let-7 microRNA family in neuroblastoma. *Nature*, **535**, 246–251.
14. van Kouwenhove,M., Kedde,M. and Agami,R. (2011) MicroRNA regulation by RNA-binding proteins and its implications for cancer. *Nat. Rev. Cancer*, **11**, 644–656.

15. Bell,J.L., Wachter,K., Muhleck,B., Pazaitis,N., Kohn,M., Lederer,M. and Huttelmaier,S. (2013) Insulin-like growth factor 2 mRNA-binding proteins (IGF2BPs): post-transcriptional drivers of cancer progression? *Cell. Mol. Life Sci.*, **70**, 2657–2675.

16. Lederer,M., Bley,N., Schleifer,C. and Huttelmaier,S. (2014) The role of the oncofetal IGF2 mRNA-binding protein 3 (IGF2BP3) in cancer. *Semin. Cancer Biol.*, **29**, 3–12.

17. Kobel,M., Weidensdorfer,D., Reinke,C., Lederer,M., Schmitt,W.D., Zeng,K., Thomssen,C., Hauptmann,S. and Huttelmaier,S. (2007) Expression of the RNA-binding protein IMP1 correlates with poor prognosis in ovarian carcinoma. *Oncogene*, **26**, 7584–7589.

18. Craig,E.A., Weber,J.D. and Spiegelman,V.S. (2012) Involvement of the mRNA binding protein CRD-BP in the regulation of metastatic melanoma cell proliferation and invasion by hypoxia. *J. Cell Sci.*, **125**, 5950–5954.

19. Stohr,N., Kohn,M., Lederer,M., Glass,M., Reinke,C., Singer,R.H. and Huttelmaier,S. (2012) IGF2BP1 promotes cell migration by regulating MK5 and PTEN signaling. *Genes Dev.*, **26**, 176–189.

20. Hamilton,K.E., Noubissi,F.K., Katti,P.S., Hahn,C.M., Davey,S.R., Lundsmith,E.T., Klein-Szanto,A.J., Rhim,A.D., Spiegelman,V.S. and Rustgi,A.K. (2013) IMP1 promotes tumor growth, dissemination and a tumor-initiating cell phenotype in colorectal cancer cell xenografts. *Carcinogenesis*, **34**, 2647–2654.

21. Ennajdaoui,H., Howard,J.M., Sterne-Weiler,T., Jahanbani,F., Coyne,D.J., Uren,P.J., Dargyte,M., Katzman,S., Draper,J.M., Wallace,A. *et al.* (2016) IGF2BP3 modulates the interaction of invasion-associated transcripts with RISC. *Cell Rep.*, **15**, 1876–1883.

22. Gutschner,T., Hammerle,M., Pazaitis,N., Bley,N., Fiskin,E., Uckelmann,H., Heim,A., Grobeta,M., Hofmann,N., Geffers,R. *et al.* (2014) Insulin-like growth factor 2 mRNA-binding protein 1 (IGF2BP1) is an important protumorigenic factor in hepatocellular carcinoma. *Hepatology*, **59**, 1900–1911.

23. Noubissi,F.K., Nikiforov,M.A., Colburn,N. and Spiegelman,V.S. (2010) Transcriptional Regulation of CRD-BP by c-myc: Implications for c-myc Functions. *Genes Cancer*, **1**, 1074–1082.

24. Degrauwe,N., Schlumpf,T.B., Janiszewska,M., Martin,P., Cauderay,A., Provero,P., Riggi,N., Suva,M.L., Paro,R. and Stamenkovic,I. (2016) The RNA binding protein IMP2 preserves glioblastoma stem cells by preventing let-7 target gene silencing. *Cell Rep.*, **15**, 1634–1647.

25. Degrauwe,N., Suva,M.L., Janiszewska,M., Riggi,N. and Stamenkovic,I. (2016) IMPs: an RNA-binding protein family that provides a link between stem cell maintenance in normal development and cancer. *Genes Dev.*, **30**, 2459–2474.

26. Nishino,J., Kim,S., Zhu,Y., Zhu,H. and Morrison,S.J. (2013) A network of heterochronic genes including Imp1 regulates temporal changes in stem cell properties. *Elife*, **2**, e00924.

27. JnBaptiste,C.K., Gurtan,A.M., Thai,K.K., Lu,V., Bhutkar,A., Su,M.J., Rotem,A., Jacks,T. and Sharp,P.A. (2017) Dicer loss and recovery induce an oncogenic switch driven by transcriptional activation of the oncofetal Imp1-3 family. *Genes Dev.*, **31**, 674–687.

28. Jonson,L., Christiansen,J., Hansen,T.V., Vikesa,J., Yamamoto,Y. and Nielsen,F.C. (2014) IMP3 RNP safe houses prevent miRNA-directed HMGA2 mRNA decay in cancer and development. *Cell Rep.*, **7**, 539–551.

29. Kobel,M., Xu,H., Bourne,P.A., Spaulding,B.O., Shih Ie,M., Mao,T.L., Soslow,R.A., Ewanowich,C.A., Kalloger,S.E., Mehl,E. *et al.* (2009) IGF2BP3 (IMP3) expression is a marker of unfavorable prognosis in ovarian carcinoma of clear cell subtype. *Mod. Pathol.*, **22**, 469–475.

30. Davidson,B., Rosenfeld,Y.B., Holth,A., Hellesylt,E., Trope,C.G., Reich,R. and Yisraeli,J.K. (2014) VICKZ2 protein expression in ovarian serous carcinoma effusions is associated with poor survival. *Hum. Pathol.*, **45**, 1520–1528.

31. Braun,J., Misiak,D., Busch,B., Krohn,K. and Huttelmaier,S. (2014) Rapid identification of regulatory microRNAs by miTRAP (miRNA trapping by RNA in vitro affinity purification). *Nucleic Acids Res.*, **42**, e66.

32. Kohn,M., Ihling,C., Sinz,A., Krohn,K. and Huttelmaier,S. (2015) The Y3** ncRNA promotes the 3′ end processing of histone mRNAs. *Genes Dev.*, **29**, 1998–2003.

33. Kim,D., Pertea,G., Trapnell,C., Pimentel,H., Kelley,R. and Salzberg,S.L. (2013) TopHat2: accurate alignment of transcriptomes in the presence of insertions, deletions and gene fusions. *Genome Biol.*, **14**, R36.

34. Langmead,B. and Salzberg,S.L. (2012) Fast gapped-read alignment with Bowtie 2. *Nat. Methods*, **9**, 357–359.

35. Liao,Y., Smyth,G.K. and Shi,W. (2014) featureCounts: an efficient general purpose program for assigning sequence reads to genomic features. *Bioinformatics*, **30**, 923–930.

36. Cunningham,F., Amode,M.R., Barrell,D., Beal,K., Billis,K., Brent,S., Carvalho-Silva,D., Clapham,P., Coates,G., Fitzgerald,S. *et al.* (2015) Ensembl 2015. *Nucleic Acids Res.*, **43**, D662–D669.

37. Kozomara,A. and Griffiths-Jones,S. (2014) miRBase: annotating high confidence microRNAs using deep sequencing data. *Nucleic Acids Res.*, **42**, D68–D73.

38. Robinson,M.D., McCarthy,D.J. and Smyth,G.K. (2010) edgeR: a Bioconductor package for differential expression analysis of digital gene expression data. *Bioinformatics*, **26**, 139–140.

39. Ru,Y., Kechris,K.J., Tabakoff,B., Hoffman,P., Radcliffe,R.A., Bowler,R., Mahaffey,S., Rossi,S., Calin,G.A., Bemis,L. *et al.* (2014) The multiMiR R package and database: integration of microRNA-target interactions along with their disease and drug associations. *Nucleic Acids Res.*, **42**, e133.

40. Hafner,M., Landthaler,M., Burger,L., Khorshid,M., Hausser,J., Berninger,P., Rothballer,A., Ascano,M. Jr, Jungkamp,A.C., Munschauer,M. *et al.* (2010) Transcriptome-wide identification of RNA-binding protein and microRNA target sites by PAR-CLIP. *Cell*, **141**, 129–141.

41. Van Nostrand,E.L., Pratt,G.A., Shishkin,A.A., Gelboin-Burkhart,C., Fang,M.Y., Sundararaman,B., Blue,S.M., Nguyen,T.B., Surka,C., Elkins,K. *et al.* (2016) Robust transcriptome-wide discovery of RNA-binding protein binding sites with enhanced CLIP (eCLIP). *Nat. Methods*, **13**, 508–514.

42. Conway,A.E., Van Nostrand,E.L., Pratt,G.A., Aigner,S., Wilbert,M.L., Sundararaman,B., Freese,P., Lambert,N.J., Sathe,S., Liang,T.Y. *et al.* (2016) Enhanced CLIP uncovers IMP Protein-RNA targets in human pluripotent stem cells important for cell adhesion and survival. *Cell Rep.*, **15**, 666–679.

43. Gottwein,E., Corcoran,D.L., Mukherjee,N., Skalsky,R.L., Hafner,M., Nusbaum,J.D., Shamulailatpam,P., Love,C.L., Dave,S.S., Tuschl,T. *et al.* (2011) Viral microRNA targetome of KSHV-infected primary effusion lymphoma cell lines. *Cell Host Microbe*, **10**, 515–526.

44. Kishore,S., Jaskiewicz,L., Burger,L., Hausser,J., Khorshid,M. and Zavolan,M. (2011) A quantitative analysis of CLIP methods for identifying binding sites of RNA-binding proteins. *Nat. Methods*, **8**, 559–564.

45. Skalsky,R.L., Corcoran,D.L., Gottwein,E., Frank,C.L., Kang,D., Hafner,M., Nusbaum,J.D., Feederle,R., Delecluse,H.J., Luftig,M.A. *et al.* (2012) The viral and cellular microRNA targetome in lymphoblastoid cell lines. *PLoS Pathog.*, **8**, e1002484.

46. Subramanian,A., Tamayo,P., Mootha,V.K., Mukherjee,S., Ebert,B.L., Gillette,M.A., Paulovich,A., Pomeroy,S.L., Golub,T.R., Lander,E.S. *et al.* (2005) Gene set enrichment analysis: a knowledge-based approach for interpreting genome-wide expression profiles. *Proc. Natl. Acad. Sci. U.S.A.*, **102**, 15545–15550.

47. Wurth,L., Papasaikas,P., Olmeda,D., Bley,N., Calvo,G.T., Guerrero,S., Cerezo-Wallis,D., Martinez-Useros,J., Garcia-Fernandez,M., Huttelmaier,S. *et al.* (2016) UNR/CSDE1 drives a post-transcriptional program to promote melanoma invasion and metastasis. *Cancer Cell*, **30**, 694–707.

48. Lanczky,A., Nagy,A., Bottai,G., Munkacsy,G., Szabo,A., Santarpia,L. and Gyorffy,B. (2016) miRpower: a web-tool to validate survival-associated miRNAs utilizing expression data from 2178 breast cancer patients. *Breast Cancer Res. Treat.*, **160**, 439–446.

49. Domcke,S., Sinha,R., Levine,D.A., Sander,C. and Schultz,N. (2013) Evaluating cell lines as tumour models by comparison of genomic profiles. *Nat. Commun.*, **4**, 2126.

50. Wachter,K., Kohn,M., Stohr,N. and Huttelmaier,S. (2013) Subcellular localization and RNP formation of IGF2BPs (IGF2 mRNA-binding proteins) is modulated by distinct RNA-binding domains. *Biol. Chem.*, **394**, 1077–1090.

51. Zhao,W., Lu,D., Liu,L., Cai,J., Zhou,Y., Yang,Y., Zhang,Y. and Zhang,J. (2017) Insulin-like growth factor 2 mRNA binding protein 3 (IGF2BP3) promotes lung tumorigenesis via attenuating p53 stability. *Oncotarget*, **8**, 93672–93687.

52. Zirkel,A., Lederer,M., Stohr,N., Pazaitis,N. and Huttelmaier,S. (2013) IGF2BP1 promotes mesenchymal cell properties and migration of tumor-derived cells by enhancing the expression of LEF1 and SNAI2 (SLUG). *Nucleic Acids Res.*, **41**, 6618–6636.

53. Mongroo,P.S., Noubissi,F.K., Cuatrecasas,M., Kalabis,J., King,C.E., Johnstone,C.N., Bowser,M.J., Castells,A., Spiegelman,V.S. and Rustgi,A.K. (2011) IMP-1 displays cross-talk with K-Ras and modulates colon cancer cell survival through the novel proapoptotic protein CYFIP2. *Cancer Res.*, **71**, 2172–2182.

54. Hart,T., Chandrashekhar,M., Aregger,M., Steinhart,Z., Brown,K.R., MacLeod,G., Mis,M., Zimmermann,M., Fradet-Turcotte,A., Sun,S. *et al.* (2015) High-resolution CRISPR screens reveal fitness genes and genotype-specific cancer liabilities. *Cell*, **163**, 1515–1526.

55. Elcheva,I., Tarapore,R.S., Bhatia,N. and Spiegelman,V.S. (2008) Overexpression of mRNA-binding protein CRD-BP in malignant melanomas. *Oncogene*, **27**, 5069–5074.

56. Elkhadragy,L., Chen,M., Miller,K., Yang,M.H. and Long,W. (2017) A regulatory BMI1/let-7i/ERK3 pathway controls the motility of head and neck cancer cells. *Mol. Oncol.*, **11**, 194–207.

57. Xu,D., Takeshita,F., Hino,Y., Fukunaga,S., Kudo,Y., Tamaki,A., Matsunaga,J., Takahashi,R.U., Takata,T., Shimamoto,A. *et al.* (2011) miR-22 represses cancer progression by inducing cellular senescence. *J. Cell Biol.*, **193**, 409–424.

58. Dai,N., Ji,F., Wright,J., Minichiello,L., Sadreyev,R. and Avruch,J. (2017) IGF2 mRNA binding protein-2 is a tumor promoter that drives cancer proliferation through its client mRNAs IGF2 and HMGA1. *Elife*, **6**, e27155.

59. Huttelmaier,S., Zenklusen,D., Lederer,M., Dictenberg,J., Lorenz,M., Meng,X., Bassell,G.J., Condeelis,J. and Singer,R.H. (2005) Spatial regulation of beta-actin translation by Src-dependent phosphorylation of ZBP1. *Nature*, **438**, 512–515.

60. Elcheva,I., Goswami,S., Noubissi,F.K. and Spiegelman,V.S. (2009) CRD-BP protects the coding region of betaTrCP1 mRNA from miR-183-mediated degradation. *Mol. Cell*, **35**, 240–246.

61. Hammerle,M., Gutschner,T., Uckelmann,H., Ozgur,S., Fiskin,E., Gross,M., Skawran,B., Geffers,R., Longerich,T., Breuhahn,K. *et al.* (2013) Posttranscriptional destabilization of the liver-specific long noncoding RNA HULC by the IGF2 mRNA-binding protein 1 (IGF2BP1). *Hepatology*, **58**, 1703–1712.

62. Li,Y., Estep,J.A. and Karginov,F.V. (2018) Transcriptome-wide identification and validation of interactions between the miRNA machinery and HuR on mRNA targets. *J. Mol. Biol.*, **430**, 285–296.

Müller et al., 2018 - SUPPLEMENTARY FIGURE LEGENDS

Supplementary Figure S1. Prognostic relevance of IGF2BPs in ovarian cancer. (**A**) Kaplan Meier (KM) analyses of all three IGF2BPs in serous ovarian carcinomas were performed by KM plotter. KM plots for overall survival (OS, *upper panel*) were determined in all serous ovarian carcinoma samples available via KM plotter. KM plots for progression free survival (PFS, *middle panel*) were determined in all serous ovarian carcinoma samples available. KM plots for serous ovarian cancer with mutated p53 is shown in the bottom panel. Hazardous ratios (HR) and statistical significance determined by KM plotter are indicated in the plots. The number of samples considered by KM plotter in best cut-off analyses are indicated below plots. (**B**) The expression of IGF2BP mRNAs in ovarian cancer-derived cells was analyzed by RNA-seq data (FPKM) provided by the cancer cell line encyclopedia (CCLE). Expression of IGF2BP paralogues in ES-2 cells is indicated by red symbols. (**C**) Representative Western blot analyses of parental ES-2 cells (WT), a ES-2 control clone (C-1) and two IGF2BP1- (sgI1, *upper panel*) or IGF2BP3-deleted (sgI3, *lower panel*) ES-2 clones. GAPDH or VCL served as loading controls.

Supplementary Figure S2. IGF2BP1 promotes oncogenic tumor cell properties. (**A**) The invasive potential of spheroids derived from IGF2BP1-deleted ES-2 cells (sgI1-1) expressing GFP, GFP-IGF2BP1 (GFP-I1) or an RNA-binding deficient mutant of IGF2BP1 (GFP-I1mut) was determined as described in (Figure 1G). The expression of GFP-fused proteins is shown in Figure 4K. The deletion of IGF2BP1 is shown in Figure S1C. (**B**) The speed of cell migration of ES-2 cells overexpressing GFP or indicated GFP-tagged IGF2BP paralogues (GFP-I1/2/3) was determined in 3D-collagen matrices (4 mg/ml) over 10h starting 60h post-transfection with indicated siRNAs for n > 50 cells per condition. (**C-E**) The spheroid viability (C), anoikis-resistance (D) and spheroid invasion (E) of GFP or GFP-IGF2BP1 (GFP-I1) overexpressing ES-2 cells were determined as described in (Figure 1D, E and G). Statistical significance was determined by Student's t-test: (*) P < 0.05; (**) P < 0.01; (***) P < 0.001.

Supplementary Figure S3. IGF2BP paralogue-specific regulation of RNA abundance in ES-2 cells. (**A-I**) Differential mRNA (A, D, G), lncRNA (B, E, H) and miRNA (C, F, I) expression (relative to siC-

transfected cells) was determined by RNA-sequencing in ES-2 cells upon IGF2BP1 (A-C), IGF2BP2 (D-F) or IGF2BP3 (G-I) depletion using siRNA pools. The FDR values and $\log_2$ fold changes of downregulated (DN, blue, FDR<0.1), upregulated (UP, red, FDR<0.1) or unchanged (black, FDR>0.1) transcripts are indicated by volcano blots. For RNA-sequencing data and DE transcripts refer to supplementary tables T1A/B.

Supplementary Figure S4. IGF2BPs regulate similar pathways in a paralogue-dependent manner. (**A, D, G**) The overlap of the "leading edge" subset mRNAs contained in the indicated pathway gene sets identified by GSEA upon the paralogue-specific depletion of IGF2BPs is indicated by Venn diagrams. For GSEA refer to supplementary table T1C. (**B, E, H**) The correlation of $\log_2$ fold changes (FC) determined upon the paralogue-specific depletion of IGF2BPs was analyzed by Pearson correlation for mRNAs comprised in indicated GSEA-identified pathway gene sets. Pearson correlation coefficients (R_P) and significance of correlation (P) are indicated. (**C, F, I**) The $\log_2$ fold change of mRNAs comprised in indicated GSEA-identified hallmark gene sets determined upon the depletion of IGF2BP paralogues is indicated by heat maps. Note that mRNAs are sorted according to fold changes determined by RNA-sequencing upon IGF2BP1 depletion. Scale bars indicating $\log_2$ FC are indicated in right panels. (**J**) Representative Western blot analysis of indicated proteins upon control (siC), IGF2BP1 (siI1), IGF2BP2 (siI2) or IGF2BP3 (siI3) depletion in ES-2 cells using siRNA pools. VCL served as loading control. (**K**) FPKM values determined for the KRAS mRNA by RNA-sequencing upon control (siC), IGF2BP1 (siI1), IGF2BP2 (siI2) or IGF2BP3 (siI3) depletion in ES-2 cells is shown as bar diagram. Error bars indicate standard deviation.

Supplementary Figure S5. IGF2BP1 regulates the expression of mRNAs associated with cell migration and tumor cell fitness. (**A**) mRNAs showing significant (FDR<0.1) deregulation upon the depletion of IGF2BP1 (siI1, *upper panel*), IGF2BP2 (siI2, *middle panel*) or IGF2BP3 (siI3, *lower panel*) were analyzed by gene annotation enrichment analysis (GAEA) using DAVID and Gene Ontology (GO-) terms for biological processes. The determined p-values and percentage of deregulated genes comprised under the respective GO terms are indicated for the top-five GO-terms identified among DN (blue) or UP (red) transcripts identified by IGF2BP depletion in ES-2 cells. For GO-term analyses also refer to supplementary table T1D. (**B, C**) Averaged and

normalized Bayesian fitness values (B) as well as Fitness scores (C) determined for genes in five tumor-derived cells by Hart et al. (52) are shown for DE mRNAs identified by the depletion of IGF2BP paralogues in ES-2 cells. The dashed line in (B) indicates the threshold of significant fitness relevance determined in (52).

Supplementary Figure S6. Analysis of IGF2BP1 mRNA binding by the conservation of CLIP sites in distinct cell lines. CLIP sites derived from eight CLIP analyses were collected and mapped to all human genes (RefSeq hg19). CLIP scores (also see material and methods) were defined as the number of experiments reporting CLIP sites for IGF2BP1 in a specific transcript or cis-element (5'UTR/CDS/3'UTR/introns). (**A**) Distribution of reported IGF2BP1 CLIP sites across the last exon of LIN28B. The top panel shows the number of overlapping CLIP sites per base pair. (**B**) Distribution of IGF2BP1 CLIP scores among protein-coding and non-coding genes. Genes known to harbor coding as well as non-coding transcripts expressed from their *loci* were not considered since the unambiguous association of CLIP sites with specific transcripts would be biased substantially. (**C**) The numbers of overlapping genes that showed maximum CLIP scores (8) for the respective cis-element is indicated by a Venn diagram. (**D-H**) The number of IGF2BP1 binding-motifs suggested by CLIP studies in the longest reported (RefSeq hg19) 3'UTR sequences of mRNAs unaffected (C) and significantly up- or downregulated upon IGF2BP1 depletion are depicted by box plots. The absolute frequency of motif occurrences was normalized to 3'UTR length. UGUG served as a control motif. Statistical significance was determined by Mann-Whitney U-test: (***) P < 0.001.

Supplementary Figure S7. IGF2BP- and AGO-association is enhanced among mRNAs downregulated by IGF2BP depletion. (**A-C**) IGF2BP and AGO CLIP scores determined in indicated cis-elements of mRNAs down- (DN) or upregulated (UP) upon the depletion of IGF2BPs in ES-2 cells are shown by box plots. For CLIP score calculation refer to materials and methods. (**D**) The expression of indicated IGF2BP1 target mRNAs was determined in IGF2BP1-deleted ES-2 cells re-expressing GFP, GFP-IGF2BP1 or a RNA-binding deficient IGF2BP1 (GFP-I1mut) using RT-qPCR. The abundance of mRNAs in GFP-IGF2BP1 expressing cells is shown relative to mRNA levels observed in GFP and GFP-I1mut expressing cells. ACTB mRNA levels served as normalization controls.

HIST1H2AC and RPLP0 mRNAs served as negative controls. Statistical significance was determined by Mann-Whitney's U-test: (*) $P < 0.05$; (**)$P < 0.01$; (***) $P < 0.001$; indicated by color-coding in (D).

Supplementary Figure S8. Phenotypic effects of IGF2BP1's downstream effectors. (**A**) The knockdown efficiency of IGF2BP1 and its effector mRNAs was monitored by RT-qPCR. ES-2 cells were transfected with indicated siRNA pools for 72h. RNA ratios were determined relative to cells transfected with control siRNAs using ACTB for internal normalization. Statistical significance was determined by Student's t-test as indicated by color-coding. (**B-D**) Representative images of spheroids/cells analyzed as described in Figure 8.

Müller et al., 2018 - Supplementary Figure S1
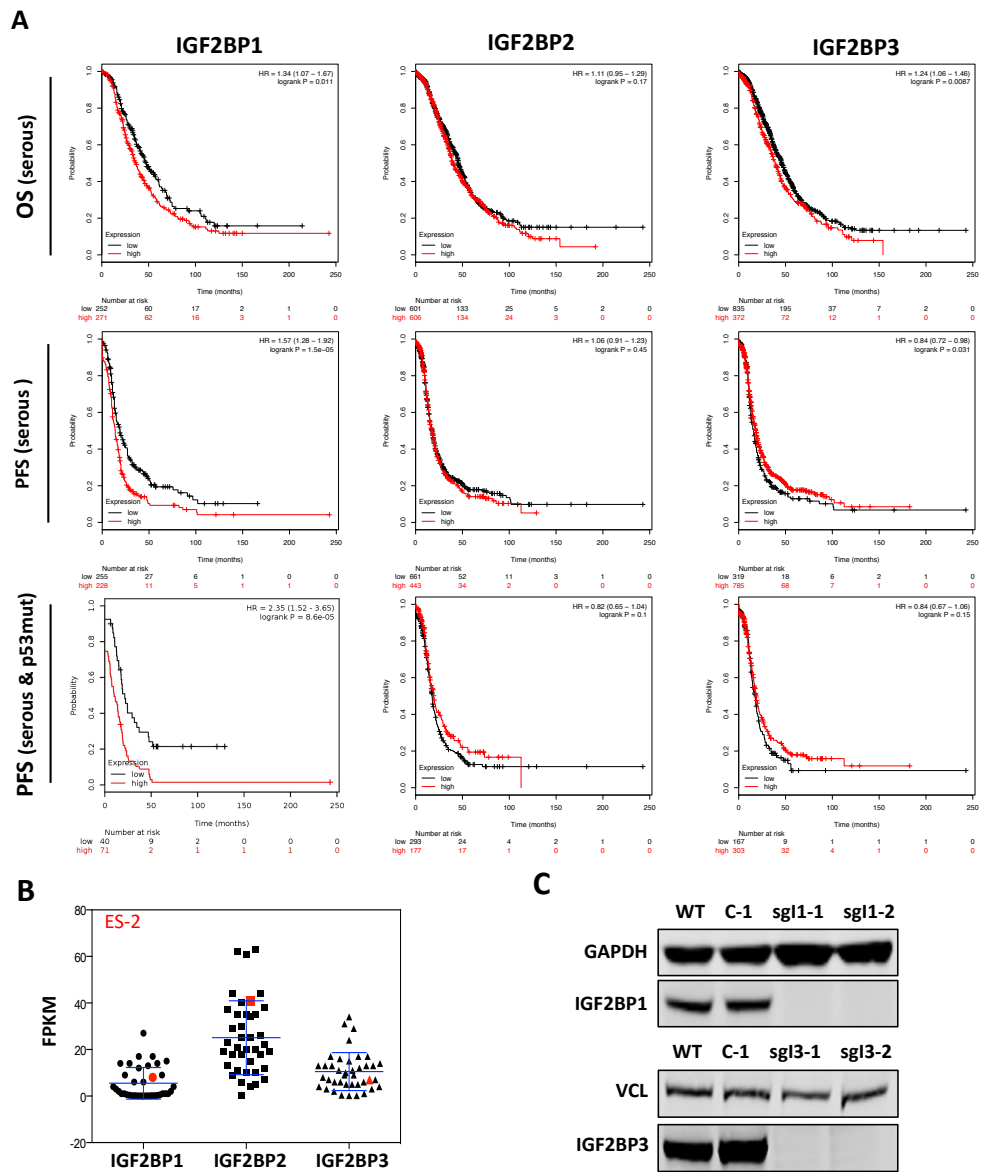
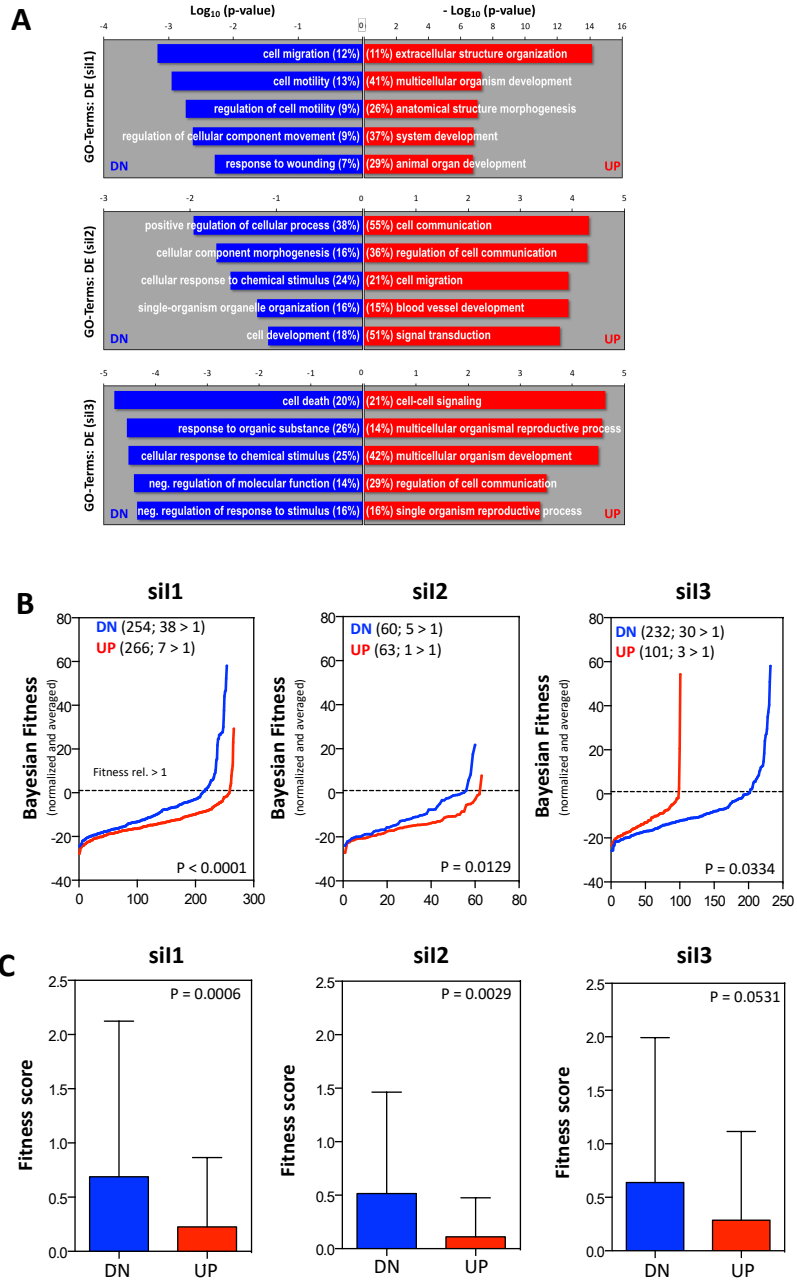**Müller et al., 2018 - Supplementary Figure S2**
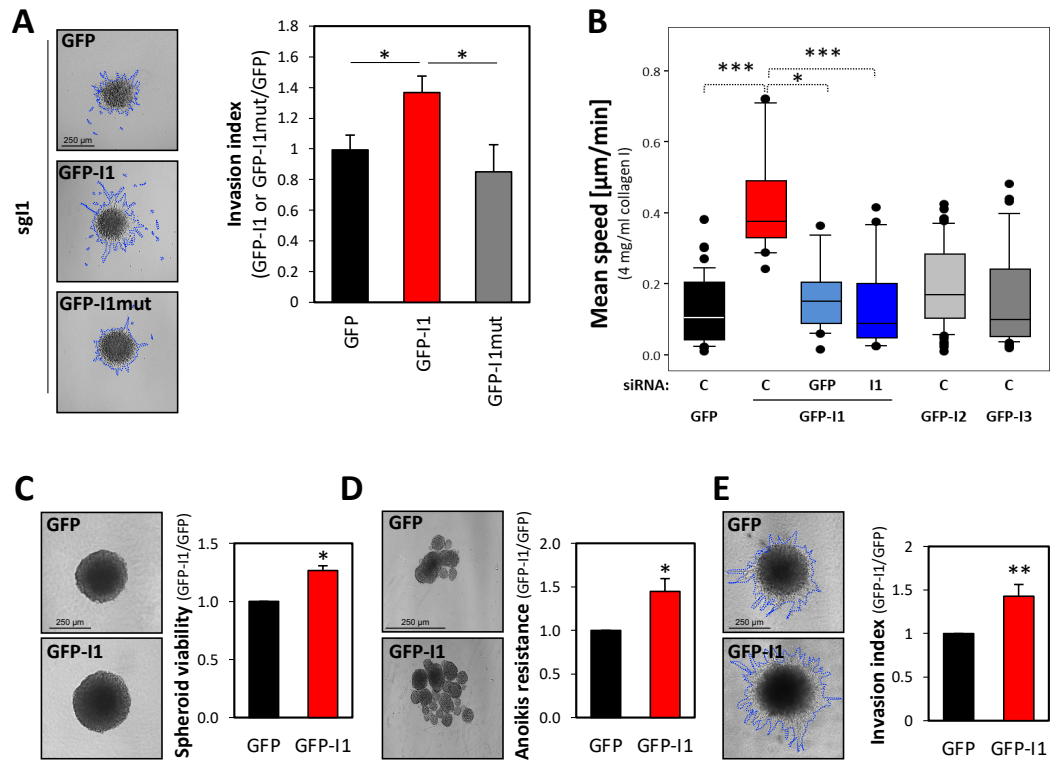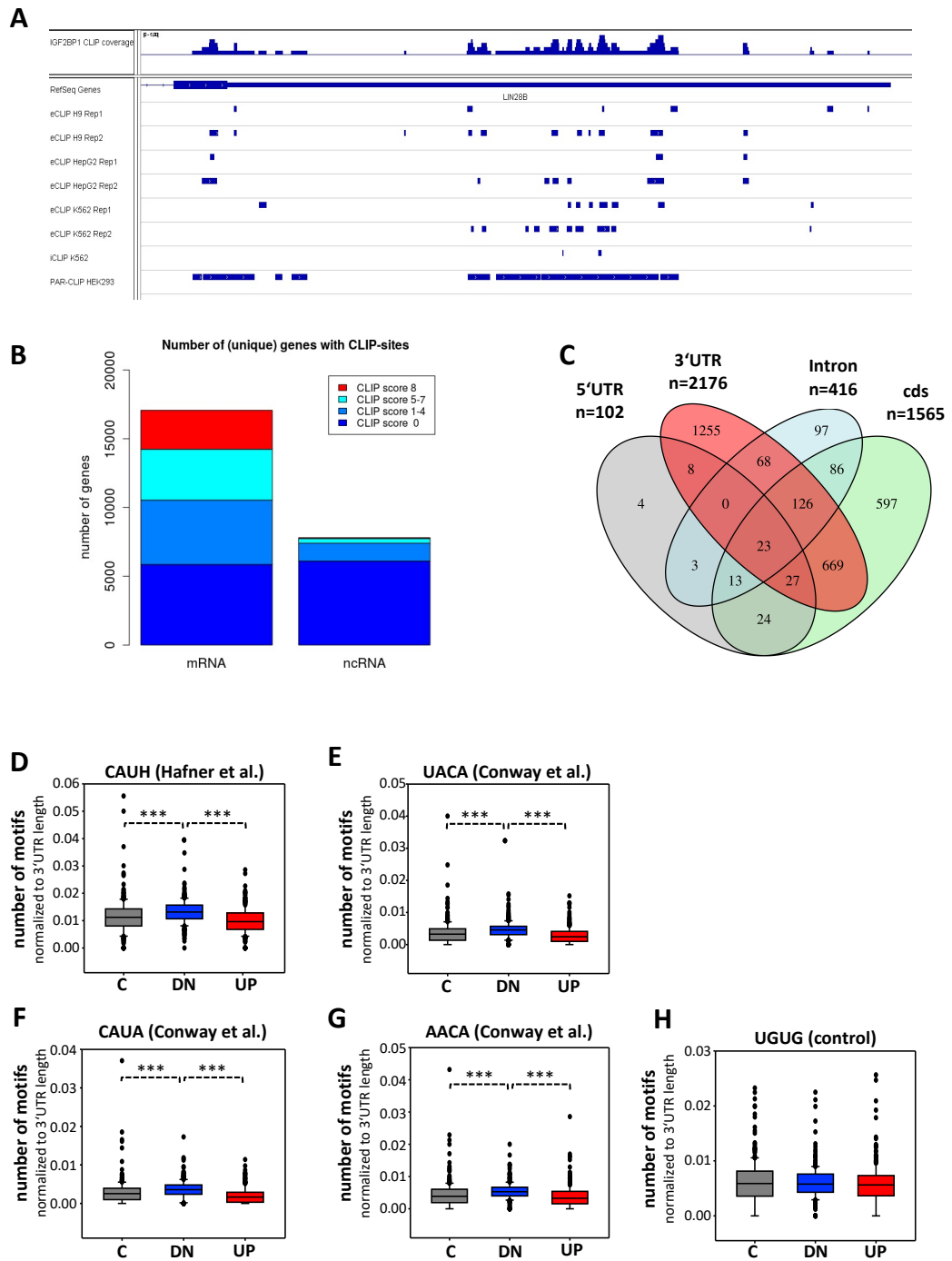
Müller et al., 2018 - Supplementary Figure S3
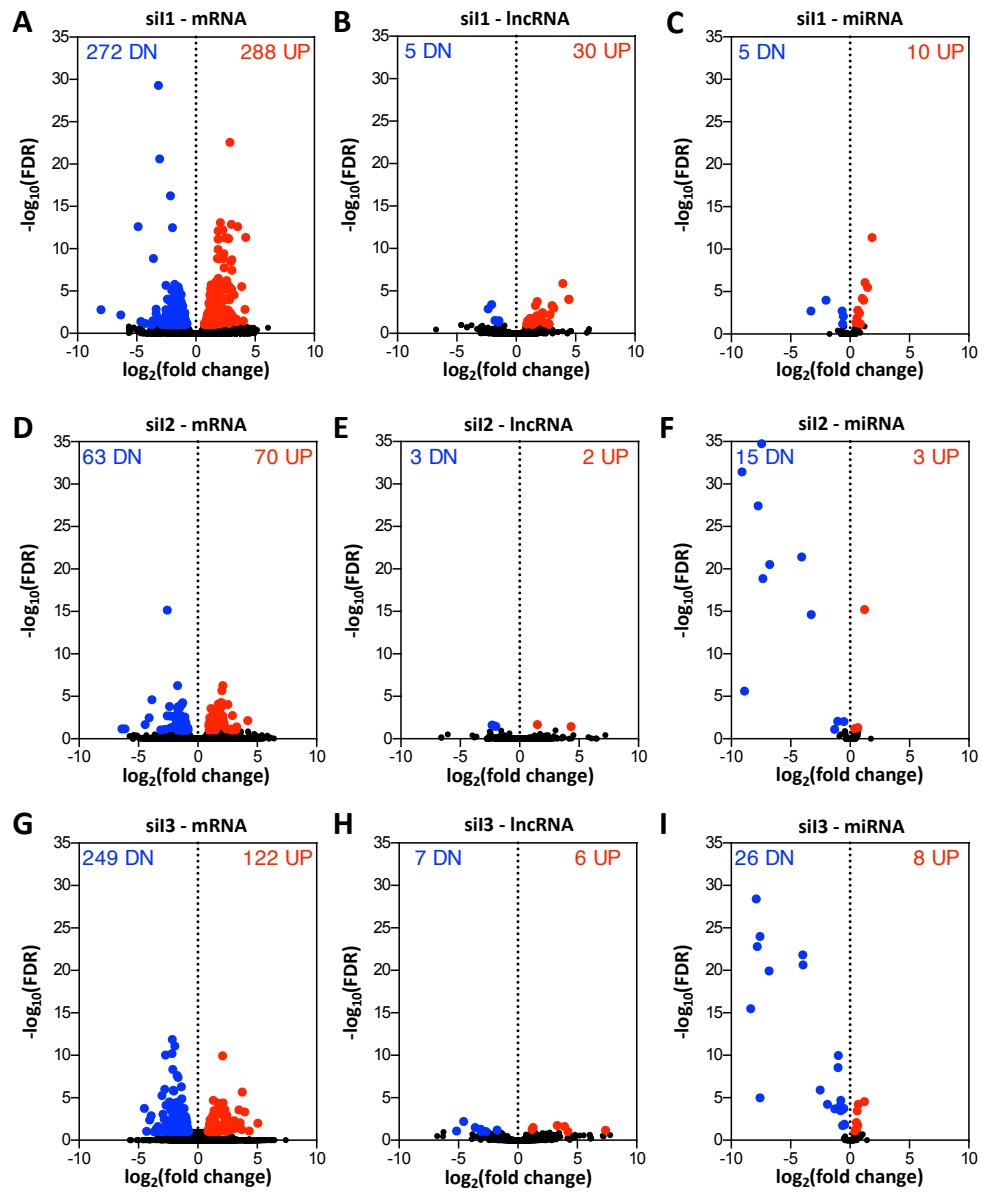
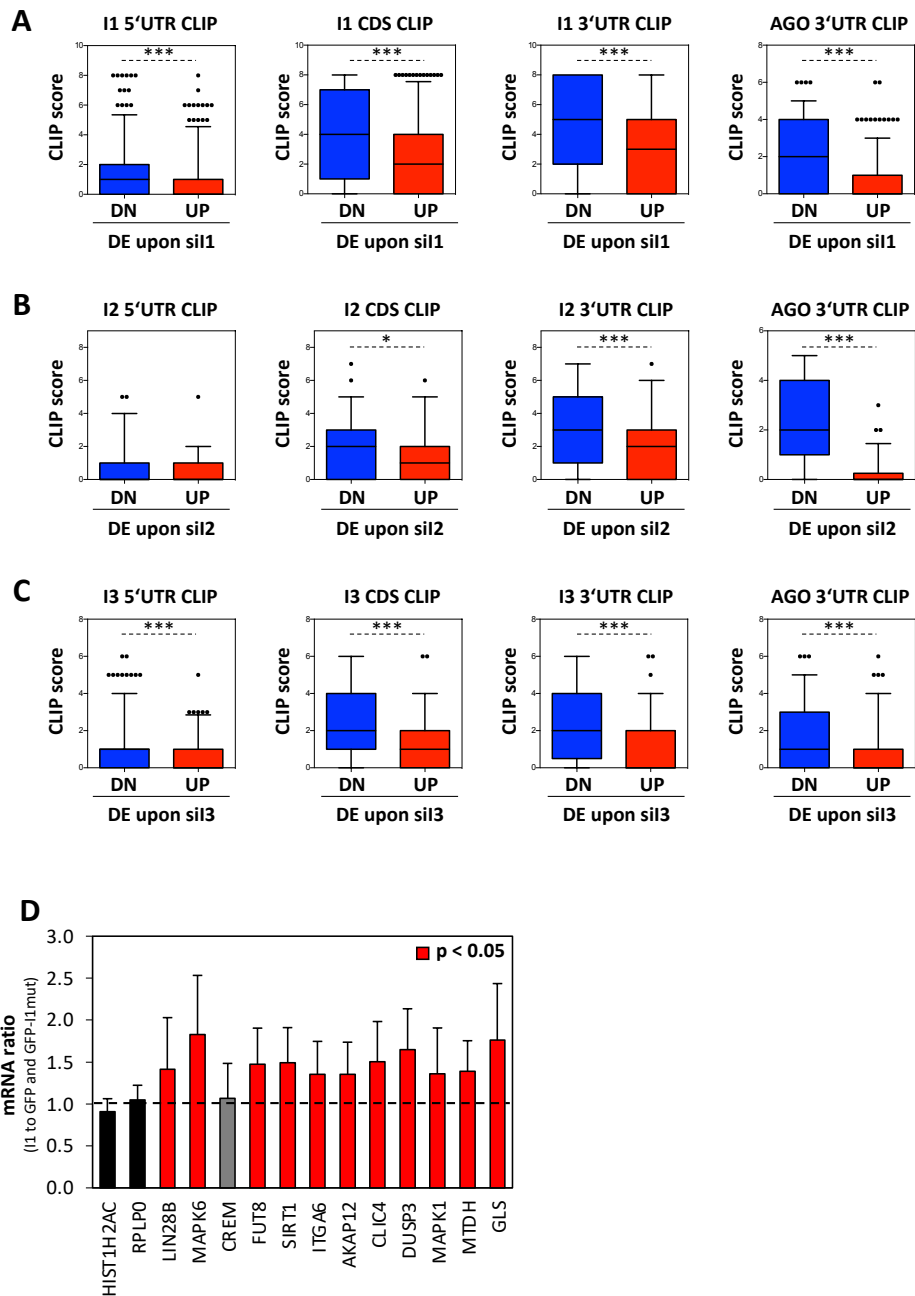## Müller et al., 2018 - Supplementary Figure S4
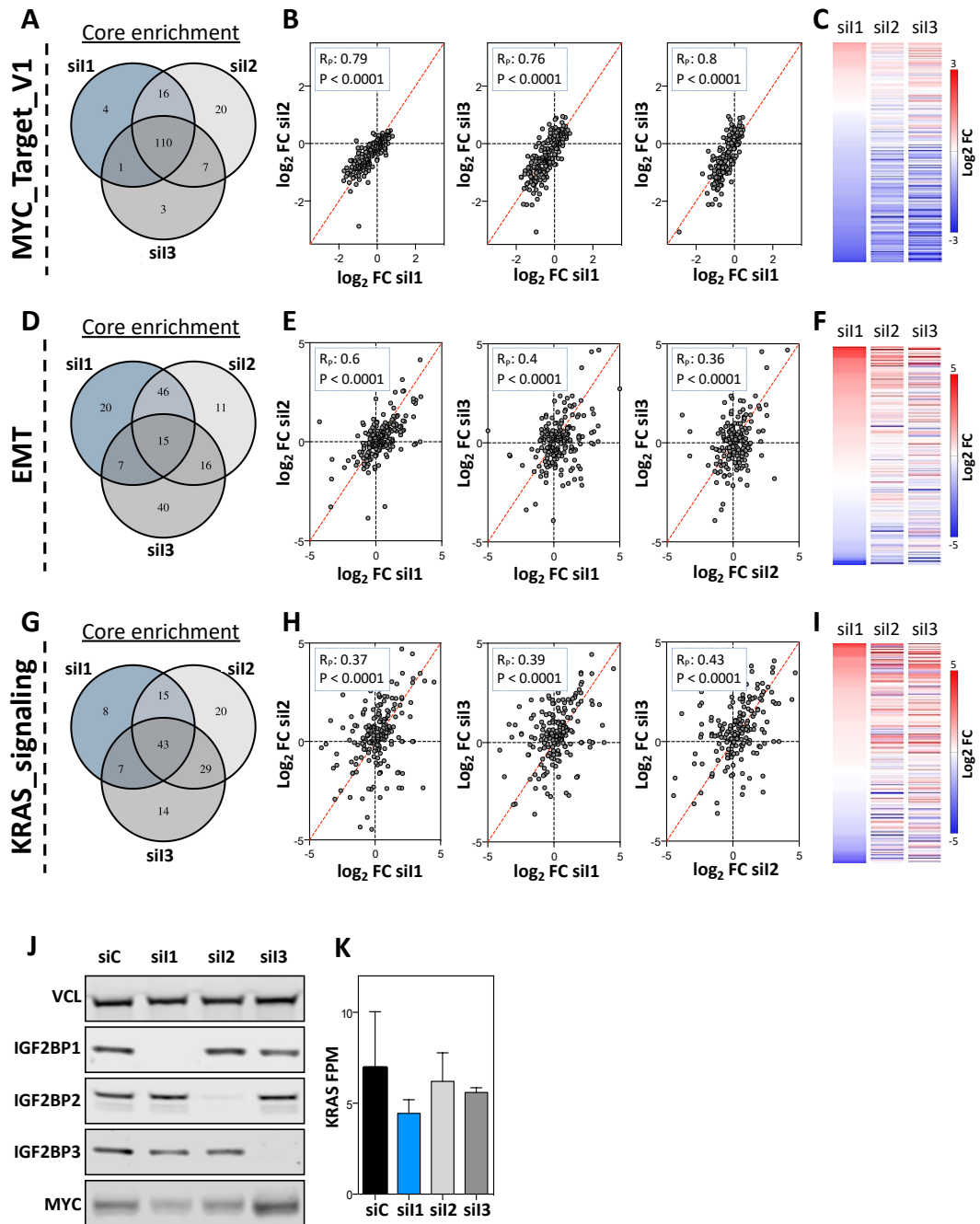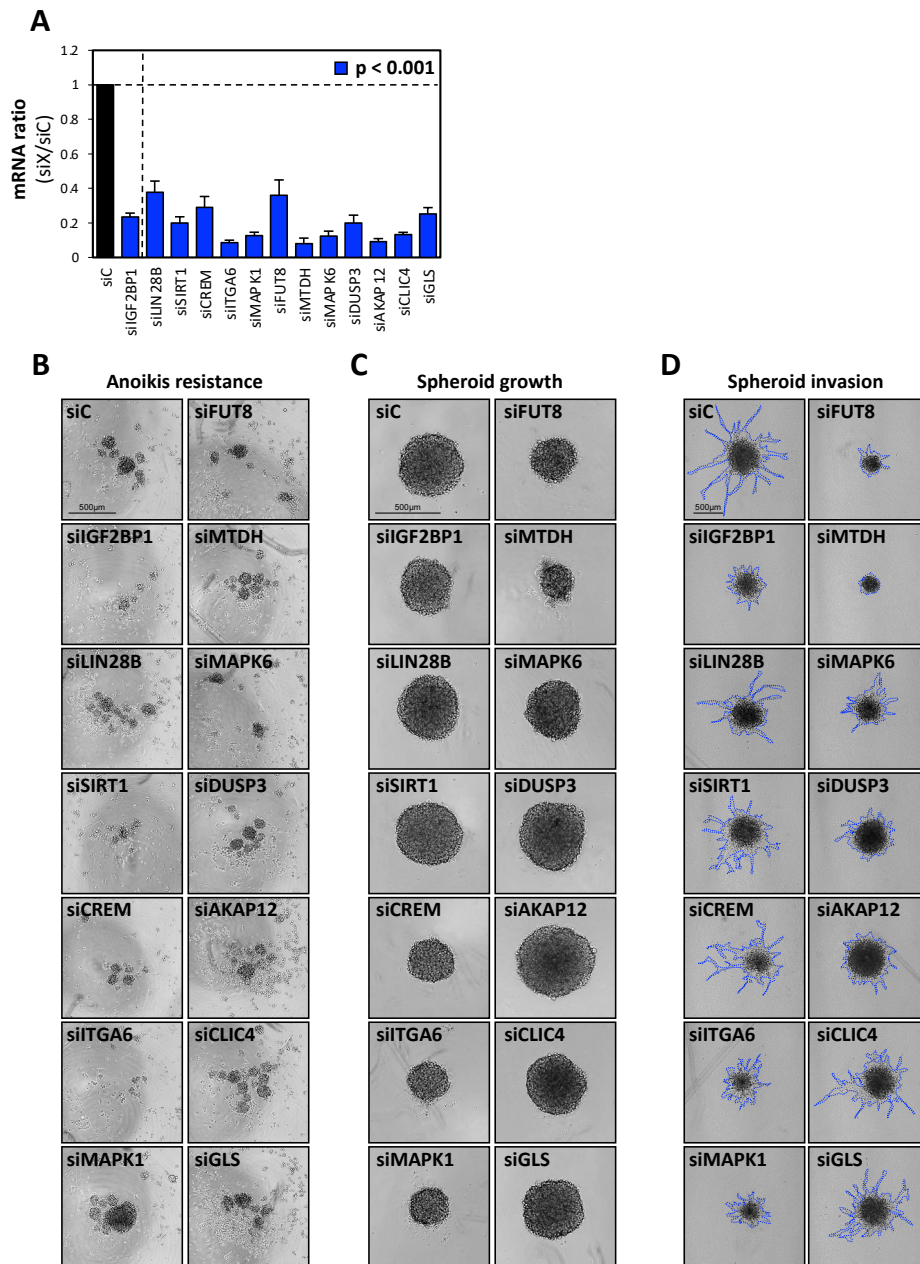
Müller et al., 2018 - Supplementary Figure S5

Müller et al., 2018 - Supplementary Figure S6

Müller et al., 2018 - Supplementary Figure S7

Müller et al., 2018 - Supplementary Figure S8

Article: IGF2BP1 promotes SRF-dependent transcription in cancer in a m⁶A- and miRNA-dependent manner

IGF2BP1 promotes SRF-dependent transcription in cancer in a m⁶A- and miRNA-dependent manner

Simon Müller[1], Markus Glaß[1], Anurag K. Singh[2], Jacob Haase[1], Nadine Bley[1], Tommy Fuchs[1], Marcell Lederer[1], Andreas Dahl[3], Huilin Huang[4,5], Jianjun Chen[4,5], Guido Posern[2] and Stefan Hüttelmaier [1,*]

[1]Institute of Molecular Medicine, Section for Molecular Cell Biology, Faculty of Medicine, Martin Luther University Halle-Wittenberg, Charles Tanford protein center, Kurt-Mothes-Str. 3a, 06120 Halle, Germany, [2]Institute for Physiological Chemistry, Medical Faculty, Martin Luther University Halle-Wittenberg, 06114 Halle (Saale), Germany, [3]Deep Sequencing Group, Center for Molecular and Cellular Bioengineering, Technische Universität Dresden, Tatzberg 47/49, 01307 Dresden, [4]Department of Systems Biology, City of Hope, Monrovia, CA 91016, USA and [5]Department of Cancer Biology, University of Cincinnati College of Medicine, Cincinnati, OH 45219, USA

ABSTRACT

The oncofetal mRNA-binding protein IGF2BP1 and the transcriptional regulator SRF modulate gene expression in cancer. In cancer cells, we demonstrate that IGF2BP1 promotes the expression of SRF in a conserved and N⁶-methyladenosine (m⁶A)-dependent manner by impairing the miRNA-directed decay of the SRF mRNA. This results in enhanced SRF-dependent transcriptional activity and promotes tumor cell growth and invasion. At the post-transcriptional level, IGF2BP1 sustains the expression of various SRF-target genes. The majority of these SRF/IGF2BP1-enhanced genes, including PDLIM7 and FOXK1, show conserved upregulation with SRF and IGF2BP1 synthesis in cancer. PDLIM7 and FOXK1 promote tumor cell growth and were reported to enhance cell invasion. Consistently, 35 SRF/IGF2BP1-dependent genes showing conserved association with SRF and IGF2BP1 expression indicate a poor overall survival probability in ovarian, liver and lung cancer. In conclusion, these findings identify the SRF/IGF2BP1-, miRNome- and m⁶A-dependent control of gene expression as a conserved oncogenic driver network in cancer.

INTRODUCTION

The mammalian IGF2 mRNA binding proteins (IGF2BPs; alias: VICKZ, CRD-BP, IMPs or ZBPs) family encompasses three RNA-binding proteins (RBPs) controlling the cytoplasmic fate of mRNAs in development, somatic cells and human diseases (1). Two members, IGF2BP1 and 3, are *bona fide* oncofetal proteins (1,2). They are abundant during development, expressed in some progenitor cells, barely observed in adult life but become upregulated or *de novo* synthesized in cancer (1,3–5). Recent studies indicate that IGF2BP1 has the most conserved 'oncogenic' role of the IGF2BP family in tumor-derived cells (6). The protein promotes a mesenchymal tumor cell phenotype characterized by altered actin dynamics, elevated migration, invasion, proliferation, self-renewal and anoikis resistance (7–9). Consistently, IGF2BP1 expression is associated with poor prognosis in various human cancers and the protein enhances the growth and metastasis of human tumor-derived cells in nude mice, as demonstrated for epithelial ovarian cancer (EOC) as well as hepatocellular carcinoma (HCC) derived tumor cells (6,10). This 'oncogenic' role of IGF2BP1 essentially relies on the impairment of mRNA decay. By associating with its target mRNAs, IGF2BP1 interferes with the degradation of target transcripts by endonucleases, as demonstrated for the MYC mRNA (11,12), or miRNA-directed decay, as shown for the vast majority of by now validated target mRNAs (6,9,13). Recent studies revealed that the association of IGF2BPs with target mRNAs, e.g. the MYC mRNA, is enhanced by the N⁶-methyladenosine (m⁶A) modification of target transcripts suggesting IGF2BPs as novel m⁶A-readers (14). Cross-linking immunoprecipitation (CLIP) analyses identified a plethora of candidate target mRNAs of IGF2BPs and revealed the 3′UTR as the mainly bound cis-element in associated transcripts (15–17). Although these studies indicate a substantial conservation of IGF2BP–mRNA association in tumor and stem cells, the phenotypic roles of IGF2BP homologs show a large variability in tumor cells derived from distinct cancers (6). The conserved phenotypic role of IGF2BP1 in tumor-derived cells suggests that the pro-

*To whom correspondence should be addressed. Tel: +49 345 5573959; Fax: +49 345 5527126; Email: stefan.huettelmaier@medizin.uni-halle.de

tein, in addition to promoting MYC synthesis, enhances additional oncogenic pathways not or barely affected by the other IGF2BP homologs.

In this study, we identify the SRF-encoding (serum response factor) mRNA as a conserved target mRNA of IGF2BP1 in cancer. SRF controls gene expression in concert with two classes of regulators: ternary complex factors (TCFs: ELK1, 3 and 4) and myocardin-related transcription factors (MRTFA and MRTFB) (18). Transcriptomic analyses revealed that SRF–MRTF driven transcription modulates the expression of genes involved in cytoskeletal regulation, cell adhesion, migration and invasion (19–21). Although partially overlapping, SRF/TCF-dependent gene expression mainly affects genes modulating proliferation and growth factor responsiveness (20,22). The SRF/MRTF-dependent control of gene expression essentially relies on RhoGTPase-signaling and actin dynamics modulating the subcellular localization and activity of MRTFs in transcription (23,24). Transcriptional control by SRF/TCFs is regulated by Mitogen-activated protein kinase-signaling (MAPK-signaling) (18,25). Thus, in concert with MRTFs and TCFs, SRF serves as a central hub modulating tumor cell migration, invasion and metastasis as well as proliferation and tumor growth in a signaling- and cytoskeleton-dependent manner (26–28). Notably, recent studies indicate that SRF destabilizes cell identity, promotes cellular reprogramming to pluripotency and when overexpressed in mice even enhances a metaplasia-like phenotype in the pancreas (29).

Here, we demonstrate that IGF2BP1 promotes SRF and SRF target genes at the post-transcriptional level suggesting it as a post-transcriptional enhancer of SRF itself as well as SRF-dependent gene expression in cancer cells. IGF2BP1 promotes SRF expression in a m^6A-dependent manner by impairing the miRNA-directed downregulation of the SRF mRNA. In addition, IGF2BP1 enhances the expression of SRF-induced target genes at the post-transcriptional level. In cancer, the SRF-IGF2BP1 directed enhancement of gene expression promotes an 'aggressive' tumor cell phenotype and is associated with poor prognosis.

MATERIALS AND METHODS

Plasmids and cloning

Information on cloning strategies including vectors, oligonucleotides used for polymerase chain reaction (PCR) and restrictions sites are summarized in Supplementary Table ST5. All constructs were validated by sequencing.

ChIP, RIP and RT-qPCR

Chromatin immunoprecipitation (ChIP) experiments were performed essentially as described previously (30). In brief, ~2.5 × 10^7 ES-2 cells were treated with formaldehyde, quenched and harvested in lysis buffer (10 mM 4-(2-hydroxyethyl)-1-piperazineethanesulfonic acid (HEPES), pH 7.9; 7.2 mM KOH; 150 mM KCl; 5 mM MgCl$_2$; 0.5% NP-40; protease inhibitors). Nuclei were enriched by centrifugation and lysed in ChIP-buffer (50 mM Tris-Cl, pH 8.0; 10 mM ethylenediaminetetraacetic acid (EDTA); 1%

sodium dodecyl sulphate (SDS); protease inhibitors) before chromatin was sheared by sonication. For ChIP, 25 μg of sheared chromatin was incubated with control (anti-IgG, Abcam ab171870) or anti-SRF (NEB 5147) antibodies overnight in dilution buffer (10 mM Tris-Cl, pH 8.0; 150 mM NaCl; 1 mM EDTA; 0.1% SDS; 1% Triton X-100; protease inhibitors). Upon extensive washing, chromatin was eluted in elution buffer (50 mM Tris-Cl, pH 8.0; 10 mM EDTA; 1% SDS), treated with Proteinase K and cross-linking was reversed overnight. DNA was finally eluted using the WIZARD®SV Gel & PCR Clean-Up System (Promega A9281) according to the manufacturer's protocol and analyzed by quantitative real-time PCR (qPCR). RNA immunoprecipitation (RIP) and quantitative RT-PCR analyses were performed essentially as recently described (6). Primers are summarized in Supplementary Table ST5.

Northern and western blotting

Northern blotting of small RNAs and semi-quantitative infrared western blotting were performed as recently described (9). Probes and antibodies are summarized in Supplementary Tables ST5 and ST7.

Luciferase reporter assays

Promoter reporter assays were performed using the MRTF-specific 3.DA reporter (24) and a TCF-dependent reporter containing 500 bp of the murine Egr1 promoter cloned into pGL3 and the pRL-tk plasmid (kind gift from Bernd Knöll, Ulm University, Germany). Cells were retransfected with siRNAs using RNAiMax for 24 h before reporter transfection with polyethylenimine and harvested for analysis the following day, as described previously (31). Firefly luciferase activity was normalized to fluorescence of co-transfected EGFP (BMG Labtech Clariostar microplate reader) and was shown relative to the control siRNA transfection.

For the analysis of miRNAs targeting the SRF 3′UTR, 48-nt long regions of the SRF 3′UTR comprising predicted miRNA targeting sites (MTSs) were cloned 3′ to the firefly luciferase open reading frame (pmirGLO, Promega). Luciferase reporter analyses were performed as previously described (9). The activities of firefly and renilla luciferases were determined 48 h post-transfection by DualGLO (Promega) according to the manufacturer's protocol. Reporters containing a minimal vector-encoded 3′UTR (empty) served as normalization controls.

RNA sequencing and differential gene expression

Libraries for RNA-sequencing (RNA-seq) were essentially prepared according to the manufacturer's protocols. For total RNA-seq, 1 μg of total RNA served as input for ribosomal RNA depletion using RiboCop v1.2 (Lexogen). The Ultra Directional RNA Library kit (NEB) was used for library generation. Sequencing was performed on an Illumina NextSeq 500 platform. For the generation of small RNA-seq libraries, 50 ng of total RNA served as input using the NEXTflex Small RNA Library Prep Kit v3 (Bio Scientific). Sequencing was performed on the Illumina HighSeq 2000 platform.

For RNA-seq data analyses, low quality read ends as well as remaining parts of sequencing adapters were clipped off using Cutadapt (v 1.14). For total and small RNA-seq analyses, reads were aligned to the human genome (UCSC GRCh38) using HiSat2 (v 2.1.0; (32)) or Bowtie2 (V 2.3.2; (33)), respectively. FeatureCounts (v 1.5.3; (34)) was used for summarizing gene-mapped reads. Ensembl (GRCh38.89; (35)) or miRBase (v 21; (36)) was used for annotations. Differential gene expression (DE) was determined by the R package edgeR (v 3.18.1; (37)) using TMM normalization.

MicroRNA-target predictions

MiRWALK 2.0 (38) was used for the analysis of transcript-specific miRNA-targeting (Supplementary Table ST3). The positions of MTSs in the 3′UTR of mRNAs were derived from TargetScan.

CLIP data analysis and CLIP scores

Peak coordinates from publicly available CLIP data (15–17), obtained from ENCODE, NCBI GEO and CLIPdb, were mapped to cis-elements (5′UTR, CDS and 3′UTR) of all annotated genes (RefSeq hg19). Cis-element specific CLIP scores were calculated as the number of datasets reporting CLIP peaks mapped to the 5′UTR, coding sequence (CDS) or 3′UTR, as previously reported (39). Thus, the CLIP score indicates the conservation of binding of a RNA-binding protein to a cis-element of a specific mRNA. For IGF2BP1, the following number of datasets was considered, resulting in CLIP scores ranging from 0 to 8: 2 PAR-CLIP (HEK293), 2 eCLIP (hESCs), 2 eCLIP (HepG2), 2 eCLIP (K562). For IGF2BP2 (CLIP score: 0–7): 2 eCLIP (hESCs), 2 eCLIP (K562), 2 iCLIP (K562), 1 PAR-CLIP (HEK293). For IGF2BP3 (CLIP score: 0–6): 1 eCLIP (hESCs), 2 eCLIP (HepG2), 2 iCLIP (K562), 1 PAR-CLIP (HEK293).

ChIP-seq data analyses. Genomic promoter-binding sites of SRF were derived from five publicly available ChIP-seq data performed in MEFs (20,40) (two studies), Ewing sarcoma-derived cells (41), H1 hESC (human embryonic stem cells) and the human lymphoblastoid cell line GM12878 (42). ChIP-scores were calculated as the number of datasets reporting ChIP-peaks mapped to the promoter region of a specific gene.

Kaplan–Meier and gene expression correlation analyses. Hazardous ratios (HRs) for indicated gene panels and tumor cohorts of serous ovarian carcinoma, lung adenocarcinoma (LUAD) and HCC were determined by the Kaplan–Meier (KM) plotter (www.kmplot.com) (43) online tool using best cutoff analyses and the multigene classifier.

Gene expression correlations. The correlation of gene expression was determined using the R2 platform (http://hgserver1.amc.nl/cgi-bin/r2/main.cgi) to analyze the indicated TCGA-provided datasets (ovarian serous cystadenocarcinoma, LUAD, liver HCC and skin cutaneous melanoma). Pearson correlation coefficients (*R* values) are summarized in Supplementary Table ST4B.

Cell culture, transfection and CRISPR/Cas9

Cells were cultured and transfected essentially as described recently (9). SiRNAs are summarized in Supplementary Table ST6. For the depletion of DICER1/DROSHA, cells were retransfected after 3 d and harvested 6 d after the initial transfection, as recently described (6). IGF2BP1 knockout cells were generated using the CRISPR/Cas9 technology and sgRNAs previously described (6). Control clones were generated by transfecting the Cas9 nuclease only. For the deletion of the bulk 3′UTR of SRF (Acc. No.: NM_003131), two CRISPR guide RNAs were used as depicted in Figure 2B. The deletion was validated by PCR amplification of the genomic locus and sequencing. Guide RNAs and PCR primers are summarized in Supplementary Table ST5.

Spheroid growth, invasion and anoikis resistance

The analyses of 3D spheroid growth, anoikis-resistance and spheroid invasion were performed as previously described (6,9). In brief, for spheroid growth and invasion 1000 cells per well (24 h post-transfection) were seeded in an ultra-low attachment round bottom 96-well plate (Corning 7007) using FBS-containing (10%) DMEM medium. Spheroid growth was monitored for 5 d by light microscopy, and viability was determined by CellTiter-GLO (Promega). Upon spheroid formation (24 h), the invasion matrix (Trevigen; 5 mg/ml) was added to monitor tumor cell infiltration for another 24 h using light microscopy. For anoikis resistance, 1000 cells per well were seeded in an ultra-low attachment flat bottom 96-well plate (Corning 3474) using Dulbecco's Modified Eagle Medium (DMEM) containing 1% fetal bovine serum (FBS). Cell growth was monitored for 5 d, and cell viability was determined as described above.

RESULTS

IGF2BP1 promotes SRF expression in cancer cells

The oncofetal mRNA-binding protein IGF2BP1 is a post-transcriptional enhancer of oncogene expression impairing the miRNA-directed degradation of its target mRNAs (6,9). To identify conserved effector networks of IGF2BP1 in HCC and EOC, IGF2BP1-dependent gene expression was analyzed in HCC-derived Huh-7 and EOC-derived ES-2 cells. To this end, mRNA abundance was monitored by RNA-seq upon the depletion of IGF2BP1 using homolog-specific siRNA pools (Figure 1A and Supplementary Table S1 (6)). The number of differentially expressed genes was higher in ES-2 than in Huh-7 cells. In part, variable effects on gene expression were expected since IGF2BP1 controls target mRNA abundance in a miRNome-dependent manner (6), and miRNA expression (the miRNome) varies between distinct tumor cell lines. Small RNA-seq confirmed a partially distinct miRNA expression in both cell lines, for instance significantly lower abundance of the let-7-5p family but elevated expression of the hepatic miR-122-5p in Huh-7 cells (Supplementary Table ST2 and Supplementary Figure S1A,B). In support of a miRNome-dependent regulation, the absolute number of let-7 target mRNAs (predicted by at least two out of four databases using MirWalk
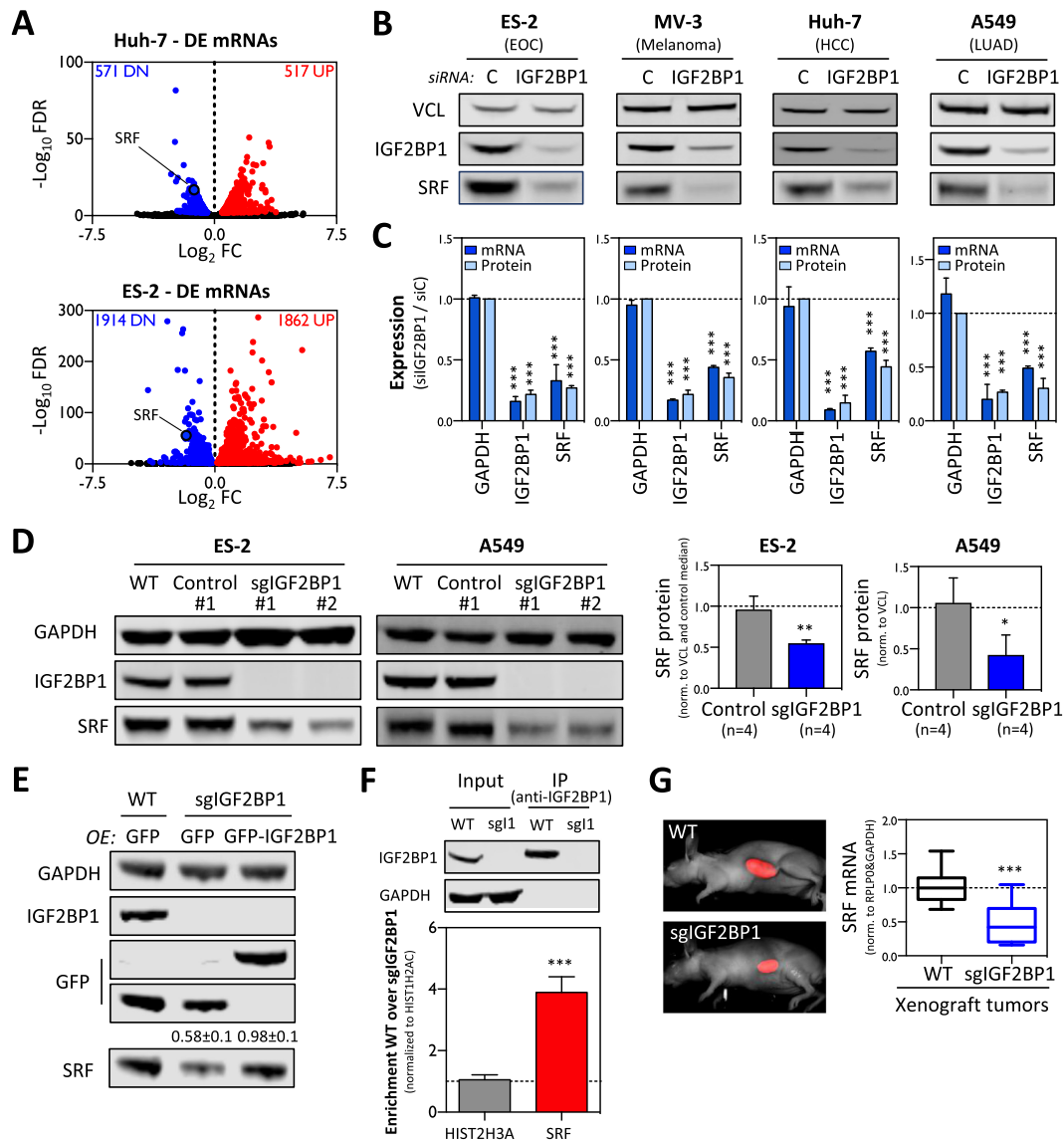
Figure 1. IGF2BP1 promotes SRF expression in cancer cells. (**A**) Volcano plots showing differential gene expression (threshold: FDR ≤ 0.01) determined by RNA-seq in Huh-7 and ES-2 cells upon IGF2BP1 depletion by siRNA pools (72 h). (**B**) Representative western blots demonstrating downregulation of SRF protein upon IGF2BP1 depletion by siRNA pools (72 h) in indicated tumor-derived cell lines. (**C**) Quantification of SRF protein and mRNA abundance upon IGF2BP1 depletion in cancer cells shown in (B). VCL served as the normalization control in three independent western blot analyses. GAPDH served as the negative control in RT-qPCR studies cross-normalized to RPLP0 expression. (**D**) Representative western blot analysis (left panel) demonstrating deletion of IGF2BP1 by CRISPR/Cas9 in two independent cell clones of ES-2 and A549 cells (sgIGF2BP1) compared to parental cells (WT) or Cas9-transfected control clones (C-1). The quantification of SRF protein levels in four control and IGF2BP1-deleted A549 and ES-2 cell clones confirmed that the deletion of IGF2BP1 results in significantly reduced SRF protein expression. GAPDH served as the loading and normalization control. (**E**) Western blotting analyses indicate that the re-expression of wild-type GFP-fused IGF2BP1 restores the expression of SRF protein in IGF2BP1-deleted ES-2 cells. GAPDH served as the loading and normalization control for the quantification of SRF protein levels in three independent studies (indicated above lower panel). (**F**) RIP analysis showing that IGF2BP1 is associated with the SRF mRNA in ES-2 cells. RNA co-purified with IGF2BP1 from parental (WT) or IGF2BP1-KO (sgI1) cells was analyzed by RT-qPCR. HIST1H2AC served as the normalization and HIST2H3A as the negative control. Error bars indicate standard deviation determined in at least three analyses. (**G**) The quantification of SRF mRNA abundance in ES-2 derived *Xenograft* tumors grafted in nude mice by RT-qPCR indicates that IGF2BP1 deletion is associated with reduced SRF expression (right panel). GAPDH and RPLP0 served as normalization controls. Unpublished images of iRFP-labeled tumors (left panel) were derived from recent studies (6). Statistical significance, as indicated by *P*-values, was determined by Student's *t*-test: (*) $P < 0.05$, (**) $P < 0.01$, (***) $P < 0.001$.

(38)) downregulated by IGF2BP1 depletion was higher in ES-2 (429) than Huh-7 (158) cells (Supplementary Figure S1C). However, IGF2BP1 interferes with miRNA-directed mRNA degradation mostly independent of primary MTS sequences. The protein preferentially associates upstream of MTSs in the 3′UTR of its target mRNAs and recruits associated transcripts to miRNA-/RISC-free mRNPs (6,9). To analyze this for the here suggested target mRNAs of IGF2BP1, we considered eight CLIP-seq (cross-linking immunoprecipitation high-throughput sequencing) studies. The CLIP score indicating the number of experiments featuring cross-link peaks between IGF2BP1 in the 5′UTR, CDS or 3′UTR of specific mRNAs was introduced to rate CLIP-reported mRNA-binding (39). This allowed the comprehensive assessment of preferred binding regions irrespective of distinct CLIP techniques and cell lines used in individual analyses. The IGF2BP1 3′UTR CLIP score was significantly higher among transcripts downregulated (DN) upon IGF2BP1 depletion in both cell lines (Supplementary Figure S1D). This suggested that mRNAs significantly downregulated in both cell lines are more likely direct target transcripts and thus effectors of IGF2BP1 that are conserved in HCC and EOC. To evaluate if IGF2BP1 depletion affected similar pathways despite the only moderate overlap of transcripts significantly (false discovery rate (FDR) < 0.01) deregulated in both cell lines, gene set enrichment analyses were performed. These revealed a striking overlap of hallmark pathways affected by the knockdown of IGF2BP1 in both cell lines (Supplementary Figure S1E and Supplementary Table ST1B). In conclusion, these findings suggested that although IGF2BP1 may have variable regulatory 'potency' on specific mRNAs in distinct cancer cells, it serves conserved functions and controls similar pathways at varying extend or significance in these cells.

Among the various transcripts downregulated in both cancer cell lines (242) was the SRF (serum response factor) mRNA encoding a transcriptional regulator modulating both proliferative and migratory/invasive tumor cell properties in a conserved manner, as previously demonstrated for IGF2BP1 (6,7). The expected similarities and conservation of SRF's and IGF2BP1's roles in modulating tumor cell properties suggested that the post-transcriptional regulator IGF2BP1 synergizes with the transcriptional regulator SRF in promoting an 'aggressive' tumor cell phenotype. Therefore, the conservation of IGF2BP1-dependent regulation of SRF expression was analyzed in a panel of four tumor cell lines derived from distinct primary cancers. These studies revealed that SRF mRNA and protein abundance was significantly decreased in all cell lines upon IGF2BP1 knockdown (Figure 1B and C). This was confirmed in additional tumor-derived cell lines (data not shown) demonstrating that the IGF2BP1-dependent upregulation of SRF expression is highly conserved in cancer cells. To validate regulation of SRF expression by IGF2BP1, the latter was deleted in ES-2 (EOC) and A549 (LUAD) cells using CRISPR/Cas9 technology. In both cell lines, the knockout of IGF2BP1 was associated with decreased SRF expression in four independent cell clones of each cell line (Figure 1D). To exclude bias by off-target effects and validate that IGF2BP1 promotes SRF expression in a RNA-binding-dependent manner, SRF protein

and mRNA abundance were monitored by knockdown recovery studies (Supplementary Figure S2A). For this, ES-2 cells were depleted for IGF2BP1 using siRNAs directed against the human IGF2BP1-encoding mRNA resulting in severely reduced SRF expression. SRF protein and mRNA levels were substantially increased by the re-expression of GFP-fused wild-type chicken Igf2bp1 (chI1; also termed ZBP1). On the contrary, SRF abundance remained reduced when re-expressing a GFP-tagged, RNA-binding deficient mutant of chicken Igf2bp1 (chI1 mut) (44), as observed in cells expressing GFP alone (control). Furthermore, SRF expression was restored in IGF2BP1-deleted ES-2 cells by the re-expression of human GFP-tagged IGF2BP1, whereas SRF abundance remained reduced in IGF2BP1-deleted cells transduced with GFP alone (Figure 1E). These findings excluded off-target effects of the used siRNA pool as well as sgRNAs used for IGF2BP1 deletion and suggested that IGF2BP1 controls SRF expression in a RNA-binding dependent manner. To elucidate if IGF2BP1 associates with the SRF mRNA in ES-2 cells, binding was analyzed by RIP. In contrast to the control transcript HIST2H3A, the SRF mRNA was significantly enriched with IGF2BP1 from parental, wild-type (WT) but not IGF2BP1-deleted (sgI1) ES-2 cells (Figure 1F). Finally, downregulated SRF synthesis upon IGF2BP1 deletion was also observed in ES-2-derived *Xenograft* tumors in nude mice (Figure 1G; tumor samples were obtained from (6)). This suggested that the IGF2BP1-dependent enhancement of SRF expression is associated with the recently reported role of IGF2BP1 in promoting tumor growth and metastasis (6).

IGF2BP1 promotes SRF expression in a 3′UTR and m⁶A-dependent manner

Consistent with IGF2BP1-CLIP studies in distinct cell lines (15–17), we recently demonstrated that IGF2BP1 impairs the miRNA-dependent downregulation of target mRNAs mainly by associating with the 3′UTR of target transcripts (6). To test if this is also observed for the SRF mRNA, three IGF2BP1-CLIP studies performed in HCC-derived HepG2, leukemia-derived K562 or hESCs were considered (16,17). In all three cell models, IGF2BP1-CLIP hits were identified in the 3′UTR of the SRF mRNA suggesting conserved regulation via this cis-element (Figure 2A). The conservation of IGF2BP1-dependent regulation was further supported by substantially decreased SRF mRNA and protein levels upon the depletion of IGF2BP1 in HepG2 cells (Supplementary Figure S3A and B). Aiming to validate regulation via the 'endogenous' 3′UTR, the vast majority of this cis-element in the *SRF* locus was deleted in A549 cells by directing Cas9 nuclease to the proximal and distal (located upstream of the polyadenylation signal) ends of the 3′UTR using two sgRNAs (Figure 2B). The biallelic deletion of the bulk 3′UTR (SRF-Δ3′UTR) was confirmed by PCR (Figure 2C). Compared to parental (WT) cells, SRF mRNA and protein abundance was substantially increased in SRF-Δ3′UTR cells suggesting that the 3′UTR essentially accounts for limiting SRF expression (Figure 2D and E; Supplementary Figure S3C). To test if the 3′UTR-dependent downregulation of SRF synthesis is IGF2BP1-dependent, IGF2BP1 was depleted in parental
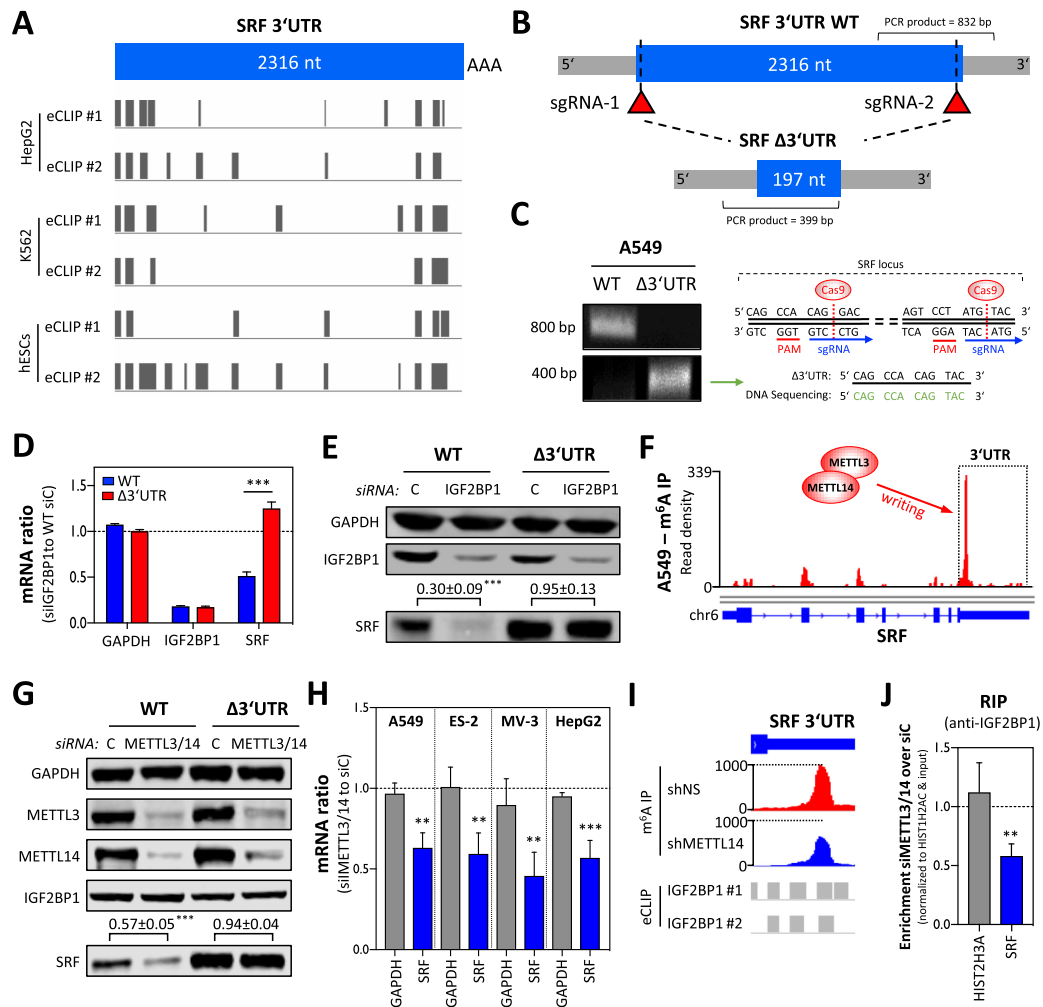
Figure 2. IGF2BP1 promotes SRF expression in a 3′UTR and m⁶A-dependent manner. (**A**) Schematic depicting the position of IGF2BP1-CLIP sites reported in the SRF 3′UTR by six experiments performed in three indicated cell lines. (**B**) Schematic showing the SRF-3′UTR deletion strategy by CRISPR/Cas9. The relative position of sgRNAs and PCR primers for validating deletion of the SRF 3′UTR are indicated. (**C**) Representative semi-quantitative PCR analysis (left panel) of parental (WT) and SRF-3′UTR-deleted (Δ3′UTR) A549 cells. The successful deletion was further validated by DNA sequencing (right panel) of PCR products (Δ3′UTR) spanning the expected cleavage sites indicated in the schematic. (**D**) RT-qPCR analysis of indicated mRNAs in parental and SRF-Δ3′UTR A549 cells upon IGF2BP1 depletion (72 h). RPLP0 served as the normalization and GAPDH as the negative control. (**E**) Representative western blot analysis of indicated proteins in cells treated as described in (D). GAPDH served as the loading and normalization control for the quantification ($n = 3$) of SRF protein levels upon IGF2BP1 depletion (relative to controls), as depicted above lower panel. (**F**) m⁶A -RIP-seq data showing m⁶A-modification of the SRF mRNA in A549 cells. Sequencing data were obtained from MeT-DB V2.0 (45). (**G**) Representative western blot analysis of indicated proteins upon METTL3/14 depletion in parental (WT) and SRF-Δ3′UTR A549 cells. Note that IGF2BP1 expression is unaffected by METTL3/14 depletion, whereas SRF protein abundance is decreased only in parental A549 cells. GAPDH served as the loading and normalization control for the quantification ($n = 3$) of SRF protein levels (relative to controls), as indicated in the lower panel. (**H**) The depletion of METTL3/14 by siRNA pools impairs SRF mRNA abundance in indicated cell lines. GAPDH served as the negative control in RT-qPCR studies cross-normalized to RPLP0 expression. (**I**) Altered m⁶A-modification of the SRF 3′UTR was determined upon METTL14 depletion in HepG2 cells by m⁶A-RIP-seq. Sequencing data were deposited according to (14). Note that the m⁶A-modified region partially overlaps with IGF2BP1-CLIP sites determined in HepG2 cells. (**J**) IGF2BP1-RIP analyses showing reduced association of the SRF mRNA with IGF2BP1 in METTL3/14-depleted A549 cells. RNA co-purified with IGF2BP1 from cells transfected with control siRNAs (siC) or METTL3/14-depleted cells was analyzed by RT-qPCR. HIST1H2AC served as the normalization and HIST2H3A as the negative control. Error bars indicate standard deviation determined in at least three analyses. Statistical significance was determined by Student's *t*-test: (**) $P < 0.01$, (***) $P < 0.001$.

and SRF-Δ3′UTR cells (Figure 2D and E). Whereas SRF mRNA and protein abundance remained largely unchanged in SRF-Δ3′UTR cells, SRF expression was significantly reduced in parental cells upon IGF2BP1 depletion. This indicated that the IGF2BP1-dependent regulation of SRF expression is strictly 3′UTR-dependent.

In recent studies, IGF2BPs were reported to enhance the expression of MYC and other target transcripts in a m^6A-dependent manner (14). The m^6A-modification of the MYC mRNA promotes the association of IGF2BP1 resulting in reduced decay of the MYC transcript and consequently enhanced the expression of this oncogene in cancer cells. The analysis of publicly available m^6A-RIP-seq data in A549 cells in the MeT-DB V2.0 database (45) indicated strong modification in the 3′UTR of the SRF mRNA (Figure 2F). To test if SRF expression is controlled in a m^6A- and 3′UTR-dependent manner, the methyltransferases METTL3 and 14 were co-depleted in parental and SRF-Δ3′UTR A549 cells. The knockdown of METTL3/14 resulted in a significant downregulation of SRF protein in parental cells (Figure 2G). In contrast, SRF protein levels remained unaltered in SRF-Δ3′UTR A549 cells upon METTL3/14 depletion. This suggested that SRF expression is controlled via m^6A-modification in the 3′UTR of the SRF mRNA. If the m^6A-dependent regulation of SRF expression is conserved, it was investigated by monitoring SRF mRNA and protein abundance upon METTL3/14 depletion in four cancer-derived cells (Figure 2H and Supplementary Figure S3D). In all analyzed cell lines, SRF mRNA and protein abundance was significantly reduced upon the co-depletion of METTL3/14. As observed in A549 cells, m^6A-RIP-seq analyses in HepG2 cells confirmed that the SRF mRNA is modified in the 3′UTR and that modification is reduced by the depletion of METTL14 (Figure 2I; m^6A-RIP-seq data were obtained from Huang *et al.* (14)). Notably, m^6A-modified nucleotides largely overlap with reported IGF2BP1-CLIP sites in HepG2 cells suggesting that the IGF2BP1-dependent regulation of SRF expression is m^6A-dependent (Figure 2I and Supplementary Figure S3E). If the depletion of METTL3/14 impairs the association of IGF2BP1 with the SRF mRNA, as reported for the MYC mRNA (14), it was analyzed by RIP. Compared to cells transfected with control siRNAs, the co-depletion significantly reduced the association of the SRF mRNA with IGF2BP1 (Figure 2J and Supplementary Figure S3F). These findings supported the view that the m^6A-modification of the SRF mRNA promotes its association with IGF2BP1, as previously reported for the MYC mRNA (14). However, IGF2BP1 also binds mRNAs independent of m^6A, e.g. (14,44). Therefore, we hypothesized that reduced m^6A-modification is partially compensated by increasing IGF2BP1 abundance. If the elevated abundance of IGF2BP1 restores SRF expression when METTL3 is depleted, it was analyzed in ES-2 cells stably overexpressing GFP (control), wild-type (I1) or RNA-binding deficient (I1mut) IGF2BP1. Upon METTL3 knockdown, SRF protein abundance was substantially enhanced in cells overexpressing GFP-IGF2BP1 when compared to I1mut- or GFP-expressing controls (Supplementary Figure S3G). These findings indicate that SRF expression is enhanced

by IGF2BP1 in a conserved, 3′UTR- and m^6A-dependent manner.

IGF2BP1 impairs the miRNA-dependent downregulation of SRF expression

Recent studies indicate that IGF2BPs control mRNA turnover largely by modulating the miRNA-dependent regulation of their target transcripts. Whereas IGF2BP3 was shown to promote or impair the miRNA-directed downregulation of target mRNAs (46), IGF2BP1 and 2 interfere with the miRNA-directed inhibition of effector expression (3,6,9). Although CLIP-hits in the 3′UTR of the SRF mRNA were reported for all three IGF2BPs, only the depletion of IGF2BP1 interfered with the expression of SRF in cancer cells (Supplementary Figure S4A and B). In agreement, IGF2BP1 expression showed the most significant and conserved association with elevated SRF expression in ovarian, skin, liver and lung cancer, as determined by Pearson correlation of RNA-sequencing data available via the TCGA (Supplementary Figure S4C). In view of recent reports, these findings suggested that IGF2BP1 promotes SRF expression in cancer by impairing the miRNA-dependent decay of the SRF mRNA. Consistently, the depletion of IGF2BP1 led to significantly enhanced decay of the SRF mRNA in ES-2 cells (Figure 3A). The analysis of miRNA expression by small RNA-seq revealed that miRNAs, predicted to target the SRF-3′UTR (3 of 4 analyzed databases; Supplementary Table ST3), showed conserved expression (median CPM (counts per million mapped reads)) in the four tumor cell lines for which the IGF2BP1-dependent control of SRF expression was demonstrated (Figure 3B, only the 10 most abundant miRNAs are shown; Supplementary Figure S4D and Supplementary Table ST2). Among these were miRNAs or miR families like miR-22-3p, 125-5p or miR-181-5p that were previously reported to downregulate SRF expression in cancer, smooth muscle and/or endothelial cells (47–50). If SRF expression is controlled by miRNAs in ES-2 cells, it was investigated by depleting DICER and DROSHA. This depletion resulted in a significant downregulation of bulk miRNA abundance, as recently shown and indicated here for miR-22 by northern blotting (Supplementary Figure S4E (6)). The decrease in miRNA levels by DICER/DROSHA knockdown was associated with a severe upregulation of SRF mRNA abundance (Figure 3C). Moreover, it abolished the downregulation of SRF mRNA levels observed upon the depletion of IGF2BP1 indicating that the protein stabilized the SRF mRNA by impairing its miRNA-directed downregulation (Figure 3D). As observed for other miRNA-controlled target mRNAs of IGF2BP1, for instance SIRT1 (6), not all predicted MTSs overlapped with reported IGF2BP1-binding sites in the SRF 3′UTR (Figure 3E). If IGF2BP1 modulates regulation by the two most abundant miRNAs predicted to target the SRF 3′UTR (miR-23a-3p and miR-125a-5p) was analyzed by luciferase reporters. These comprised 48-nt long fragments of the SRF 3′UTR including the predicted MTSs (Figure 3F, left panel). In ES-2 cells deleted for IGF2BP1, reporter activities were significantly decreased compared to parental cells (Figure 3F, right panel). This suggested
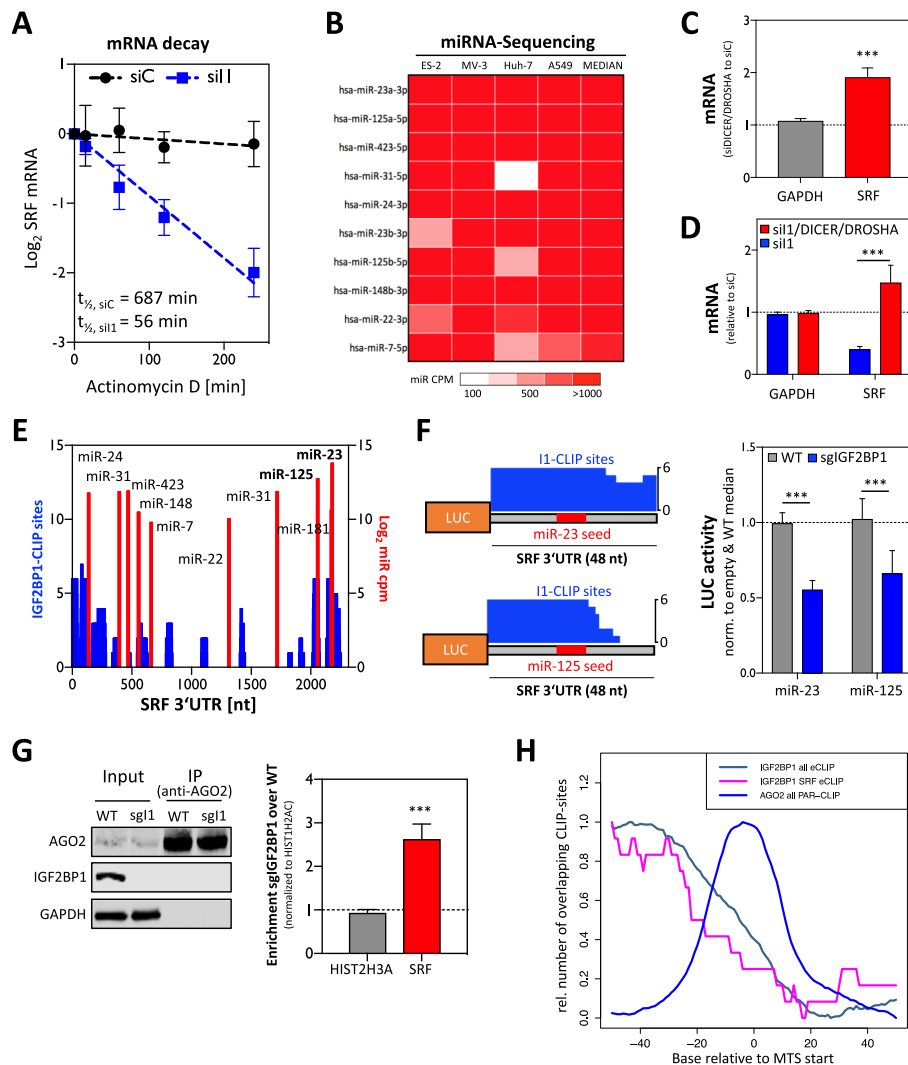
Figure 3. IGF2BP1 promotes SRF expression in a miRNA-dependent manner. (**A**) The decay of the SRF mRNA was monitored by RT-qPCR in ES-2 cells treated with actinomycin D for the indicated time upon transfection of control (siC) or IGF2BP1-directed siRNA pools. The reduction of the SRF mRNA half-life by IGF2BP1 knockdown is indicated in the graph. (**B**) Heatmap indicating the expression of the 10 most abundant and 'conserved' miRNAs, predicted to target the SRF 3′UTR, in the analyzed tumor-derived cell lines. MiRNAs are sorted by median expression (CPM, count per million) and color codes of mRNA abundance are shown in the lower panel. (**C**) RT-qPCR analysis demonstrating the upregulation (relative to controls, siC-transfected) of the SRF mRNA upon DICER/DROSHA depletion in ES-2 cells. GAPDH served as the negative and RPLP0 as the normalization control. (**D**) RT-qPCR analysis of SRF mRNA levels upon IGF2BP1 or IGF2BP1/DICER/DROSHA depletion relative to controls (siC-transfected). RPLP0 served as the normalization control and GAPDH as the negative control. (**E**) The number of CLIP studies showing overlapping IGF2BP1-CLIP sites (CLIP score at nucleotide resolution) in the SRF 3′UTR (blue), and the position (*x*-axis) of miRNA targeting sites (red) are shown for the SRF 3′UTR. MiRNA abundance (right axis, red) is indicated as log₂ CPM for 10 'SRF-targeting' miRNAs showing conserved expression in the cancer cells analyzed. (**F**) Schematic (left panel) showing luciferase reporter constructs comprising indicated regions of the SRF 3′UTR including predicted MTSs for miR-23a-3p and miR-125a-5p. Note that miR-seeds (red) overlap with IGF2BP1-binding sites (blue) suggested by eCLIP analyses (CLIP score at nucleotide resolution is indicated). Luciferase reporter analysis (right panel) demonstrating reduced activity of indicated reporters in IGF2BP1-deleted (sgIGF2BP1, blue) compared to parental ES-2 cells (grey). (**G**) RIP analysis showing the enhanced association of the SRF mRNA with AGO2 in IGF2BP1-deleted ES-2 cells. Immunoprecipitation was analyzed by western blotting (left panel). RNA co-purified with AGO2 from WT or IGF2BP1-deleted (sgI1) ES-2 cells was analyzed by RT-qPCR (right panel). HIST1H2AC served as the normalization and HIST2H3A as the negative control. (**H**) The relative number of overlapping CLIP sites determined for IGF2BP1 and AGO2 in the proximity of MTSs, as recently reported (6), is shown relative to the start of MTSs predicted by TargetScan for human mRNAs (hg19; IGF2BP1 all eCLIP) or the SRF 3′UTR (IGF2BP1 SRF eCLIP). Error bars indicate standard deviation determined in at least three analyses. Statistical significance was determined by Student's *t*-test: (***) *P* < 0.001.

that IGF2BP1 impaired miRNA-directed downregulation by associating with the respective SRF-derived elements as reported by CLIP analyses. To test if IGF2BP1 interferes with RISC-association of the SRF mRNA in cells, as previously proposed for other target mRNAs (39), AGO2-RIP studies were performed in parental and IGF2BP1-deleted ES-2 cells. These studies showed that the deletion of IGF2BP1 significantly promotes the association of the SRF mRNA with AGO2 (Figure 3G). Finally, the inspection of IGF2BP1-CLIP sites in the vicinity of MTSs in the SRF 3′UTR confirmed the preference of IGF2BP1-binding upstream of MTSs, as previously reported by transcriptome-wide analyses (Figure 3H (6)). In conclusion, these findings indicate that IGF2BP1 impairs the miRNA-directed down-regulation of SRF expression.

Previous studies indicate that IGF2BP1 associates with ELAVL1 (HuR), as well as other RBPs in cytoplasmic mRNPs and controls target mRNA fate, e.g. of the MYC mRNA, in concert with these co-factors (51). ELAVL1 is a key regulator of mRNA turnover and translation promoting or impairing miRNA-directed regulation of its target mRNAs (52). Accordingly, it was tempting to speculate that both proteins cooperate or antagonize each other in the miRNA-dependent regulation of SRF expression. This was analyzed by depleting IGF2BP1 and ELAVL1 in A549 cells. Whereas SRF protein levels were decreased by IGF2BP1 knockdown, they remained unchanged upon the depletion of ELAVL1 (Supplementary Figure S5A). The analysis of IGF2BP1- and ELAVL1-mRNA binding, as reported by CLIP studies, revealed that although both proteins preferentially associate in the 5′-proximity of MTSs they show substantially distinct binding properties at MTSs and the 3′-proximity of miRNA targeting sites (Supplementary Figure S5B). Although these findings do not exclude that ELAVL1 and IGF2BP1 co-regulate the miRNA-dependent regulation of some mRNAs, they provide strong evidence that the IGF2BP1-dependent regulation of the SRF mRNA is independent of ELAVL1.

IGF2BP1 promotes SRF-dependent transcription in cancer cells

SRF modulates gene expression in concert with two groups of signal-regulated co-factors, TCFs (ELK1, 3 and 4) and MRTFs (MRTFA and MRTFB). In concert with these co-regulators and their upstream signaling cascades, SRF-dependent transcriptional control modulates cell proliferation, contractility and pro-invasive behavior (40). RNA-sequencing indicated that the depletion of IGF2BP1 in ES-2 cells only impaired the expression of SRF whereas the abundance of co-factor encoding mRNAs remained unchanged (Figure 4A). This suggested that IGF2BP1 depletion interferes with SRF/TCF- as well as SRF/MRTF-dependent transcriptional regulation in cancer cells mainly by reducing cellular SRF abundance. This was analyzed by monitoring the activity of SRF/TCF- and SRF/MRTF-dependent luciferase reports in cancer cells upon the depletion of IGF2BP1 or SRF (Figure 4B and C). Notably, IGF2BP1 expression remained unchanged upon SRF depletion. The activity of both reporters was substantially diminished by the depletion of either IGF2BP1 or SRF

in all cancer cells analyzed. The only exception was observed in A549 cells in which SRF/TCF-dependent reporters were barely affected by IGF2BP1 or SRF depletion for unknown reasons. In Huh-7 cells, the depletion of IGF2BP1 showed only moderate effects on the activity of MRTF-reporters when compared to the knockdown of SRF. This could be a result of the constitutively high Rho-dependent activation of MRTFs due to DLC-1 deficiency in Huh-7 cells (53). Despite the obvious, cell type-dependent and variable extent of IGF2BP1/SRF-directed regulation, the presented findings suggested that IGF2BP1 and SRF exhibit similar effects on promoting a pro-proliferative and pro-invasive gene expression signature in tumor cells. This regulation was likely to mainly rely on the IGF2BP1-dependent upregulation of SRF expression and the consequent cell type-dependent enhancement of SRF/MRTF- as well as SRF/TCF-controlled transcription. To test if IGF2BP1 and SRF modulate tumor cell viability, spheroid growth was monitored upon their depletion (Figure 4D). The knockdown of both factors substantially decreased the growth of ES-2 derived spheroids when cultured in the presence of 10% FBS indicating that both proteins are essential for tumor cell growth or proliferation (Figure 4D). How IGF2BP1 or SRF influence tumor cell viability at low adhesion and mitogen stimulation (FBS, 1%) was analyzed by anoikis resistance assays upon depleting both factors in ES-2 cells (Figure 4E). Whereas IGF2BP1 knockdown impaired cell viability as previously reported (6), anoikis resistance remained largely unaffected by the depletion of SRF. This revealed that IGF2BP1 also serves SRF-independent roles in cancer cells and thus supports the notion that IGF2BP1 promotes an 'aggressive' tumor cell phenotype via pleiotropic effectors (6). SRF-dependent transcriptional regulation is a key modulator of cytoskeletal dynamics and was shown to promote tumor cell invasion and experimental metastasis (26), as recently shown for IGF2BP1 in EOC-derived cells (6). In agreement, the depletion of both factors substantially interfered with spheroid invasion in ES-2 cells (Figure 4F). In summary, these findings demonstrate that IGF2BP1 promotes SRF-dependent transcriptional regulation and that both factors likely synergize in promoting an 'aggressive' tumor cell phenotype.

IGF2BP1 promotes SRF-dependent transcription at the post-transcriptional level in cancer

The regulation of SRF-dependent transcription by IGF2BP1 in cancer cells and the partial 'phenocopy' observed upon IGF2BP1 and SRF depletion in ES-2 cells suggested that both factors synergize in promoting a pro-proliferative and invasive tumor cell phenotype. In view of reported functions of SRF and IGF2BP1, one plausible molecular mechanism underlying this synergy could be that IGF2BP1 promotes SRF-dependent transcription at the post-transcriptional level by impairing the degradation of SRF-driven transcripts. This implies that elevated IGF2BP1 expression partially restores SRF/IGF2BP1-dependent cell properties in a RNA-binding dependent manner when SRF is reduced. To test this assumption at the phenotypic level, spheroid viability was monitored upon SRF depletion in ES-2 cells
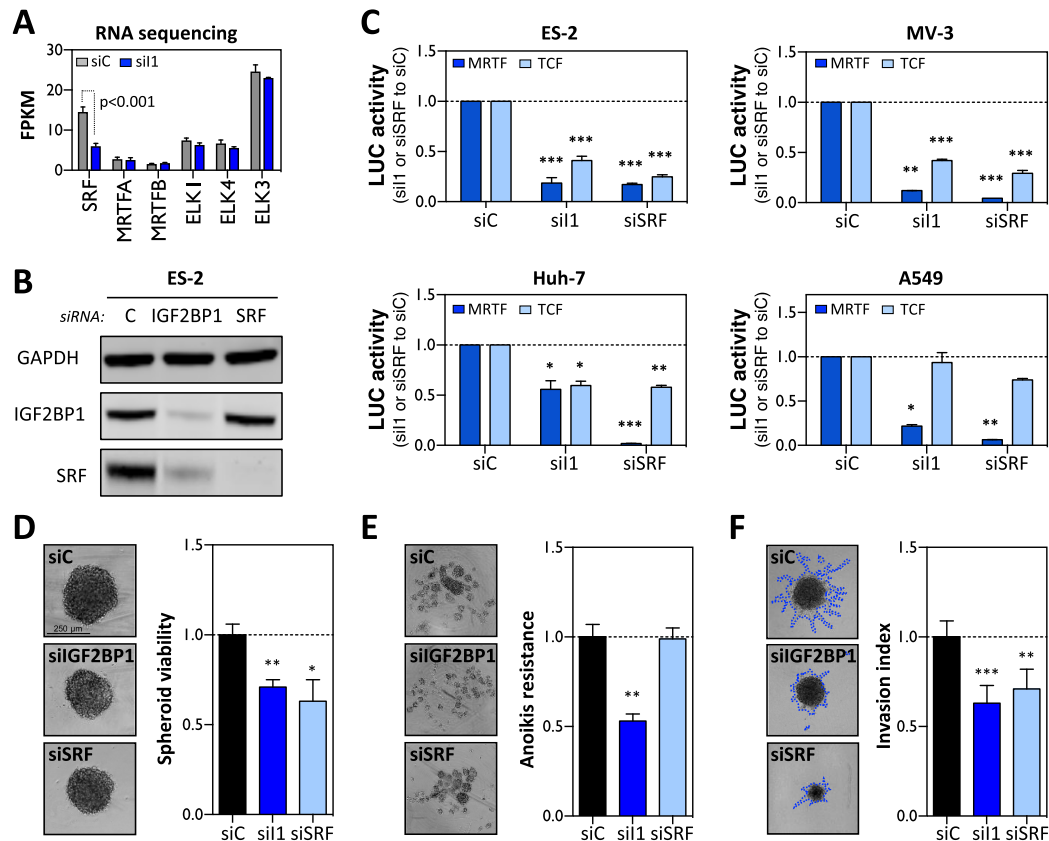
Figure 4. IGF2BP1 promotes SRF-dependent transcription. (**A**) The abundance of indicated mRNAs was determined by RNA-seq (shown as FPKM; fragments per kilobase per million mapped reads) in ES-2 cells transfected with control (siC) or IGF2BP1-directed (siI1) siRNAs. (**B**) Representative western blot analysis of indicated proteins in ES-2 cells transfected with control (siC), IGF2BP1- (siI1) or SRF-directed (siSRF) siRNA pools for 72 h. (**C**) Luciferase reporter assays using MRTF-dependent (dark blue) or TCF-dependent (light blue) promoter constructs in the indicated cell lines upon IGF2BP1- or SRF-depletion by siRNA pools. Reporter activity was determined relative to cells transfected with control (siC) siRNAs, 48 h post-transfection. (**D**) The viability of ES-2 derived spheroids cultured at 10% FBS in concave ultra-low attachment plates was determined by Cell-titer GLO (Promega) 72 h post-transfection with indicated siRNA pools. Cells transfected with control siRNA (siC) served as control and the median viability was set to one. (**E**) Anoikis-resistance of ES-2 cells was determined relative to controls (median set to one) by Cell-titer GLO 72 h post-transfection with indicated siRNA pools. Cells were cultured in planar ultra-low attachment plates at 1% FBS. (**F**) The invasive potential of ES-2 spheroids in 3D matrigel matrix was analyzed 72 h post-transfection of indicated siRNA pools. The relative invasion index (median of controls set to one) was determined by the perimeters of the invasive front (traced by blue dashed line) normalized to spheroid body perimeter. Representative images of cell spheroids are shown in left panels (D–F). Error bars indicate standard deviation determined in at least three analyses. Statistical significance was determined by Student's t-test: (*) $P < 0.05$, (**) $P < 0.01$, (***) $P < 0.001$.

expressing GFP, GFP-IGF2BP1 (I1) or a RNA-binding deficient IGF2BP1 (I1mut) mutant (Figure 5A). The analysis of absolute spheroid size (area) and viability (relative to cells transfected with control siRNAs, siC) revealed that wild-type IGF2BP1 significantly enhanced spheroid growth when SRF was depleted (Figure 5B). In contrast, spheroid growth and viability remained unchanged by the overexpression of RNA-binding deficient IGF2BP1 when compared to GFP-expressing controls. This supported the view that elevated IGF2BP1 expression partially compensated for reduced SRF-dependent transcript synthesis by the post-transcriptional stabilization of mRNAs regulated by SRF at the transcriptional level. Aiming to identify tran-

scripts subjected to co-regulation by SRF and IGF2BP1 in ES-2 cells, differential gene expression was monitored by RNA-seq upon the knockdown of SRF (Supplementary Figure S6A and Supplementary Table ST4A). Comparative analysis of differential gene expression upon IGF2BP1 or SRF depletion in ES-2 cells identified a substantial number of genes up- (489) or downregulated (539) by the knockdown of both factors (Figure 5C). To identify conserved candidates for co-regulation by IGF2BP1 and SRF in cancer, the correlation of candidate transcript expression with IGF2BP1 or SRF mRNA abundance in four primary cancers was determined (*R*, Correlation coefficient; Supplementary Table S4B). The median of correlation
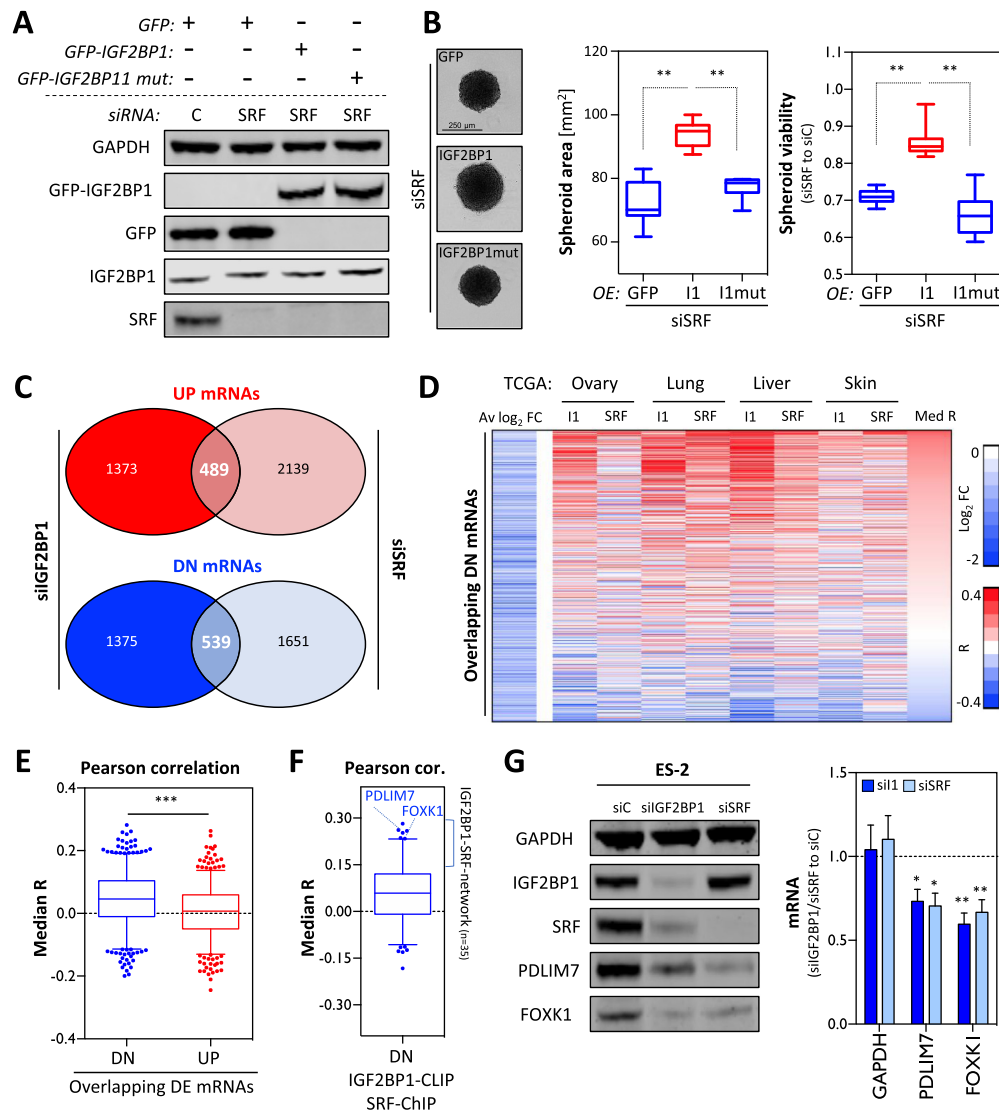
Figure 5. IGF2BP1 and SRF synergize in promoting gene expression in cancer. (**A**) Representative western blot analysis of control (siC) and SRF-depletion (72 h) in ES-2 cells expressing GFP, GFP-IGF2BP1 (GFP-I1) or RNA-binding deficient IGF2BP1 (GFP-I1 mut). (**B**) The maximal area (middle panel) and viability of ES-2 derived spheroids (right panel) transfected as indicated in (A) were derived by inspecting light microscopy images and Cell titer GLO assays (as in Figure 4D), respectively. Representative images are shown in the left panel. Cells transfected with control siRNA (siC) served as control and the median viability was set to one. (**C**) The overlap of mRNAs significantly (FDR $\leq$ 0.01) up- (UP, red) or downregulated (DN, blue) in ES-2 cells upon the depletion of IGF2BP1 and SRF is shown by Venn diagrams. Numbers indicate transcripts with significantly deregulated expression upon the depletion of IGF2BP1 and/or SRF. (**D**) The expression of genes downregulated by SRF and IGF2BP1 depletion in ES-2 cells was tested by Pearson correlation in indicated cancers using TCGA-derived RNA-seq data. The average log2 fold change (right) of gene expression in ES-2 cells (Av log$_2$ FC) upon depletion and correlation coefficients (R) determined for IGF2BP1 and SRF in indicated cancers are shown for each downregulated gene by a heatmap. Genes are ranked by the median correlation (Med R) of gene expression (with SRF and IGF2BP1) indicated on the right. Scale bars for the Av log$_2$ FC and R are shown in the right panel. (**E**) The median R values determined as described in (D) are shown by box plots for genes significantly down- (blue) or upregulated (red) upon IGF2BP1 and SRF depletion in ES-2 cells. (**F**) The median R values of downregulated genes with a 3′UTR CLIP score $\geq$ 4 and SRF-ChIP-score $\geq$ 1 are shown by a box plot. Genes with a median R greater 0.15 (I1-SRF-network, $n = 35$), including PDLIM7 and FOXK1, were considered for further analyses. (**G**) Representative western blot (left panel) and RT-qPCR (right panel) analyses of indicated proteins and FOXK1 as well as PDLIM7 mRNAs in ES-2 cells transfected with control (siC), IGF2BP1- or SRF-directed siRNAs (72 h). GAPDH served as the loading control (**WB**) or the negative control (RT-qPCR). RPLP0 served as the normalization control in RT-qPCR analyses. Error bars indicate standard deviation determined in at least three analyses. Statistical significance was determined by Student's *t*-test: (*) P < 0.05, (**) P < 0.01, (***) P < 0.001.

coefficient was significantly higher for genes downregulated (DN) by the depletion of IGF2BP1 and SRF in ES-2 cells than for upregulated (UP) genes for which the median *R* was slightly above zero (Figure 5E). This suggested that potentially 'oncogenic' effectors of SRF/IGF2BP1 are identified by a conserved positive association with SRF/IGF2BP1-expression in cancer and downregulation upon SRF and IGF2BP1 depletion in cancer-derived cells. To identify candidate transcripts enhanced by SRF at the transcriptional level and promoted by IGF2BP1 at the post-transcriptional level, the median *R* of DN-mRNAs with conserved SRF-promoter binding (ChIP-score ≥ 1; Supplementary Table S4C) and IGF2BP1-3′UTR association (CLIP score ≥ 4) was determined (Figure 5F and Supplementary Table S4C). Although SRF-promoter and IGF2BP1-3′UTR association appeared conserved for only 257 of 539 DN-transcripts, the vast majority of these mRNAs showed positively associated expression with SRF and IGF2BP1 in the four cancers analyzed. To validate the oncogenic role of SRF/IGF2BP1-enhanced effector, 35 transcripts with median *R* values above 0.15 determined by correlation analyses, reported SRF-promoter binding and IGF2BP1-3′UTR association were picked for further analyses. Notably, the identified genes included the previously reported IGF2BP1 target mRNA MKI67 (10). Gene annotation enrichment analyses suggested cell proliferation as a major, shared role of the identified genes (Supplementary Table S4C). Two of these 35 mRNAs, PDLIM7 and FOXK1, showing a significant and positive association with both, IGF2BP1 and SRF expression in cancer, as indicated for HCC and EOC (Supplementary Figure S6C), were chosen for validating regulation by IGF2BP1 and SRF.

The abundance of PDLIM7 and FOXK1 protein and mRNA was significantly reduced by the knockdown of IGF2BP1 and SRF in ES-2 cells (Figure 5G). SRF-ChIP studies performed in ES-2 cells confirmed the binding of SRF to the promoters of FOXK1 and PDLIM7 providing further evidence that SRF promotes the synthesis of the respective transcripts (Figure 6A). IGF2BP1-CLIP sites reported in HepG2, K562, HEK293 and hESCs suggested that binding of IGF2BP1 to the 3′UTRs of FOXK1 and PDLIM7 is conserved (Figure 6B). To evaluate, if IGF2BP1 restores FOXK1 and PDLIM7 expression when SRF is reduced, as observed in phenotypic analyses (see Figure 5A), ES-2 cells stably expressing GFP, wild-type or RNA-binding deficient IGF2BP1 were transfected with control (siC) or SRF-directed siRNA pools (Figure 6C). The abundance of FOXK1 and PDLIM7 protein and mRNA was significantly increased in cells expressing wild-type IGF2BP1. These findings suggested that IGF2BP1 partially restores the expression of SRF target genes by stabilizing the respective mRNAs. This regulation was associated with a substantial recovery of spheroid growth upon SRF depletion (see Figure 5A and B) suggesting that FOXK1 and PDLIM7 are part of a SRF/IGF2BP1-dependent 'effector network' in cancer cells. In support of this, the depletion of FOXK1 and PDLIM7 significantly impaired the growth and viability of ES-2 spheroids, as observed upon the knockdown of IGF2BP1 and SRF (Figure 6D and E). To validate that the regulation of

FOXK1 and PDLIM7 by IGF2BP1/SRF is conserved in cancer cells, the abundance of both mRNAs was monitored upon the depletion of IGF2BP1 in two additional cell lines, A549 and HepG2 (Figure 6F). Both transcripts (FOXK1 and PDLIM7) were decreased upon the knockdown of IGF2BP1 suggesting a substantial conservation of SRF/IGF2BP1-dependent regulation of both factors in cancer cells. If the SRF/IGF2BP1-dependent enhancement of FOXK1 and PDLIM7 has prognostic value in cancer, it was evaluated by Kaplan–Meier analyses using KM plotter (43). Next to evaluating the prognostic value of single gene expression, KM plotter also enables gene set studies. In ovarian cancer, elevated expression of the 'oncogenic gene set' comprising IGF2BP1, SRF, FOXK1 and PDLIM7 was not significantly ($P = 0.077$) associated with poor overall survival (OS) but showed the expected trend with a HR of 1.22 (Supplementary Figure S7A). Significant prognostic value of the gene set was observed when analyzing progression-free survival (PFS: HR, 1.33; $P = 0.0059$) in ovarian cancer. This was even further pronounced when determining PFS probability only in p53-mutated ovarian cancer where the gene set was significantly associated with a poor prognosis ($PFS_{p53-mut}$: HR, 1.84; $P = 0.0034$). Notably, ES-2 cells were reported to be p53-mutated and were proposed as suitable cell models for studying serous ovarian cancer cell properties (54). Assuming that SRF/IGF2BP1-directed gene expression serves conserved oncogenic roles, we next analyzed the prognostic value of the identified prime candidate gene network comprising 35 genes next to SRF and IGF2BP1 (see Figure 5F and Supplementary Table ST4C). In contrast to the small gene set (IGF2BP1, SRF, FOXK1 and PDLIM7), the enlarged gene set (35 genes plus IGF2BP1 and SRF) was significantly associated with poor OS probability in serous ovarian cancer, HCC as well as LUAD, as supported by HR values ranging from 1.52 to 2.15 (Figure 6G and Supplementary Figure S7B). In conclusion, these findings indicate that the SRF/IGF2BP1-dependent control of gene expression in cancer is largely conserved, promotes the synthesis of factors enhancing tumor cell growth and is associated with unfavorable prognosis in three solid cancers.

DISCUSSION

Here, we demonstrate that the mRNA-binding protein IGF2BP1 is a conserved post-transcriptional enhancer of SRF-driven transcription in cancer. The protein impairs the miRNA-directed degradation of the SRF mRNA resulting in elevated SRF abundance and transcriptional activity (Figures 1, 3 and 4). Genomic deletion of the bulk 3′UTR of SRF abrogates IGF2BP1-dependent regulation and enhances SRF expression indicating that SRF expression is essentially controlled via its 3′UTR (Figure 2). This observation supports the recently reported major mode of IGF2BP1-directed regulation in cancer cells, the impairment of miRNA-directed downregulation of target mRNAs (6,9). Concomitantly, this observation underpins the physiological relevance of miRNA-directed control of SRF expression reported in cancer cells, endothelial and (smooth) muscle cells, e.g. (47–50).
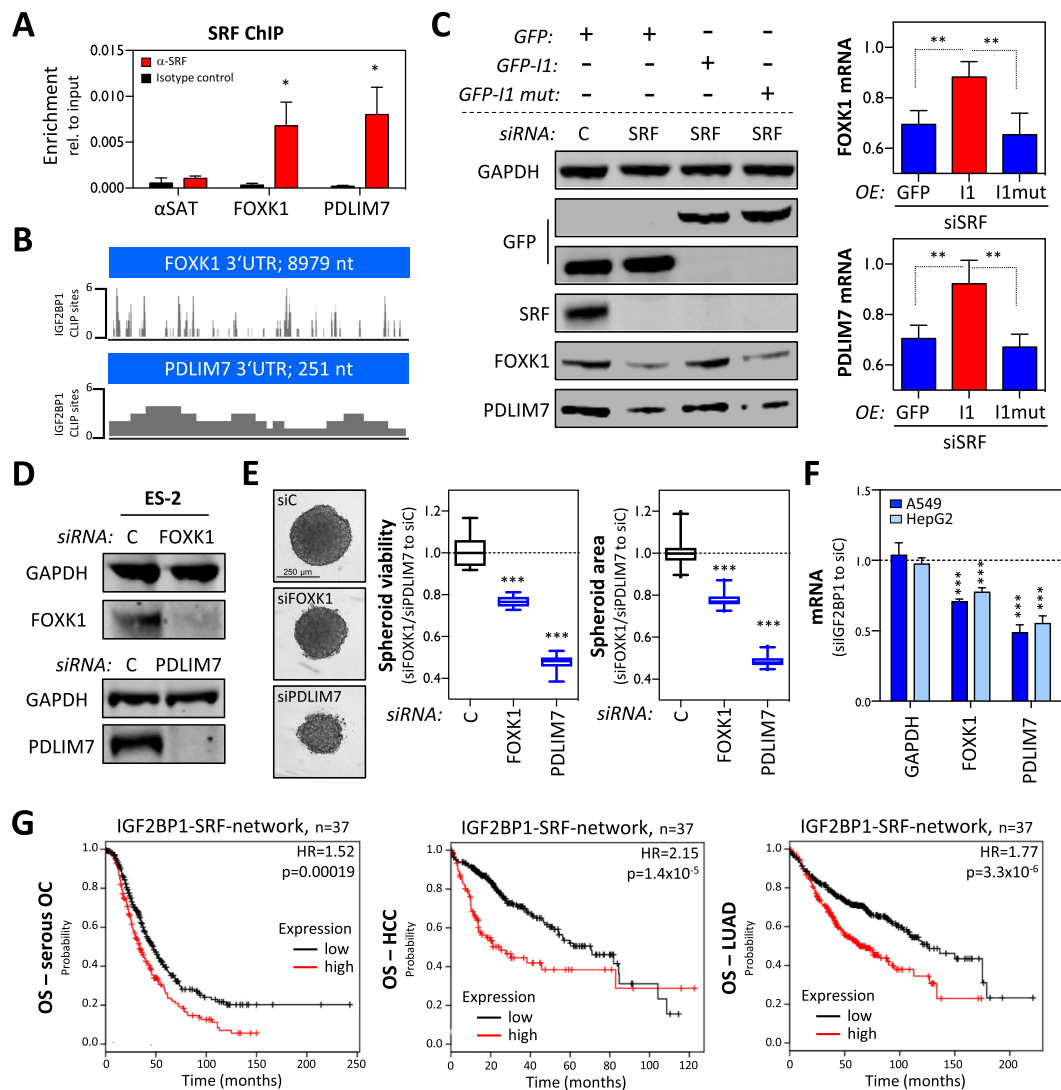
Figure 6. The SRF/IGF2BP1-dependent control of gene expression promotes the expression of 'oncogenic' factors. (**A**) SRF-ChIP analysis of FOXK1 and PDLIM7 in ES-2 cells. The enrichment of promoter regions with SRF (red) or isotype control (black) of indicated genes or satellite DNA (SAT; negative control) was determined relative to inputs by qPCR. (**B**) Schematic indicating the position of IGF2BP1-CLIP hits (CLIP score) in the 3'UTR of indicated genes. (**C**) Representative western blot (left panel) and RT-qPCR (right panel) analyses of indicated proteins and mRNAs in ES-2 cells treated as indicated in Figure 5A. GAPDH served as the loading control in WB and the normalization control in RT-qPCR analyses. (**D**) Representative western blot analyses of indicated proteins in ES-2 cells transfected with control (siC), FOXK1- or PDLIM7-directed siRNA pools (72 h). GAPDH served as the loading control. (**E**) The viability and size (area) of ES-2 derived spheroids (right panel) transfected with siRNA pools as indicated in (D) was monitored by Cell-titer GLO 72 h (viability) and light microscopy (size) post-transfection, as described in Figure 4D. Representative images are shown in the left panel. Cells transfected with control siRNA (siC) served as control and the median viability or area was set to one. (**F**) The abundance of indicated mRNAs was determined in A549 or HepG2 cells transfected with control or IGF2BP1-directed siRNA pools (72 h). GAPDH served as the negative and RPLP0 as a normalization control. (**G**) Kaplan–Meier analyses of the 37 I1-SRF-network genes were performed in indicated cancer datasets using the multigene classifier of KM plotter. The OS probability along with HR and *P*-values determined by KM plotter is shown. Error bars indicate standard deviation determined in at least three analyses. Statistical significance was determined by Student's *t*-test: (*) P < 0.05, (**) *P* < 0.01, (***) *P* < 0.001.

Recent studies have identified IGF2BPs as novel m^{6}A-readers in cancer (14). N^6-methyladenosine modification in the coding region stability determinant (CRD) of the MYC mRNA enhances the association of IGF2BPs and interferes with the endonuclease-directed decay of the MYC mRNA (11). This enhances the expression of the MYC oncogene in cancer cells, as previously reported in EOC- and HCC-derived cancer cells (10,12). Here, we present the first evidence that SRF expression is enhanced in a IGF2BP1- and m^{6}A-dependent manner, as recently reported for MYC. However, in contrast to the latter, m^{6}A-/IGF2BP1-dependent regulation is strictly 3′UTR-dependent (Figure 2). This confirms IGF2BP1 as a conserved 'oncogenic' m^{6}A-reader in cancer and supports the view that IGF2BP1 impairs the miRNA-directed decay of target mRNAs by sequestering transcripts in miRNA-/RISC-free mRNPs (6,9). This mode of regulation is expected to essentially rely on modulating the efficiency, presumably the affinity, of IGF2BP1–mRNA association, as shown here by reduced binding of IGF2BP1 to the SRF mRNA upon METTL3/14 depletion (Figure 2J) and previously demonstrated for the MYC mRNA (14). In an equilibrium, IGF2BP1–mRNA association accordingly relies on the concentration of IGF2BP1 and m^{6}A-modified target mRNAs. Consistently, reduced m^{6}A-modification is partially compensated when IGF2BP1 abundance is upregulated (Supplementary Figure S3G). Although remaining partially contradictory, m^{6}A-modification was proposed to promote oncogenesis in some malignancies including HCC, where METTL3 expression is a significant predictor of poor OS probability (55). Together this suggests that the 'oncogenic potential' of IGF2BP1 is enhanced in cancers with upregulated m^{6}A-modification in IGF2BP1-target mRNAs.

The conserved regulation of SRF expression by IGF2BP1 essentially relies on the post-transcriptional enhancement of SRF expression that by itself is expected to promote oncogenesis. Recent studies show that the upregulation of SRF enhances pluripotency by interfering with cell identity and induces a metaplasia-like phenotype in the pancreas of transgenic mice (29). The oncogenic role of upregulated SRF expression is further enhanced by the IGF2BP1-dependent sustainment of SRF-target gene expression demonstrated here for PDLIM7 and FOXK1 (Figures 5G and 6C). In agreement with promoting tumor cell vitality (Figure 6E), PDLIM7 was shown to stabilizes MDM2 by interfering with its autoubiquitination resulting in reduced responsiveness toward CDK4/6-inhibition by PD03329921 in cancer cells (56,57). In support of findings presented here (Figure 6E), analyses in EOC-, HCC-derived and other cancer cells indicate that the transcriptional regulator FOXK1 promotes the proliferation and metastatic potential of tumor cells in a conserved manner (58,59). Moreover, FOXK1 synergizes with SRF in controlling the transcription of smooth muscle α-actin and cathepsin-A (60). This suggests that the SRF/IGF2BP1-dependent regulation of gene expression also influences the abundance and/or activity of transcriptional co-regulators of SRF. Whereas FOXK1 is enhanced by SRF/IGF2BP1-dependent regulation, the expression of the two main co-factor groups of SRF, MRTFs and TCFs (18) remained

unaffected by IGF2BP1 (Figure 4A). However, IGF2BP1 is a potent post-transcriptional regulator of actin dynamics controlling ACTB protein synthesis as well as MAPK4/MK5/HSP27-dependent regulation of cellular G/F-actin ratios (7,61). Thus, it is tempting to speculate that, next to regulating SRF abundance, IGF2BP1 also modulates the actin-dependent MRTF/SRF (transcriptional) activity, something that needs to be addressed in further detail by follow-up studies. Likewise, IGF2BP1 probably influences the MAPK-modulated activity of SRF/TCF-dependent transcriptional control in cancer cells. IGF2BPs promote the synthesis of growth factors like IGF2 and consistently enhances ERK1/2-activity in liver cancer cells (62,63). At the post-transcriptional level, SRF/IGF2BP1-dependent regulation probably relies on the miRNA-dependent stabilization of SRF-enhanced mRNAs by IGF2BP1. In addition to reports demonstrating miRNA-dependent control of at least FOXK1 (64), the *in silico* prediction of miRNAs targeting PDLIM7 or FOXK1 mRNAs identified various, partially tumor-suppressive miRNAs like members of the let-7-5p, miR-34-5p or miR-181-5p families (data not shown). Taken together, this suggests that IGF2BP1 promotes SRF-dependent transcription in a largely miRNome- and potentially m^{6}A-dependent manner in cancer.

The majority of transcripts enhanced by SRF/IGF2BP1 in ES-2 cells show a conserved association with SRF/IGF2BP1-expression in cancer (Figure 5D–F). Their expression is associated with an overall poor survival probability in ovarian, liver and lung cancer supporting the notion that SRF/IGF2BP1-enhanced gene expression is a conserved driver of oncogenesis that promotes both tumor growth and metastasis (6,26). Moreover, SRF/IGF2BP1-driven gene expression may also enhance a stem-like tumor cell phenotype, as supported by the recently reported role of SRF in promoting pluripotency and various studies indicating IGF2BPs to sustain stem-like cell properties (4,29). In conclusion, these findings suggest SRF/IGF2BP1-dependent gene expression as a novel therapeutic hub in cancer treatment. While targeting SRF-dependent transcription likely poses various, broad and undesired side-effects, the targeting of IGF2BP1 may be advantageous. The protein is essentially absent in adult life, and *de novo* synthesis is only observed in cancer. Targeting IGF2BP1 could thus provide a strategy to impair 'oncogenic' gene expression including genes enhanced by the co-regulation of SRF/IGF2BP1.

DATA AVAILABILITY

Total RNA- as well as small RNA-Seq data have been deposited at GEO (GSE116136).

SUPPLEMENTARY DATA

Supplementary Data are available at NAR Online.

ACKNOWLEDGEMENTS

REFERENCES

1. Bell,J.L., Wachter,K., Muhleck,B., Pazaitis,N., Kohn,M., Lederer,M. and Huttelmaier,S. (2013) Insulin-like growth factor 2 mRNA-binding proteins (IGF2BPs): post-transcriptional drivers of cancer progression? *Cell. Mol. Life Sci.*, **70**, 2657–2675.
2. Lederer,M., Bley,N., Schleifer,C. and Huttelmaier,S. (2014) The role of the oncofetal IGF2 mRNA-binding protein 3 (IGF2BP3) in cancer. *Semin. Cancer Biol.*, **29**, 3–12.
3. Degrauwe,N., Schlumpf,T.B., Janiszewska,M., Martin,P., Cauderay,A., Provero,P., Riggi,N., Suva,M.L., Paro,R. and Stamenkovic,I. (2016) The RNA binding protein IMP2 preserves glioblastoma stem cells by preventing let-7 target gene silencing. *Cell Rep.*, **15**, 1634–1647.
4. Degrauwe,N., Suva,M.L., Janiszewska,M., Riggi,N. and Stamenkovic,I. (2016) IMPs: an RNA-binding protein family that provides a link between stem cell maintenance in normal development and cancer. *Genes Dev.*, **30**, 2459–2474.
5. Nishino,J., Kim,S., Zhu,Y., Zhu,H. and Morrison,S.J. (2013) A network of heterochronic genes including Imp1 regulates temporal changes in stem cell properties. *Elife*, **2**, e00924.
6. Muller,S., Bley,N., Glass,M., Busch,B., Rousseau,V., Misiak,D., Fuchs,T., Lederer,M. and Huttelmaier,S. (2018) IGF2BP1 enhances an aggressive tumor cell phenotype by impairing miRNA-directed downregulation of oncogenic factors. *Nucleic Acids Res.*, **46**, 6285–6303.
7. Stohr,N., Kohn,M., Lederer,M., Glass,M., Reinke,C., Singer,R.H. and Huttelmaier,S. (2012) IGF2BP1 promotes cell migration by regulating MK5 and PTEN signaling. *Genes Dev.*, **26**, 176–189.
8. Zirkel,A., Lederer,M., Stohr,N., Pazaitis,N. and Huttelmaier,S. (2013) IGF2BP1 promotes mesenchymal cell properties and migration of tumor-derived cells by enhancing the expression of LEF1 and SNAI2 (SLUG). *Nucleic Acids Res.*, **41**, 6618–6636.
9. Busch,B., Bley,N., Muller,S., Glass,M., Misiak,D., Lederer,M., Vetter,M., Strauss,H.G., Thomssen,C. and Huttelmaier,S. (2016) The oncogenic triangle of HMGA2, LIN28B and IGF2BP1 antagonizes tumor-suppressive actions of the let-7 family. *Nucleic Acids Res.*, **44**, 3845–3864.
10. Gutschner,T., Hammerle,M., Pazaitis,N., Bley,N., Fiskin,E., Uckelmann,H., Heim,A., Grobeta,M., Hofmann,N., Geffers,R. *et al.* (2014) Insulin-like growth factor 2 mRNA-binding protein 1 (IGF2BP1) is an important protumorigenic factor in hepatocellular carcinoma. *Hepatology*, **59**, 1900–1911.
11. Lemm,I. and Ross,J. (2002) Regulation of c-myc mRNA decay by translational pausing in a coding region instability determinant. *Mol. Cell. Biol.*, **22**, 3959–3969.
12. Kobel,M., Weidensdorfer,D., Reinke,C., Lederer,M., Schmitt,W.D., Zeng,K., Thomssen,C., Hauptmann,S. and Huttelmaier,S. (2007) Expression of the RNA-binding protein IMP1 correlates with poor prognosis in ovarian carcinoma. *Oncogene*, **26**, 7584–7589.
13. Noubissi,F.K., Elcheva,I., Bhatia,N., Shakoori,A., Ougolkov,A., Liu,J., Minamoto,T., Ross,J., Fuchs,S.Y. and Spiegelman,V.S. (2006) CRD-BP mediates stabilization of betaTrCP1 and c-myc mRNA in response to beta-catenin signalling. *Nature*, **441**, 898–901.
14. Huang,H., Weng,H., Sun,W., Qin,X., Shi,H., Wu,H., Zhao,B.S., Mesquita,A., Liu,C., Yuan,C.L. *et al.* (2018) Recognition of RNA N(6)-methyladenosine by IGF2BP proteins enhances mRNA stability and translation. *Nat. Cell Biol.*, **20**, 285–295.
15. Hafner,M., Landthaler,M., Burger,L., Khorshid,M., Hausser,J., Berninger,P., Rothballer,A., Ascano,M. Jr., Jungkamp,A.C., Munschauer,M. *et al.* (2010) Transcriptome-wide identification of RNA-binding protein and microRNA target sites by PAR-CLIP. *Cell*, **141**, 129–141.
16. Van Nostrand,E.L., Pratt,G.A., Shishkin,A.A., Gelboin-Burkhart,C., Fang,M.Y., Sundararaman,B., Blue,S.M., Nguyen,T.B., Surka,C., Elkins,K. *et al.* (2016) Robust transcriptome-wide discovery of RNA-binding protein binding sites with enhanced CLIP (eCLIP). *Nat. Methods*, **13**, 508–514.
17. Conway,A.E., Van Nostrand,E.L., Pratt,G.A., Aigner,S., Wilbert,M.L., Sundararaman,B., Freese,P., Lambert,N.J., Sathe,S., Liang,T.Y. *et al.* (2016) Enhanced CLIP uncovers IMP Protein-RNA targets in human pluripotent stem cells important for cell adhesion and survival. *Cell Rep.*, **15**, 666–679.
18. Clark,K.A. and Graves,B.J. (2014) Dual views of SRF: a genomic exposure. *Genes Dev.*, **28**, 926–928.
19. Descot,A., Hoffmann,R., Shaposhnikov,D., Reschke,M., Ullrich,A. and Posern,G. (2009) Negative regulation of the EGFR-MAPK cascade by actin-MAL-mediated Mig6/Errfi-1 induction. *Mol. Cell*, **35**, 291–304.
20. Esnault,C., Stewart,A., Gualdrini,F., East,P., Horswell,S., Matthews,N. and Treisman,R. (2014) Rho-actin signaling to the MRTF coactivators dominates the immediate transcriptional response to serum in fibroblasts. *Genes Dev.*, **28**, 943–958.
21. Leitner,L., Shaposhnikov,D., Mengel,A., Descot,A., Julien,S., Hoffmann,R. and Posern,G. (2011) MAL/MRTF-A controls migration of non-invasive cells by upregulation of cytoskeleton-associated proteins. *J. Cell Sci.*, **124**, 4318–4331.
22. Boros,J., Donaldson,I.J., O'Donnell,A., Odrowaz,Z.A., Zeef,L., Lupien,M., Meyer,C.A., Liu,X.S., Brown,M. and Sharrocks,A.D. (2009) Elucidation of the ELK1 target gene network reveals a role in the coordinate regulation of core components of the gene regulation machinery. *Genome Res.*, **19**, 1963–1973.
23. Olson,E.N. and Nordheim,A. (2010) Linking actin dynamics and gene transcription to drive cellular motile functions. *Nat. Rev. Mol. Cell Biol.*, **11**, 353–365.
24. Miralles,F., Posern,G., Zaromytidou,A.I. and Treisman,R. (2003) Actin dynamics control SRF activity by regulation of its coactivator MAL. *Cell*, **113**, 329–342.
25. Esnault,C., Gualdrini,F., Horswell,S., Kelly,G., Stewart,A., East,P., Matthews,N. and Treisman,R. (2017) ERK-induced activation of TCF family of SRF cofactors initiates a chromatin modification cascade associated with transcription. *Mol. Cell*, **65**, 1081–1095.
26. Medjkane,S., Perez-Sanchez,C., Gaggioli,C., Sahai,E. and Treisman,R. (2009) Myocardin-related transcription factors and SRF are required for cytoskeletal dynamics and experimental metastasis. *Nat. Cell Biol.*, **11**, 257–268.
27. Ro,S. (2016) Multi-phenotypic role of serum response factor in the gastrointestinal system. *J. Neurogastroenterol. Motil.*, **22**, 193–200.
28. Miano,J.M., Long,X. and Fujiwara,K. (2007) Serum response factor: master regulator of the actin cytoskeleton and contractile apparatus. *Am. J. Physiol. Cell Physiol.*, **292**, C70–C81.
29. Ikeda,T., Hikichi,T., Miura,H., Shibata,H., Mitsunaga,K., Yamada,Y., Woltjen,K., Miyamoto,K., Hiratani,I., Yamada,Y. *et al.* (2018) Srf destabilizes cellular identity by suppressing cell-type-specific gene expression programs. *Nat. Commun.*, **9**, 1387.
30. Carey,M.F., Peterson,C.L. and Smale,S.T. (2009) Chromatin immunoprecipitation (ChIP). *Cold Spring Harb. Protoc.*, **2009**, doi:10.1101/pdb.prot5279.
31. Weissbach,J., Schikora,F., Weber,A., Kessels,M. and Posern,G. (2016) Myocardin-Related transcription factor a activation by competition with WH2 domain proteins for actin binding. *Mol. Cell. Biol.*, **36**, 1526–1539.
32. Kim,D., Langmead,B. and Salzberg,S.L. (2015) HISAT: a fast spliced aligner with low memory requirements. *Nat. Methods*, **12**, 357–360.
33. Langmead,B. and Salzberg,S.L. (2012) Fast gapped-read alignment with Bowtie 2. *Nat. Methods*, **9**, 357–359.

390 Nucleic Acids Research, 2019, Vol. 47, No. 1

34. Liao,Y., Smyth,G.K. and Shi,W. (2014) featureCounts: an efficient general purpose program for assigning sequence reads to genomic features. *Bioinformatics*, **30**, 923–930.

35. Yates,A., Akanni,W., Amode,M.R., Barrell,D., Billis,K., Carvalho-Silva,D., Cummins,C., Clapham,P., Fitzgerald,S., Gil,L. *et al.* (2016) Ensembl 2016. *Nucleic Acids Res.*, **44**, D710–D716.

36. Kozomara,A. and Griffiths-Jones,S. (2014) miRBase: annotating high confidence microRNAs using deep sequencing data. *Nucleic Acids Res.*, **42**, D68–D73.

37. Robinson,M.D., McCarthy,D.J. and Smyth,G.K. (2010) edgeR: a Bioconductor package for differential expression analysis of digital gene expression data. *Bioinformatics*, **26**, 139–140.

38. Dweep,H. and Gretz,N. (2015) miRWalk2.0: a comprehensive atlas of microRNA-target interactions. *Nat. Methods*, **12**, 697.

39. Muller,S., Bley,N., Glass,M., Busch,B., Rousseau,V., Misiak,D., Fuchs,T., Lederer,M. and Huttelmaier,S. (2018) IGF2BP1 enhances an aggressive tumor cell phenotype by impairing miRNA-directed downregulation of oncogenic factors. *Nucleic Acids Res.*, **46**, 6285–6303.

40. Gualdrini,F., Esnault,C., Horswell,S., Stewart,A., Matthews,N. and Treisman,R. (2016) SRF Co-factors control the balance between cell proliferation and contractility. *Mol. Cell*, **64**, 1048–1061.

41. Katschnig,A.M., Kauer,M.O., Schwentner,R., Tomazou,E.M., Mutz,C.N., Linder,M., Sibilia,M., Alonso,J., Aryee,D.N.T. and Kovar,H. (2017) EWS-FLI1 perturbs MRTFB/YAP-1/TEAD target gene regulation inhibiting cytoskeletal autoregulatory feedback in Ewing sarcoma. *Oncogene*, **36**, 5995–6005.

42. Sikora-Wohlfeld,W., Ackermann,M., Christodoulou,E.G., Singaravelu,K. and Beyer,A. (2013) Assessing computational methods for transcription factor target gene identification based on ChIP-seq data. *PLoS Comput. Biol.*, **9**, e1003342.

43. Lanczky,A., Nagy,A., Bottai,G., Munkacsy,G., Szabo,A., Santarpia,L. and Gyorffy,B. (2016) miRpower: a web-tool to validate survival-associated miRNAs utilizing expression data from 2178 breast cancer patients. *Breast Cancer Res. Treat.*, **160**, 439–446.

44. Wachter,K., Kohn,M., Stohr,N. and Huttelmaier,S. (2013) Subcellular localization and RNP formation of IGF2BPs (IGF2 mRNA-binding proteins) is modulated by distinct RNA-binding domains. *Biol. Chem.*, **394**, 1077–1090.

45. Liu,H., Wang,H., Wei,Z., Zhang,S., Hua,G., Zhang,S.W., Zhang,L., Gao,S.J., Meng,J., Chen,X. *et al.* (2018) MeT-DB V2.0: elucidating context-specific functions of N6-methyl-adenosine methyltranscriptome. *Nucleic Acids Res.*, **46**, D281–D287.

46. Ennajdaoui,H., Howard,J.M., Sterne-Weiler,T., Jahanbani,F., Coyne,D.J., Uren,P.J., Dargyte,M., Katzman,S., Draper,J.M., Wallace,A. *et al.* (2016) IGF2BP3 modulates the interaction of Invasion-Associated transcripts with RISC. *Cell Rep.*, **15**, 1876–1883.

47. Chen,Z., Wang,M., Huang,K., He,Q., Li,H. and Chang,G. (2018) MicroRNA-125b affects vascular smooth muscle cell function by targeting serum response factor. *Cell. Physiol. Biochem.*, **46**, 1566–1580.

48. Su,Z., Zhang,M., Xu,M., Li,X., Tan,J., Xu,Y., Pan,X., Chen,N., Chen,X. and Zhou,Q. (2018) MicroRNA181c inhibits prostate cancer cell growth and invasion by targeting multiple ERK signaling pathway components. *Prostate*, **78**, 343–352.

49. Xu,D., Guo,Y., Liu,T., Li,S. and Sun,Y. (2017) miR-22 contributes to endosulfan-induced endothelial dysfunction by targeting SRF in HUVECs. *Toxicol. Lett.*, **269**, 33–40.

50. Wei,X., Hou,X., Li,J. and Liu,Y. (2017) miRNA-181a/b regulates phenotypes of vessel smooth muscle cells through serum response factor. *DNA Cell Biol.*, **36**, 127–135.

51. Weidensdorfer,D., Stohr,N., Baude,A., Lederer,M., Kohn,M., Schierhorn,A., Buchmeier,S., Wahle,E. and Huttelmaier,S. (2009) Control of c-myc mRNA stability by IGF2BP1-associated cytoplasmic RNPs. *RNA*, **15**, 104–115.

52. Srikantan,S., Tominaga,K. and Gorospe,M. (2012) Functional interplay between RNA-binding protein HuR and microRNAs. *Curr. Protein Pept. Sci.*, **13**, 372–379.

53. Muehlich,S., Hampl,V., Khalid,S., Singer,S., Frank,N., Breuhahn,K., Gudermann,T. and Prywes,R. (2012) The transcriptional coactivators megakaryoblastic leukemia 1/2 mediate the effects of loss of the tumor suppressor deleted in liver cancer 1. *Oncogene*, **31**, 3913–3923.

54. Domcke,S., Sinha,R., Levine,D.A., Sander,C. and Schultz,N. (2013) Evaluating cell lines as tumour models by comparison of genomic profiles. *Nat. Commun.*, **4**, 2126.

55. Deng,X., Su,R., Weng,H., Huang,H., Li,Z. and Chen,J. (2018) RNA N(6)-methyladenosine modification in cancers: current status and perspectives. *Cell Res.*, **28**, 507–517.

56. Klein,M.E., Dickson,M.A., Antonescu,C., Qin,L.X., Dooley,S.J., Barlas,A., Manova,K., Schwartz,G.K., Crago,A.M., Singer,S. *et al.* (2018) PDLIM7 and CDH18 regulate the turnover of MDM2 during CDK4/6 inhibitor therapy-induced senescence. *Oncogene*, **37**, 5066–5078.

57. Jung,C.R., Lim,J.H., Choi,Y., Kim,D.G., Kang,K.J., Noh,S.M. and Im,D.S. (2010) Enigma negatively regulates p53 through MDM2 and promotes tumor cell survival in mice. *J. Clin. Invest.*, **120**, 4493–4506.

58. Li,J., Yu,Z., He,L., Zhou,D., Xie,S., Hou,H. and Geng,X. (2017) Knockdown of FOXK1 inhibited the proliferation, migration and invasion in hepatocellular carcinoma cells. *Biomed. Pharmacother.*, **92**, 270–276.

59. Li,L., Gong,M., Zhao,Y., Zhao,X. and Li,Q. (2017) FOXK1 facilitates cell proliferation through regulating the expression of p21, and promotes metastasis in ovarian cancer. *Oncotarget*, **8**, 70441–70451.

60. Freddie,C.T., Ji,Z., Marais,A. and Sharrocks,A.D. (2007) Functional interactions between the Forkhead transcription factor FOXK1 and the MADS-box protein SRF. *Nucleic Acids Res.*, **35**, 5203–5212.

61. Huttelmaier,S., Zenklusen,D., Lederer,M., Dictenberg,J., Lorenz,M., Meng,X., Bassell,G.J., Condeelis,J. and Singer,R.H. (2005) Spatial regulation of beta-actin translation by Src-dependent phosphorylation of ZBP1. *Nature*, **438**, 512–515.

62. Xu,Y., Zheng,Y., Liu,H. and Li,T. (2017) Modulation of IGF2BP1 by long non-coding RNA HCG11 suppresses apoptosis of hepatocellular carcinoma cells via MAPK signaling transduction. *Int. J. Oncol.*, **51**, 791–800.

63. Dai,N., Christiansen,J., Nielsen,F.C. and Avruch,J. (2013) mTOR complex 2 phosphorylates IMP1 cotranslationally to promote IGF2 production and the proliferation of mouse embryonic fibroblasts. *Genes Dev.*, **27**, 301–312.

64. Zhang,P., Tang,W.M., Zhang,H., Li,Y.Q., Peng,Y., Wang,J., Liu,G.N., Huang,X.T., Zhao,J.J., Li,G. *et al.* (2017) MiR-646 inhibited cell proliferation and EMT-induced metastasis by targeting FOXK1 in gastric cancer. *Br. J. Cancer*, **117**, 525–534.

Müller et al., 2018 - SUPPLEMENTARY FIGURE LEGENDS

Supplementary Figure S1. IGF2BP1-dependent control of gene expression in ES-2 and Huh-7 cells. (A) Correlation analysis of miRNA expression, as determined by small RNA-seq (supplementary Table T2), in Huh-7 and ES-2 cells. Downregulated expression of the let-7-5p family (red) and upregulation of miR- 122-5p (blue) in Huh-7 cells is indicated along with the determined Correlation coefficient (R), R squared value (R2) and statistical significance (p-value). (B) The expression (CPM; counts per million mapped reads) of all nine let-7-5p family members in ES-2 and Huh-7 cells was determined by small RNA-sequencing and summed up over two biological replicates. (C) The overlap of mRNAs significantly (FDR ≤ 0.01) up- (UP, red) or downregulated (DN, blue) in the indicated cell lines upon IGF2BP1 depletion is shown by Venn diagrams. Numbers indicate transcripts with significantly deregulated expression in analyzed cell lines. (D) The IGF2BP1 3'UTR-CLIP scores determined for mRNAs significantly down- (DN, blue) or upregulated (UP, red) in Huh-7 or ES-2 cell are depicted by box plots. (E) Gene set enrichment analysis (GSEA) of IGF2BP1-depleted Huh-7 (top panel) and ES-2 (bottom panel) cells. Genes were ranked according to their fold change. Note that the same pathways are significantly affected by IGF2BP1 depletion (also see supplementary Table 1B). Statistical significance was determined by Student's t-test: (**) $P < 0.01$, (***) $P < 0.001$.

Supplementary Figure S2. (A) Knockdown-recovery study indicating that wild type chicken Igf2bp1 restores SRF protein (left panel) and mRNA (right panel) expression in ES-2 cells. RPLP0 served as the internal normalization control in RT-qPCR analyses. Cells stably expressing indicated proteins were previously reported (9). Statistical significance was determined by Student's t-test: (***) $P < 0.001$.

Supplementary Figure S3. IGF2BP1 controls SRF expression in HepG2 cells in an m^6A-dependent manner. (A) RT-qPCR analyses demonstrate the downregulation (relative to controls, siC-transfected) of the SRF mRNA upon IGF2BP1 depletion in HepG2 cells by siRNA pools (72h). GAPDH served as the negative and RPLP0 as the normalization control. (B) Representative Western blot analysis of indicated proteins in HepG2 cells transfected with control (siC) or IGF2BP1-directed siRNA pools as in A. (C) RT-qPCR analysis showing the upregulation (relative to controls, parental A549 cells) of the SRF mRNA upon deletion of the bulk 3'UTR. GAPDH served as the negative and RPLP0 as the normalization control. Error bars indicate standard deviation determined in at least three analyses. (D) The depletion of METTL3 and METTL14 by siRNA pools impairs SRF protein expression in indicated cell lines. GAPDH served as the loading and negative control. Representative Western blots are shown. (E) The enlargement of Fig. 2I shows m^6A-RIP-seq reads in the 3'UTR in HepG2 cells transfected with control shRNAs (red) or METTL14-directed shRNAs (blue), as reported by (14). Clip hits in the respective region reported by eCLIP analyses in HepG2 cells are shown in the lower panel. (F) IGF2BP1- immunoprecipitation analyzed in Fig. 2J was evaluated by Western blotting in control-transfected (C) or METTL3/14-depleted (M3/14)

cells. GAPDH served as the loading control in input fractions. (G) Representative Western blot analysis of indicated proteins showing that elevated expression of GFP- tagged wild type IGF2BP1 (I1) restores SRF protein abundance when METTL3 is depleted in ES-2 cells. Note that SRF protein abundance remains unaffected in cells expressing GFP or RNA-binding deficient IGF2BP1 (I1mut). GAPDH served as the loading control. Statistical significance was determined by Student's t-test: (**) $P < 0.01$, (***) $P < 0.001$.

Supplementary Figure S4. IGF2BP1-dependent regulation of SRF expression is IGF2BP paralogue specific. (A) Representative Western blot analysis in indicated cell lines demonstrating that only the depletion of IGF2BP1 impairs SRF protein abundance in cancer cells. Cells were transfected with control (siC) or siRNA pools directed against IGF2BP paralogues (IGF2BP1, 2 and 3) for 72h. VCL served as the loading control. (B) Schematic indicating the position of CLIP sites reported for IGF2BP1-3 in the SRF 3'UTR by eight (IGF2BP1), seven (IGF2BP2) or six (IGF2BP3) experiments performed in HepG2, K562, HEK293 or hESC cells, as indicated in material and methods. VCL served as the loading control. (C) The expression of SRF and IGF2BP1 was tested for Pearson correlation in indicated cancers using TCGA-derived RNA-seq data. The determined correlation coefficients for each analysis as well as the median correlation coefficient (Trend) are indicated by a heat map. Scale bars for R values are shown in the lower panel. (D) MiRNA expression was determined by small RNA-seq of two biological replicates of indicated cell lines (left panel). The CPM of 598 miRNAs predicted by at least 3 of 4 databases (miRWalk, RNA22, TargetScan, miRanda) to target the SRF 3'UTR are shown by a heat map (right panel). MiRNAs are sorted according to the median CPM determined in the analyzed cell lines. Scale bars for CPM values are shown in the lower panel. (E) The depletion of DICER and DROSHA, as well as miR-22 upon DICER/DROSHA knockdown in ES-2 cells, was monitored by Western blotting (upper panel, WB) or Northern blotting (lower panel, NB). VCL, 5S rRNA and the U6 snRNA served as loading controls in WB or NB, respectively. Representative blots are shown.

Supplementary Figure S5. (A) SRF protein expression was analyzed by Western blotting upon the depletion of IGF2BP1 or ELAVL1 in A549 cells (72 h). Note that only the depletion of IGF2BP1 results in reduced SRF protein abundance. GAPDH served as the loading control. A representative Western blot is shown. (B) The relative number of overlapping CLIP sites determined for IGF2BP1, ELAVL1 and AGO2 in the proximity of MTSs, as recently reported (6), are shown relative to the start of MTSs predicted by TargetScan for human mRNAs (hg19; IGF2BP1 all eCLIP) or the SRF 3'UTR (IGF2BP1 SRF eCLIP).

Supplementary Figure S6. Co-regulation of gene expression by IGF2BP1 and SRF in ES-2 cells. (A) Volcano plot showing differential gene expression (threshold: FDR ≤ 0.01) determined by RNA-seq in ES-2 cells upon SRF depletion using siRNA pools (72h). (B) The expression of genes upregulated by SRF and IGF2BP1 depletion in ES-2 cells was tested for Pearson correlation in indicated cancers using TCGA- derived RNA-seq data. The average log2 fold change (right) of gene

expression in ES-2 cells (Av log$_2$ FC) upon depletion and correlation coefficients (R) determined for IGF2BP1 and SRF in indicated cancers are shown for each upregulated gene by a heat map. Genes are sorted according to the median correlation coefficient (Med R) of gene expression (with SRF and IGF2BP1) indicated on the right. Scale bars for the Av log$_2$ FC and R are shown in the right panel. (C) Pearson correlation analysis of indicated genes in TCGA-derived RNA-seq data of ovarian (ovary) and liver cancer. The number of considered tumor samples, correlation coefficients (R) and statistical significance determined by the R2 database are indicated. Correlations coefficients for all genes analyzed in TCGA-provided datasets (Ovary, Lung, Liver and Skin) are summarized in supplementary Table T4B.

Supplementary Figure S7. SRF/IGF2BP1-directed gene expression is associated with an unfavorable prognosis in cancer. (A) Kaplan Meier analyses of the small gene set (IGF2BP1, SRF, PDLIM7 and FOXK1; see Figure 6G) were performed in an ovarian data set using the multigene classifier of KM plotter. The overall (OS) survival probability in all serous ovarian cancer samples (left panel), the progression-free survival probability (PFS) in all (middle panel) or p53-mutated (right panel) serous ovarian cancer samples accessible via KM plotter are shown. (B) Kaplan Meier analyses of the 37 I1- SRF-network genes (see Figure 6G) in serous ovarian cancer (left panel) and p53-mutated serous ovarian cancer (right panel) were performed by KM plotter using the multi gene classifier. The overall (OS) or progression-free (PFS) survival probability along with hazardous ratios (HR) and p values determined by KM plotter are shown.
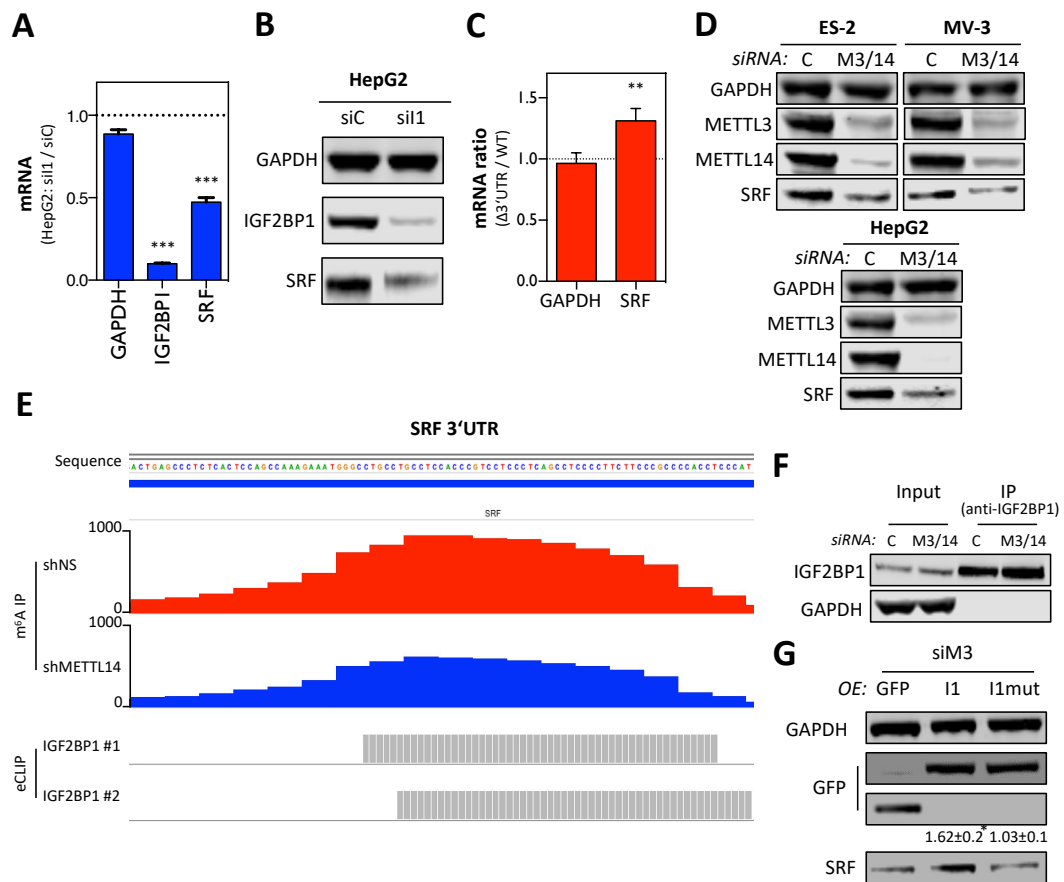
Müller et al., 2019 - Supplementary Figure S1
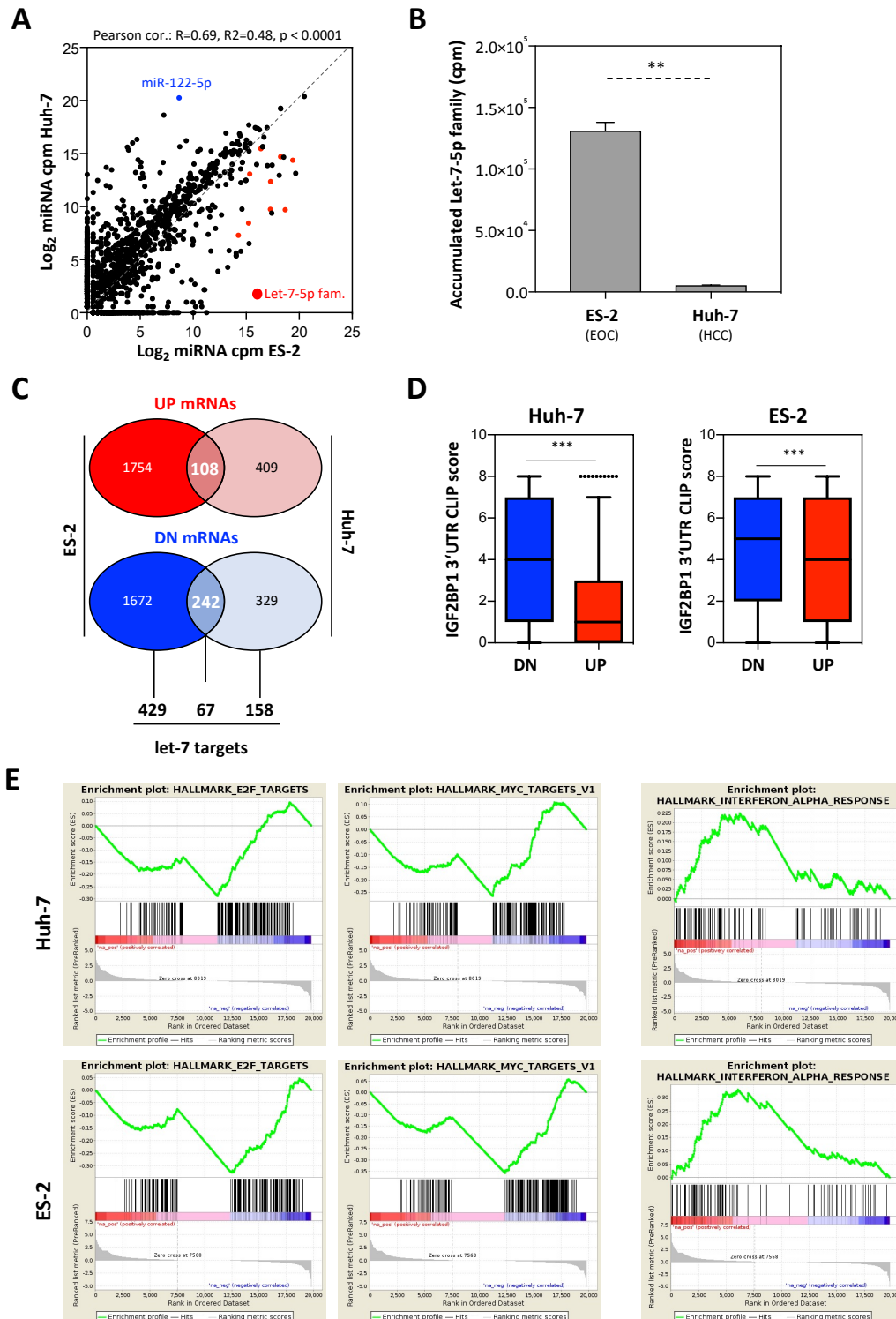
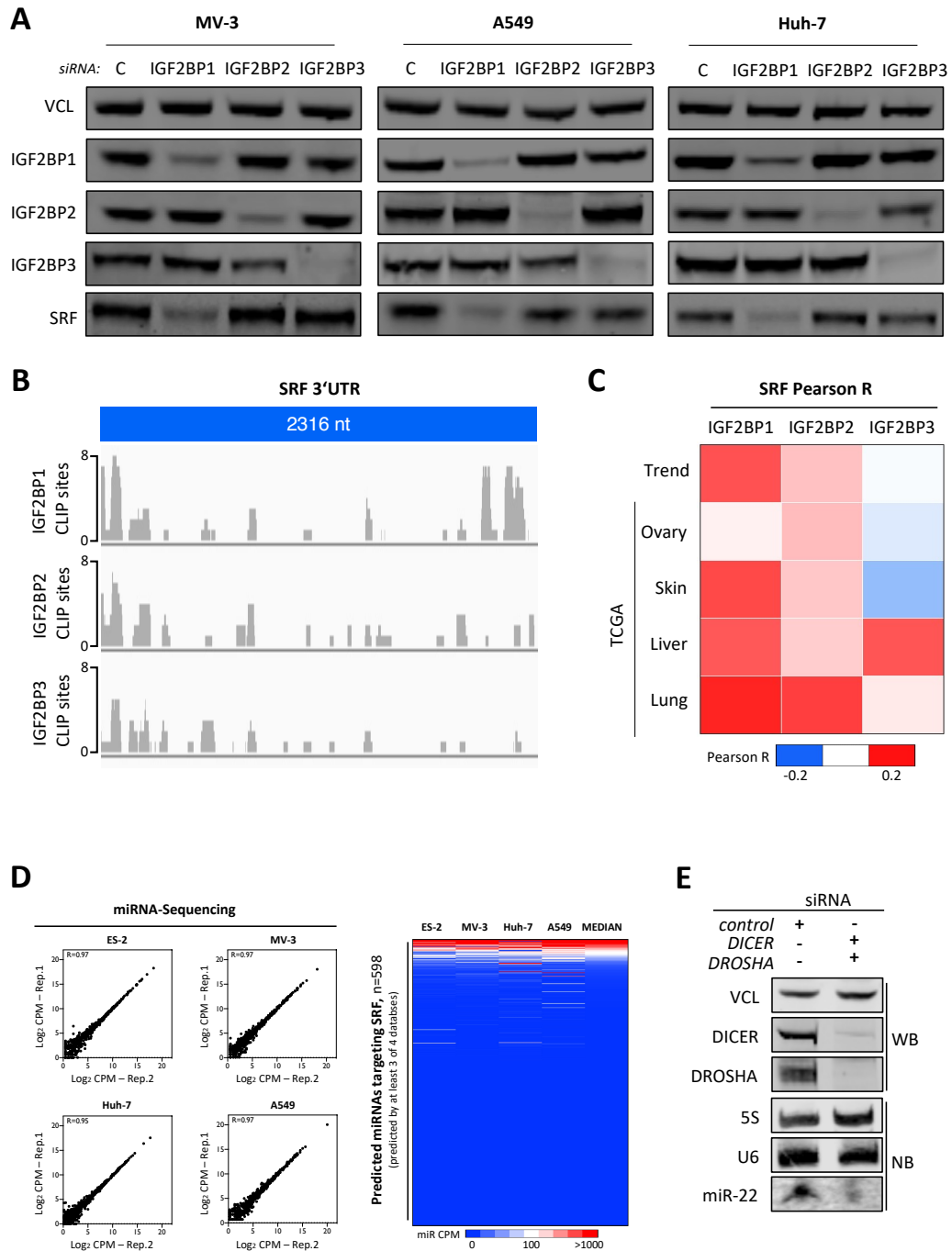**Müller et al., 2019 - Supplementary Figure S2**
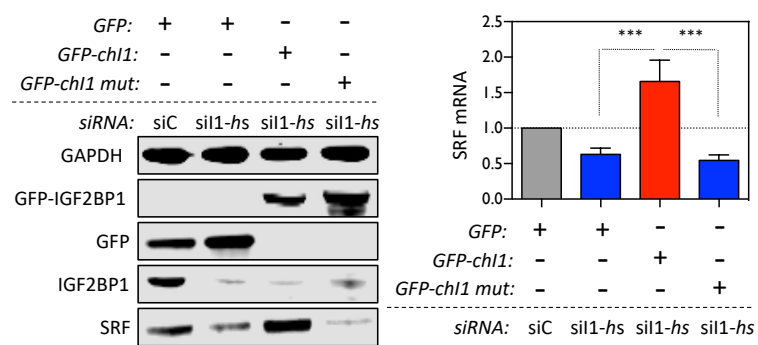
A

Müller et al., 2019 - Supplementary Figure S3

Müller et al., 2019 - Supplementary Figure S4

A

B

SRF 3'UTR

C

SRF Pearson R

D

miRNA-Sequencing

E

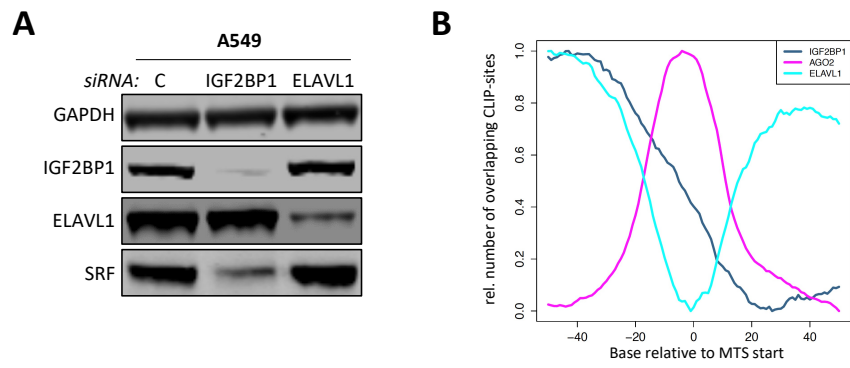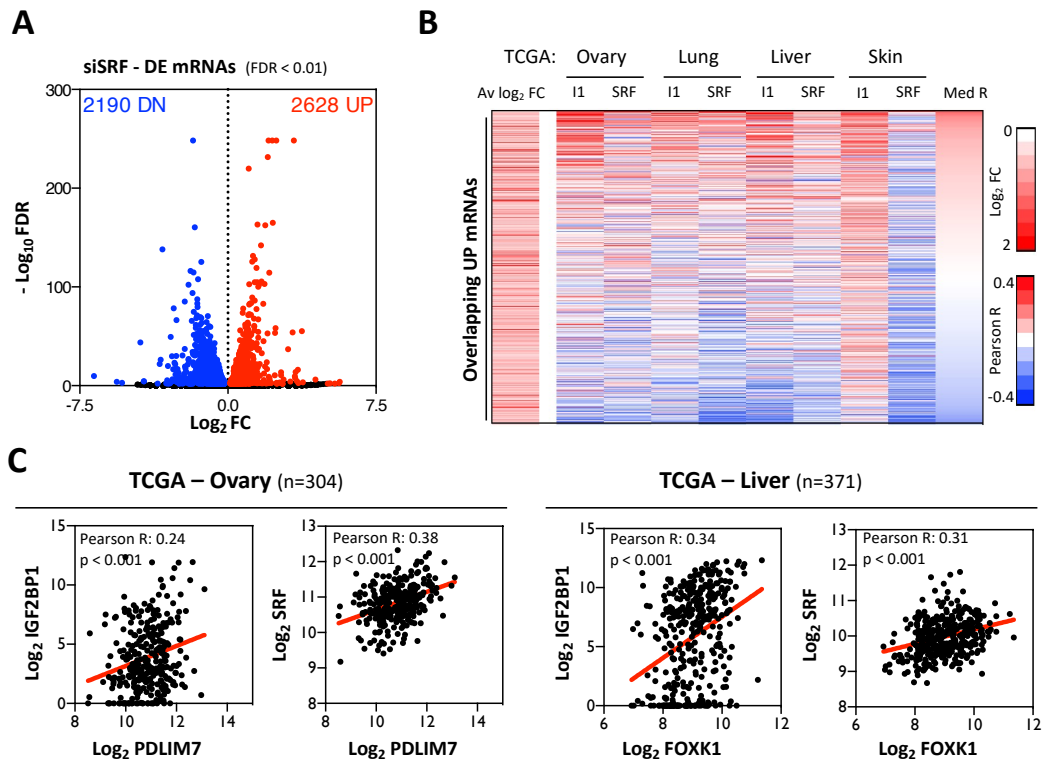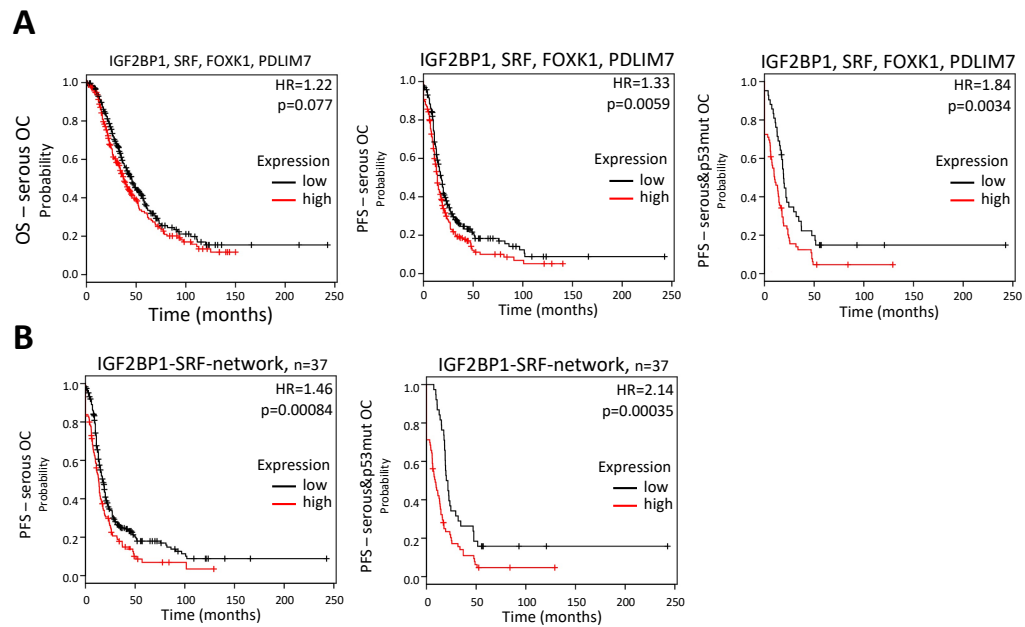**Müller et al., 2019 - Supplementary Figure S5**

Müller et al., 2019 - Supplementary Figure S6

Müller et al., 2019 - Supplementary Figure S7

Article: The oncofetal RNA-binding protein IGF2BP1 is a druggable, post-transcriptional super-enhancer of E2F-driven gene expression in cancer

The oncofetal RNA-binding protein IGF2BP1 is a druggable, post-transcriptional super-enhancer of E2F-driven gene expression in cancer

Simon Müller[1,*], Nadine Bley[1], Bianca Busch[1], Markus Glaß[1], Marcell Lederer[1], Claudia Misiak[1], Tommy Fuchs[1], Alice Wedler[1], Jacob Haase[1], Jean Borges Bertoldo[1], Patrick Michl[2] and Stefan Hüttelmaier [1,*]

[1]Institute of Molecular Medicine, Section for Molecular Cell Biology, Faculty of Medicine, Martin Luther University Halle-Wittenberg, 06120 Halle, Germany and [2]Department of Internal Medicine I, Faculty of Medicine, Martin Luther University Halle/Wittenberg, 06120 Halle, Germany

ABSTRACT

The IGF2 mRNA-binding protein 1 (IGF2BP1) is a non-catalytic post-transcriptional enhancer of tumor growth upregulated and associated with adverse prognosis in solid cancers. However, conserved effector pathway(s) and the feasibility of targeting IGF2BP1 in cancer remained elusive. We reveal that IGF2BP1 is a post-transcriptional enhancer of the E2F-driven hallmark in solid cancers. IGF2BP1 promotes G1/S cell cycle transition by stabilizing mRNAs encoding positive regulators of this checkpoint like E2F1. This IGF2BP1-driven shortening of the G1 cell cycle phase relies on 3′UTR-, miRNA- and m⁶A-dependent regulation and suggests enhancement of cell cycle progression by m⁶A-modifications across cancers. In addition to E2F transcription factors, IGF2BP1 also stabilizes E2F-driven transcripts directly indicating post-transcriptional 'super'-enhancer role of the protein in E2F-driven gene expression in cancer. The small molecule BTYNB disrupts this enhancer function by impairing IGF2BP1-RNA association. Consistently, BTYNB interferes with E2F-driven gene expression and tumor growth in experimental mouse tumor models.

INTRODUCTION

RNA-binding proteins (RBPs), including the IGF2 mRNA-binding protein (IGF2BP) family are crucial regulators of tumor and stem cell fate (1–3). CLIP (cross-linking immunoprecipitation) studies suggest a plethora of mostly overlapping IGF2BP target mRNAs (4,5).

Despite promiscuous RNA-binding properties and distinct, partially oncofetal expression patterns, all IGF2BP paralogues show an 'oncogenic' potential in cancer (6,7). However, among IGF2BPs, only IGF2BP1 shows strong conservation of oncogenic potential in cancer-derived cell lines (8,9). This was largely attributed to the inhibition of MYC mRNA decay by IGF2BP1 (10). This regulation, however, is an exception, since all IGF2BPs impair MYC mRNA turnover due to hindering cleavage by endonucleases in the coding region of MYC (11,12). The main role of IGF2BP1 in cancer cells is the impairment of miRNA/RISC-directed mRNA decay by safe-guarding target mRNAs in cytoplasmic mRNPs (8,13–15). Recently, IGF2BPs were identified as m⁶A-readers, associating preferentially with N⁶-methyladenosine modified target mRNAs (12). Validated for two mRNAs, MYC and SRF, m⁶A-enhanced mRNA association of IGF2BPs results in elevated mRNA stabilization and enforced expression of MYC and SRF, respectively (12,16). Despite consistent stimulation of tumor cell proliferation and tumor growth by IGF2BP1, conserved effector pathways remained unknown. Here, we reveal that IGF2BP1 stabilizes E2F1–3 mRNAs leading to enhanced E2F-driven gene expression and cell cycle progression in cancer cells. E2F-dependent regulation is frequently deregulated in cancer and tightly linked to the control of self-renewal versus differentiation potential of pluripotent stem cells (17,18). In cancer as well as progenitor cells, E2F expression is subjected to largely conserved regulation by various microRNAs (17,19). Surprisingly, regulation of E2F expression by RBPs was only reported for pumilio proteins (20). PUM1 and 2 were shown to impair E2F3 mRNA translation and promote miRNA-directed silencing of E2F3 expression in cancer cells, suggesting a rather tumor-suppressive role of both RBPs. In contrast, IGF2BP1 is considered to act in an

*To whom correspondence should be addressed. Tel: +49 345 5573959; Fax: +49 345 5527126; Email: stefan.huettelmaier@medizin.uni-halle.de
Correspondence may also be addressed to Simon Müller. Email: simon.mueller@medizin.uni-halle.de

oncogenic manner. Accordingly, a small molecule inhibitor of the protein, termed BTYNB (21), was recently reported. BTYNB was shown to impair the association of IGF2BP1 with the MYC RNA *in vitro* and 2D proliferation of various tumor cells. However, if BTYNB also interferes with other, conserved effector pathways of IGF2BP1 in cancer cells and impacts tumor growth remained largely elusive.

MATERIALS AND METHODS

Animal handling and ethics approvals

Immunodeficient athymic nude mice (FOXN1[nu/nu]) were obtained from Charles River. Animals were handled according to the guidelines of the Martin Luther University. Permission was granted by a local ethical review committee. For subcutaneous xenograft assays 1×10^5 iRFP-labeled ES-2 cells or 2.5×10^5 iRFP-labeled A549 cells (stably transduced using iRFP encoding lentiviruses) were harvested in media supplemented with 50% (v/v) matrigel (Sigma) and injected into the left flank of six-week old female immunodeficient athymic nude mice. For intraperitoneal assays 1×10^5 iRFP-labeled ES-2 cells were harvested in PBS and injected into six-week old female immunodeficient athymic nude mice. Mice were held with access to chlorophyll-free food to avoid background noise in iRFP image acquisition. Subcutaneous tumor growth and volume were measured and monitored by non-invasive near-infrared imaging using a Pearl Trilogy Imaging System (LI-COR). Tumor volume was calculated using the formula $0.52 \times L_1 \times L_2 \times L_3$. The mice were sacrificed, once the first tumor reached a diameter of 1.5 cm. For monitoring intraperitoneal tumor growth, isofluran-anaesthetized mice were weekly monitored by near-infrared imaging. Intraperitoneal fluorescence intensity of iRFP-labeled cells was quantified using the Image Studio software (LI-COR). Where indicated, ES-2 cells were pre-incubated with DMSO or 5 μM BTYNB for 24 h prior to injection, in suspension containing DMSO or BTYNB, into athymic nude mice. Prior injection, viable cells were counted using trypan blue and a TC20 Cell Counter (Bio-Rad).

Cell cycle analyses

For cell cycle analyses, cells were harvested with trypsin (72 h post-transfection or otherwise indicated), fixed overnight in 70% ethanol at −20°C. DNA was stained with propidium iodide (Miltenyi Biotec; diluted 1:1000) at 37°C for 30 min in PBS supplemented with RNAse A (2 μg/ml; Sigma Aldrich) to deplete RNA. The DNA content was measured by flow cytometry using a MACS Quant Analyzer (Miltenyi Biotec) and analyzed using FlowJo. The FUCCI system was used to analyze the length of cell cycle phases. ES-2 cells, stably transduced with IncuCyte® Cell Cycle Red/Green Lentivirus Reagent (Sartorius), were transfected with indicated siRNAs. Cells in the G2/M phase were enriched by FACS based on their green fluorescence using a FACS Melody sorter (BD Bioscience) 24 h post-transfection. Cell cycles phases were monitored based on their fluorescence using an IncuCyte S3 (Sartorius) starting immediately after sorting. Cell segmentation and quantification was performed using the Cell-By-Cell module (In-

cuCyte S3; Sartorius). Single cell tracking was subsequently processed using ImageJ.

Cell culture and transfections

HepG2 (ATCC, RRID: CVCL_0027), A549 (ATCC, RRID: CVCL_0023), ES-2 (ATCC, RRID: CVCL_3509), MV3 (RRID: CVCL_W280) and PANC-1 (ATCC, RRID: CVCL_0480) and HEK293T/17 (ATCC, RRID:CVCL_1926) were cultured in Dulbecco's modified Eagle's medium (DMEM) supplemented with 10% fetal bovine serum (FBS) at 37°C and 5% CO_2.

Transfection of cells with DNA or siRNAs was performed using Lipofectamine 3000 or Lipofectamine RNAiMAX (Thermo Fisher Scientific) according to the manufacturer's instructions. For the production of lentiviral particles 2.8×10^6 HEK293T/17 cells were transfected using Lipofectamine 3000, the packaging plasmids psPax2 (Addgene: Plasmid #12260) and pMD2.G (Addgene: Plasmid #12259) and the lentiviral expression pLVX vector encoding iRFP, GFP, GFP-IGF2BP1 or GFP-IGF2BP1 KHmutant. For luciferase reporter studies 1×10^5 cells were transfected using Lipofectamine 3000 and pmir-GLO or NanoLuc plasmids. For genomic deletions via CRISPR/Cas9 5×10^5 cells were transfected using Lipofectamine 3000, Cas9- and sgRNA-encoding plasmids (see CRISPR/Cas9 section). For the gene-specific depletion with siRNAs 5×10^5 cells were transfected using 9 μl Lipofectamine RNAiMAX and 15nM siRNAs. Plasmids and siRNAs used are summarized in Supplementary Table S10.

The inhibitors BTYNB (Cayman Chemical) or Palbociclib (Selleckchem) were used at indicated concentrations. For RNA decay analyses, cells were treated with actinomycin D (5 μM, Sigma Aldrich) for indicated time points 72 h upon transfection.

Lentiviral transduction

Lentiviral particle-containing supernatants were collected 24 and 48 h upon transfection of HEK293T/17 cells. Titers were analyzed 48 h post-infection of HEK293T/17 cells and determined by flow cytometry (GFP or iRFP) using a MACS Quant Analyzer (Miltenyi BioTec). Lentiviral transduction for downstream experiments was accomplished at 10 MOI (multiplicity of infection).

CRISPR/Cas9-mediated genomic deletions

For the CRISPR/Cas9-mediated genomic deletions in the *IGF2BP1* and *METTL3* loci, A549 cells were transfected with two CRISPR sgRNA-encoding plasmids (IGF2BP1: psg_RFP_IGF2BP1_Ex6, psg_RFP_IGF2BP1_Ex7; METTL3: psg_RFP_METTL3_Ex3–1, psg_RFP_METTL3_Ex3–2) and a Cas9 nuclease-encoding plasmids (pcDNA_Cas9_T2A_GFP). For the genomic deletion of the E2F1 3′UTR locus, PANC-1 cells were transfected with two CRISPR sgRNA-encoding (psg_RFP_E2F1_3p1, psg_RFP_E2F1_3p2, encoding sgRNAs targeting the last exon of E2F1 downstream of the stop-codon and upstream of the polyA-signal) and a Cas9

nuclease-encoding plasmids (pcDNA_Cas9_T2A_GFP). Single cell clones were generated by seeding one RFP- and GFP-positive cell per well using a FACS Melody sorter (BD Bioscience) 48 h post-transfection. The deletion of IGF2BP1 and METTL3 was validated by western blotting. The bi-allelic deletion of the E2F1 3′UTR in the *E2F1* gene locus was validated by PCR on isolated genomic DNA of single cell clones. CRISPR sgRNAs, plasmids and PCR primer are summarized in Supplementary Table S10.

Luciferase assays

The E2F1–3′UTR (NM_005225.3) was amplified on genomic DNA and cloned in the pmirGLO plasmid (Promega, pmirGLO_E2F1_3p). Dual-GLO Luciferase reporter analyses were performed according to manufacturer's protocols. Luciferase activities (Firefly and Renilla) were determined 48 h post-transfection of reporters. Reporters containing a minimal vector-encoded 3′UTR (MCS) served as normalization controls. For luciferase reporter studies on the E2F-transcriptional activity, four E2F binding elements were cloned upstream of a minimal, NanoLuc-driving promoter (Promega, pNL3.1_4xE2F). NanoLuc reporter analyses were performed according to manufacturer's protocols. Luciferase activities were determined 48 h post-transfection of reporters. Reporters containing a minimal promoter served as normalization controls.

Plasmids and cloning

Cloning strategies including plasmids, oligonucleotides used for PCR and restriction sites are summarized in Supplementary Table S10. All constructs were validated by sequencing.

RNA sequencing and differential gene expression

Libraries for RNA-sequencing (RNA-seq) were generated according to the manufacturer's instructions. For total RNA-seq, 1 μg of total RNA served as input for rRNA depletion using RiboCop v1.2 (Lexogen). The Ultra Directional RNA Library kit (NEB) was used for strand-specific library generation. Library preparation and sequencing was performed on an Illumina NextSeq 500 platform at the Deep Sequencing Group (TU Dreseden). For the preparation of small RNA-seq libraries, 50 ng of total RNA served as input using the NEXTflex Small RNA Library Prep Kit v3 (Bio Scientific). Sequencing was performed on the Illumina HighSeq 2000 platform at the Deep Sequencing Group (TU Dreseden). For mRNA-seq libraries, total RNA served as input for a polyA-enrichment using oligo dT beads. Library preparation and sequencing was performed by Novogene (Hong Kong) on an Illumina HiSeq platform. First, Low quality read ends as well as remaining parts of sequencing adapters were clipped off using Cutadapt (V 1.6). For total and small RNA-seq analyses reads were aligned to the human genome (UCSC GRCh37/hg19) using TopHat2 (V 2.0.13) or Bowtie2 (V 2.2.4), respectively. FeatureCounts (V 1.4.6) was used for summarizing gene-mapped reads. Ensembl (GRCh37.75) or miRBase (V 20) were used for annotations (see supplementary table T1A). Differentially gene

expression (DE) was determined by edgeR (V 3.12) using TMM normalization, as described previously (8).

Kaplan–Meier analyses

For survival analyses, Kaplan–Meier plots and Hazard ratios (HR) were determined using GEPIA 2 (http://gepia2.cancer-pku.cn/#survival) based on the expression status of indicated genes in TCGA data sets with median group cut-off.

MicroRNA–Target predictions

miRWalk 2.0 (http://zmf.umm.uni-heidelberg.de/apps/zmf/mirwalk2/), (22) was used for the analysis of miRNA-targeting in the 3′UTR of the E2F1 transcript (NM: 0055225.3). The following databases were considered: miR-Walk, miRDB, PITA, MicroT4, miRMap, RNA22, mi-Randa, miRNAMap, RNAhybrid, miRBridge, PICTAR2 and Targetscan (Supplementary Table S6).

IGF2BP1-CLIP and m⁶A-RIP- data analysis

IGF2BP1 CLIP data were analyzed as previously described (8). In brief, peak genomic coordinates from publicly available IGF2BP1-CLIP data (4,5,23) were obtained from ENCODE (24), NCBI GEO (4) and CLIPdb (25), were mapped to all annotated genes (RefSeq hg19) using bedtools (26). For IGF2BP1-binding, the following number of datasets was considered: two PAR-CLIP (HEK293), two eCLIP (hESCs), two eCLIP (HepG2) and two eCLIP (K562). For the analysis of transcript-specific m^6A-modification, m⁶A-RIP-seq data, performed in A549 cells, were considered and obtained from MeT-DB (V2.0, (27)).

Gene expression and correlation analysis

We obtained gene-level RNA-seq read counts of TCGA primary tumor samples and GTEx V7 normal tissue via the GDC data portal (portal.gdc.cancer.gov) and the GTEx portal (gtexportal.org), respectively, for the indicated tumor cohorts. Differential gene expression was assessed using R/edgeR (pmid: 19910308) by applying TMM normalization. Respective tumor and normal tissue sample data were normalized together to avoid composition bias. CPM transformation was utilized to obtain normalized expression values. For correlation analyses, RNA-seq data sets for protein-coding genes were log_2-(FPKM+1)-transformed and the Pearson correlation coefficient with IGF2BP1 was determined.

Gene set enrichment analysis (GSEA)

Gene set enrichment analyses (GSEA) were performed on pre-ranked lists using the GSEA-software (V3.0, (28)) with MSigDB (V7.0, (29)) gene sets for Hallmarks and KEGG pathways. All protein-coding genes were ranked according to the correlation coefficient with IGF2BP1 in TCGA RNA-seq data or the fold change determined upon IGF2BP1 knockdown or knockout by RNA-seq.

Cell proliferation, spheroid, self-renewal and clonogenic assays

For the assessment of cell proliferation in 2D culture systems, 2.5×10^4 cells were plated 24 h upon transfection and the amount of cells as well as propidium iodide-negative/-positive cells were determined by flow cytometry at indicated time points using a MACS Quant Analyzer (Miltenyi Biotec). In addition, cell confluency and vitality were determined by using an IncuCyte S3 system (Sartorius) with 10× magnification and CellTiter Glo (Promega) according to manufacturer's protocols. For spheroid growth in 3D culture systems, 1×10^3 cells were seeded in 96-well round-bottom ultra-low attachment plates (Corning) 24 h post-transfection. Spheroid formation was induced by centrifugation for 3 min at 300 g. Spheroid growth was monitored for five additional days by bright-field microscopy using an IncuCyte S3 system (Sartorius) with 10× magnification. Additionally, cell viability was determined by using CellTiter Glo (Promega). For anchorage-independent growth and self-renewal, 1×10^3 cells were seeded 24 h post-transfection in a layer of soft agar mixed with cell culture medium (0.35% agar) on another layer of soft agar containing a higher concentration (0.5% agar). Growth and colony formation were monitored for 14 days with medium exchange every 3 days, as described previously (30). Colonies were stained using MTT (Sigma-Aldrich). The number of colonies was determined by using the 2D Colony Analyzer tool of the MiToBo package for the Fiji software (http://fiji.sc). For clonogenic assays, 200 cells were seeded in six-well plates 24 h post-transfection. Colony formation was analyzed 14 days upon seeding. Colonies were stained by using 0.01% crystal violet for 60 min. Number of colonies were determined by using the 2D Colony Analyzer tool of the MiToBo package for the Fiji software.

Drug synergy matrix screen

For the analysis of synergy between BTYNB and Palbociclib, the viability of ES-2 cells was determined 72 h upon drug exposure using CellTiter GLO in a drug matrix screen at indicated concentrations. Synergy relief maps were generated using the SynergyFinder web application (https://synergyfinder.fimm.fi, (31)) and the ZIP (Zero interaction potency) method.

RNA isolation and RT-q-PCR

Total RNA from cell line experiments was isolated by using TRIzol. RNA integrity was determined on a Bioanalyzer 2100 (Agilent). For cDNA synthesis, two μg total RNA served as a template using M-MLV Reverse Transcriptase (Promega) and random hexamer primers following manufacturer's protocols. qPCR analysis was performed using a LightCycler 480 II (Roche) with the ORA™ qPCR Green ROX L Mix (highQu) using following PCR reactions: 5 min / 95°C, 45 cycles of 10 s/95°C, 10 s/60°C and 20 s/72°C. Primer pairs spanning an exon/exon borders were selected using Primer Blast (https://www.ncbi.nlm.nih.gov/tools/primer-blast/). Sequences are summarized in Supplementary Table S10. Relative RNA abundance was determined by the $\Delta\Delta C_t$ method, as previously described (8).

Nascent RNA capture

The Click-iT Nascent RNA Capture Kit (Thermo Fisher) was used for the purification of newly synthesized RNAs according to manufacturer's protocol. In brief, PANC-1 cells were transfected with control or IGF2BP1-directed siRNAs for 72 h. Cells were further incubated with 0.2 mM 5-ethynyl uridine (EU) for 4 h. Total RNA was prepared using TRIzol. 10 μg of total RNA served as input for the biotinylation of the EU-labeled RNA by click reaction using 1 mM biotin azide. 1 μg of biotinylated RNA served as input for the purification of nascent RNAs using Streptavidin T1 magnetic beads. Total RNA and purified nascent RNA served as templates for cDNA-synthesis and qPCR analysis.

RNA co-Immunoprecipitation (RIP)

For RNA co-immunoprecipitations (RIP) cell extracts (1×10^7 per condition) were prepared on ice using RIP buffer (10 mM HEPES, 150 mM KCl, 5 mM $MgCl_2$, 0.5% NP40, pH 7.0). Cleared lysates were incubated with indicated antibodies (anti-IGF2BP1- or anti-AGO2-antibodies) and Protein G Dynabeads (Life Technologies) for 60 min at room temperature (RT). After three washing steps with RIP buffer, protein–RNA complexes were eluted by addition of 1%SDS and 65°C/10 min. Protein enrichment was analyzed by western blotting. Co-purified RNAs were extracted using TRIZOL and analyzed by RT-q-PCR.

Western blotting

Infrared western blotting analyses were performed as previously described (8). In brief, total protein of harvested cells was extracted in lysis-buffer (50 mM Tris–HCl (pH 7.4), 50 mM NaCl, 2 mM $MgCl_2$, 1% SDS) supplemented with protease and phosphatase inhibitor cocktails (Sigma-Aldrich). Protein expression was analyzed by Western blotting with indicated primary antibodies by using fluorescence-coupled secondary antibodies and an infra-red scanner (LICOR). Antibodies used are indicated in Supplementary Table S10.

Statistics

All experiments were performed at least in biological triplicates. Statistical significance was tested by a parametric Student's *t*-test on equally distributed data. Otherwise, a non-parametric Mann–Whitney-test was performed. For Kaplan–Meier analyses, statistical significance was determined by log-rank analyses.

RESULTS

IGF2BP1 is a conserved enhancer of tumor cell proliferation

The IGF2 mRNA-binding protein 1 (IGF2BP1) promotes the proliferation and *in vivo* growth of tumor cells derived from a variety of solid cancers (8,9,32). In agreement, the meta-analysis of 33 TCGA-provided cancer transcriptome data sets, including 9282 tumor samples, indicated that high IGF2BP1 expression is associated with reduced overall survival probability (Figure 1A). For 9 out of 33 cancers, high IGF2BP1 mRNA expression was
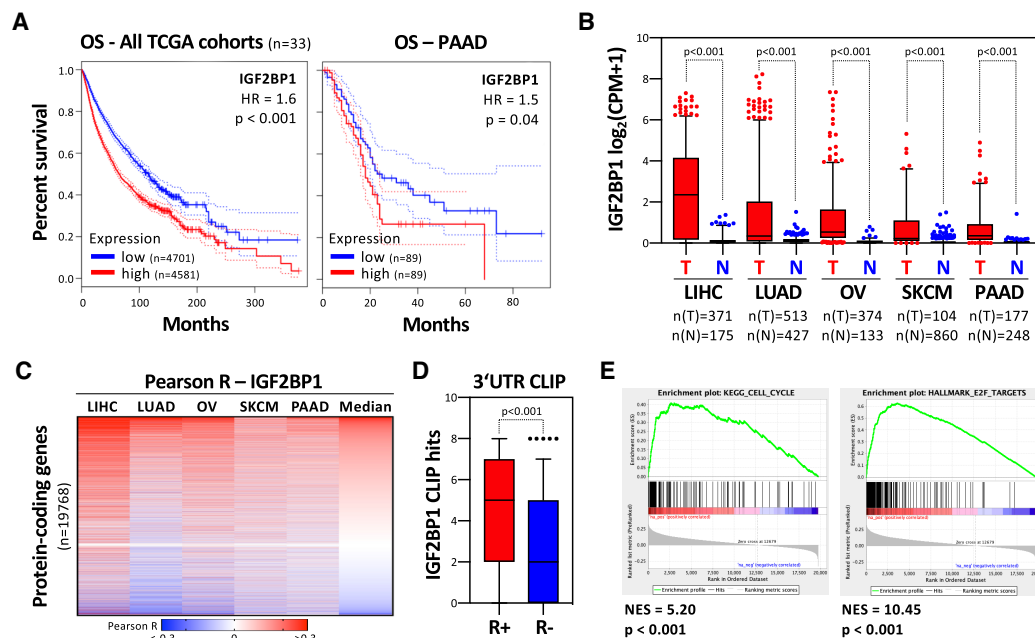
Figure 1. IGF2BP1 is a conserved pro-oncogenic RBP in human cancer. (**A**) Kaplan–Meier plots of overall survival analyses (median cutoff) based on IGF2BP1 mRNA expression. Overall survival was analyzed for all TCGA (The Cancer Genome Atlas) tumor cohorts (9282 patients, left) and the PAAD cohort (Pancreatic Adenocarcinoma, 178 patients, right). Red, high expression of IGF2BP1; Blue, low expression of IGF2BP1. HR, hazard ratio; p, logrank p value. (**B**) Box plots showing the IGF2BP1 expression in tumor and normal tissues for indicated cancers. Data were derived from the TCGA (T, red boxes) and GTEx (N, blue boxes) portal. The number (*n*) of analyzed samples is indicated. LIHC, liver hepatocellular carcinoma; LUAD, lung adenocarcinoma; OV, ovarian carcinoma; SKCM, skin cutaneous melanoma; PAAD, pancreatic adenocarcinoma. (**C**) Heatmap of correlation coefficients (R) determined for protein-coding gene and IGF2BP1 expression. *R* values were determined in indicated TCGA data sets and ranked according to median correlation coefficient. Scale bar in lower panel. (**D**) Box plots of experiments indicating IGF2BP1 CLIP hits in the 3′UTR of mRNAs showing positive (R+; $R > 0.15$, $n = 2039$) or negative (R–; $R \leftarrow 0.15$, $n = 155$) association with IGF2BP1 expression in cancers analyzed in (C). (**E**) Gene set enrichment analysis (GSEA) of IGF2BP1-correlated gene expression in the five cancers analyzed in (C). GSEA was performed on ranked median correlation coefficient determined in (C). KEGG pathway 'Cell Cycle' (left) and the Hallmark pathway 'E2F Targets' (right) are shown. NES, normalized enrichment score. Statistical significance was determined by Mann–Whitney test.

significantly ($P < 0.05$) associated with adverse prognosis (Supplementary Figure S1A). This included pancreatic adenocarcinoma (Figure 1A; PAAD). In the vast majority of cancers, IGF2BP1 synthesis was substantially up-regulated, supporting its oncofetal expression and conserved prognostic relevance. Among cancers with substantially upregulated IGF2BP1 expression were four with reported pro-oncogenic roles of IGF2BP1 (LIHC, LUAD, OV and SKCM) as well as PAAD (Figure 1B). In these five cancers, IGF2BP1 followed by LIN28B were the in average most upregulated mRNA-binding proteins (mRBPs) among 660 detected and reported by the RBP census (Supplementary Figure S1B) (33). IGF2BP1 is a known regulator of mRNA stability and associated with a plethora of mRNAs. CLIP studies in different cell types suggested thousands of IGF2BP1-bound mRNAs. So far, many studies focused on the IGF2BP1-dependent stabilization of the MYC mRNA. Surprising in view of the reported MYC/N-enhancing role of IGF2BPs (10,12,34), no significant association of IGF2BP1 and MYC was observed across 33 cancers or the five cancers (LIHC, LUAD, OV, SKCM and PAAD) with expected or validated pro-oncogenic roles of

IGF2BP1 (Supplementary Figure S1C, D). This suggested that IGF2BP1 acts via largely cancer-specific pathways or that its most conserved effector pathway(s) across cancer types remained unknown.

Aiming to identify key candidate effector pathways, IGF2BP1-associated expression of protein-coding genes was investigated in the aforementioned five cancers (Supplementary Table S1). The median correlation coefficient was used to rank genes and distinguish two major groups, genes showing positive (R+) or negative (R–) correlation with IGF2BP1 expression (Figure 1C). The investigation of IGF2BP1–3′UTR association, re-analyzed in eight independent CLIP studies performed in four distinct cell types (8), suggested an enrichment of conserved 3′UTR-binding among the positively correlated (R+) transcripts (Figure 1D). This supported IGF2BP1's role as a mainly 3′UTR-dependent mRNA-stabilizing mRBP in cancer. Gene set enrichment analyses (GSEA) of genes ranked by their determined median association with IGF2BP1 expression in the five investigated solid cancers demonstrated a striking enrichment of R+-genes in the E2F_TARGETS hallmark as well as the KEGG_CELL_CYCLE gene sets (Figure 1E;

Supplementary Table S2). This significant enrichment was also observed in each of the five investigated cancers suggesting E2F-driven gene expression as a conserved effector pathway of IGF2BP1 in cancer (Supplementary Figure S2A–C; Table S2).

IGF2BP1 promotes cell cycle progression in cancer-derived cells

If and how IGF2BP1 controls E2F-dependent cell cycle control and proliferation was initially investigated in PAAD-derived PANC-1 cells. IGF2BP1 depletion impaired spheroid growth, significantly decreased 2D cell proliferation and elevated doubling time approximately twofold (Figure 2A; Supplementary Figure S3A, B). Cell cycle progression analyses showed that IGF2BP1 knockdown led to an enrichment of cells in G1 (Figure 2B, C). Importantly, IGF2BP1 depletion was not associated with increased apoptosis, as indicated by barely observed subG1 cell fractions or dead cells, monitored by PI-labeling (Supplementary Figure S3C). IGF2BP1 knockdown also impaired colony formation and clonogenicity suggesting a pivotal role of cell cycle control and sustained self-renewal potential (Supplementary Figure S3D, E). Impaired G1/S-progression upon IGF2BP1 depletion was also observed in four cell lines derived from the four other cancers investigated here (Figure 2D; Supplementary Figure S4A). The monitoring of cell cycle progression at the single cell level (65 divisions) in IGF2BP1-depleted ES-2 cells (OV-derived), using the FUCCI technology (35), demonstrated that IGF2BP1 depletion exclusively prolonged the G1 phase, approximately twofold (Figure 2E, F). Population analyses over 72 h including 4800 cells confirmed this by indicating a substantial increase of cells in G1 and decrease in the S phase upon knockdown (Supplementary Figure S4B, C). This was further evaluated by IGF2BP1 deletion (KO) in LUAD-derived A549 cells. IGF2BP1-KO impaired spheroid growth (Supplementary Figure S4D), as previously observed in other cancer-derived cells (8). Furthermore, spheroid growth was significantly enhanced in A549 knockout cells by the re-expression of wild type (WT) GFP-tagged IGF2BP1 (Supplementary Figure S4E). Compared to GFP re-expressing controls, viability remained essentially unchanged by the re-expression of an RNA-binding deficient mutant GFP-IGF2BP1 (MUT). This indicated the importance of the IGF2BP1's RNA-binding capacity in controlling tumor cell proliferation and spheroid growth. In nude mice, IGF2BP1 deletion substantially interfered with the growth of A549-derived xenograft tumors (Figure 2G). Concise with its depletion, IGF2BP1 loss resulted in an increase of A549 cells in G1 without enhanced subG1 cell fractions (Figure 2H, I). This indicated, IGF2BP1 is a conserved regulator of G1/S-transition in cancer cells, controlling tumor cell proliferation *in vitro* and tumor growth *in vivo*.

IGF2BP1 regulates the E2F-dependent control of G1/S-transition

To identify conserved key effector-encoding mRNAs of IGF2BP1-dependent control of G1/S-transition, the expression of protein-coding genes was monitored upon IGF2BP1 depletion by RNA-seq in five tumor cell lines (Supplementary Table S3). For GSEA, protein-coding genes were ranked by their median or cell-specific fold change of expression (Figure 3A). This indicated conserved and significant downregulation of the E2F_TARGET and KEGG cell cycle gene sets in median and all individual cell models, including IGF2BP1-KO A549 cells (Figure 3B, C; Supplementary Figure S5A; Supplementary Table S4). In agreement, IGF2BP1 depletion resulted in the largely conserved downregulation of factors promoting G1/S transition (Figure 3D, left panel; Supplementary Table S5). These genes also showed significant and concise association with IGF2BP1 expression in the five respective primary cancers (Figure 3D, right panel). No evidence for IGF2BP1-dependent regulation of factors impairing G1/S transition, e.g. RB1, was observed. Surprisingly, significant downregulation of MYC mRNA abundance was only determined in HepG2 and MV3 cells, supporting previous studies (9,12). In view of lacking correlation of IGF2BP1 and MYC mRNAs across cancers (see Supplementary Figure S1C and S1D), this provided further evidence that IGF2BP1-dependent regulation of MYC mRNA levels is rather cell-type specific. In contrast, these findings indicated a pivotal role of IGF2BP1 in regulating E2F-driven transcription in a concise manner across different cancers and tumor cell lines. This was tested further for the E2F1–3 transcription factors, well known enhancers of G1/S transition (17). In all analyzed cancer cells, IGF2BP1 depletion significantly reduced E2F1–3 mRNA levels, with the exception of A549 cells where E2F3 transcripts were modestly elevated (Figure 3D). In agreement with decreased mRNA abundance, E2F1 protein expression was substantially reduced in all tested cancer cell lines upon IGF2BP1 depletion (Figure 3E). Likewise, E2F2 and E2F3 protein levels were decreased by IGF2BP1 knockdown in PANC-1 cells (Supplementary Figure S5C). Notably, downregulation of E2F1 protein was also observed in A549 IGF2BP1-KO cells (Supplementary Figure S5D). Furthermore, E2F1 mRNA levels were strongly reduced in xenograft tumors lacking IGF2BP1 (Figure 3F). In GFP-expressing A549 cells deleted for IGF2BP1, E2F1 mRNA and protein levels were reduced nearly twofold compared to parental cells (Figure 3G, GFP; Supplementary Figure S5E). The re-expression of wild type IGF2BP1 restored E2F1 mRNA and protein expression (Figure 3G, WT; Supplementary Figure S5E). This was not observed upon the re-expression of RNA-binding deficient IGF2BP1, suggesting that IGF2BP1 controls E2F1 expression in an RNA-binding dependent manner (Figure 3G, MUT; Supplementary Figure S5E (8)).

IGF2BP1 regulates E2F1 expression in a 3′UTR- and miRNA-dependent manner

IGF2BP1's main and conserved role in cancer-derived cells relies on the 3′UTR- and miRNA-dependent regulation of mRNA turnover (8). IGF2BP1-mRNA association reported by CLIP indicated conserved binding to the 3′UTR of the E2F1 mRNA (Figure 4A). Preferred 3′UTR-binding was also observed for other transcripts encoding positive regulators of G1/S transition (Supplementary Figure S5B). 3′UTR-dependent regulation was tested for E2F1 using
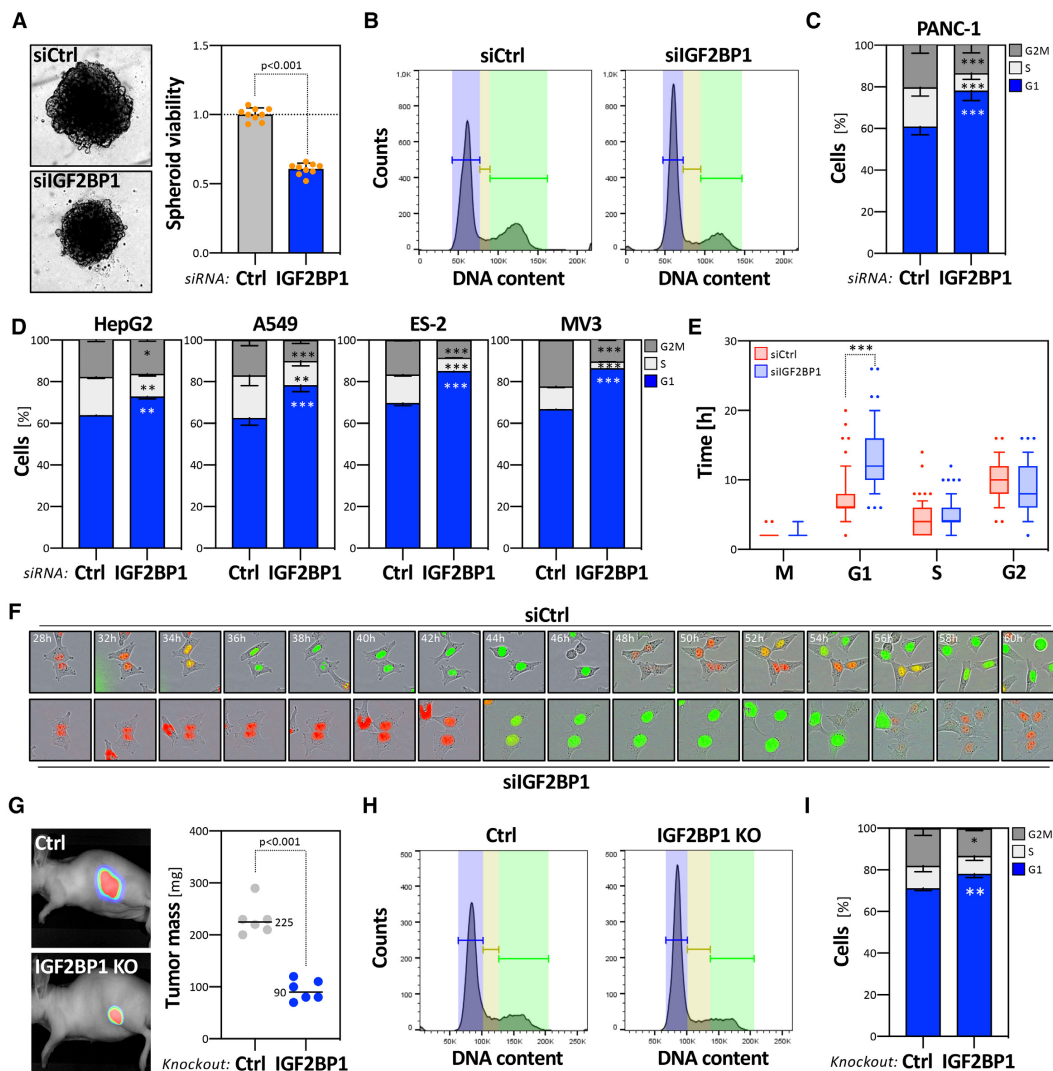
Figure 2. IGF2BP1 promotes proliferation and cell cycle progression in cancer cells. (**A**) PANC-1 cells were transfected with control (siCtrl, gray) or IGF2BP1-directed siRNA pools (siIGF2BP1, blue). Representative PANC-1 spheroids 6 days post-transfection are indicated in the left panel. The viability of PANC-1 spheroids was determined by CellTiter GLO (right panel). Orange dots represent median-normalized values of three spheroids analyzed in three independent studies. (**B–D**) PANC-1 cell cycle phase distribution upon transfection with control (**B**, left panel) or IGF2BP1-directed (**B**, right panel) siRNAs, as determined by PI-labeling and flow cytometry. Fractions of PANC-1 (**C**) or HepG2, A549, ES-2 and MV3 (**D**) cells in each cell cycle phase were quantified in three independent knockdown analyses. (**E**) Box plots showing the duration of cell cycle phases upon control (siCtrl, red) or IGF2BP1-depletion (siIGF2BP1, blue). ES-2 cells were stably transduced with the FUCCI system (Sartorius). The length of cell cycle phases was determined over 66 (control, red) and 80 (IGF2BP1-depleted, blue) cell divisions. (**F**) Representative images of cells with segmentation mask overlays analyzed in (E) at indicated time post transfection with control- (upper panel) or IGF2BP1-directed (bottom panel) siRNAs. Red, G1 phase; Green, G2 phase; Yellow, S phase. (**G**) Parental (Ctrl) and IGF2BP1-deleted (KO) A549 cells expressing iRFP were injected (sc) into nude mice (6 mice per condition) and the growth of xenograft tumors was monitored by near-infrared imaging. Representative images are shown in the left panel (42 days post-injection). Final tumor mass is shown by box plots (right panel). (**H, I**) Cell cycle analysis, as presented in (B, C) of parental and IGF2BP1-deleted A549 cells. Statistical significance was determined by Mann–Whitney test: *P <0.05; **P < 0.01; ***P < 0.001.
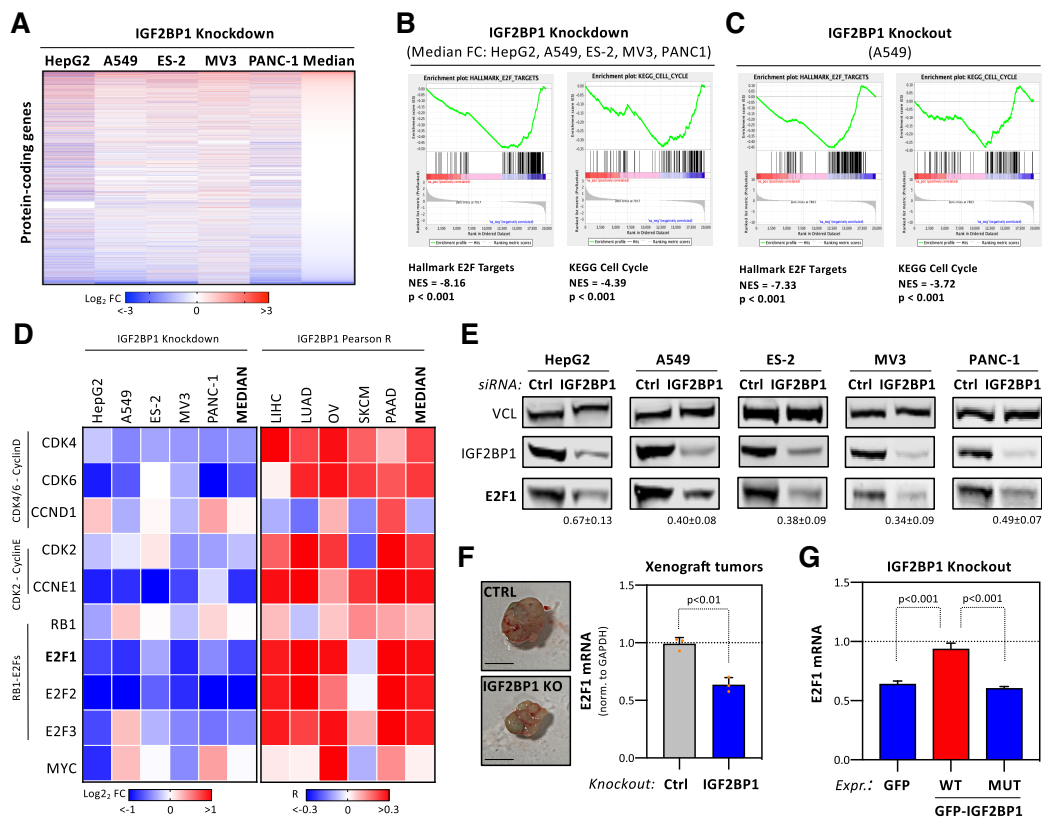
Figure 3. IGF2BP1 controls G1/S cell cycle transition of cancer cells. (**A**) Heatmap indicating the fold change (FC) of mRNAs upon IGF2BP1-depletion in indicated cancer cell lines 72 h post-transfection of siRNAs. The abundance of mRNAs was monitored by RNA sequencing. Genes were ranked according to their median FC determined in five cancer cell lines. (**B, C**) Gene set enrichment analysis (GSEA) of median FC of protein-coding genes upon IGF2BP1 depletion in five cancer cell lines (**B**) or upon IGF2BP1 knockout in A549 cells (**C**). Results for the KEGG pathway 'Cell Cycle' (left) and the Hallmark pathway 'E2F Targets' (right) are shown. NES, normalized enrichment score. (**D**) Heatmap depicting the fold change of indicated mRNAs upon IGF2BP1 depletion in cancer cells (left) and their correlation (coefficient) with IGF2BP1 mRNA expression in indicated cancers (right). Median fold change or correlation coefficients are indicated in most right columns. (**E**) Representative Western blot analyses of E2F1 upon IGF2BP1 depletion in indicated cancer cell lines. Vinculin (VCL) served as a loading and normalization control. Average fold change and standard deviation of E2F1 protein levels, determined in three independent analyses are indicated in bottom panel. (**F**) RT-q-PCR analysis of E2F1 mRNA levels in excised xenograft tumors (Figure 2G). Representative images of tumors are shown in the left panel. E2F1 expression was determined in three control and IGF2BP1-KO tumors by normalization to GAPDH. (**G**) RT-q-PCR analysis of E2F1 mRNA levels in IGF2BP1-KO A549 cells expressing GFP, GFP-IGF2BP1 (WT) or an RNA-binding deficient GFP-IGF2BP1 (MUT) normalized to parental A549 cells. RPLP0 served as normalization control. Statistical significance was determined by Student's t-test.

E2F1–3′UTR containing luciferase reporters. IGF2BP1 depletion resulted in conserved downregulation of reporter activity in all analyzed cancer cell lines (Figure 4B). This was further investigated by deleting the E2F1–3′UTR in PANC-1 cells by sgRNAs directing Cas9-cleavage 3′-to the stop codon and 5′-to the polyadenylation signal (Figure 4C). IGF2BP1 expression remained unaffected by homozygous deletion of the bulk E2F1–3′UTR. However, 3′UTR-deletion abolished downregulation of E2F1 mRNA levels observed upon IGF2BP1 knockdown in parental PANC-1 cells (Figure 4D). These findings strongly suggested that IGF2BP1 controls E2F1 mRNA turnover via the 3′UTR. In accord, IGF2BP1 knockdown significantly enhanced decay of the E2F1 mRNA upon blocking transcription by actinomycin D (Figure 4E; ActD). Notably, although IGF2BP1 depletion reduced total E2F1 mRNA levels, the synthesis of nascent E2F1 mRNAs remained essentially unchanged (Supplementary Figure S6A). Together, this indicated that IGF2BP1 exclusively controls E2F1 mRNA turnover without substantial deregulation of E2F1 mRNA synthesis.

E2F1 expression is controlled at various levels including miRNA-directed inhibition via the 3′UTR (17,19). To identify conserved miRNAs controlling E2F1 synthesis, the expression of miRNAs was monitored in the five investigated cell lines (Supplementary Table S6). MiRNA abundance was then plotted over the number of databases, analyzed via MiRWalk2.0, predicting miRNA targeting at the
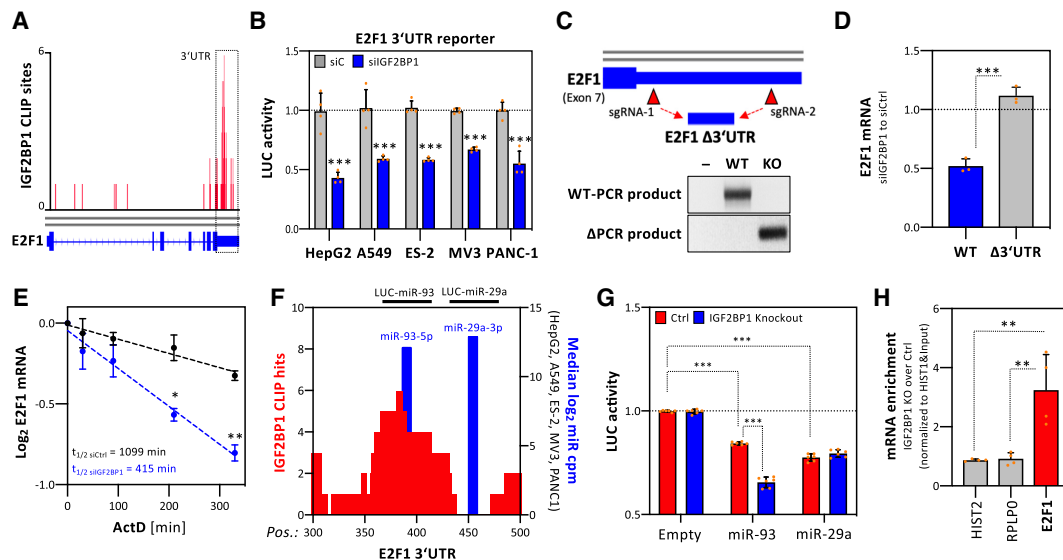
Figure 4. IGF2BP1 enhances E2F1 mRNA stability in a 3′UTR- and miRNA-dependent manner. (**A**) IGF2BP1 CLIP profile of the E2F1 mRNA. The 3′UTR is highlighted by dashed lines. (**B**) E2F1 3′UTR luciferase activity in indicated cancer cells upon control- or IGF2BP1-depletion. Reporter activities, normalized to a control reporter, were determined in four independent experiments. (**C**) Experimental strategy of the genomic deletion of the E2F1 3′UTR by the Cas9 nuclease using indicated CRISPR guide RNAs (sgRNAs) (Top panel). Representative PCR analysis on genomic DNA of parental PANC-1 (WT) and an E2F1 3′UTR-deleted PANC-1 cell clone (KO). (**D**) RT-q-PCR analysis of E2F1 mRNA levels upon IGF2BP1 depletion in parental PANC-1 (WT, blue) or the E2F1 3′UTR-deleted PANC-1 cell clone (Δ3′UTR, grey) normalized to control-transfected cells. RPLP0 served as internal normalization control. (**E**) E2F1 mRNA decay was monitored by RT-q-PCR in control- (black) or IGF2BP1-depleted (blue) PANC-1 cells upon indicated time of Actinomycin D (ActD) treatment. Error bars indicated standard deviation. Average mRNA half-life, determined in three independent studies, is indicated. (**F**) The graph depicts the number of CLIP studies showing overlapping IGF2BP1-CLIP sites (left axis, red; CLIP hits) and the position (x-axis) of miRNA targeting sites (blue) in the E2F1 3′UTR. MiRNA abundance (right axis, blue) is indicated as median $\log_2$ cpm determined by small RNA-seq of indicated cell lines. Luciferase reporter comprising indicated regions of the E2F1–3′UTR (LUC-miR-93, LUC-miR-29a) and analyzed in (G), are indicated in the top panel. (**G**) Luciferase reporter analysis demonstrating activity of indicated reporters in parental (Ctrl, red) or IGF2BP1-knockout (blue) A549 cells. Reporter activities, normalized to a control reporter without miRNA targeting site (Empty), were determined in three independent experiments with two technical replicates each. (**H**) Co-purification of mRNAs with AGO2 in parental (Ctrl) or IGF2BP1-knockout A549 cells was analyzed by immunoprecipitation using anti-AGO2 antibodies and RT-q-PCR analysis (right panel). HIST2 and RPLP0 served as negative controls. HIST1 served as normalization control. Statistical significance was determined by Student's *t*-test: *P <0.05; **P < 0.01; ***P < 0.001.

E2F1–3′UTR (Supplementary Figure S6B). These studies revealed high and conserved abundance of various miR-NAs with *in silico* predicted or validated E2F1 repression, e.g. miR-29a-3p and miR-93–5p (19). IGF2BP1 binding sites in the E2F1 3′UTR reported by CLIP studies overlap with the predicted seed region of the miR-93–5p family (Figure 4F). In contrast, no CLIP-reported binding was observed in the predicted miR-29a-3p seed. To test if IGF2BP1 modulates regulation by these miRNAs via predicted targeting sites, we analyzed luciferase reporters containing 48 nucleotide long E2F1 3′UTR regions including the aforementioned miRNA seeds (Figure 4G). Luciferase activity for both reporters was reduced in A549 cells compared to a reporter encoding a minimal 3′UTR suggesting regulation by miRNAs, as predicted. However, in A549 cells deleted for IGF2BP1, activity of the miR-93-5p reporter was significantly decreased compared to parental cells. In contrast, activity of the miR-29a-3p reporter remained unaffected by IGF2BP1 deletion, suggesting that IGF2BP1 impairs miR-93–5p directed regulation by impairing miRNA regulation due to binding at or in proximity to the miR targeting site. To exclude bias by IGF2BP1-

KO, this was further investigated by analyzing miR-93-5p reporter activity upon IGF2BP1 knockdown (Supplementary Figure S6C). As observed in IGF2BP1-KO cells, reporter activity was also decreased upon IGF2BP1 depletion. Finally, we analyzed AGO2-association of the E2F1 mRNA by RIP in A549 cells. In comparison to parental cells, AGO2-association of control mRNAs remained unaffected by IGF2BP1 deletion (Figure 4H, Supplementary Figure S6D). In sharp contrast, AGO2-E2F1 mRNA association was increased in IGF2BP1-KO cells, indicating that IGF2BP1 impairs miRNA-directed downregulation of E2F1 expression.

The E2F pathway is controlled by IGF2BP1 in an m6A-dependent manner

IGF2BPs are major m6A-readers in cancer, showing an m6A-dependent increase in target mRNA association (12,16). In A549 and other cells, m6A-RIP studies indicated preferential m6A-modification of E2F1–3 mRNAs in the 3′UTR close to the stop codon (Figure 5A, B). All these mRNAs were consistently decreased by IGF2BP1 depletion
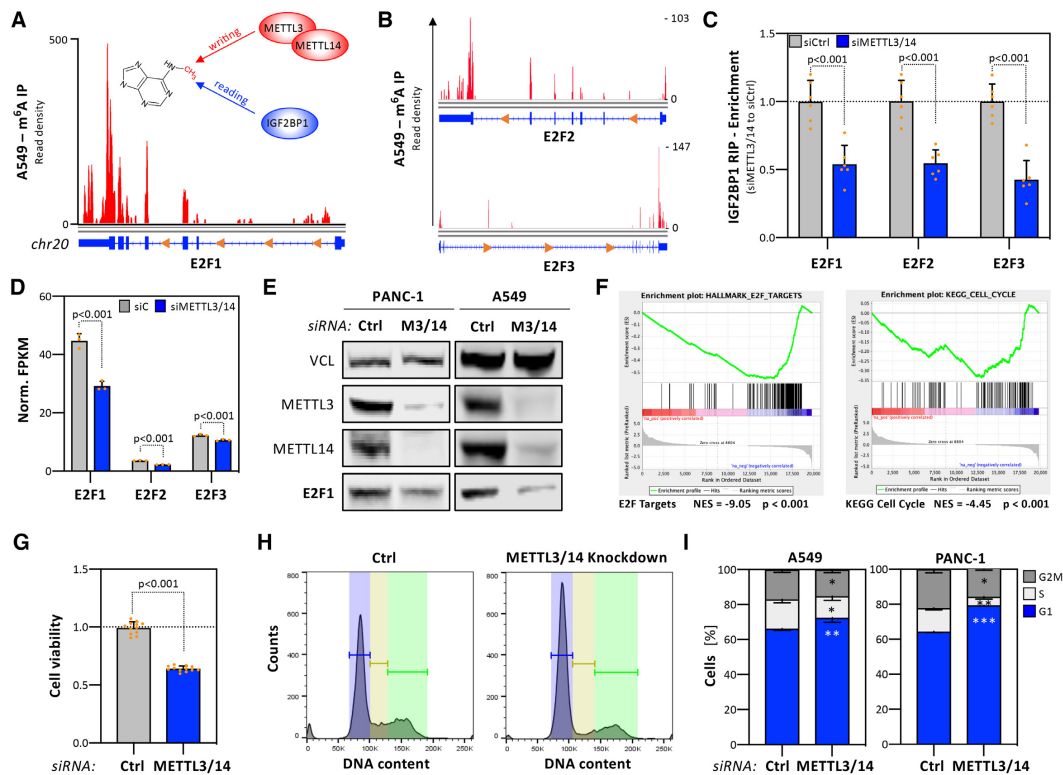
Figure 5. The E2F-dependent cell cycle progression controlled by IGF2BP1 is m^{6}A-dependent. (A, B) N^6-Methyladenosine RIP-seq profile of the E2F1 (**A**), E2F2 and E2F3 (**B**) mRNAs determined in A549 cells. Data were obtained from MeT-DB V2.0. The m^{6}A-writing enzymes METTL3 and METTL14 as well as IGF2BP1 as an m^{6}A-reader are indicated. (**C**) Co-purification of indicated mRNAs with IGF2BP1 in control- (gray, siCtrl) or METTL3/14-depleted (blue, siMETTL3/14) PANC-1 cells was analyzed by RIP using anti-IGF2BP1 antibodies and RT-q-PCR analysis. HIST1 served as normalization control. (**D**) Abundance of E2F1–3 mRNAs determined by RNA-seq upon transfection of indicated siRNAs in PANC-1 cells as shown in (**C**). (**E**) Representative Western blot analysis of indicated proteins upon control- and METTL3/14 depletion in PANC-1 (left) and A549 (right) cells. VCL served as loading control. (**F**) Gene set enrichment analysis (GSEA) of protein-coding genes upon METTL3/14 co-depletion in PANC-1 cells. Protein-coding genes were ranked by their fold change of mRNA abundance determined by RNA-seq as shown in (**D**). Results for the Hallmark pathway 'E2F Targets' (left) and the KEGG pathway 'Cell Cycle' (right) are shown. NES, normalized enrichment score. (**G**) PANC-1 cells were transfected with indicated siRNAs (grey, siCtrl; siMETTL3/14, blue). The viability of PANC-1 spheroids was determined 6 days post-transfection by CellTiter GLO, as described in Figure 2A. (**H, I**) Cell cycle progression analyses of control- or METTL4/14-depleted PANC-1 and A549 cells (**I**), as described in Figure 2B, C. Representative cell cycle phase distribution in PANC-1 cells is shown in (**H**). Statistical significance was determined by Mann–Whitney test: $*P < 0.05$; $**P < 0.01$; $***P < 0.001$.

and show conserved 3′UTR-association in IGF2BP1-CLIP studies (Figure 3D, 4A; Supplementary Figure S5B). In PANC-1 cells, IGF2BP1-RIP studies demonstrated that co-depletion of METTL3/14, crucial for m^{6}A-modification of mRNAs, significantly reduced IGF2BP1-association of all three mRNAs (Figure 5C). In PANC-1 cells, METTL3/14 co-depletion resulted in reduced E2F1–3 mRNA and protein levels (Figure 5D, E; Supplementary Figure S6E and Table S7). The co-depletion of METTL3/14 and METTL3-deletion by CRISPR/Cas9 in A549 cells led to reduced E2F1 expression without affecting IGF2BP1 abundance (Figure 5E; Supplementary Figure S6F). GSEA of gene expression determined by RNA-seq upon METTL3/14 co-depletion confirmed significant downregulation of E2F-target and KEGG cell cycle gene sets (Figure 5F; Supple-

mentary Table S8). This was associated with impaired cell viability and cell cycle progression, evidenced by accumulation of cells in G1 (Figure 5G–I). Furthermore, the expression of IGF2BP1, METTL3 and METTL14 is strongly correlated with E2F1–3 expression ($R = 0.4$) across 33 TCGA tumor cohorts (Supplementary Figure S6G). In sum, this indicated that IGF2BP1 promotes E2F-driven G1/S transition in an m^{6}A-dependent manner.

IGF2BP1 is a post-transcriptional super-enhancer of E2F-dependent transcription

Our studies suggested that IGF2BP1 is a conserved post-transcriptional enhancer of E2F-driven transcription in cancer. In agreement, the activity of E2F-promoter lu-

ciferase reporters was consistently decreased by IGF2BP1 depletion in all here investigated cancer cell lines (Figure 6A). The evaluation of IGF2BP1-CLIP studies revealed enriched 3′UTR-association of E2F_TARGET transcripts among mRNAs downregulated by IGF2BP1 depletion in five cancer cell lines (Figure 6B, dark to light blue). Moreover, E2F_TARGET genes showed a strong correlation of downregulation upon IGF2BP1 depletion in cancer cell lines and IGF2BP1-associated expression in the corresponding primary cancers (Figure 6C). This suggested that IGF2BP1 promotes the synthesis of E2F-driven gene expression via E2Fs and stabilizes the respective mRNAs. This was analyzed for four E2F-driven transcripts: DSCC1, BUB1B, MKI67 and GINS1 (Figure 6C, red). These were among 31 transcripts (black and red) showing association with IGF2BP1 in primary tumors (R > 0.15) and consistent downregulation ($\log_2 FC < -0.5$) upon IGF2BP1 depletion in cancer cells (Figure 6C, dashed lines). IGF2BP1-CLIP indicated conserved and 3′UTR-directed association for all four mRNAs (Supplementary Figure S7A). Notably, one transcript, the proliferation marker Ki-67 (MKI67), is stabilized by IGF2BP1 in hepatocellular carcinoma (9). RNA-seq confirmed that all four mRNAs were downregulated by IGF2BP1 knockdown and the co-depletion of E2F1–3 (Figure 6D; Supplementary Table S9). Co-depletion of E2F1–3 resulted in severely impaired 2D proliferation and spheroid growth, as expected (Supplementary Figure S7B, C). The analysis of mRNA turnover upon blocking transcription indicated significant destabilization of all four transcripts upon IGF2BP1 knockdown (Figure 6E). Like observed for IGF2BP1 (see Figure 1A), the mRNA expression of the 31 identified E2F/IGF2BP1-binding factors was associated with a significantly reduced survival probability across 33 cancers (Figure 6F). Moreover, these genes showed conserved association with IGF2BP1 expression across these 33 cancers as well as the aforementioned five cancers primarily investigated here (Supplementary Figure S7D). In conclusion, this indicated that IGF2BP1 is a post-transcriptional 'super'-enhancer of E2F-driven gene expression. The protein promotes the E2F hallmark pathway by enhancing E2F1–3 abundance and stabilizes E2F-driven oncogenic transcripts.

BTYNB inhibits enhancement of E2F-driven gene expression by IGF2BP1

Previous studies reported a small molecule inhibitor, BTYNB (21), impairing association of IGF2BP1 with the MYC RNA *in vitro*. BTYNB interfered with cancer cell proliferation and expression of some prior known IGF2BP1 target transcripts. This suggested that this lead compound may as well disrupt E2F/IGF2BP1-driven gene expression. BTYNB exposure (48 h) impaired the viability of LUAD-derived A549 cells (Figure 7A). IGF2BP1-RIP analyses demonstrated that BTYNB treatment for 24 h, when cell vitality was barely affected (data not shown), is associated with reduced binding of IGF2BP1 to the E2F1 mRNA (Figure 7B; Supplementary Figure S8B). In contrast, IGF2BP1-association with the E2F1 mRNA remained essentially unaffected by treatment (24 h) with Palbociclib (36), a CDK4/6-targeting cell cycle inhibitor

currently in phase 4 clinical trials (Supplementary Figure S8B, C). These findings suggested that BTYNB impairs IGF2BP1-association with the E2F1 mRNA. Consistently, BTYNB also led to significantly reduced activity of E2F1–3′UTR luciferase reporters and decreased E2F1 expression at the protein as well as mRNA level (Figure 7C, D). Likewise, BTYNB decreased E2F1 expression and vitality of all other here investigated cancer cell lines without affecting IGF2BP1 abundance (Figure 7E; Supplementary Figure S8A). If BTYNB also impacts the expression of prior identified E2F1-driven target transcripts of IGF2BP1 (DSCC1, BUB1B, MKI67 and GINS1) was analyzed by IGF2BP1-RIP and monitoring steady state mRNA levels in A549 cells. In agreement with reduced IGF2BP1-association of the four mRNAs, steady state levels of all four transcripts were markedly reduced upon BTYNB exposure of A549 as well as all other cancer cell lines investigated (Figure 7F; Supplementary Figure S8D, E).

How BTYNB treatment impairs tumor initiation and growth was analyzed in iRFP-labeled (near infrared red fluorescent protein) ES-2 cells. In these, the deletion of IGF2BP1 impaired the growth of subcutaneous (s.c.) xenograft tumors and interfered with metastasis (8). ES-2 cells exposed to BTYNB, prior (24 h) and during s.c. injection of viable tumor cells, formed tumors at the same efficiency observed for DMSO-treated controls (Figure 7G; Supplementary Figure S8F). However, already 7 days post s.c. injection tumor growth was markedly reduced by BTYNB. This was observed up to 3 weeks post last BTYNB treatment. A major problem of ovarian cancer progression is the rapid spread of malignancies in the peritoneum. If BTYNB also interferes with the peritoneal growth of ES-2 cells was monitored upon intraperitoneal (i.p.) injection. BTYNB treatment impaired both, the growth and spread of tumor cells with reduced tumor burden observed up to 2 weeks after the last treatment (Figure 7H; Supplementary Figure S8G).

Our studies implied that the indirect, IGF2BP1-directed impairment of E2F-driven gene expression by BTYNB synergizes with other cell cycle inhibitors like Palbociclib, targeting activating kinases upstream of E2Fs. This was tested by matrix analysis of combinatorial treatment in ES-2 cells. These analyses revealed synergy scores larger than 7, indicating additive effects (Synergy score between –10 and 10) of BTYNB and Palbociclib according to the ZIP (zero interaction potency) synergy model (Figure 7I). Notably, additivity or even synergy was observed already at low concentrations of both compounds, providing promising evidence that the inhibition of IGF2BP1-RNA association by BTYNB is beneficial in combined treatment aiming to impair tumor cell proliferation.

DISCUSSION

Our studies reveal that IGF2BP1 is the first RBP acting as a conserved post-transcriptional enhancer of E2F-driven gene expression and G1/S-transition in cancer cells and tumors. In consequence, IGF2BP1 promotes tumor cell proliferation *in vitro* and tumor growth *in vivo*. The concisely observed, proliferation-stimulating role of IGF2BP1 was largely attributed to the m^{6}A-dependent stabilization of
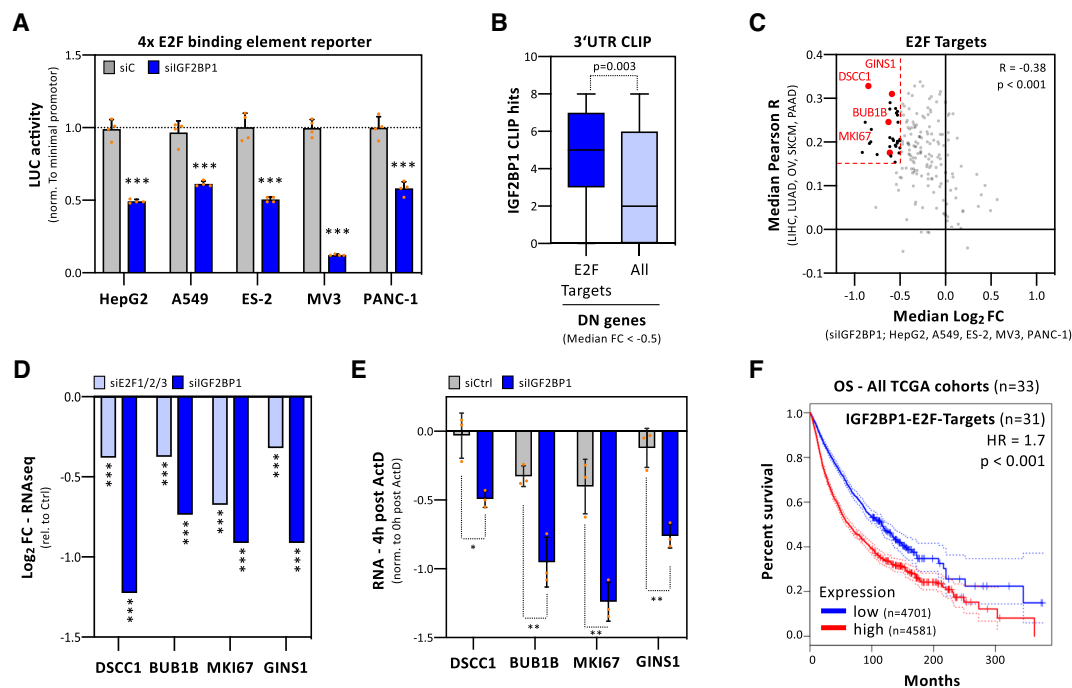
Figure 6. IGF2BP1 is a post-transcriptional enhancer of E2F-driven genes. (**A**) E2F-responsive promoter studies. Luciferase activities, normalized to minimal promoter activity, were determined in indicated cancer cells upon control- (gray) or IGF2BP1-depletion (blue) in four independent experiments. (**B**) Box plots of IGF2BP1 CLIP hits in the 3′UTR of mRNAs showing a median $\log_2 FC < -0.5$ upon IGF2BP1 depletion, as determined in five cancer cell lines (see Figure 3A). E2F Targets, $n = 196$; All, $n = 1280$. (**C**) The median correlation coefficient (R) of E2F target genes with IGF2BP1 in indicated primary cancers was plotted against the median $\log_2 FC$ observed upon IGF2BP1 depletion in indicated cancer cells. Dashed lines distinguish genes with $R > 0.15$ and $\log_2 FC \leftarrow 0.5$ ($n = 31$). (**D**) $\log_2$ FC of DSCC1, BUB1B, MKI67 and GINS1 upon E2F1/2/3- or IGF2BP1-depletion in PANC-1 cells, as determined by RNA seq. (**E**) mRNA decay of indicated genes was monitored by RT-q-PCR in control- (gray) or IGF2BP1-depleted (blue) PANC-1 cells upon 4h of Actinomycin D (ActD) treatment and normalized to RNA levels prior ActD treatment. Error bars indicated standard deviation in three independent studies. RPLP0 served as internal normalization control. (**F**) Kaplan–Meier plots of overall survival analyses (median cutoff) based on the expression of 31 IGF2BP1 and E2F target mRNA (as shown in C) expression. Overall survival was analyzed for all 33 TCGA tumor cohorts (9282 patients). HR, hazard ratio; *P*, logrank *P* value. Statistical significance was determined by Mann–Whitney test: $*P < 0.05$; $**P < 0.01$; $***P < 0.001$.

the MYC mRNA (9,10,12). However, IGF2BP1 and MYC mRNA expression appear barely correlated in most cancers and IGF2BP1 ablation results in conserved and exclusive impairment of G1/S transition. In contrast, disturbed cell cycle progression upon MYC depletion is variable, primarily leading to the enrichment of cancer cells in the S or G2/M phases (37). This clearly indicates that the specific role of IGF2BP1 in promoting G1/S-transition involves additional effector pathways controlling this checkpoint. We reveal that IGF2BP1 is a conserved regulator of E2F-driven gene expression, promoting the expression of E2F transcription factors and other positive regulators of G1/S transition like CDK2/4/6 as well as CCNE1 in an RNA-binding dependent manner. The only prior reported RBPs controlling E2F expression are PUM1 and 2, which promote miRNA-dependent repression of E2F3 mRNA translation (17,20). In contrast, IGF2BP1 impairs downregulation of the E2F1 mRNA by miRNAs. This unravels the first, conserved post-transcriptional enhancer of E2F-dependent cell cycle progression. The IGF2BP1-directed inhibition of target mRNA downregulation by

miRNAs relies on their recruitment to miRNA/RISC-devoid IGF2BP1-mRNPs (14). The expression of positive regulators of G1/S transition, including E2Fs, is substantially impaired by abundant miRNAs emphasizing the potency of post-transcriptional control of cell cycle progression in cancer and stem cells (17,19,38). In addition to E2F1, IGF2BP1 directly stabilizes E2F-driven transcripts encoding cell cycle regulators like Ki-67. This identifies IGF2BP1 as a conserved post-transcriptional super-enhancer of E2F-transcription, promoting E2F activity over the cell type and mitogen-dependent restriction point of G1/S transition (17). Thus, our studies also provide an explanation for the conserved role of IGF2BPs in promoting the self-renewal of stem-like cells (2,39). E2F-driven transcription serves multiple roles in stem cells, including potentially cell cycle-independent regulation (18). Intriguingly, however, the 'cell cycle length hypothesis' implies that expanded time spent in the G1 phase increases the probability of guidance cues to induce differentiation of progenitor cells (40). Consistently, the overexpression of CDK4/cyclinD1 shortens G1 and promotes both, the gen-
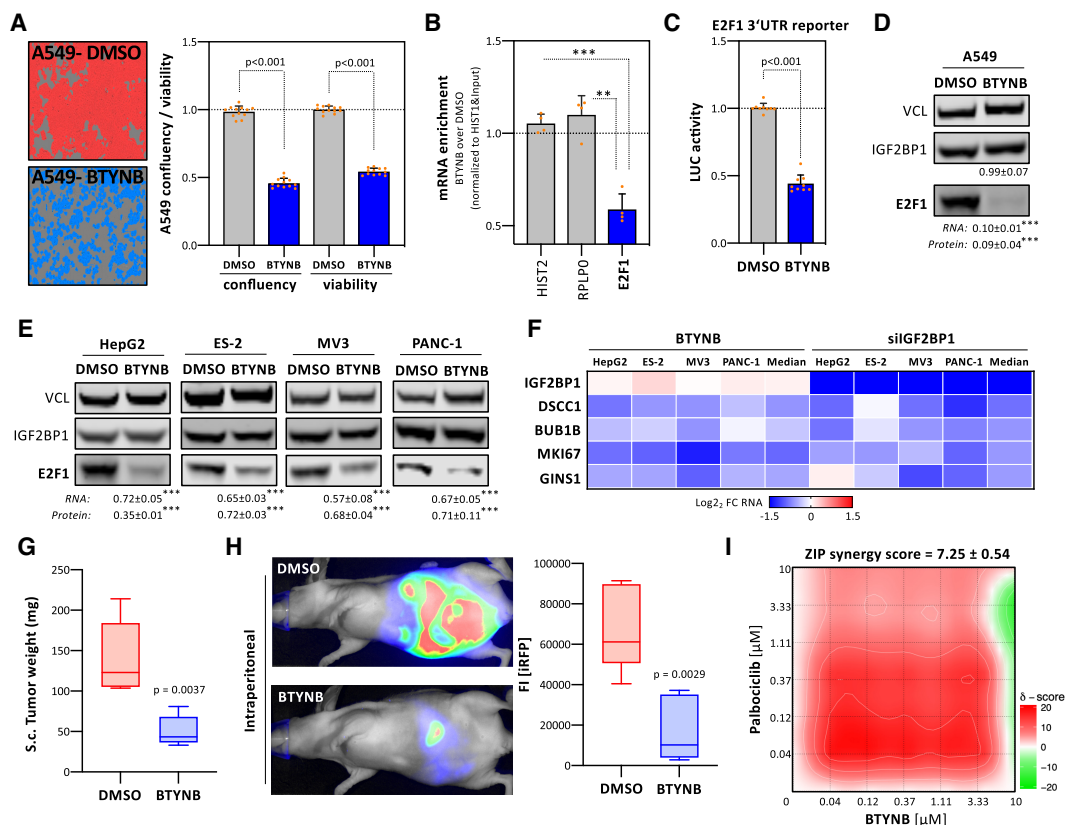
Figure 7. BTYNB impairs IGF2BP1's post-transcriptional super-enhancer function in E2F-driven gene expression. (**A**) A549 cells were treated with DMSO (red) or 5 μM BTYNB (blue) for 48 h. Representative images are indicated in the left panel. Cell confluency and viability were determined by an IncuCyte S3 analyzer and CellTiter GLO (right panel). (**B**) Co-purification of mRNAs with IGF2BP1 in A549 cells upon treatment with 5 μM BTYNB (48 h) was analyzed by immunoprecipitation using anti-IGF2BP1 antibodies and RT-q-PCR analysis. HIST2 and RPLP0 served as negative controls. HIST1 served as normalization control. (**C**) E2F1 3′UTR luciferase activity in A549 cells upon DMSO- or BTYNB (5 μM) treatment. Reporter activities were determined in three independent experiments, including three technical replicates each, as described in Figure 4B. (**D, E**) Western blot analysis of E2F1 protein level upon DMSO or BTYNB (5 μM, 48 h) treatment in indicated cancer cells. The fold change of E2F1 protein and mRNA levels, determined by RT-q-PCR, upon BTYNB treatment is indicated in bottom panel. (**F**) Heatmap showing $\log_2$ FC of indicated mRNAs upon 5 μM BTYNB treatment (left) or IGF2BP1 depletion (right) in indicated cancer cells. (G, H) iRFP-labeled ES-2 cells were treated with DMSO or 5 μM BTYNB for 24h and injected sc (**G**) or ip (**H**) into nude mice (5 mice per condition). The mass of final sc tumors (G) is shown by box plots. Representative images indicating iRFP-labeled intraperitoneal tumors are shown in the left panel (H). The total, final iRFP fluorescence intensity (FI) of ip tumor burden is indicated by box plots (H, right panel). (**I**) Relief plot showing the ZIP synergy for combined treatment with BTYNB and Palbociclib (72 h) at indicated concentrations in 2D-cultured ES-2 cells. Cell viability was determined using Cell Titer GLO. Synergy maps were generated using the SynergyFinder web application (https://synergyfinder.fimm.fi, (31)). ZIP (zero interaction potency) synergy scores were determined in four independent experiments. Synergy scores are color-coded (scores < −10, antagonistic, green; scores > 10, synergistic, red). Statistical significance was determined by Mann–Whitney test: *P <0.05; **P < 0.01; ***P < 0.001.

eration and expansion of neural stem cells (41). The opposite, a substantial prolongation of G1, is observed when ablating IGF2BP1 expression. This suggests that IGF2BP1 favors an undifferentiated, stem-like cell phenotype with high self-renewal potential by shortening G1 due to enhanced G1/S transition. This is concise with IGF2BP1's broad expression in cancer cell lines and substantial upregulation in progressed cancers. In these, the protein conveys elevated proliferation, self-renewal potential and anchorage-independent growth along with enforced expression of stem cell factors like LIN28B (8,14,42). A key observa-

tion of our study is that IGF2BP1/E2F-controlled cell cycle progression is apparently m[6]A-dependent. This emphasizes and substantially expands the recently reported m[6]A-reader role of IGF2BP1 (12,16). Far more important, however, these findings provide a mechanistic rational explaining the conserved growth-promoting role of METTL3/14 in cancer models, that remained controversial (43). Our study strongly suggests that METTL3/14-directed m[6]A-modification is a conserved mechanism promoting elevated cell cycle progression in IGF2BP1-expressing cancers. The enforcement of tumor cell proliferation is further ampli-

fied by the IGF2BP1-dependent stabilization of some E2F-driven mRNAs, encoding regulators of proliferation like Ki-67. This post-transcriptional 'super'-enhancer function of IGF2BP1 is impaired by the small molecule BTYNB. The reported inhibition of IGF2BP1-RNA association and tumor cell proliferation by BTYNB impairing suggested that IGF2BP1-driven tumorigenesis is druggable in principal (21). Notably, however, MYC expression remained largely unchanged at BTYNB concentrations sufficient to substantially impair E2F expression and cell vitality. Moreover, putative off-target effects of BTYNB remain unknown so far. Nonetheless, we present evidence that BTYNB impairs IGF2BP1-dependent stabilization of mRNAs encoding factors, which promote cell cycle and cancer progression. The severe inhibition of tumor growth and peritoneal spread by BTYNB demonstrated in experimental tumor models provides strong, pre-clinical evidence that the therapeutic inhibition of IGF2BP1 is feasible. The conserved roles of IGF2BP1 and inhibitory potency of BTYNB revealed here suggest a broad therapeutic target potential of IGF2BP1 in the treatment of solid cancers. Furthermore, BTYNB acts in an additive manner with Palbociclib, a cell cycle inhibitor targeting key E2F-activiating kinases, mainly CDK4 and CDK6 (36). Thus, our studies provide pre-clinical evidence that combined treatment with BTYNB, impairing IGF2BP1-RNA association, is beneficial for cell cycle inhibition, e.g. by Palbociclib, in cancer treatment.

DATA AVAILABILITY

RNA-sequencing data are deposited on GEO: GSE146807
Flow cytometry data are deposited on FLOW Repository: FR-FCM-Z2DE, FR-FCM-Z2DG, FR-FCM-Z2DF, FR-FCM-Z2ET, FR-FCM-Z2DW

SUPPLEMENTARY DATA

Supplementary Data are available at NAR Online.

REFERENCES

1. Hattori,A., Buac,K. and Ito,T. (2016) Regulation of stem cell self-renewal and oncogenesis by RNA-binding proteins. *Adv. Exp. Med. Biol.*, **907**, 153–188.
2. Degrauwe,N., Suva,M.L., Janiszewska,M., Riggi,N. and Stamenkovic,I. (2016) IMPs: an RNA-binding protein family that provides a link between stem cell maintenance in normal development and cancer. *Genes Dev.*, **30**, 2459–2474.
3. Pereira,B., Billaud,M. and Almeida,R. (2017) RNA-binding proteins in cancer: old players and new actors. *Trends Cancer*, **3**, 506–528.
4. Conway,A.E., Van Nostrand,E.L., Pratt,G.A., Aigner,S., Wilbert,M.L., Sundararaman,B., Freese,P., Lambert,N.J., Sathe,S., Liang,T.Y. *et al.* (2016) Enhanced CLIP uncovers IMP protein-RNA targets in human pluripotent stem cells important for cell adhesion and survival. *Cell Rep.*, **15**, 666–679.
5. Hafner,M., Landthaler,M., Burger,L., Khorshid,M., Hausser,J., Berninger,P., Rothballer,A., Ascano,M. Jr., Jungkamp,A.C., Munschauer,M. *et al.* (2010) Transcriptome-wide identification of RNA-binding protein and microRNA target sites by PAR-CLIP. *Cell*, **141**, 129–141.
6. Bell,J.L., Wachter,K., Muhleck,B., Pazaitis,N., Kohn,M., Lederer,M. and Huttelmaier,S. (2013) Insulin-like growth factor 2 mRNA-binding proteins (IGF2BPs): post-transcriptional drivers of cancer progression? *Cell. Mol. Life Sci.*, **70**, 2657–2675.
7. Lederer,M., Bley,N., Schleifer,C. and Huttelmaier,S. (2014) The role of the oncofetal IGF2 mRNA-binding protein 3 (IGF2BP3) in cancer. *Semin. Cancer Biol.*, **29**, 3–12.
8. Muller,S., Bley,N., Glass,M., Busch,B., Rousseau,V., Misiak,D., Fuchs,T., Lederer,M. and Huttelmaier,S. (2018) IGF2BP1 enhances an aggressive tumor cell phenotype by impairing miRNA-directed downregulation of oncogenic factors. *Nucleic Acids Res.*, **46**, 6285–6303.
9. Gutschner,T., Hammerle,M., Pazaitis,N., Bley,N., Fiskin,E., Uckelmann,H., Heim,A., Grobeta,M., Hofmann,N., Geffers,R. *et al.* (2014) Insulin-like growth factor 2 mRNA-binding protein 1 (IGF2BP1) is an important protumorigenic factor in hepatocellular carcinoma. *Hepatology*, **59**, 1900–1911.
10. Kobel,M., Weidensdorfer,D., Reinke,C., Lederer,M., Schmitt,W.D., Zeng,K., Thomssen,C., Hauptmann,S. and Huttelmaier,S. (2007) Expression of the RNA-binding protein IMP1 correlates with poor prognosis in ovarian carcinoma. *Oncogene*, **26**, 7584–7589.
11. Lemm,I. and Ross,J. (2002) Regulation of c-myc mRNA decay by translational pausing in a coding region instability determinant. *Mol. Cell. Biol.*, **22**, 3959–3969.
12. Huang,H., Weng,H., Sun,W., Qin,X., Shi,H., Wu,H., Zhao,B.S., Mesquita,A., Liu,C., Yuan,C.L. *et al.* (2018) Recognition of RNA N(6)-methyladenosine by IGF2BP proteins enhances mRNA stability and translation. *Nat. Cell Biol.*, **20**, 285–295.
13. Elcheva,I., Goswami,S., Noubissi,F.K. and Spiegelman,V.S. (2009) CRD-BP protects the coding region of betaTrCP1 mRNA from miR-183-mediated degradation. *Mol. Cell*, **35**, 240–246.
14. Busch,B., Bley,N., Muller,S., Glass,M., Misiak,D., Lederer,M., Vetter,M., Strauss,H.G., Thomssen,C. and Huttelmaier,S. (2016) The oncogenic triangle of HMGA2, LIN28B and IGF2BP1 antagonizes tumor-suppressive actions of the let-7 family. *Nucleic Acids Res.*, **44**, 3845–3864.
15. Jonson,L., Christiansen,J., Hansen,T.V.O., Vikesa,J., Yamamoto,Y. and Nielsen,F.C. (2014) IMP3 RNP safe houses prevent miRNA-directed HMGA2 mRNA decay in cancer and development. *Cell Rep.*, **7**, 539–551.
16. Muller,S., Glass,M., Singh,A.K., Haase,J., Bley,N., Fuchs,T., Lederer,M., Dahl,A., Huang,H., Chen,J. *et al.* (2019) IGF2BP1 promotes SRF-dependent transcription in cancer in a m6A- and miRNA-dependent manner. *Nucleic Acids Res.*, **47**, 375–390.
17. Kent,L.N. and Leone,G. (2019) The broken cycle: E2F dysfunction in cancer. *Nat. Rev. Cancer*, **19**, 326–338.
18. Julian,L.M. and Blais,A. (2015) Transcriptional control of stem cell fate by E2Fs and pocket proteins. *Front Genet*, **6**, 161.
19. Emmrich,S. and Putzer,B.M. (2010) Checks and balances: E2F-microRNA crosstalk in cancer control. *Cell Cycle*, **9**, 2555–2567.
20. Miles,W.O., Tschop,K., Herr,A., Ji,J.Y. and Dyson,N.J. (2012) Pumilio facilitates miRNA regulation of the E2F3 oncogene. *Genes Dev.*, **26**, 356–368.

21. Mahapatra,L., Andruska,N., Mao,C., Le,J. and Shapiro,D.J. (2017) A novel IMP1 inhibitor, BTYNB, targets c-Myc and inhibits melanoma and ovarian cancer cell proliferation. *Transl Oncol*, **10**, 818–827.

22. Dweep,H. and Gretz,N. (2015) miRWalk2.0: a comprehensive atlas of microRNA-target interactions. *Nat. Methods*, **12**, 697.

23. Van Nostrand,E.L., Pratt,G.A., Shishkin,A.A., Gelboin-Burkhart,C., Fang,M.Y., Sundararaman,B., Blue,S.M., Nguyen,T.B., Surka,C., Elkins,K. *et al.* (2016) Robust transcriptome-wide discovery of RNA-binding protein binding sites with enhanced CLIP (eCLIP). *Nat. Methods*, **13**, 508–514.

24. Consortium,E.P. (2012) An integrated encyclopedia of DNA elements in the human genome. *Nature*, **489**, 57–74.

25. Yang,Y.C., Di,C., Hu,B., Zhou,M., Liu,Y., Song,N., Li,Y., Umetsu,J. and Lu,Z.J. (2015) CLIPdb: a CLIP-seq database for protein-RNA interactions. *BMC Genomics*, **16**, 51.

26. Quinlan,A.R. (2014) BEDTools: the Swiss-Army Tool for genome feature analysis. *Curr Protoc Bioinformatics*, **47**, doi:10.1002/0471250953.bi1112s47.

27. Liu,H., Flores,M.A., Meng,J., Zhang,L., Zhao,X., Rao,M.K., Chen,Y. and Huang,Y. (2015) MeT-DB: a database of transcriptome methylation in mammalian cells. *Nucleic. Acids. Res.*, **43**, D197–D203.

28. Subramanian,A., Tamayo,P., Mootha,V.K., Mukherjee,S., Ebert,B.L., Gillette,M.A., Paulovich,A., Pomeroy,S.L., Golub,T.R., Lander,E.S. *et al.* (2005) Gene set enrichment analysis: a knowledge-based approach for interpreting genome-wide expression profiles. *Proc. Natl. Acad. Sci. U.S.A.*, **102**, 15545–15550.

29. Liberzon,A., Birger,C., Thorvaldsdottir,H., Ghandi,M., Mesirov,J.P. and Tamayo,P. (2015) The Molecular Signatures Database (MSigDB) hallmark gene set collection. *Cell Syst.*, **1**, 417–425.

30. Marshall,G.M., Bell,J.L., Koach,J., Tan,O., Kim,P., Malyukova,A., Thomas,W., Sekyere,E.O., Liu,T., Cunningham,A.M. *et al.* (2010) TRIM16 acts as a tumour suppressor by inhibitory effects on cytoplasmic vimentin and nuclear E2F1 in neuroblastoma cells. *Oncogene*, **29**, 6172–6183.

31. Ianevski,A., Giri,A.K. and Aittokallio,T. (2020) SynergyFinder 2.0: visual analytics of multi-drug combination synergies. *Nucleic Acids Res.*, **48**, W488–W493.

32. Rosenfeld,Y.B., Krumbein,M., Yeffet,A., Schiffmann,N., Mishalian,I., Pikarsky,E., Oberman,F., Fridlender,Z. and Yisraeli,J.K. (2019) VICKZ1 enhances tumor progression and metastasis in lung adenocarcinomas in mice. *Oncogene*, **38**, 4169–4181.

33. Gerstberger,S., Hafner,M. and Tuschl,T. (2014) A census of human RNA-binding proteins. *Nat. Rev. Genet.*, **15**, 829–845.

34. Bell,J.L., Turlapati,R., Liu,T., Schulte,J.H. and Huttelmaier,S. (2015) IGF2BP1 harbors prognostic significance by gene gain and diverse expression in neuroblastoma. *J. Clin. Oncol.*, **33**, 1285–1293.

35. Sakaue-Sawano,A., Kurokawa,H., Morimura,T., Hanyu,A., Hama,H., Osawa,H., Kashiwagi,S., Fukami,K., Miyata,T., Miyoshi,H. *et al.* (2008) Visualizing spatiotemporal dynamics of multicellular cell-cycle progression. *Cell*, **132**, 487–498.

36. Fry,D.W., Harvey,P.J., Keller,P.R., Elliott,W.L., Meade,M., Trachet,E., Albassam,M., Zheng,X., Leopold,W.R., Pryer,N.K. *et al.* (2004) Specific inhibition of cyclin-dependent kinase 4/6 by PD 0332991 and associated antitumor activity in human tumor xenografts. *Mol. Cancer Ther.*, **3**, 1427–1438.

37. Wang,H., Mannava,S., Grachtchouk,V., Zhuang,D., Soengas,M.S., Gudkov,A.V., Prochownik,E.V. and Nikiforov,M.A. (2008) c-Myc depletion inhibits proliferation of human tumor cells at various stages of the cell cycle. *Oncogene*, **27**, 1905–1915.

38. Gangaraju,V.K. and Lin,H. (2009) MicroRNAs: key regulators of stem cells. *Nat. Rev. Mol. Cell Biol.*, **10**, 116–125.

39. Cao,J., Mu,Q. and Huang,H. (2018) The roles of insulin-like growth factor 2 mRNA-binding protein 2 in cancer and cancer stem cells. *Stem Cells Int.*, **2018**, 4217259.

40. Lange,C. and Calegari,F. (2010) Cdks and cyclins link G1 length and differentiation of embryonic, neural and hematopoietic stem cells. *Cell Cycle*, **9**, 1893–1900.

41. Lange,C., Huttner,W.B. and Calegari,F. (2009) Cdk4/cyclinD1 overexpression in neural stem cells shortens G1, delays neurogenesis, and promotes the generation and expansion of basal progenitors. *Cell Stem Cell*, **5**, 320–331.

42. Shyh-Chang,N. and Daley,G.Q. (2013) Lin28: primal regulator of growth and metabolism in stem cells. *Cell Stem Cell*, **12**, 395–406.

43. Lan,Q., Liu,P.Y., Haase,J., Bell,J.L., Huttelmaier,S. and Liu,T. (2019) The critical role of RNA m(6)A methylation in cancer. *Cancer Res.*, **79**, 1285–1292.

Müller et al., 2020 – SUPPLEMENTARY FIGURE LEGENDS

Supplementary Figure S1 - IGF2BP1 is a conserved oncoRBP in solid human cancer. (A) Heatmap of IGF2BP1 Hazard ratios (HR) with indicated p-values. Overall survival (median cutoff) was analyzed for indicated TCGA tumor cohorts. (B) Heatmap showing the log2 FC of mRBP-encoding mRNAs (n=660, left heatmap) in indicated TCGA tumor cohorts to corresponding GTEx normal tissue samples based on RNA sequencing. mRBPs were ranked according to their average FC. The log2 FC of the 10 most upregulated mRBPs is depicted by a heatmap enlargement (right panel). (C, D) Scatter plots of IGF2BP1 and MYC expression across all TCGA tumor cohorts (n =33, C) and five indicated TCGA cancer cohorts (D).

Supplementary Figure S2 - IGF2BP1 expression shows conserved association with enhanced proliferation in solid cancer. (A) Violin plots of correlation coefficients (R) determined for protein-coding genes and IGF2BP1 expression in the indicated TCGA tumor cohorts. (B, C) Gene set enrichment analysis (GSEA) of IGF2BP1-correlated gene expression in the five indicated TCGA tumor cohorts. GSEA was performed on the ranked correlation coefficients determined in A. GSEA plots for indicated cancer cohorts are shown for the cancer Hallmark pathway "E2F targets" (B) and KEGG pathway "Cell Cycle" (C). NES, normalized enrichment score.

Supplementary Figure S3 - IGF2BP1 is a conserved regulator of tumor cell proliferation and clonogenic growth. (A-C) PANC-1 cells were transfected with control (siCtrl, grey) or IGF2BP1-directed siRNA pools (siIGF2BP1, blue). Cells were counted at indicated time points post-transfection by flow cytometry (A) and the doubling time was calculated (B) in three independent experiments. The percentage of Propidium iodide (PI) positive and negative PANC-1 cells (C) was determined by flow cytometry upon transfection of indicated siRNAs. (D, E) Quantification of colony formation and clonogenic growth of PANC-1 cells transfected with indicated siRNAs. Representative images of colony formation in soft agar (D, left panel) and clonogenicity studies (E, left panel) are shown. Statistical significance was determined by Mann-Whitney-Test: *, $p<0.05$; **, $p< 0.01$; ***, $p< 0.001$.

Supplementary Figure S4 - IGF2BP1 is a conserved enhancer of G1/S transition in cancer-derived cells. (A) Representative cell cycle phase distribution upon transfection with control (siCtrl) or IGF2BP1-directed siRNAs in indicated cancer cells, as determined by PI-labeling and flow cytometry. (B, C) ES-2 cells were stably transduced with the FUCCI system (Sartorius) and transfected with control (siCtrl) or IGF2BP1-directed siRNAs. Cells were synchronized in G2 phase (green fluorescence) 20h post-transfection by cell sorting (FACS) and monitored for indicated time in the IncuCyte Live Cell Imaging system. Cell segmentation and classification was performed using the Cell-by-Cell module and representative images overlayed with segmentation masks are shown (B). Difference between IGF2BP1 depleted and control cells is shown for the respective cell cycle phases over time for n > 4000 objects (C). Error bars indicate standard error

of three independent experiments. Red, G1 phase; Green, G2 phase; Yellow, S phase. (D) Spheroid growth of parental (Ctrl) and IGF2BP1-deleted (KO) A549 cells. Representative A549 spheroids 5 days post-seeding are indicated in the left panel. The viability of spheroids was determined by Cell-titer GLO (right panel). (E) Spheroid growth analysis of IGF2BP1-KO A549 cells expressing GFP, GFP-IGF2BP1 (WT) or an RNA-binding deficient GFP-IGF2BP1 (MUT). Spheroid viability was determined using Cell Titer GLO and normalized to median cell vitality observed in GFP-expressing controls. Error bars indicate standard deviation of at least three independent analyses with at least four analyzed spheroids. Statistical significance was determined by Mann-Whitney-Test.

Supplementary Figure S5 - IGF2BP1 is a conserved regulator of E2F-driven gene expression in cancer-derived cells. (A) Gene set enrichment analysis (GSEA) of protein-coding gene fold changes upon IGF2BP1 depletion in five indicated cancer cell lines the median fold change determined in the respective analyses as shown in Figure 3. GSEA plots for the Hallmark pathway "E2F Targets" (top panel) and the KEGG pathway "Cell Cycle" (bottom panel) are shown. NES, normalized enrichment score. (B) IGF2BP1 CLIP profile of the indicated mRNAs. The 3'UTR is highlighted by dashed lines. (C-E) Representative Western blot analyses of E2F2 and E2F3 protein expression upon IGF2BP1-depletion in PANC-1 cells (C), of E2F1 protein upon IGF2BP1 deletion in A549 (D) cells by CRISPR/Cas9 and of E2F1 protein in IGF2BP1-KO A549 cells expressing GFP, GFP-IGF2BP1 (WT) or an RNA-binding deficient GFP-IGF2BP1 (MUT) (E). Vinculin (VCL) served as loading and normalization control. Average fold changes and standard deviation of E2F1/2/3 protein levels, determined in three independent analyses are indicated in bottom panels. (E) Scatter Plots of IGF2BP1, METTL3, METTL14 (x-axis) and E2F1, E2F2, E2F3 (y-axis and in plot) expression across all TCGA tumor cohorts (33 cohorts, 9282 patients) determined by GEPIA2. Pearson correlation coefficient and p-value are indicated.

Supplementary Figure S6 – IGF2BP1 controls E2F1 mRNA abundance in a miRNA- and m6A-dependent manner. (A) RT-qPCR analysis of indicated mRNA levels in total RNA (blue) or nascent RNA (grey) fractions upon IGF2BP1-depletion normalized to control-transfected PANC-1 cells. RPLP0 served as normalization control. Nascent RNAs were purified using the Click-iT Nascent RNA Capture Kit (Thermo Fisher) upon labeling newly synthesized transcripts with 5-ethynyl uridine for 4h (72h post-transfection of siRNAs). (B) Abundance of miRNAs targeting the E2F1 3'UTR. MiRNA expression, determined by small RNA sequencing in five cancer cell lines, is indicated as median cpm along with the number of 12 investigated databases predicting miRNA binding sites (MBS), as analyzed by miRWalk2.0. (C) Luciferase reporter analysis demonstrating activity of indicated reporters in control- (siCtrl, red) or IGF2BP1-depleted (siIGF2BP1, blue) A549 cells. Reporter activities, normalized to a control reporter without miRNA targeting site (Empty), were determined in three independent experiments with two technical replicates each. (D) Immunoprecipitation of AGO2 in parental (Ctrl) or IGF2BP1-knockout A549 cells was confirmed

by Western blotting (left panel). VCL served as negative control. (E, F) Representative Western blot analyses of E2F2 and E2F3 proteins upon METTL3 and METTL14-depletion in PANC-1 cells (E) and of E2F1 protein upon METTL3 deletion (F) in A549 by CRISPR/Cas9. Vinculin (VCL) served as loading and normalization control. Average fold changes and standard deviation of E2F1/2/3 protein levels, determined in three independent analyses are indicated in bottom panels. (G) Scatter Plots of IGF2BP1, METTL3, METTL14 (x-axis) and E2F1, E2F2, E2F3 (y-axis and in plot) expression across all TCGA tumor cohorts (33 cohorts, 9282 patients) determined by GEPIA2. Pearson correlation coefficient and p-value are indicated.

Supplementary Figure S7 - IGF2BP1 is a post-transcriptional super-enhancer of E2F-driven gene expression in cancer. (A) IGF2BP1 CLIP profile in the 3'UTR of the indicated E2F-driven mRNAs. The length of the 3'UTRs is shown. (B, C) PANC-1 cells were transfected with control (siC, black) or E2F1/2/3-directed siRNA pools (siE2F1+2+3, blue). The viability of 2D-cultured PANC-1 cells (B) and PANC-1 spheroids (C, right panel) was determined by Cell-titer GLO 6 days post-transfection. Representative PANC-1 spheroids are shown in the left panel (c). Statistical significance was determined by Mann-Whitney-Test: **, p< 0.01; ***, p< 0.001. (D) Scatter Plots of IGF2BP1 (x-axis) and indicated mRNAs (y-axis and in plot) expression across all TCGA tumor cohorts (33 cohorts, 9282 patients, top panel) and the LIHC, LUAD, OV, SKCM and PAAD cohorts (bottom panel) determined by GEPIA2. The correlation of IGF2BP1 and the 31 gene signature shown in Figure 6C is depicted in the right scatter plot. Correlation coefficients (R) and p-values are indicated in plots.

Supplementary Figure S8 - BTYNB is a potent inhibitor of IGF2BP1-driven tumor cell proliferation and tumor growth. (A) Indicated cancer cells were treated with DMSO (grey) or 5 µM BTYNB (blue) for 48 h. Representative images of PANC-1 cells are indicated in the left panel. Cell viability was determined by Cell-titer GLO (right panel). (B) Immunoprecipitation of IGF2BP1 in A549 cells treated with DMSO, 5 µM BTYNB or 5µM Palbociclib for 24h was confirmed by Western blotting. VCL served as negative control. (C, D) Co-purification of indicated mRNAs with IGF2BP1 in DMSO-, Palbociclib-treated (5µM for 24h, C) or BTYNB-treated (5µM for 24h, D) A549 cells was analyzed by RIP using anti-IGF2BP1 antibodies and RT-qPCR analysis. The enrichment of mRNAs in BTYNB-treated over DMSO-treated cells is shown. HIST1 mRNA served as normalization control. (E) RT-q-PCR analysis of mRNA levels upon BTYNB treatment in A549 cells normalized to DMSO-treated cells as in Figure 7A-D. RPLP0 served as internal normalization control. (F, G) iRFP-labeled ES-2 cells were treated with DMSO or 5 µM BTYNB for 24h and upon s.c. (F) or i.p. (G) injection into nude mice (5 mice per condition). Representative images indicating iRFP-labeled tumors at indicated times are shown in the left panels. Quantifications of tumor volumes (F) or fluorescence intensity (FI, G) are shown in the right panels. (G, bottom panel) Arrows indicate i.p. tumors 14 days post-injection in an enlargement of the region indicated by a dashed box in the middle panel. Statistical significance was determined by Mann-Whitney-Test. Exact p-values are indicated.
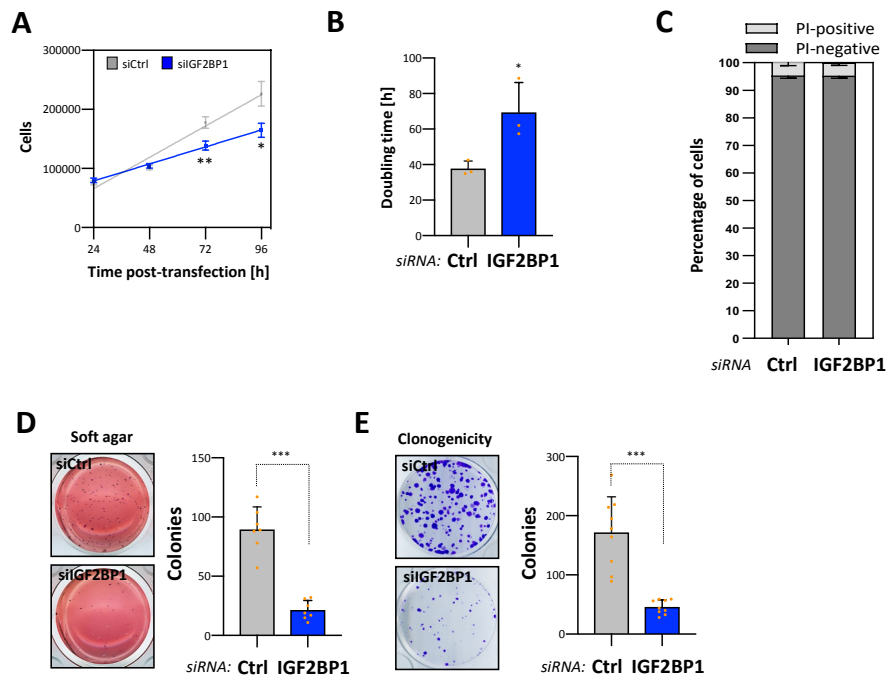
Müller et al., 2020 - Supplementary Figure S1
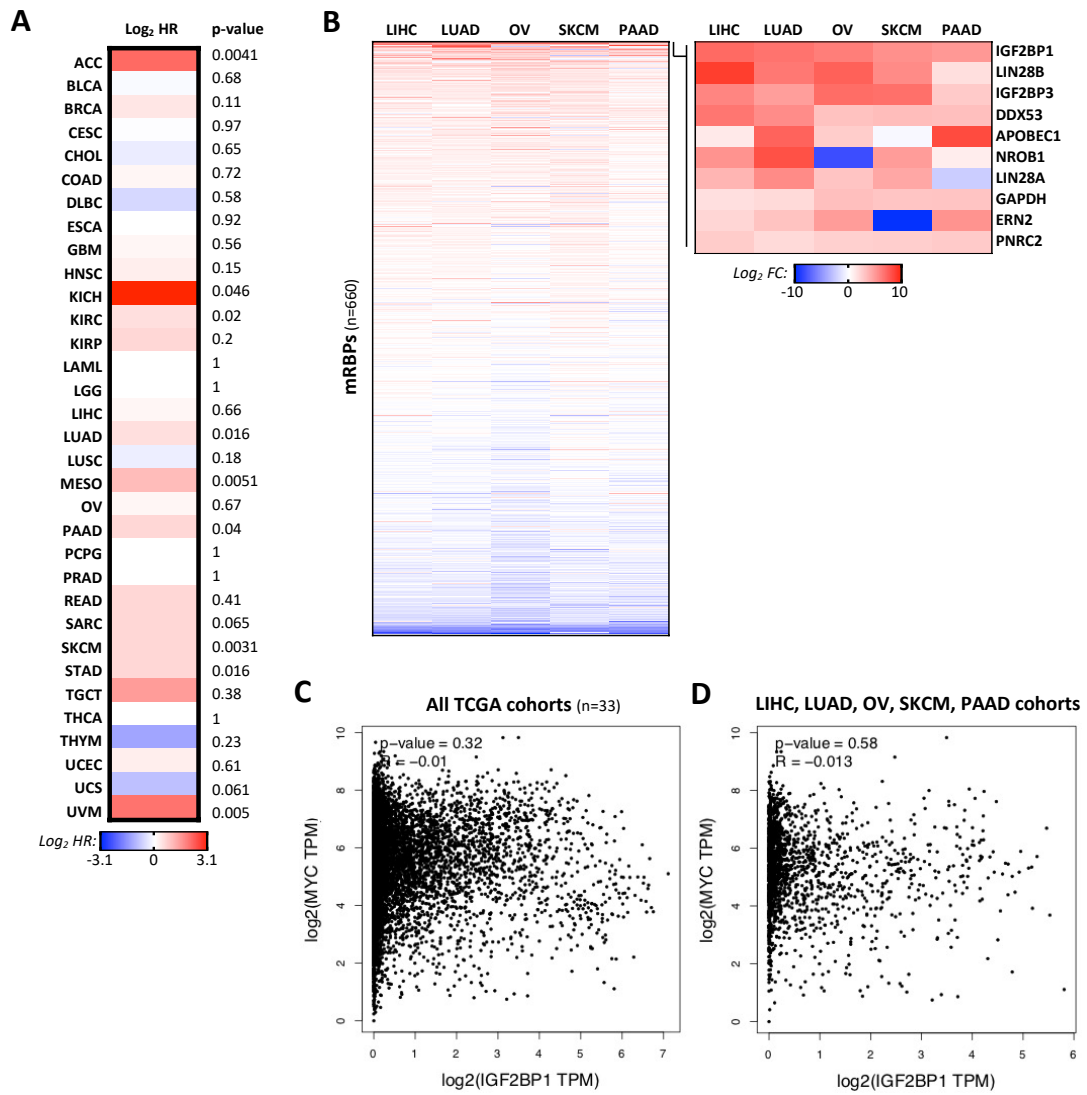
Müller et al., 2020 - Supplementary Figure S2
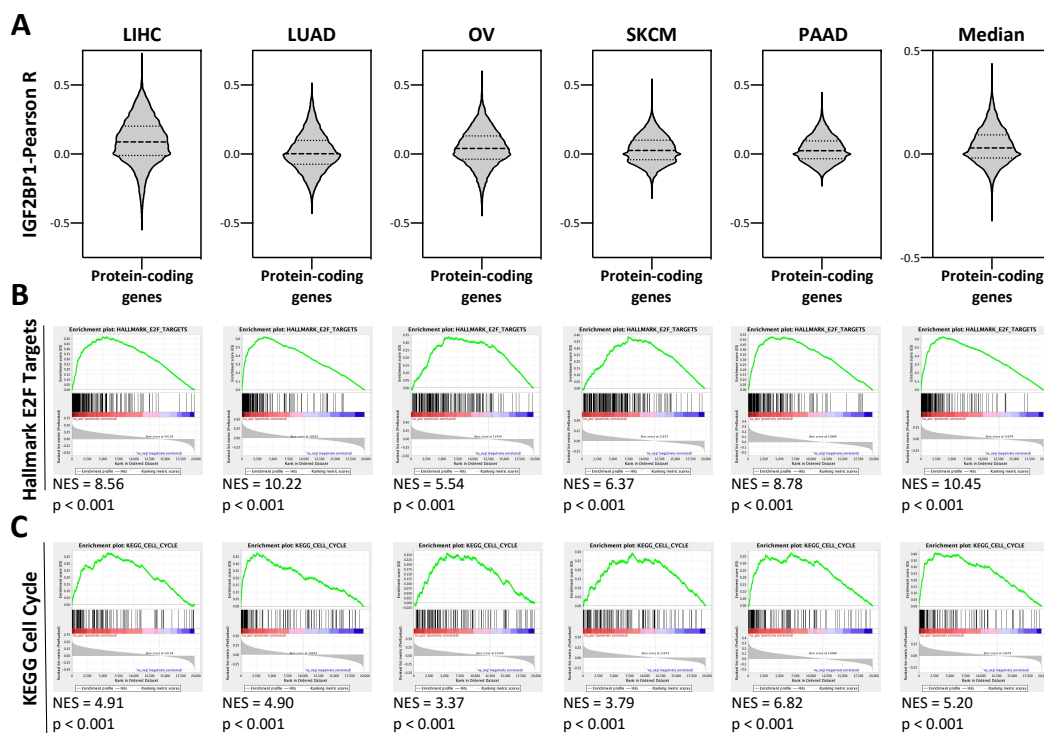
Müller et al., 2020 - Supplementary Figure S3

Müller et al., 2020 - Supplementary Figure S4

A

B

C

D

E

A549 – IGF2BP1 Knockout

Müller et al., 2020 - Supplementary Figure S5

A

	HepG2	A549	ES-2	MV3	PANC1	Median FC

Hallmark E2F Targets

| NES = -4.45 | NES = -3.60 | NES = -5.20 | NES = -8.97 | NES = -7.37 | NES = -3.51 |
| p < 0.001 | p < 0.001 | p < 0.001 | p < 0.001 | p < 0.001 | p < 0.001 |

KEGG Cell Cycle

| NES = -4.14 | NES = -1.95 | NES = -2.26 | NES = -4.55 | NES = -3.78 | NES = -2.75 |
| p < 0.001 | p = 0.002 | p = 0.002 | p = 0.002 | p = 0.002 | p = 0.002 |

B

IGF2BP1 CLIP sites

E2F2, E2F3, CDK2, CDK4, CDK6, CCNE1, CCND1, MYC — 3'UTR

C

PANC-1

siRNA: Ctrl IGF2BP1

VCL
IGF2BP1
E2F2 0.42±0.05
E2F3 0.46±0.07

D

A549

Knockout: Ctrl IGF2BP1

VCL
IGF2BP1
E2F1 0.51±0.20

E

GFP-IGF2BP1

Expr.: GFP WT MUT

VCL
GFP
E2F1 1.68±0.11 0.97±0.26
***

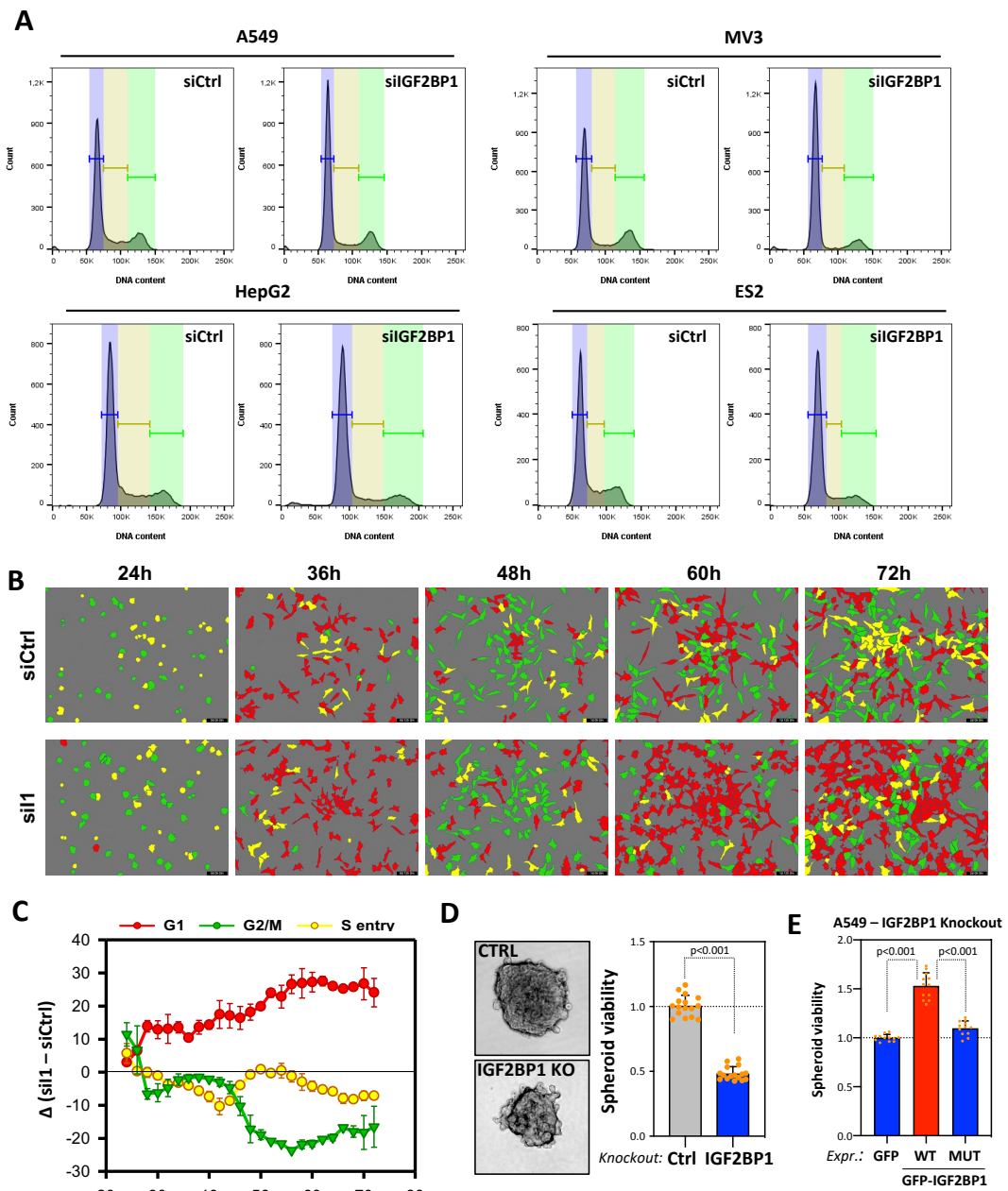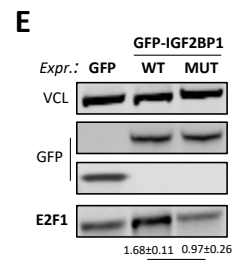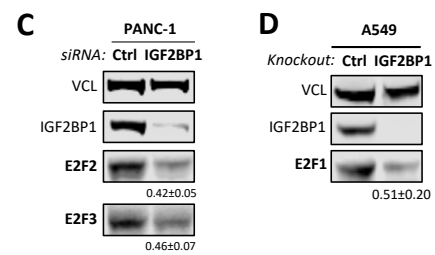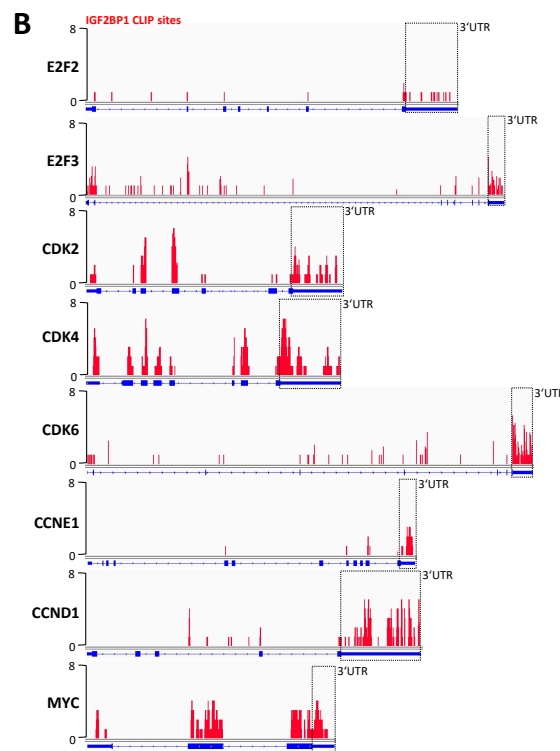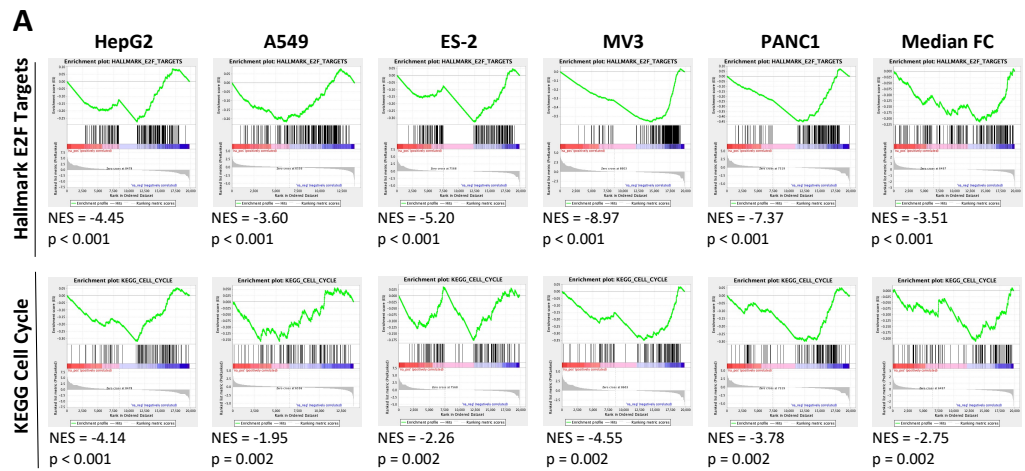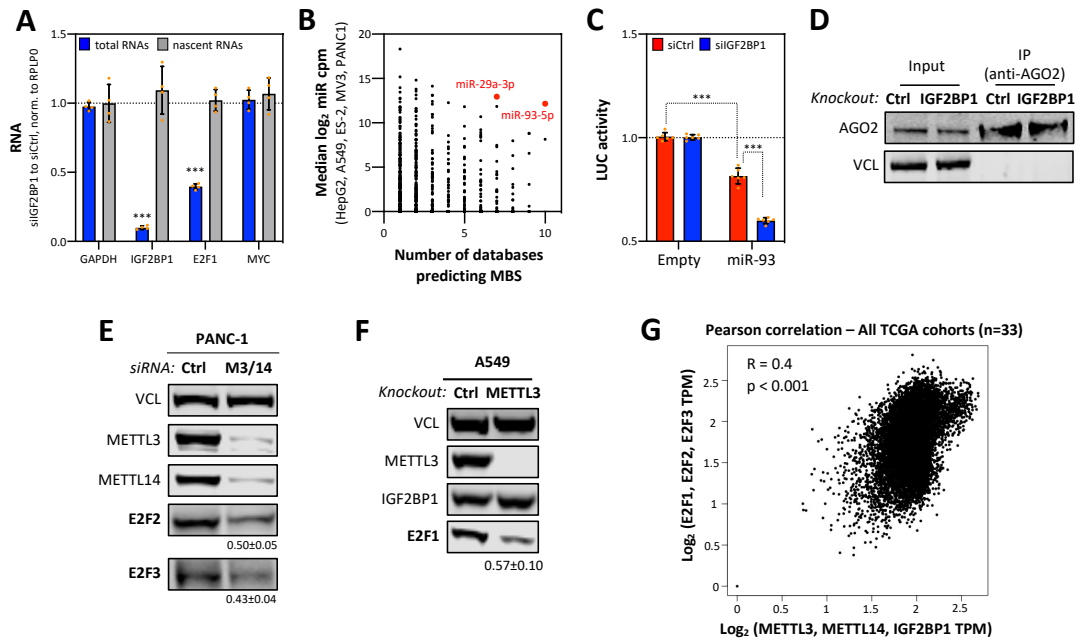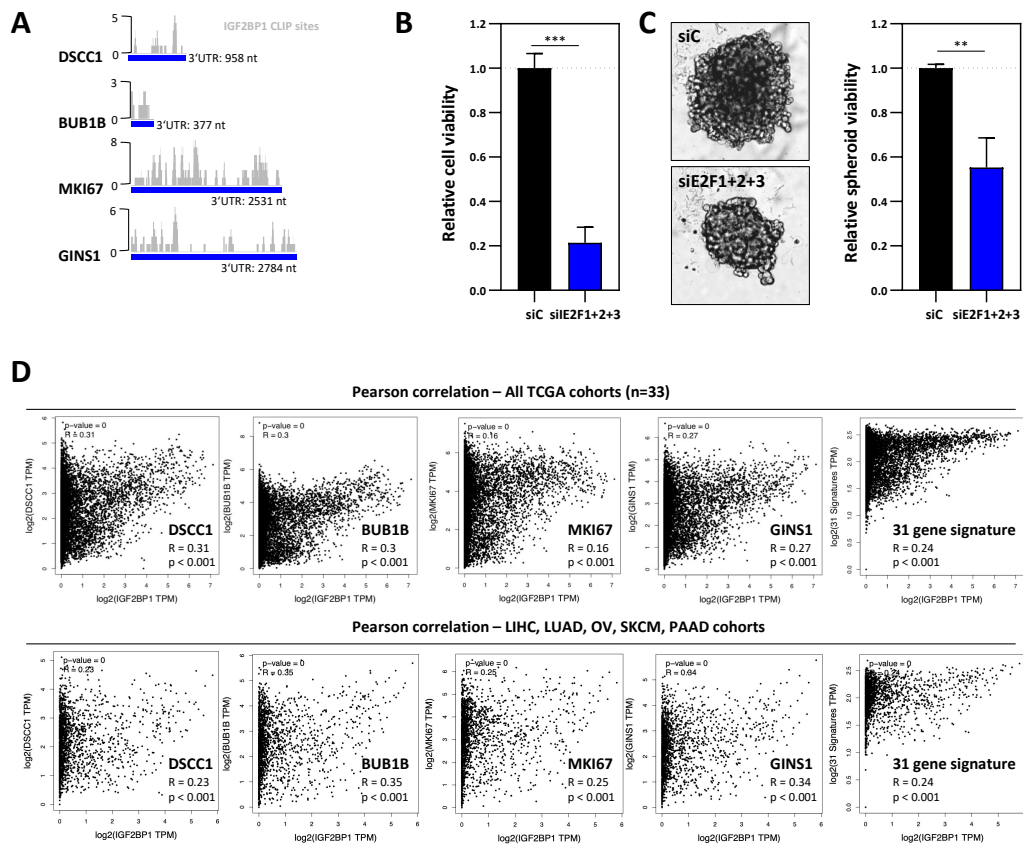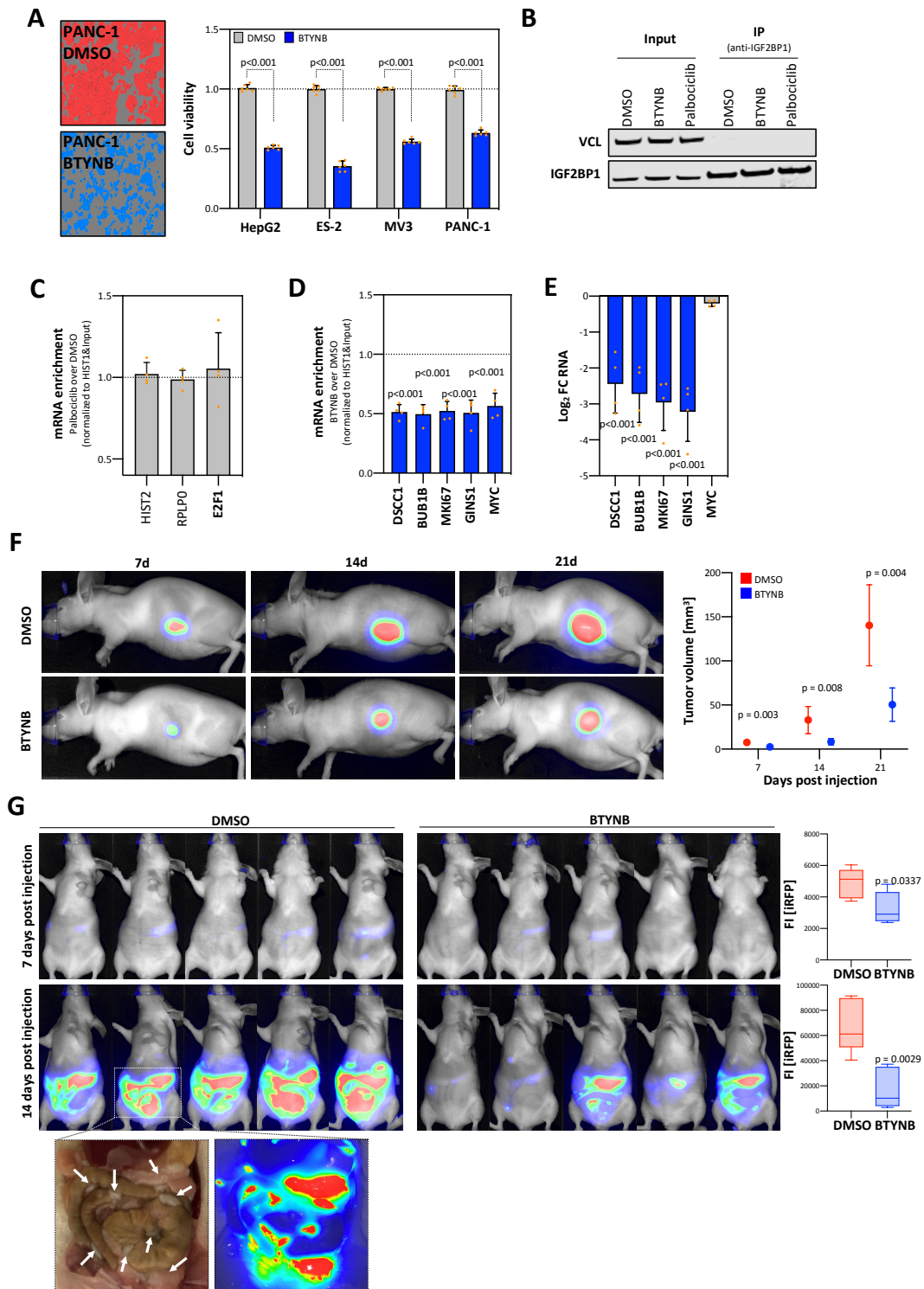## Müller et al., 2020 - Supplementary Figure S6

Müller et al., 2020 - Supplementary Figure S7

Müller et al., 2020 - Supplementary Figure S8

V REFERENCES

Agarwal, V., Bell, G.W., Nam, J.W., and Bartel, D.P. (2015). Predicting effective microRNA target sites in mammalian mRNAs. Elife *4*.

Allegri, L., Baldan, F., Roy, S., Aube, J., Russo, D., Filetti, S., and Damante, G. (2019). The HuR CMLD-2 inhibitor exhibits antitumor effects via MAD2 downregulation in thyroid cancer cells. Sci Rep *9*, 7374.

Anczukow, O., Akerman, M., Clery, A., Wu, J., Shen, C., Shirole, N.H., Raimer, A., Sun, S., Jensen, M.A., Hua, Y., *et al.* (2015). SRSF1-Regulated Alternative Splicing in Breast Cancer. Mol Cell *60*, 105-117.

Asangani, I.A., Rasheed, S.A., Nikolova, D.A., Leupold, J.H., Colburn, N.H., Post, S., and Allgayer, H. (2008). MicroRNA-21 (miR-21) post-transcriptionally downregulates tumor suppressor Pdcd4 and stimulates invasion, intravasation and metastasis in colorectal cancer. Oncogene *27*, 2128-2136.

Balzeau, J., Menezes, M.R., Cao, S., and Hagan, J.P. (2017). The LIN28/let-7 Pathway in Cancer. Front Genet *8*, 31.

Barbagallo, D., Caponnetto, A., Brex, D., Mirabella, F., Barbagallo, C., Lauretta, G., Morrone, A., Certo, F., Broggi, G., Caltabiano, R., *et al.* (2019). CircSMARCA5 Regulates VEGFA mRNA Splicing and Angiogenesis in Glioblastoma Multiforme Through the Binding of SRSF1. Cancers (Basel) *11*.

Barbieri, I., and Kouzarides, T. (2020). Role of RNA modifications in cancer. Nat Rev Cancer *20*, 303-322.

Barbieri, I., Tzelepis, K., Pandolfini, L., Shi, J., Millan-Zambrano, G., Robson, S.C., Aspris, D., Migliori, V., Bannister, A.J., Han, N., *et al.* (2017). Promoter-bound METTL3 maintains myeloid leukaemia by m(6)A-dependent translation control. Nature *552*, 126-131.

Bardhan, K., Anagnostou, T., and Boussiotis, V.A. (2016). The PD1:PD-L1/2 Pathway from Discovery to Clinical Implementation. Front Immunol *7*, 550.

Bartel, D.P. (2004). MicroRNAs: genomics, biogenesis, mechanism, and function. Cell *116*, 281-297.

Bava, F.A., Eliscovich, C., Ferreira, P.G., Minana, B., Ben-Dov, C., Guigo, R., Valcarcel, J., and Mendez, R. (2013). CPEB1 coordinates alternative 3'-UTR formation with translational regulation. Nature *495*, 121-125.

Behm-Ansmant, I., Rehwinkel, J., Doerks, T., Stark, A., Bork, P., and Izaurralde, E. (2006). mRNA degradation by miRNAs and GW182 requires both CCR4:NOT deadenylase and DCP1:DCP2 decapping complexes. Genes Dev *20*, 1885-1898.

Behrmann, E., Loerke, J., Budkevich, T.V., Yamamoto, K., Schmidt, A., Penczek, P.A., Vos, M.R., Burger, J., Mielke, T., Scheerer, P., *et al.* (2015). Structural snapshots of actively translating human ribosomes. Cell *161*, 845-857.

Bell, J.L., Turlapati, R., Liu, T., Schulte, J.H., and Huttelmaier, S. (2015). IGF2BP1 harbors prognostic significance by gene gain and diverse expression in neuroblastoma. J Clin Oncol *33*, 1285-1293.

Bell, J.L., Wachter, K., Muhleck, B., Pazaitis, N., Kohn, M., Lederer, M., and Huttelmaier, S. (2013). Insulin-like growth factor 2 mRNA-binding proteins (IGF2BPs): post-transcriptional drivers of cancer progression? Cell Mol Life Sci *70*, 2657-2675.

Berezikov, E., Chung, W.J., Willis, J., Cuppen, E., and Lai, E.C. (2007). Mammalian mirtron genes. Mol Cell *28*, 328-336.

Bley, N., Schott, A., Muller, S., Misiak, D., Lederer, M., Fuchs, T., Assmann, C., Glass, M., Ihling, C., Sinz, A., *et al.* (2021). IGF2BP1 is a targetable SRC/MAPK-dependent driver of invasive growth in ovarian cancer. RNA Biol *18*, 391-403.

Bogucka, K., Marini, F., Rosigkeit, S., Schloeder, J., Jonuleit, H., David, K., Schlackow, M., and Rajalingam, K. (2021). ERK3/MAPK6 is required for KRAS-mediated NSCLC tumorigenesis. Cancer Gene Ther *28*, 359-374.

Boudoukha, S., Cuvellier, S., and Polesskaya, A. (2010). Role of the RNA-binding protein IMP-2 in muscle cell motility. Mol Cell Biol *30*, 5710-5725.

Boyerinas, B., Park, S.M., Hau, A., Murmann, A.E., and Peter, M.E. (2010). The role of let-7 in cell differentiation and cancer. Endocr Relat Cancer *17*, F19-36.

Boyerinas, B., Park, S.M., Shomron, N., Hedegaard, M.M., Vinther, J., Andersen, J.S., Feig, C., Xu, J., Burge, C.B., and Peter, M.E. (2008). Identification of let-7-regulated oncofetal genes. Cancer Res *68*, 2587-2591.

Braun, J., Misiak, D., Busch, B., Krohn, K., and Huttelmaier, S. (2014). Rapid identification of regulatory microRNAs by miTRAP (miRNA trapping by RNA in vitro affinity purification). Nucleic Acids Res *42*, e66.

Busch, B., Bley, N., Muller, S., Glass, M., Misiak, D., Lederer, M., Vetter, M., Strauss, H.G., Thomssen, C., and Huttelmaier, S. (2016). The oncogenic triangle of HMGA2, LIN28B and IGF2BP1 antagonizes tumor-suppressive actions of the let-7 family. Nucleic Acids Res *44*, 3845-3864.

REFERENCES

Bussing, I., Slack, F.J., and Grosshans, H. (2008). let-7 microRNAs in development, stem cells and cancer. Trends Mol Med *14*, 400-409.

Calin, G.A., Dumitru, C.D., Shimizu, M., Bichi, R., Zupo, S., Noch, E., Aldler, H., Rattan, S., Keating, M., Rai, K., *et al.* (2002). Frequent deletions and down-regulation of micro- RNA genes miR15 and miR16 at 13q14 in chronic lymphocytic leukemia. Proc Natl Acad Sci U S A *99*, 15524-15529.

Castello, A., Horos, R., Strein, C., Fischer, B., Eichelbaum, K., Steinmetz, L.M., Krijgsveld, J., and Hentze, M.W. (2013). System-wide identification of RNA-binding proteins by interactome capture. Nat Protoc *8*, 491-500.

Chang, K.Y., and Ramos, A. (2005). The double-stranded RNA-binding motif, a versatile macromolecular docking platform. FEBS J *272*, 2109-2117.

Chao, J.A., Patskovsky, Y., Patel, V., Levy, M., Almo, S.C., and Singer, R.H. (2010). ZBP1 recognition of beta-actin zipcode induces RNA looping. Genes Dev *24*, 148-158.

Chen, H.M., Lin, C.C., Chen, W.S., Jiang, J.K., Yang, S.H., Chang, S.C., Ho, C.L., Yang, C.C., Huang, S.C., Chao, Y., *et al.* (2021). Insulin-Like Growth Factor 2 mRNA-Binding Protein 1 (IGF2BP1) Is a Prognostic Biomarker and Associated with Chemotherapy Responsiveness in Colorectal Cancer. Int J Mol Sci *22*.

Chen, M., Wei, L., Law, C.T., Tsang, F.H., Shen, J., Cheng, C.L., Tsang, L.H., Ho, D.W., Chiu, D.K., Lee, J.M., *et al.* (2018). RNA N6-methyladenosine methyltransferase-like 3 promotes liver cancer progression through YTHDF2-dependent posttranscriptional silencing of SOCS2. Hepatology *67*, 2254-2270.

Christiansen, J., Kolte, A.M., Hansen, T., and Nielsen, F.C. (2009). IGF2 mRNA-binding protein 2: biological function and putative role in type 2 diabetes. J Mol Endocrinol *43*, 187-195.

Cimmino, A., Calin, G.A., Fabbri, M., Iorio, M.V., Ferracin, M., Shimizu, M., Wojcik, S.E., Aqeilan, R.I., Zupo, S., Dono, M., *et al.* (2005). miR-15 and miR-16 induce apoptosis by targeting BCL2. Proc Natl Acad Sci U S A *102*, 13944-13949.

Clery, A., Blatter, M., and Allain, F.H. (2008). RNA recognition motifs: boring? Not quite. Curr Opin Struct Biol *18*, 290-298.

Concepcion, C.P., Bonetti, C., and Ventura, A. (2012). The microRNA-17-92 family of microRNA clusters in development and disease. Cancer J *18*, 262-267.

Cong, L., Ran, F.A., Cox, D., Lin, S., Barretto, R., Habib, N., Hsu, P.D., Wu, X., Jiang, W., Marraffini, L.A., *et al.* (2013). Multiplex genome engineering using CRISPR/Cas systems. Science *339*, 819-823.

Conn, S.J., Pillman, K.A., Toubia, J., Conn, V.M., Salmanidis, M., Phillips, C.A., Roslan, S., Schreiber, A.W., Gregory, P.A., and Goodall, G.J. (2015). The RNA binding protein quaking regulates formation of circRNAs. Cell *160*, 1125-1134.

Conway, A.E., Van Nostrand, E.L., Pratt, G.A., Aigner, S., Wilbert, M.L., Sundararaman, B., Freese, P., Lambert, N.J., Sathe, S., Liang, T.Y., *et al.* (2016). Enhanced CLIP Uncovers IMP Protein-RNA Targets in Human Pluripotent Stem Cells Important for Cell Adhesion and Survival. Cell Rep *15*, 666-679.

Cortez, M.A., Ivan, C., Valdecanas, D., Wang, X., Peltier, H.J., Ye, Y., Araujo, L., Carbone, D.P., Shilo, K., Giri, D.K., *et al.* (2016). PDL1 Regulation by p53 via miR-34. J Natl Cancer Inst *108*.

Craig, E.A., Weber, J.D., and Spiegelman, V.S. (2012). Involvement of the mRNA binding protein CRD-BP in the regulation of metastatic melanoma cell proliferation and invasion by hypoxia. J Cell Sci *125*, 5950-5954.

Crick, F. (1970). Central dogma of molecular biology. Nature *227*, 561-563.

Crick, F.H. (1958). On protein synthesis. Symp Soc Exp Biol *12*, 138-163.

D'Ambrogio, A., Nagaoka, K., and Richter, J.D. (2013). Translational control of cell growth and malignancy by the CPEBs. Nat Rev Cancer *13*, 283-290.

Dagil, R., Ball, N.J., Ogrodowicz, R.W., Hobor, F., Purkiss, A.G., Kelly, G., Martin, S.R., Taylor, I.A., and Ramos, A. (2019). IMP1 KH1 and KH2 domains create a structural platform with unique RNA recognition and re-modelling properties. Nucleic Acids Res *47*, 4334-4348.

Dai, N., Ji, F., Wright, J., Minichiello, L., Sadreyev, R., and Avruch, J. (2017). IGF2 mRNA binding protein-2 is a tumor promoter that drives cancer proliferation through its client mRNAs IGF2 and HMGA1. Elife *6*.

Dai, N., Rapley, J., Angel, M., Yanik, M.F., Blower, M.D., and Avruch, J. (2011). mTOR phosphorylates IMP2 to promote IGF2 mRNA translation by internal ribosomal entry. Genes Dev *25*, 1159-1172.

Dai, N., Zhao, L., Wrighting, D., Kramer, D., Majithia, A., Wang, Y., Cracan, V., Borges-Rivera, D., Mootha, V.K., Nahrendorf, M., *et al.* (2015). IGF2BP2/IMP2-Deficient mice resist obesity through enhanced translation of Ucp1 mRNA and Other mRNAs encoding mitochondrial proteins. Cell Metab *21*, 609-621.

Davidson, B., Rosenfeld, Y.B., Holth, A., Hellesylt, E., Trope, C.G., Reich, R., and Yisraeli, J.K. (2014). VICKZ2 protein expression in ovarian serous carcinoma effusions is associated with poor survival. Hum Pathol *45*, 1520-1528.

de Miguel, F.J., Sharma, R.D., Pajares, M.J., Montuenga, L.M., Rubio, A., and Pio, R. (2014). Identification of alternative splicing events regulated by the oncogenic factor SRSF1 in lung cancer. Cancer Res *74*, 1105-1115.

Dedes, K.J., Natrajan, R., Lambros, M.B., Geyer, F.C., Lopez-Garcia, M.A., Savage, K., Jones, R.L., and Reis-Filho, J.S. (2011). Down-regulation of the miRNA master regulators Drosha and Dicer is associated with specific subgroups of breast cancer. Eur J Cancer *47*, 138-150.

Degrauwe, N., Schlumpf, T.B., Janiszewska, M., Martin, P., Cauderay, A., Provero, P., Riggi, N., Suva, M.L., Paro, R., and Stamenkovic, I. (2016a). The RNA Binding Protein IMP2 Preserves Glioblastoma Stem Cells by Preventing let-7 Target Gene Silencing. Cell Rep *15*, 1634-1647.

Degrauwe, N., Suva, M.L., Janiszewska, M., Riggi, N., and Stamenkovic, I. (2016b). IMPs: an RNA-binding protein family that provides a link between stem cell maintenance in normal development and cancer. Genes Dev *30*, 2459-2474.

Delaunay, S., and Frye, M. (2019). RNA modifications regulating cell fate in cancer. Nat Cell Biol *21*, 552-559.

Denkert, C., Koch, I., von Keyserlingk, N., Noske, A., Niesporek, S., Dietel, M., and Weichert, W. (2006). Expression of the ELAV-like protein HuR in human colon cancer: association with tumor stage and cyclooxygenase-2. Mod Pathol *19*, 1261-1269.

Denkert, C., Weichert, W., Pest, S., Koch, I., Licht, D., Kobel, M., Reles, A., Sehouli, J., Dietel, M., and Hauptmann, S. (2004a). Overexpression of the embryonic-lethal abnormal vision-like protein HuR in ovarian carcinoma is a prognostic factor and is associated with increased cyclooxygenase 2 expression. Cancer Res *64*, 189-195.

Denkert, C., Weichert, W., Winzer, K.J., Muller, B.M., Noske, A., Niesporek, S., Kristiansen, G., Guski, H., Dietel, M., and Hauptmann, S. (2004b). Expression of the ELAV-like protein HuR is associated with higher tumor grade and increased cyclooxygenase-2 expression in human breast carcinoma. Clin Cancer Res *10*, 5580-5586.

Dews, M., Homayouni, A., Yu, D., Murphy, D., Sevignani, C., Wentzel, E., Furth, E.E., Lee, W.M., Enders, G.H., Mendell, J.T., et al. (2006). Augmentation of tumor angiogenesis by a Myc-activated microRNA cluster. Nat Genet *38*, 1060-1065.

Dhiman, G., Srivastava, N., Goyal, M., Rakha, E., Lothion-Roy, J., Mongan, N.P., Miftakhova, R.R., Khaiboullina, S.F., Rizvanov, A.A., and Baranwal, M. (2019). Metadherin: A Therapeutic Target in Multiple Cancers. Front Oncol *9*, 349.

Di Martino, M.T., Leone, E., Amodio, N., Foresta, U., Lionetti, M., Pitari, M.R., Cantafio, M.E., Gulla, A., Conforti, F., Morelli, E., et al. (2012). Synthetic miR-34a mimics as a novel therapeutic agent for multiple myeloma: in vitro and in vivo evidence. Clin Cancer Res *18*, 6260-6270.

Doyle, G.A., Betz, N.A., Leeds, P.F., Fleisig, A.J., Prokipcak, R.D., and Ross, J. (1998). The c-myc coding region determinant-binding protein: a member of a family of KH domain RNA-binding proteins. Nucleic Acids Res *26*, 5036-5044.

Dreyfuss, G., Kim, V.N., and Kataoka, N. (2002). Messenger-RNA-binding proteins and the messages they carry. Nat Rev Mol Cell Biol *3*, 195-205.

Dvinge, H., Kim, E., Abdel-Wahab, O., and Bradley, R.K. (2016). RNA splicing factors as oncoproteins and tumour suppressors. Nat Rev Cancer *16*, 413-430.

Dweep, H., Sticht, C., Pandey, P., and Gretz, N. (2011). miRWalk--database: prediction of possible miRNA binding sites by "walking" the genes of three genomes. J Biomed Inform *44*, 839-847.

Eichhorn, S.W., Guo, H., McGeary, S.E., Rodriguez-Mias, R.A., Shin, C., Baek, D., Hsu, S.H., Ghoshal, K., Villen, J., and Bartel, D.P. (2014). mRNA destabilization is the dominant effect of mammalian microRNAs by the time substantial repression ensues. Mol Cell *56*, 104-115.

Elcheva, I., Goswami, S., Noubissi, F.K., and Spiegelman, V.S. (2009). CRD-BP protects the coding region of betaTrCP1 mRNA from miR-183-mediated degradation. Mol Cell *35*, 240-246.

Elkhadragy, L., Chen, M., Miller, K., Yang, M.H., and Long, W. (2017). A regulatory BMI1/let-7i/ERK3 pathway controls the motility of head and neck cancer cells. Mol Oncol *11*, 194-207.

Elkon, R., Ugalde, A.P., and Agami, R. (2013). Alternative cleavage and polyadenylation: extent, regulation and function. Nat Rev Genet *14*, 496-506.

Ender, C., Krek, A., Friedlander, M.R., Beitzinger, M., Weinmann, L., Chen, W., Pfeffer, S., Rajewsky, N., and Meister, G. (2008). A human snoRNA with microRNA-like functions. Mol Cell *32*, 519-528.

REFERENCES

Ennajdaoui, H., Howard, J.M., Sterne-Weiler, T., Jahanbani, F., Coyne, D.J., Uren, P.J., Dargyte, M., Katzman, S., Draper, J.M., Wallace, A., *et al.* (2016). IGF2BP3 Modulates the Interaction of Invasion-Associated Transcripts with RISC. Cell Rep *15*, 1876-1883.

Esquela-Kerscher, A., and Slack, F.J. (2006). Oncomirs - microRNAs with a role in cancer. Nat Rev Cancer *6*, 259-269.

Farina, K.L., Huttelmaier, S., Musunuru, K., Darnell, R., and Singer, R.H. (2003). Two ZBP1 KH domains facilitate beta-actin mRNA localization, granule formation, and cytoskeletal attachment. J Cell Biol *160*, 77-87.

Fawzy, I.O., Hamza, M.T., Hosny, K.A., Esmat, G., El Tayebi, H.M., and Abdelaziz, A.I. (2015). miR-1275: A single microRNA that targets the three IGF2-mRNA-binding proteins hindering tumor growth in hepatocellular carcinoma. FEBS Lett *589*, 2257-2265.

Feng, Y.H., and Tsao, C.J. (2016). Emerging role of microRNA-21 in cancer. Biomed Rep *5*, 395-402.

Ferraro, A., Kontos, C.K., Boni, T., Bantounas, I., Siakouli, D., Kosmidou, V., Vlassi, M., Spyridakis, Y., Tsipras, I., Zografos, G., *et al.* (2014). Epigenetic regulation of miR-21 in colorectal cancer: ITGB4 as a novel miR-21 target and a three-gene network (miR-21-ITGBeta4-PDCD4) as predictor of metastatic tumor potential. Epigenetics *9*, 129-141.

Filippova, N., Yang, X., Ananthan, S., Sorochinsky, A., Hackney, J.R., Gentry, Z., Bae, S., King, P., and Nabors, L.B. (2017). Hu antigen R (HuR) multimerization contributes to glioma disease progression. J Biol Chem *292*, 16999-17010.

Fischer, D.C., Noack, K., Runnebaum, I.B., Watermann, D.O., Kieback, D.G., Stamm, S., and Stickeler, E. (2004). Expression of splicing factors in human ovarian cancer. Oncol Rep *11*, 1085-1090.

Font, J., and Mackay, J.P. (2010). Beyond DNA: zinc finger domains as RNA-binding modules. Methods Mol Biol *649*, 479-491.

Fox, R.G., Lytle, N.K., Jaquish, D.V., Park, F.D., Ito, T., Bajaj, J., Koechlein, C.S., Zimdahl, B., Yano, M., Kopp, J., *et al.* (2016). Image-based detection and targeting of therapy resistance in pancreatic adenocarcinoma. Nature *534*, 407-411.

Frankel, L.B., Christoffersen, N.R., Jacobsen, A., Lindow, M., Krogh, A., and Lund, A.H. (2008). Programmed cell death 4 (PDCD4) is an important functional target of the microRNA miR-21 in breast cancer cells. J Biol Chem *283*, 1026-1033.

Friedman, R.C., Farh, K.K., Burge, C.B., and Bartel, D.P. (2009). Most mammalian mRNAs are conserved targets of microRNAs. Genome Res *19*, 92-105.

Fujita, S., Ito, T., Mizutani, T., Minoguchi, S., Yamamichi, N., Sakurai, K., and Iba, H. (2008). miR-21 Gene expression triggered by AP-1 is sustained through a double-negative feedback mechanism. J Mol Biol *378*, 492-504.

Garneau, N.L., Wilusz, J., and Wilusz, C.J. (2007). The highways and byways of mRNA decay. Nat Rev Mol Cell Biol *8*, 113-126.

Gebauer, F., Schwarzl, T., Valcarcel, J., and Hentze, M.W. (2021). RNA-binding proteins in human genetic disease. Nat Rev Genet *22*, 185-198.

Gerstberger, S., Hafner, M., and Tuschl, T. (2014). A census of human RNA-binding proteins. Nat Rev Genet *15*, 829-845.

Glass, M., Misiak, D., Bley, N., Muller, S., Hagemann, S., Busch, B., Rausch, A., and Huttelmaier, S. (2021). IGF2BP1, a Conserved Regulator of RNA Turnover in Cancer. Front Mol Biosci *8*, 632219.

Gong, F., Ren, P., Zhang, Y., Jiang, J., and Zhang, H. (2016). MicroRNAs-491-5p suppresses cell proliferation and invasion by inhibiting IGF2BP1 in non-small cell lung cancer. Am J Transl Res *8*, 485-495.

Goswami, S., Tarapore, R.S., Poenitzsch Strong, A.M., TeSlaa, J.J., Grinblat, Y., Setaluri, V., and Spiegelman, V.S. (2015). MicroRNA-340-mediated degradation of microphthalmia-associated transcription factor (MITF) mRNA is inhibited by coding region determinant-binding protein (CRD-BP). J Biol Chem *290*, 384-395.

Grimson, A., Farh, K.K., Johnston, W.K., Garrett-Engele, P., Lim, L.P., and Bartel, D.P. (2007). MicroRNA targeting specificity in mammals: determinants beyond seed pairing. Mol Cell *27*, 91-105.

Gruber, A.J., and Zavolan, M. (2019). Alternative cleavage and polyadenylation in health and disease. Nat Rev Genet *20*, 599-614.

Gualdrini, F., Esnault, C., Horswell, S., Stewart, A., Matthews, N., and Treisman, R. (2016). SRF Co-factors Control the Balance between Cell Proliferation and Contractility. Mol Cell *64*, 1048-1061.

Guo, H., Ingolia, N.T., Weissman, J.S., and Bartel, D.P. (2010). Mammalian microRNAs predominantly act to decrease target mRNA levels. Nature *466*, 835-840.

Gutschner, T., Hammerle, M., Pazaitis, N., Bley, N., Fiskin, E., Uckelmann, H., Heim, A., Grobeta, M., Hofmann, N., Geffers, R., *et al.* (2014). Insulin-like growth factor 2 mRNA-binding protein 1 (IGF2BP1) is an important protumorigenic factor in hepatocellular carcinoma. Hepatology *59*, 1900-1911.

Ha, M., and Kim, V.N. (2014). Regulation of microRNA biogenesis. Nat Rev Mol Cell Biol *15*, 509-524.

Haase, J., Misiak, D., Bauer, M., Pazaitis, N., Braun, J., Potschke, R., Mensch, A., Bell, J.L., Dralle, H., Siebolts, U., *et al.* (2021). IGF2BP1 is the first positive marker for anaplastic thyroid carcinoma diagnosis. Mod Pathol *34*, 32-41.

Hafner, M., Landthaler, M., Burger, L., Khorshid, M., Hausser, J., Berninger, P., Rothballer, A., Ascano, M., Jr., Jungkamp, A.C., Munschauer, M., *et al.* (2010). Transcriptome-wide identification of RNA-binding protein and microRNA target sites by PAR-CLIP. Cell *141*, 129-141.

Hagan, J.P., Piskounova, E., and Gregory, R.I. (2009). Lin28 recruits the TUTase Zcchc11 to inhibit let-7 maturation in mouse embryonic stem cells. Nat Struct Mol Biol *16*, 1021-1025.

Hamilton, K.E., Noubissi, F.K., Katti, P.S., Hahn, C.M., Davey, S.R., Lundsmith, E.T., Klein-Szanto, A.J., Rhim, A.D., Spiegelman, V.S., and Rustgi, A.K. (2013). IMP1 promotes tumor growth, dissemination and a tumor-initiating cell phenotype in colorectal cancer cell xenografts. Carcinogenesis *34*, 2647-2654.

Hammerle, M., Gutschner, T., Uckelmann, H., Ozgur, S., Fiskin, E., Gross, M., Skawran, B., Geffers, R., Longerich, T., Breuhahn, K., *et al.* (2013). Posttranscriptional destabilization of the liver-specific long noncoding RNA HULC by the IGF2 mRNA-binding protein 1 (IGF2BP1). Hepatology *58*, 1703-1712.

Hanahan, D., and Weinberg, R.A. (2000). The hallmarks of cancer. Cell *100*, 57-70.

Hanahan, D., and Weinberg, R.A. (2011). Hallmarks of cancer: the next generation. Cell *144*, 646-674.

Hannus, M., Beitzinger, M., Engelmann, J.C., Weickert, M.T., Spang, R., Hannus, S., and Meister, G. (2014). siPools: highly complex but accurately defined siRNA pools eliminate off-target effects. Nucleic Acids Res *42*, 8049-8061.

Hansen, T.V., Hammer, N.A., Nielsen, J., Madsen, M., Dalbaeck, C., Wewer, U.M., Christiansen, J., and Nielsen, F.C. (2004). Dwarfism and impaired gut development in insulin-like growth factor II mRNA-binding protein 1-deficient mice. Mol Cell Biol *24*, 4448-4464.

Hatley, M.E., Patrick, D.M., Garcia, M.R., Richardson, J.A., Bassel-Duby, R., van Rooij, E., and Olson, E.N. (2010). Modulation of K-Ras-dependent lung tumorigenesis by MicroRNA-21. Cancer Cell *18*, 282-293.

Hentze, M.W., Castello, A., Schwarzl, T., and Preiss, T. (2018). A brave new world of RNA-binding proteins. Nat Rev Mol Cell Biol *19*, 327-341.

Heo, I., Joo, C., Kim, Y.K., Ha, M., Yoon, M.J., Cho, J., Yeom, K.H., Han, J., and Kim, V.N. (2009). TUT4 in concert with Lin28 suppresses microRNA biogenesis through pre-microRNA uridylation. Cell *138*, 696-708.

Heravi-Moussavi, A., Anglesio, M.S., Cheng, S.W., Senz, J., Yang, W., Prentice, L., Fejes, A.P., Chow, C., Tone, A., Kalloger, S.E., *et al.* (2012). Recurrent somatic DICER1 mutations in nonepithelial ovarian cancers. N Engl J Med *366*, 234-242.

Hernandez, J., Bechara, E., Schlesinger, D., Delgado, J., Serrano, L., and Valcarcel, J. (2016). Tumor suppressor properties of the splicing regulatory factor RBM10. RNA Biol *13*, 466-472.

Hosono, Y., Niknafs, Y.S., Prensner, J.R., Iyer, M.K., Dhanasekaran, S.M., Mehra, R., Pitchiaya, S., Tien, J., Escara-Wilke, J., Poliakov, A., *et al.* (2017). Oncogenic Role of THOR, a Conserved Cancer/Testis Long Non-coding RNA. Cell *171*, 1559-1572 e1520.

Hsu, K.F., Shen, M.R., Huang, Y.F., Cheng, Y.M., Lin, S.H., Chow, N.H., Cheng, S.W., Chou, C.Y., and Ho, C.L. (2015). Overexpression of the RNA-binding proteins Lin28B and IGF2BP3 (IMP3) is associated with chemoresistance and poor disease outcome in ovarian cancer. Br J Cancer *113*, 414-424.

Hsu, P.D., Scott, D.A., Weinstein, J.A., Ran, F.A., Konermann, S., Agarwala, V., Li, Y., Fine, E.J., Wu, X., Shalem, O., *et al.* (2013). DNA targeting specificity of RNA-guided Cas9 nucleases. Nat Biotechnol *31*, 827-832.

Huang, H., Weng, H., and Chen, J. (2020a). m(6)A Modification in Coding and Non-coding RNAs: Roles and Therapeutic Implications in Cancer. Cancer Cell *37*, 270-288.

Huang, H., Weng, H., Sun, W., Qin, X., Shi, H., Wu, H., Zhao, B.S., Mesquita, A., Liu, C., Yuan, C.L., *et al.* (2018a). Recognition of RNA N(6)-methyladenosine by IGF2BP proteins enhances mRNA stability and translation. Nat Cell Biol *20*, 285-295.

Huang, Q., Guo, H., Wang, S., Ma, Y., Chen, H., Li, H., Li, J., Li, X., Yang, F., Qiu, M., *et al.* (2020b). A novel circular RNA, circXPO1, promotes lung adenocarcinoma progression by interacting with IGF2BP1. Cell Death Dis *11*, 1031.

Huang, X., Zhang, H., Guo, X., Zhu, Z., Cai, H., and Kong, X. (2018b). Insulin-like growth factor 2 mRNA-binding protein 1 (IGF2BP1) in cancer. J Hematol Oncol *11*, 88.

Hughes, J.P., Rees, S., Kalindjian, S.B., and Philpott, K.L. (2011). Principles of early drug discovery. Br J Pharmacol *162*, 1239-1249.

Huntzinger, E., and Izaurralde, E. (2011). Gene silencing by microRNAs: contributions of translational repression and mRNA decay. Nat Rev Genet *12*, 99-110.

REFERENCES

Huttelmaier, S., Zenklusen, D., Lederer, M., Dictenberg, J., Lorenz, M., Meng, X., Bassell, G.J., Condeelis, J., and Singer, R.H. (2005). Spatial regulation of beta-actin translation by Src-dependent phosphorylation of ZBP1. Nature *438*, 512-515.

Ipsaro, J.J., and Joshua-Tor, L. (2015). From guide to target: molecular insights into eukaryotic RNA-interference machinery. Nat Struct Mol Biol *22*, 20-28.

Izaguirre, D.I., Zhu, W., Hai, T., Cheung, H.C., Krahe, R., and Cote, G.J. (2012). PTBP1-dependent regulation of USP5 alternative RNA splicing plays a role in glioblastoma tumorigenesis. Mol Carcinog *51*, 895-906.

Jiang, T., Li, M., Li, Q., Guo, Z., Sun, X., Zhang, X., Liu, Y., Yao, W., and Xiao, P. (2017). MicroRNA-98-5p Inhibits Cell Proliferation and Induces Cell Apoptosis in Hepatocellular Carcinoma via Targeting IGF2BP1. Oncol Res *25*, 1117-1127.

Jo, M.H., Shin, S., Jung, S.R., Kim, E., Song, J.J., and Hohng, S. (2015). Human Argonaute 2 Has Diverse Reaction Pathways on Target RNAs. Mol Cell *59*, 117-124.

Johnson, S.M., Grosshans, H., Shingara, J., Byrom, M., Jarvis, R., Cheng, A., Labourier, E., Reinert, K.L., Brown, D., and Slack, F.J. (2005). RAS is regulated by the let-7 microRNA family. Cell *120*, 635-647.

Jonas, S., and Izaurralde, E. (2015). Towards a molecular understanding of microRNA-mediated gene silencing. Nat Rev Genet *16*, 421-433.

Jonson, L., Christiansen, J., Hansen, T.V.O., Vikesa, J., Yamamoto, Y., and Nielsen, F.C. (2014). IMP3 RNP safe houses prevent miRNA-directed HMGA2 mRNA decay in cancer and development. Cell Rep *7*, 539-551.

Jonson, L., Vikesaa, J., Krogh, A., Nielsen, L.K., Hansen, T., Borup, R., Johnsen, A.H., Christiansen, J., and Nielsen, F.C. (2007). Molecular composition of IMP1 ribonucleoprotein granules. Mol Cell Proteomics *6*, 798-811.

Jurica, M.S., and Moore, M.J. (2003). Pre-mRNA splicing: awash in a sea of proteins. Mol Cell *12*, 5-14.

Kang, D., Lee, Y., and Lee, J.S. (2020). RNA-Binding Proteins in Cancer: Functional and Therapeutic Perspectives. Cancers (Basel) *12*.

Karni, R., de Stanchina, E., Lowe, S.W., Sinha, R., Mu, D., and Krainer, A.R. (2007). The gene encoding the splicing factor SF2/ASF is a proto-oncogene. Nat Struct Mol Biol *14*, 185-193.

Karube, Y., Tanaka, H., Osada, H., Tomida, S., Tatematsu, Y., Yanagisawa, K., Yatabe, Y., Takamizawa, J., Miyoshi, S., Mitsudomi, T., *et al.* (2005). Reduced expression of Dicer associated with poor prognosis in lung cancer patients. Cancer Sci *96*, 111-115.

Kasinski, A.L., and Slack, F.J. (2011). Epigenetics and genetics. MicroRNAs en route to the clinic: progress in validating and targeting microRNAs for cancer therapy. Nat Rev Cancer *11*, 849-864.

Kato, T., Hayama, S., Yamabuki, T., Ishikawa, N., Miyamoto, M., Ito, T., Tsuchiya, E., Kondo, S., Nakamura, Y., and Daigo, Y. (2007). Increased expression of insulin-like growth factor-II messenger RNA-binding protein 1 is associated with tumor progression in patients with lung cancer. Clin Cancer Res *13*, 434-442.

Kaur, K., Wu, X., Fields, J.K., Johnson, D.K., Lan, L., Pratt, M., Somoza, A.D., Wang, C.C.C., Karanicolas, J., Oakley, B.R., *et al.* (2017). The fungal natural product azaphilone-9 binds to HuR and inhibits HuR-RNA interaction in vitro. PLoS One *12*, e0175471.

Kent, L.N., and Leone, G. (2019). The broken cycle: E2F dysfunction in cancer. Nat Rev Cancer *19*, 326-338.

Khabar, K.S. (2005). The AU-rich transcriptome: more than interferons and cytokines, and its role in disease. J Interferon Cytokine Res *25*, 1-10.

Kim, V.N. (2005). MicroRNA biogenesis: coordinated cropping and dicing. Nat Rev Mol Cell Biol *6*, 376-385.

Kim, Y.K., Kim, B., and Kim, V.N. (2016). Re-evaluation of the roles of DROSHA, Export in 5, and DICER in microRNA biogenesis. Proc Natl Acad Sci U S A *113*, E1881-1889.

Kobel, M., Weidensdorfer, D., Reinke, C., Lederer, M., Schmitt, W.D., Zeng, K., Thomssen, C., Hauptmann, S., and Huttelmaier, S. (2007). Expression of the RNA-binding protein IMP1 correlates with poor prognosis in ovarian carcinoma. Oncogene *26*, 7584-7589.

Kobel, M., Xu, H., Bourne, P.A., Spaulding, B.O., Shih Ie, M., Mao, T.L., Soslow, R.A., Ewanowich, C.A., Kalloger, S.E., Mehl, E., *et al.* (2009). IGF2BP3 (IMP3) expression is a marker of unfavorable prognosis in ovarian carcinoma of clear cell subtype. Mod Pathol *22*, 469-475.

Kohn, M., Lederer, M., Wachter, K., and Huttelmaier, S. (2010). Near-infrared (NIR) dye-labeled RNAs identify binding of ZBP1 to the noncoding Y3-RNA. RNA *16*, 1420-1428.

Konig, J., Zarnack, K., Rot, G., Curk, T., Kayikci, M., Zupan, B., Turner, D.J., Luscombe, N.M., and Ule, J. (2011). iCLIP--transcriptome-wide mapping of protein-RNA interactions with individual nucleotide resolution. J Vis Exp.

Koralov, S.B., Muljo, S.A., Galler, G.R., Krek, A., Chakraborty, T., Kanellopoulou, C., Jensen, K., Cobb, B.S., Merkenschlager, M., Rajewsky, N., *et al.* (2008). Dicer ablation affects antibody diversity and cell survival in the B lymphocyte lineage. Cell *132*, 860-874.

Kozomara, A., Birgaoanu, M., and Griffiths-Jones, S. (2019). miRBase: from microRNA sequences to function. Nucleic Acids Res *47*, D155-D162.

Krichevsky, A.M., and Gabriely, G. (2009). miR-21: a small multi-faceted RNA. J Cell Mol Med *13*, 39-53.

Laderian, B., and Fojo, T. (2017). CDK4/6 Inhibition as a therapeutic strategy in breast cancer: palbociclib, ribociclib, and abemaciclib. Semin Oncol *44*, 395-403.

Lagos-Quintana, M., Rauhut, R., Lendeckel, W., and Tuschl, T. (2001). Identification of novel genes coding for small expressed RNAs. Science *294*, 853-858.

Lal, P., Cerofolini, L., D'Agostino, V.G., Zucal, C., Fuccio, C., Bonomo, I., Dassi, E., Giuntini, S., Di Maio, D., Vishwakarma, V., *et al.* (2017). Regulation of HuR structure and function by dihydrotanshinone-I. Nucleic Acids Res *45*, 9514-9527.

Lang, M., Berry, D., Passecker, K., Mesteri, I., Bhuju, S., Ebner, F., Sedlyarov, V., Evstatiev, R., Dammann, K., Loy, A., *et al.* (2017). HuR Small-Molecule Inhibitor Elicits Differential Effects in Adenomatosis Polyposis and Colorectal Carcinogenesis. Cancer Res *77*, 2424-2438.

Lederer, M., Bley, N., Schleifer, C., and Huttelmaier, S. (2014). The role of the oncofetal IGF2 mRNA-binding protein 3 (IGF2BP3) in cancer. Semin Cancer Biol *29*, 3-12.

Lee, Y.S., and Dutta, A. (2007). The tumor suppressor microRNA let-7 represses the HMGA2 oncogene. Genes Dev *21*, 1025-1030.

Lemm, I., and Ross, J. (2002). Regulation of c-myc mRNA decay by translational pausing in a coding region instability determinant. Mol Cell Biol *22*, 3959-3969.

Lewis, B.P., Burge, C.B., and Bartel, D.P. (2005). Conserved seed pairing, often flanked by adenosines, indicates that thousands of human genes are microRNA targets. Cell *120*, 15-20.

Li, L., Yuan, L., Luo, J., Gao, J., Guo, J., and Xie, X. (2013). MiR-34a inhibits proliferation and migration of breast cancer through down-regulation of Bcl-2 and SIRT1. Clin Exp Med *13*, 109-117.

Li, T., Hu, P.S., Zuo, Z., Lin, J.F., Li, X., Wu, Q.N., Chen, Z.H., Zeng, Z.L., Wang, F., Zheng, J., *et al.* (2019). METTL3 facilitates tumor progression via an m(6)A-IGF2BP2-dependent mechanism in colorectal carcinoma. Mol Cancer *18*, 112.

Li, T., Wan, Y., Su, Z., Li, J., Han, M., and Zhou, C. (2020). SRF Potentiates Colon Cancer Metastasis and Progression in a microRNA-214/PTK6-Dependent Manner. Cancer Manag Res *12*, 6477-6491.

Li, Z., Weng, H., Su, R., Weng, X., Zuo, Z., Li, C., Huang, H., Nachtergaele, S., Dong, L., Hu, C., *et al.* (2017). FTO Plays an Oncogenic Role in Acute Myeloid Leukemia as a N(6)-Methyladenosine RNA Demethylase. Cancer Cell *31*, 127-141.

Liao, B., Hu, Y., Herrick, D.J., and Brewer, G. (2005). The RNA-binding protein IMP-3 is a translational activator of insulin-like growth factor II leader-3 mRNA during proliferation of human K562 leukemia cells. J Biol Chem *280*, 18517-18524.

Lin, S., Choe, J., Du, P., Triboulet, R., and Gregory, R.I. (2016). The m(6)A Methyltransferase METTL3 Promotes Translation in Human Cancer Cells. Mol Cell *62*, 335-345.

Lin, S., and Gregory, R.I. (2015). MicroRNA biogenesis pathways in cancer. Nat Rev Cancer *15*, 321-333.

Linder, P., and Jankowsky, E. (2011). From unwinding to clamping - the DEAD box RNA helicase family. Nat Rev Mol Cell Biol *12*, 505-516.

Liu, C., Kelnar, K., Liu, B., Chen, X., Calhoun-Davis, T., Li, H., Patrawala, L., Yan, H., Jeter, C., Honorio, S., *et al.* (2011). The microRNA miR-34a inhibits prostate cancer stem cells and metastasis by directly repressing CD44. Nat Med *17*, 211-215.

Liu, J., Eckert, M.A., Harada, B.T., Liu, S.M., Lu, Z., Yu, K., Tienda, S.M., Chryplewicz, A., Zhu, A.C., Yang, Y., *et al.* (2018). m(6)A mRNA methylation regulates AKT activity to promote the proliferation and tumorigenicity of endometrial cancer. Nat Cell Biol *20*, 1074-1083.

Liu, L., Michowski, W., Kolodziejczyk, A., and Sicinski, P. (2019). The cell cycle in stem cell proliferation, pluripotency and differentiation. Nat Cell Biol *21*, 1060-1067.

Lukong, K.E., Chang, K.W., Khandjian, E.W., and Richard, S. (2008). RNA-binding proteins in human genetic disease. Trends Genet *24*, 416-425.

Luo, Y., Na, Z., and Slavoff, S.A. (2018). P-Bodies: Composition, Properties, and Functions. Biochemistry *57*, 2424-2431.

REFERENCES

Mahaira, L.G., Katsara, O., Pappou, E., Iliopoulou, E.G., Fortis, S., Antsaklis, A., Fotinopoulos, P., Baxevanis, C.N., Papamichail, M., and Perez, S.A. (2014). IGF2BP1 expression in human mesenchymal stem cells significantly affects their proliferation and is under the epigenetic control of TET1/2 demethylases. Stem Cells Dev *23*, 2501-2512.

Mahapatra, L., Andruska, N., Mao, C., Le, J., and Shapiro, D.J. (2017). A Novel IMP1 Inhibitor, BTYNB, Targets c-Myc and Inhibits Melanoma and Ovarian Cancer Cell Proliferation. Transl Oncol *10*, 818-827.

Maizels, Y., Oberman, F., Miloslavski, R., Ginzach, N., Berman, M., and Yisraeli, J.K. (2015). Localization of cofilin mRNA to the leading edge of migrating cells promotes directed cell migration. J Cell Sci *128*, 1922-1933.

Mancarella, C., and Scotlandi, K. (2019). IGF2BP3 From Physiology to Cancer: Novel Discoveries, Unsolved Issues, and Future Perspectives. Front Cell Dev Biol *7*, 363.

Mathelier, A., and Carbone, A. (2013). Large scale chromosomal mapping of human microRNA structural clusters. Nucleic Acids Res *41*, 4392-4408.

Medjkane, S., Perez-Sanchez, C., Gaggioli, C., Sahai, E., and Treisman, R. (2009). Myocardin-related transcription factors and SRF are required for cytoskeletal dynamics and experimental metastasis. Nat Cell Biol *11*, 257-268.

Meisner, N.C., Hintersteiner, M., Mueller, K., Bauer, R., Seifert, J.M., Naegeli, H.U., Ottl, J., Oberer, L., Guenat, C., Moss, S., *et al.* (2007). Identification and mechanistic characterization of low-molecular-weight inhibitors for HuR. Nat Chem Biol *3*, 508-515.

Melo, S.A., Moutinho, C., Ropero, S., Calin, G.A., Rossi, S., Spizzo, R., Fernandez, A.F., Davalos, V., Villanueva, A., Montoya, G., *et al.* (2010). A genetic defect in exportin-5 traps precursor microRNAs in the nucleus of cancer cells. Cancer Cell *18*, 303-315.

Meng, F., Henson, R., Wehbe-Janek, H., Ghoshal, K., Jacob, S.T., and Patel, T. (2007). MicroRNA-21 regulates expression of the PTEN tumor suppressor gene in human hepatocellular cancer. Gastroenterology *133*, 647-658.

Merritt, W.M., Lin, Y.G., Han, L.Y., Kamat, A.A., Spannuth, W.A., Schmandt, R., Urbauer, D., Pennacchio, L.A., Cheng, J.F., Nick, A.M., *et al.* (2008). Dicer, Drosha, and outcomes in patients with ovarian cancer. N Engl J Med *359*, 2641-2650.

Meyer, K.D., Saletore, Y., Zumbo, P., Elemento, O., Mason, C.E., and Jaffrey, S.R. (2012). Comprehensive analysis of mRNA methylation reveals enrichment in 3' UTRs and near stop codons. Cell *149*, 1635-1646.

Miano, J.M. (2010). Role of serum response factor in the pathogenesis of disease. Lab Invest *90*, 1274-1284.

Miles, W.O., Tschop, K., Herr, A., Ji, J.Y., and Dyson, N.J. (2012). Pumilio facilitates miRNA regulation of the E2F3 oncogene. Genes Dev *26*, 356-368.

Misso, G., Di Martino, M.T., De Rosa, G., Farooqi, A.A., Lombardi, A., Campani, V., Zarone, M.R., Gulla, A., Tagliaferri, P., Tassone, P., *et al.* (2014). Mir-34: a new weapon against cancer? Mol Ther Nucleic Acids *3*, e194.

Mitchell, S.F., and Parker, R. (2014). Principles and properties of eukaryotic mRNPs. Mol Cell *54*, 547-558.

Mogilyansky, E., and Rigoutsos, I. (2013). The miR-17/92 cluster: a comprehensive update on its genomics, genetics, functions and increasingly important and numerous roles in health and disease. Cell Death Differ *20*, 1603-1614.

Mohibi, S., Chen, X., and Zhang, J. (2019). Cancer the'RBP'eutics-RNA-binding proteins as therapeutic targets for cancer. Pharmacol Ther *203*, 107390.

Mongroo, P.S., Noubissi, F.K., Cuatrecasas, M., Kalabis, J., King, C.E., Johnstone, C.N., Bowser, M.J., Castells, A., Spiegelman, V.S., and Rustgi, A.K. (2011). IMP-1 displays cross-talk with K-Ras and modulates colon cancer cell survival through the novel proapoptotic protein CYFIP2. Cancer Res *71*, 2172-2182.

Mrena, J., Wiksten, J.P., Thiel, A., Kokkola, A., Pohjola, L., Lundin, J., Nordling, S., Ristimaki, A., and Haglund, C. (2005). Cyclooxygenase-2 is an independent prognostic factor in gastric cancer and its expression is regulated by the messenger RNA stability factor HuR. Clin Cancer Res *11*, 7362-7368.

Mueller-Pillasch, F., Lacher, U., Wallrapp, C., Micha, A., Zimmerhackl, F., Hameister, H., Varga, G., Friess, H., Buchler, M., Beger, H.G., *et al.* (1997). Cloning of a gene highly overexpressed in cancer coding for a novel KH-domain containing protein. Oncogene *14*, 2729-2733.

Muller, S., Bley, N., Busch, B., Glass, M., Lederer, M., Misiak, C., Fuchs, T., Wedler, A., Haase, J., Bertoldo, J.B., *et al.* (2020). The oncofetal RNA-binding protein IGF2BP1 is a druggable, post-transcriptional super-enhancer of E2F-driven gene expression in cancer. Nucleic Acids Res *48*, 8576-8590.

Muller, S., Bley, N., Glass, M., Busch, B., Rousseau, V., Misiak, D., Fuchs, T., Lederer, M., and Huttelmaier, S. (2018). IGF2BP1 enhances an aggressive tumor cell phenotype by impairing miRNA-directed downregulation of oncogenic factors. Nucleic Acids Res *46*, 6285-6303.

Muller, S., Glass, M., Singh, A.K., Haase, J., Bley, N., Fuchs, T., Lederer, M., Dahl, A., Huang, H., Chen, J., *et al.* (2019). IGF2BP1 promotes SRF-dependent transcription in cancer in a m6A- and miRNA-dependent manner. Nucleic Acids Res *47*, 375-390.

Nam, E.J., Yoon, H., Kim, S.W., Kim, H., Kim, Y.T., Kim, J.H., Kim, J.W., and Kim, S. (2008). MicroRNA expression profiles in serous ovarian carcinoma. Clin Cancer Res *14*, 2690-2695.

Neganova, I., Zhang, X., Atkinson, S., and Lako, M. (2009). Expression and functional analysis of G1 to S regulatory components reveals an important role for CDK2 in cell cycle regulation in human embryonic stem cells. Oncogene *28*, 20-30.

Nicoloso, M.S., Spizzo, R., Shimizu, M., Rossi, S., and Calin, G.A. (2009). MicroRNAs--the micro steering wheel of tumour metastases. Nat Rev Cancer *9*, 293-302.

Nielsen, F.C., Nielsen, J., Kristensen, M.A., Koch, G., and Christiansen, J. (2002). Cytoplasmic trafficking of IGF-II mRNA-binding protein by conserved KH domains. J Cell Sci *115*, 2087-2097.

Nielsen, J., Christiansen, J., Lykke-Andersen, J., Johnsen, A.H., Wewer, U.M., and Nielsen, F.C. (1999). A family of insulin-like growth factor II mRNA-binding proteins represses translation in late development. Mol Cell Biol *19*, 1262-1270.

Nielsen, J., Kristensen, M.A., Willemoes, M., Nielsen, F.C., and Christiansen, J. (2004). Sequential dimerization of human zipcode-binding protein IMP1 on RNA: a cooperative mechanism providing RNP stability. Nucleic Acids Res *32*, 4368-4376.

Nilsen, T.W., and Graveley, B.R. (2010). Expansion of the eukaryotic proteome by alternative splicing. Nature *463*, 457-463.

Nishino, J., Kim, S., Zhu, Y., Zhu, H., and Morrison, S.J. (2013). A network of heterochronic genes including Imp1 regulates temporal changes in stem cell properties. Elife *2*, e00924.

Niu, J., Zhao, X., Liu, Q., and Yang, J. (2017). Knockdown of MSI1 inhibited the cell proliferation of human osteosarcoma cells by targeting p21 and p27. Oncol Lett *14*, 5271-5278.

Noubissi, F.K., Elcheva, I., Bhatia, N., Shakoori, A., Ougolkov, A., Liu, J., Minamoto, T., Ross, J., Fuchs, S.Y., and Spiegelman, V.S. (2006). CRD-BP mediates stabilization of betaTrCP1 and c-myc mRNA in response to beta-catenin signalling. Nature *441*, 898-901.

Noubissi, F.K., Goswami, S., Sanek, N.A., Kawakami, K., Minamoto, T., Moser, A., Grinblat, Y., and Spiegelman, V.S. (2009). Wnt signaling stimulates transcriptional outcome of the Hedgehog pathway by stabilizing GLI1 mRNA. Cancer Res *69*, 8572-8578.

Noubissi, F.K., Nikiforov, M.A., Colburn, N., and Spiegelman, V.S. (2010). Transcriptional Regulation of CRD-BP by c-myc: Implications for c-myc Functions. Genes Cancer *1*, 1074-1082.

Oleynikov, Y., and Singer, R.H. (2003). Real-time visualization of ZBP1 association with beta-actin mRNA during transcription and localization. Curr Biol *13*, 199-207.

Pardoll, D.M. (2012). The blockade of immune checkpoints in cancer immunotherapy. Nat Rev Cancer *12*, 252-264.

Park, S.M., Gonen, M., Vu, L., Minuesa, G., Tivnan, P., Barlowe, T.S., Taggart, J., Lu, Y., Deering, R.P., Hacohen, N., *et al.* (2015). Musashi2 sustains the mixed-lineage leukemia-driven stem cell regulatory program. J Clin Invest *125*, 1286-1298.

Park, S.M., Shell, S., Radjabi, A.R., Schickel, R., Feig, C., Boyerinas, B., Dinulescu, D.M., Lengyel, E., and Peter, M.E. (2007). Let-7 prevents early cancer progression by suppressing expression of the embryonic gene HMGA2. Cell Cycle *6*, 2585-2590.

Paronetto, M.P., Cappellari, M., Busa, R., Pedrotti, S., Vitali, R., Comstock, C., Hyslop, T., Knudsen, K.E., and Sette, C. (2010). Alternative splicing of the cyclin D1 proto-oncogene is regulated by the RNA-binding protein Sam68. Cancer Res *70*, 229-239.

Patel, V.L., Mitra, S., Harris, R., Buxbaum, A.R., Lionnet, T., Brenowitz, M., Girvin, M., Levy, M., Almo, S.C., Singer, R.H., *et al.* (2012). Spatial arrangement of an RNA zipcode identifies mRNAs under post-transcriptional control. Genes Dev *26*, 43-53.

Peng, Y., and Croce, C.M. (2016). The role of MicroRNAs in human cancer. Signal Transduct Target Ther *1*, 15004.

Pereira, B., Billaud, M., and Almeida, R. (2017). RNA-Binding Proteins in Cancer: Old Players and New Actors. Trends Cancer *3*, 506-528.

Perez-Guijarro, E., Karras, P., Cifdaloz, M., Martinez-Herranz, R., Canon, E., Grana, O., Horcajada-Reales, C., Alonso-Curbelo, D., Calvo, T.G., Gomez-Lopez, G., *et al.* (2016). Lineage-specific roles of the cytoplasmic polyadenylation factor CPEB4 in the regulation of melanoma drivers. Nat Commun *7*, 13418.

Perycz, M., Urbanska, A.S., Krawczyk, P.S., Parobczak, K., and Jaworski, J. (2011). Zipcode binding protein 1 regulates the development of dendritic arbors in hippocampal neurons. J Neurosci *31*, 5271-5285.

REFERENCES

Piskounova, E., Viswanathan, S.R., Janas, M., LaPierre, R.J., Daley, G.Q., Sliz, P., and Gregory, R.I. (2008). Determinants of microRNA processing inhibition by the developmentally regulated RNA-binding protein Lin28. J Biol Chem *283*, 21310-21314.

Plaschka, C., Lin, P.C., and Nagai, K. (2017). Structure of a pre-catalytic spliceosome. Nature *546*, 617-621.

Proudfoot, N.J. (2011). Ending the message: poly(A) signals then and now. Genes Dev *25*, 1770-1782.

Pu, J., Wang, J., Qin, Z., Wang, A., Zhang, Y., Wu, X., Wu, Y., Li, W., Xu, Z., Lu, Y., *et al.* (2020). IGF2BP2 Promotes Liver Cancer Growth Through an m6A-FEN1-Dependent Mechanism. Front Oncol *10*, 578816.

Qin, X., Sun, L., and Wang, J. (2017). Restoration of microRNA-708 sensitizes ovarian cancer cells to cisplatin via IGF2BP1/Akt pathway. Cell Biol Int *41*, 1110-1118.

Qu, Y., Pan, S., Kang, M., Dong, R., and Zhao, J. (2016). MicroRNA-150 functions as a tumor suppressor in osteosarcoma by targeting IGF2BP1. Tumour Biol *37*, 5275-5284.

Ran, F.A., Hsu, P.D., Lin, C.Y., Gootenberg, J.S., Konermann, S., Trevino, A.E., Scott, D.A., Inoue, A., Matoba, S., Zhang, Y., *et al.* (2013). Double nicking by RNA-guided CRISPR Cas9 for enhanced genome editing specificity. Cell *154*, 1380-1389.

Rebucci, M., Sermeus, A., Leonard, E., Delaive, E., Dieu, M., Fransolet, M., Arnould, T., and Michiels, C. (2015). miRNA-196b inhibits cell proliferation and induces apoptosis in HepG2 cells by targeting IGF2BP1. Mol Cancer *14*, 79.

Rokavec, M., Oner, M.G., Li, H., Jackstadt, R., Jiang, L., Lodygin, D., Kaller, M., Horst, D., Ziegler, P.K., Schwitalla, S., *et al.* (2014). IL-6R/STAT3/miR-34a feedback loop promotes EMT-mediated colorectal cancer invasion and metastasis. J Clin Invest *124*, 1853-1867.

Ross, A.F., Oleynikov, Y., Kislauskis, E.H., Taneja, K.L., and Singer, R.H. (1997). Characterization of a beta-actin mRNA zipcode-binding protein. Mol Cell Biol *17*, 2158-2165.

Roundtree, I.A., Evans, M.E., Pan, T., and He, C. (2017). Dynamic RNA Modifications in Gene Expression Regulation. Cell *169*, 1187-1200.

Roush, S., and Slack, F.J. (2008). The let-7 family of microRNAs. Trends Cell Biol *18*, 505-516.

Runge, S., Nielsen, F.C., Nielsen, J., Lykke-Andersen, J., Wewer, U.M., and Christiansen, J. (2000). H19 RNA binds four molecules of insulin-like growth factor II mRNA-binding protein. J Biol Chem *275*, 29562-29569.

Rupaimoole, R., and Slack, F.J. (2017). MicroRNA therapeutics: towards a new era for the management of cancer and other diseases. Nat Rev Drug Discov *16*, 203-222.

Sampson, V.B., Rong, N.H., Han, J., Yang, Q., Aris, V., Soteropoulos, P., Petrelli, N.J., Dunn, S.P., and Krueger, L.J. (2007). MicroRNA let-7a down-regulates MYC and reverts MYC-induced growth in Burkitt lymphoma cells. Cancer Res *67*, 9762-9770.

Schneider, T., Hung, L.H., Aziz, M., Wilmen, A., Thaum, S., Wagner, J., Janowski, R., Muller, S., Schreiner, S., Friedhoff, P., *et al.* (2019). Combinatorial recognition of clustered RNA elements by the multidomain RNA-binding protein IMP3. Nat Commun *10*, 2266.

Sempere, L.F., Christensen, M., Silahtaroglu, A., Bak, M., Heath, C.V., Schwartz, G., Wells, W., Kauppinen, S., and Cole, C.N. (2007). Altered MicroRNA expression confined to specific epithelial cell subpopulations in breast cancer. Cancer Res *67*, 11612-11620.

Sempere, L.F., Freemantle, S., Pitha-Rowe, I., Moss, E., Dmitrovsky, E., and Ambros, V. (2004). Expression profiling of mammalian microRNAs uncovers a subset of brain-expressed microRNAs with possible roles in murine and human neuronal differentiation. Genome Biol *5*, R13.

Shell, S., Park, S.M., Radjabi, A.R., Schickel, R., Kistner, E.O., Jewell, D.A., Feig, C., Lengyel, E., and Peter, M.E. (2007). Let-7 expression defines two differentiation stages of cancer. Proc Natl Acad Sci U S A *104*, 11400-11405.

Shen, J., Xia, W., Khotskaya, Y.B., Huo, L., Nakanishi, K., Lim, S.O., Du, Y., Wang, Y., Chang, W.C., Chen, C.H., *et al.* (2013). EGFR modulates microRNA maturation in response to hypoxia through phosphorylation of AGO2. Nature *497*, 383-387.

Shi, R., Yu, X., Wang, Y., Sun, J., Sun, Q., Xia, W., Dong, G., Wang, A., Gao, Z., Jiang, F., *et al.* (2017). Expression profile, clinical significance, and biological function of insulin-like growth factor 2 messenger RNA-binding proteins in non-small cell lung cancer. Tumour Biol *39*, 1010428317695928.

Shuman, S. (2002). What messenger RNA capping tells us about eukaryotic evolution. Nat Rev Mol Cell Biol *3*, 619-625.

Singh, G., Pratt, G., Yeo, G.W., and Moore, M.J. (2015). The Clothes Make the mRNA: Past and Present Trends in mRNP Fashion. Annu Rev Biochem *84*, 325-354.

Song, T., Zheng, Y., Wang, Y., Katz, Z., Liu, X., Chen, S., Singer, R.H., and Gu, W. (2015). Specific interaction of KIF11 with ZBP1 regulates the transport of beta-actin mRNA and cell motility. J Cell Sci *128*, 1001-1010.

Sparanese, D., and Lee, C.H. (2007). CRD-BP shields c-myc and MDR-1 RNA from endonucleolytic attack by a mammalian endoribonuclease. Nucleic Acids Res *35*, 1209-1221.

Srikantan, S., Abdelmohsen, K., Lee, E.K., Tominaga, K., Subaran, S.S., Kuwano, Y., Kulshrestha, R., Panchakshari, R., Kim, H.H., Yang, X., *et al.* (2011). Translational control of TOP2A influences doxorubicin efficacy. Mol Cell Biol *31*, 3790-3801.

Stohr, N., Kohn, M., Lederer, M., Glass, M., Reinke, C., Singer, R.H., and Huttelmaier, S. (2012). IGF2BP1 promotes cell migration by regulating MK5 and PTEN signaling. Genes Dev *26*, 176-189.

Su, Y., Xiong, J., Hu, J., Wei, X., Zhang, X., and Rao, L. (2016). MicroRNA-140-5p targets insulin like growth factor 2 mRNA binding protein 1 (IGF2BP1) to suppress cervical cancer growth and metastasis. Oncotarget *7*, 68397-68411.

Sun, L., Fazal, F.M., Li, P., Broughton, J.P., Lee, B., Tang, L., Huang, W., Kool, E.T., Chang, H.Y., and Zhang, Q.C. (2019). RNA structure maps across mammalian cellular compartments. Nat Struct Mol Biol *26*, 322-330.

Tessier, C.R., Doyle, G.A., Clark, B.A., Pitot, H.C., and Ross, J. (2004). Mammary tumor induction in transgenic mice expressing an RNA-binding protein. Cancer Res *64*, 209-214.

Torres, A., Torres, K., Paszkowski, T., Jodlowska-Jedrych, B., Radomanski, T., Ksiazek, A., and Maciejewski, R. (2011). Major regulators of microRNAs biogenesis Dicer and Drosha are down-regulated in endometrial cancer. Tumour Biol *32*, 769-776.

Truitt, M.L., and Ruggero, D. (2016). New frontiers in translational control of the cancer genome. Nat Rev Cancer *16*, 288-304.

Ustianenko, D., Hrossova, D., Potesil, D., Chalupnikova, K., Hrazdilova, K., Pachernik, J., Cetkovska, K., Uldrijan, S., Zdrahal, Z., and Vanacova, S. (2013). Mammalian DIS3L2 exoribonuclease targets the uridylated precursors of let-7 miRNAs. RNA *19*, 1632-1638.

Valverde, R., Edwards, L., and Regan, L. (2008). Structure and function of KH domains. FEBS J *275*, 2712-2726.

van Kouwenhove, M., Kedde, M., and Agami, R. (2011). MicroRNA regulation by RNA-binding proteins and its implications for cancer. Nat Rev Cancer *11*, 644-656.

Van Nostrand, E.L., Pratt, G.A., Shishkin, A.A., Gelboin-Burkhart, C., Fang, M.Y., Sundararaman, B., Blue, S.M., Nguyen, T.B., Surka, C., Elkins, K., *et al.* (2016). Robust transcriptome-wide discovery of RNA-binding protein binding sites with enhanced CLIP (eCLIP). Nat Methods *13*, 508-514.

Vanharanta, S., Marney, C.B., Shu, W., Valiente, M., Zou, Y., Mele, A., Darnell, R.B., and Massague, J. (2014). Loss of the multifunctional RNA-binding protein RBM47 as a source of selectable metastatic traits in breast cancer. Elife *3*.

Ventura, A., Young, A.G., Winslow, M.M., Lintault, L., Meissner, A., Erkeland, S.J., Newman, J., Bronson, R.T., Crowley, D., Stone, J.R., *et al.* (2008). Targeted deletion reveals essential and overlapping functions of the miR-17 through 92 family of miRNA clusters. Cell *132*, 875-886.

Vikesaa, J., Hansen, T.V., Jonson, L., Borup, R., Wewer, U.M., Christiansen, J., and Nielsen, F.C. (2006). RNA-binding IMPs promote cell adhesion and invadopodia formation. EMBO J *25*, 1456-1468.

Viswanathan, S.R., Powers, J.T., Einhorn, W., Hoshida, Y., Ng, T.L., Toffanin, S., O'Sullivan, M., Lu, J., Phillips, L.A., Lockhart, V.L., *et al.* (2009). Lin28 promotes transformation and is associated with advanced human malignancies. Nat Genet *41*, 843-848.

Vo, D.T., Abdelmohsen, K., Martindale, J.L., Qiao, M., Tominaga, K., Burton, T.L., Gelfond, J.A., Brenner, A.J., Patel, V., Trageser, D., *et al.* (2012). The oncogenic RNA-binding protein Musashi1 is regulated by HuR via mRNA translation and stability in glioblastoma cells. Mol Cancer Res *10*, 143-155.

Vu, L.P., Pickering, B.F., Cheng, Y., Zaccara, S., Nguyen, D., Minuesa, G., Chou, T., Chow, A., Saletore, Y., MacKay, M., *et al.* (2017). The N(6)-methyladenosine (m6A)-forming enzyme METTL3 controls myeloid differentiation of normal hematopoietic and leukemia cells. Nat Med *23*, 1369-1376.

Wachter, K., Kohn, M., Stohr, N., and Huttelmaier, S. (2013). Subcellular localization and RNP formation of IGF2BPs (IGF2 mRNA-binding proteins) is modulated by distinct RNA-binding domains. Biol Chem *394*, 1077-1090.

Wang, J., Guo, Y., Chu, H., Guan, Y., Bi, J., and Wang, B. (2013). Multiple functions of the RNA-binding protein HuR in cancer progression, treatment responses and prognosis. Int J Mol Sci *14*, 10015-10041.

Wang, J., Wang, B., Bi, J., and Zhang, C. (2011). Cytoplasmic HuR expression correlates with angiogenesis, lymphangiogenesis, and poor outcome in lung cancer. Med Oncol *28 Suppl 1*, S577-585.

Wang, P., Zhang, L., Zhang, J., and Xu, G. (2018a). MicroRNA-124-3p inhibits cell growth and metastasis in cervical cancer by targeting IGF2BP1. Exp Ther Med *15*, 1385-1393.

Wang, R.J., Li, J.W., Bao, B.H., Wu, H.C., Du, Z.H., Su, J.L., Zhang, M.H., and Liang, H.Q. (2015a). MicroRNA-873 (miRNA-873) inhibits glioblastoma tumorigenesis and metastasis by suppressing the expression of IGF2BP1. J Biol Chem *290*, 8938-8948.

Wang, T., Wang, G., Hao, D., Liu, X., Wang, D., Ning, N., and Li, X. (2015b). Aberrant regulation of the LIN28A/LIN28B and let-7 loop in human malignant tumors and its effects on the hallmarks of cancer. Mol Cancer *14*, 125.

Wang, X., Cao, L., Wang, Y., Wang, X., Liu, N., and You, Y. (2012). Regulation of let-7 and its target oncogenes (Review). Oncol Lett *3*, 955-960.

Wang, X., Chen, S., Gao, Y., Yu, C., Nie, Z., Lu, R., Sun, Y., and Guan, Z. (2021). MicroRNA-125b inhibits the proliferation of vascular smooth muscle cells induced by platelet-derived growth factor BB. Exp Ther Med *22*, 791.

Wang, X., Li, J., Dong, K., Lin, F., Long, M., Ouyang, Y., Wei, J., Chen, X., Weng, Y., He, T., *et al.* (2015c). Tumor suppressor miR-34a targets PD-L1 and functions as a potential immunotherapeutic target in acute myeloid leukemia. Cell Signal *27*, 443-452.

Wang, Y., Chen, D., Qian, H., Tsai, Y.S., Shao, S., Liu, Q., Dominguez, D., and Wang, Z. (2014). The splicing factor RBM4 controls apoptosis, proliferation, and migration to suppress tumor progression. Cancer Cell *26*, 374-389.

Wang, Z.L., Li, B., Luo, Y.X., Lin, Q., Liu, S.R., Zhang, X.Q., Zhou, H., Yang, J.H., and Qu, L.H. (2018b). Comprehensive Genomic Characterization of RNA-Binding Proteins across Human Cancers. Cell Rep *22*, 286-298.

Warzecha, C.C., Sato, T.K., Nabet, B., Hogenesch, J.B., and Carstens, R.P. (2009). ESRP1 and ESRP2 are epithelial cell-type-specific regulators of FGFR2 splicing. Mol Cell *33*, 591-601.

Weber, T.S., Jaehnert, I., Schichor, C., Or-Guil, M., and Carneiro, J. (2014). Quantifying the length and variance of the eukaryotic cell cycle phases by a stochastic model and dual nucleoside pulse labelling. PLoS Comput Biol *10*, e1003616.

Weidensdorfer, D., Stohr, N., Baude, A., Lederer, M., Kohn, M., Schierhorn, A., Buchmeier, S., Wahle, E., and Huttelmaier, S. (2009). Control of c-myc mRNA stability by IGF2BP1-associated cytoplasmic RNPs. RNA *15*, 104-115.

Wightman, B., Ha, I., and Ruvkun, G. (1993). Posttranscriptional regulation of the heterochronic gene lin-14 by lin-4 mediates temporal pattern formation in C. elegans. Cell *75*, 855-862.

Wu, X., Gardashova, G., Lan, L., Han, S., Zhong, C., Marquez, R.T., Wei, L., Wood, S., Roy, S., Gowthaman, R., *et al.* (2020). Targeting the interaction between RNA-binding protein HuR and FOXQ1 suppresses breast cancer invasion and metastasis. Commun Biol *3*, 193.

Xiao, L., and Wang, J.Y. (2011). Posttranscriptional regulation of gene expression in epithelial cells by polyamines. Methods Mol Biol *720*, 67-79.

Xiao, W., Adhikari, S., Dahal, U., Chen, Y.S., Hao, Y.J., Sun, B.F., Sun, H.Y., Li, A., Ping, X.L., Lai, W.Y., *et al.* (2016). Nuclear m(6)A Reader YTHDC1 Regulates mRNA Splicing. Mol Cell *61*, 507-519.

Xie, F., Huang, C., Liu, F., Zhang, H., Xiao, X., Sun, J., Zhang, X., and Jiang, G. (2021). CircPTPRA blocks the recognition of RNA N(6)-methyladenosine through interacting with IGF2BP1 to suppress bladder cancer progression. Mol Cancer *20*, 68.

Xu, D., Guo, Y., Liu, T., Li, S., and Sun, Y. (2017a). miR-22 contributes to endosulfan-induced endothelial dysfunction by targeting SRF in HUVECs. Toxicol Lett *269*, 33-40.

Xu, L.F., Wu, Z.P., Chen, Y., Zhu, Q.S., Hamidi, S., and Navab, R. (2014). MicroRNA-21 (miR-21) regulates cellular proliferation, invasion, migration, and apoptosis by targeting PTEN, RECK and Bcl-2 in lung squamous carcinoma, Gejiu City, China. PLoS One *9*, e103698.

Xu, Y., Zheng, Y., Liu, H., and Li, T. (2017b). Modulation of IGF2BP1 by long non-coding RNA HCG11 suppresses apoptosis of hepatocellular carcinoma cells via MAPK signaling transduction. Int J Oncol *51*, 791-800.

Xue, X., Liu, Y., Wang, Y., Meng, M., Wang, K., Zang, X., Zhao, S., Sun, X., Cui, L., Pan, L., *et al.* (2016). MiR-21 and MiR-155 promote non-small cell lung cancer progression by downregulating SOCS1, SOCS6, and PTEN. Oncotarget *7*, 84508-84519.

Yae, T., Tsuchihashi, K., Ishimoto, T., Motohara, T., Yoshikawa, M., Yoshida, G.J., Wada, T., Masuko, T., Mogushi, K., Tanaka, H., *et al.* (2012). Alternative splicing of CD44 mRNA by ESRP1 enhances lung colonization of metastatic cancer cell. Nat Commun *3*, 883.

Yamakuchi, M., and Lowenstein, C.J. (2009). MiR-34, SIRT1 and p53: the feedback loop. Cell Cycle *8*, 712-715.

Yamashita, A., Chang, T.C., Yamashita, Y., Zhu, W., Zhong, Z., Chen, C.Y., and Shyu, A.B. (2005). Concerted action of poly(A) nucleases and decapping enzyme in mammalian mRNA turnover. Nat Struct Mol Biol *12*, 1054-1063.

Yanaihara, N., Caplen, N., Bowman, E., Seike, M., Kumamoto, K., Yi, M., Stephens, R.M., Okamoto, A., Yokota, J., Tanaka, T., *et al.* (2006). Unique microRNA molecular profiles in lung cancer diagnosis and prognosis. Cancer Cell *9*, 189-198.

Yang, Y., Meng, H., Peng, Q., Yang, X., Gan, R., Zhao, L., Chen, Z., Lu, J., and Meng, Q.H. (2015). Downregulation of microRNA-21 expression restrains non-small cell lung cancer cell proliferation and migration through upregulation of programmed cell death 4. Cancer Gene Ther *22*, 23-29.

Yisraeli, J.K. (2005). VICKZ proteins: a multi-talented family of regulatory RNA-binding proteins. Biol Cell *97*, 87-96.

Youn, J.Y., Dunham, W.H., Hong, S.J., Knight, J.D.R., Bashkurov, M., Chen, G.I., Bagci, H., Rathod, B., MacLeod, G., Eng, S.W.M., *et al.* (2018). High-Density Proximity Mapping Reveals the Subcellular Organization of mRNA-Associated Granules and Bodies. Mol Cell *69*, 517-532 e511.

Yu, F., Yao, H., Zhu, P., Zhang, X., Pan, Q., Gong, C., Huang, Y., Hu, X., Su, F., Lieberman, J., *et al.* (2007). let-7 regulates self renewal and tumorigenicity of breast cancer cells. Cell *131*, 1109-1123.

Zaccara, S., Ries, R.J., and Jaffrey, S.R. (2019). Reading, writing and erasing mRNA methylation. Nat Rev Mol Cell Biol *20*, 608-624.

Zhang, J., Cheng, J., Zeng, Z., Wang, Y., Li, X., Xie, Q., Jia, J., Yan, Y., Guo, Z., Gao, J., *et al.* (2015). Comprehensive profiling of novel microRNA-9 targets and a tumor suppressor role of microRNA-9 via targeting IGF2BP1 in hepatocellular carcinoma. Oncotarget *6*, 42040-42052.

Zhao, W., Lu, D., Liu, L., Cai, J., Zhou, Y., Yang, Y., Zhang, Y., and Zhang, J. (2017). Insulin-like growth factor 2 mRNA binding protein 3 (IGF2BP3) promotes lung tumorigenesis via attenuating p53 stability. Oncotarget *8*, 93672-93687.

Zheng, X., Peng, Q., Wang, L., Zhang, X., Huang, L., Wang, J., and Qin, Z. (2020). Serine/arginine-rich splicing factors: the bridge linking alternative splicing and cancer. Int J Biol Sci *16*, 2442-2453.

Zhou, X., Zhang, C.Z., Lu, S.X., Chen, G.G., Li, L.Z., Liu, L.L., Yi, C., Fu, J., Hu, W., Wen, J.M., *et al.* (2015). miR-625 suppresses tumour migration and invasion by targeting IGF2BP1 in hepatocellular carcinoma. Oncogene *34*, 965-977.

Zhou, Z.J., Dai, Z., Zhou, S.L., Fu, X.T., Zhao, Y.M., Shi, Y.H., Zhou, J., and Fan, J. (2013). Overexpression of HnRNP A1 promotes tumor invasion through regulating CD44v6 and indicates poor prognosis for hepatocellular carcinoma. Int J Cancer *132*, 1080-1089.

Zielke, N., and Edgar, B.A. (2015). FUCCI sensors: powerful new tools for analysis of cell proliferation. Wiley Interdiscip Rev Dev Biol *4*, 469-487.

Zirkel, A., Lederer, M., Stohr, N., Pazaitis, N., and Huttelmaier, S. (2013). IGF2BP1 promotes mesenchymal cell properties and migration of tumor-derived cells by enhancing the expression of LEF1 and SNAI2 (SLUG). Nucleic Acids Res *41*, 6618-6636.

Zucconi, B.E., and Wilson, G.M. (2011). Modulation of neoplastic gene regulatory pathways by the RNA-binding factor AUF1. Front Biosci (Landmark Ed) *16*, 2307-2325.

VI APPENDIX

Abbreviations

3′	3-prime
5′	5-prime
A	adenine
AML	acute myeloid leukemia
APA	alternative cleavage and polyadenylation
ARE	AU-rich element
ASO	anti-sense oligonucleotide
CDS	coding sequence
ChIP	chromatin immunoprecipitation
circNA	circular RNA
CLIP	cross-linking immunoprecipitation
CRD	coding region stability determinant
CRISPR	class 2 clustered regularly interspaced short palindromic repeat
CSD	cold shock domain
DN	downregulated
DNA	deoxyribonucleic acid
dT	deoxythymidine
eCLIP	enhanced CLIP
ECM	extracellular matrix
EMT	epithelial-mesenchymal-transition
FDA	food and drug administration
FUCCI	fluorescent ubiquitination-based cell cycle indicator
GEEG	glycine-glutamate-glutamate-glycine
GFP	green fluorescent protein
GSEA	gene set enrichment analysis
GTEx	genotype-tissue expression project
GTP	guanosine 5′-triphosphate
GXXG	glycine-any residue-any residue-glycine
iCLIP	individual-nucleotide resolution CLIP
iRFP	near-infrared fluorescent protein
KEGG	Kyoto encyclopedia of genes and genomes
KH	hnRNP K homology
lncRNA	long non-coding RNA
m^6A	N^6-methyladenosine
m^7G	7-methylguanosine
miRNA	microRNA

miRISC	miRNA-induced silencing complex
miTRAP	miRNA trapping by RNA in vitro affinity purification
mRBP	mRNA-binding protein
mRNA	messenger RNA
mRNP	messenger RNP
MTS	miRNA targeting site
ncRNA	non-coding RNA
ncRNP	non-coding RNP
NHEJ	non-homologous end joining repair
nt	nulceotide
OS	overall survival
PAR-CLIP	photoactivatable-ribonucleoside-enhanced CLIP
PFS	progression-free survival
pre-mRNA	precursor mRNA
pre-miRNA	precursor miRNA
pre-RISC	precursor RISC
pri-miRNA	primary miRNA
RBD	RNA-binding domain
RBP	RNA-binding protein
RIC	RNA interactome capture
RNP	ribonucleoprotein complex
RRM	RNA recognition motif
rRNA	ribosomal RNA
RNA	ribonucleic acid
siRNA	small interfering RNA
sgRNA	single guide RNA
SNP	single nucleotide polymorphism
snoRNA	small nucleolar RNA
TCGA	the cancer genome atlas
TPM	transcripts per million
tRNA	transfer RNA
TUTase	terminal uridylyl transferase
UP	upregulated
UTR	untranslated region
UV	ultraviolet
YTH	YT521-B homology

List of figures

List of publications

* shared first-authorship; # shared correspondence

Busch B*, Bley N*, **Müller S***, Glass M, Misiak D, Lederer M, Vetter M, Strauss HG, Thomssen C, Hüttelmaier S (2016) The oncogenic triangle of HMGA2, LIN28B and IGF2BP1 antagonizes tumor-suppressive actions of the let-7 family. **Nucleic Acids Res** 44: 3845-3864

Müller S*, Bley N*, Glass M*, Busch B, Rousseau V, Misiak D, Fuchs T, Lederer M, Hüttelmaier S (2018) IGF2BP1 enhances an aggressive tumor cell phenotype by impairing miRNA-directed downregulation of oncogenic factors. **Nucleic Acids Res** 46: 6285-6303

Müller S, Glass M, Singh AK, Haase J, Bley N, Fuchs T, Lederer M, Dahl A, Huang H, Chen J et al (2019) IGF2BP1 promotes SRF-dependent transcription in cancer in a m^6A- and miRNA-dependent manner. **Nucleic Acids Res** 47: 375-390

Schneider T, Hung LH, Aziz M, Wilmen A, Thaum S, Wagner J, Janowski R, **Müller S**, Schreiner S, Friedhoff P et al (2019) Combinatorial recognition of clustered RNA elements by the multidomain RNA-binding protein IMP3. **Nat Commun** 10: 2266

Müller S[#], Bley N, Busch B, Glass M, Lederer M, Misiak C, Fuchs T, Wedler A, Haase J, Bertoldo JB et al (2020a) The oncofetal RNA-binding protein IGF2BP1 is a druggable, post-transcriptional super-enhancer of E2F-driven gene expression in cancer. **Nucleic Acids Res** 48: 8576-8590

Müller S[*], Wedler A[*], Breuer J[*], Glass M, Bley N, Lederer M, Haase J, Misiak C, Fuchs T, Ottmann A et al (2020b) Synthetic circular miR-21 RNA decoys enhance tumor suppressor expression and impair tumor growth in mice. **NAR Cancer** 2: zcaa014

Glass M, Misiak D, Bley N, **Müller S**, Hagemann S, Busch B, Rausch A, Hüttelmaier S (2021) IGF2BP1, a Conserved Regulator of RNA Turnover in Cancer. **Front Mol Biosci** 8: 632219

Bley N, Hmedat A, **Müller S**, Rolnik R, Rausch A, Lederer M, Hüttelmaier S (2021a) Musashi-1-A Stemness RBP for Cancer Therapy? **Biology (Basel)** 10

Bley N, Schott A, **Müller S**, Misiak D, Lederer M, Fuchs T, Assmann C, Glass M, Ihling C, Sinz A et al (2021b) IGF2BP1 is a targetable SRC/MAPK-dependent driver of invasive growth in ovarian cancer. **RNA Biol** 18: 391-403

Lederer M, **Müller S**, Glass M, Bley N, Ihling C, Sinz A, Hüttelmaier S (2021) Oncogenic Potential of the Dual-Function Protein MEX3A. **Biology (Basel)** 10

Erklärung

Hiermit erkläre ich, dass ich meine Dissertationsschrift selbständig und ohne fremde Hilfe verfasst habe. Ich habe keine anderen als die von mir angegebenen Quellen und Hilfsmittel benutzt. Die aus den benutzten Werken wörtlich oder inhaltlich entnommenen Stellen habe ich als solche kenntlich gemacht.

Mit der vorliegenden Arbeit bewerbe ich mich erstmals um die Erlangung des Doktorgrades.

Halle (Saale), Oktober 2021

Simon Müller

Danksagung

An dieser Stelle gilt mein Dank all denen, die mich während meiner Arbeit im Labor und der Anfertigung dieser Dissertation unterstützt haben:

An erster Stelle richtet sich mein größter Dank an meinen Doktorvater Prof. Dr. Stefan Hüttelmaier. Ich danke dir für dein stetiges Engagement, jede erdenkliche Unterstützung, all die wissenschaftlichen Freiheiten, die anregenden Diskussionen und die konstruktive Kritik in den letzten Jahren. Die unzähligen Gespräche auf intellektueller und persönlicher Ebene werden mir immer in Erinnerung bleiben. Du hast mir die Möglichkeit gegeben, spannenden Fragestellungen nachzugehen, wissenschaftliche Kongresse zu besuchen und meine Ergebnisse zu veröffentlichen - Danke.

Darüber hinaus danke ich vor allem Dr. Nadine Bley. Du hast mich Ende 2014 in Stefan's Arbeitsgruppe aufgenommen und mich an IGF2BPs herangeführt. Du hattest immer ein offenes Ohr für wissenschaftliche und private Diskussionen, die mich stets weitergebracht haben. Ohne dich und all deine Hilfe wäre meine Dissertation in der Form nicht möglich gewesen.

Meinen besonderen Dank möchte ich auch Dr. Marcell Lederer und Dr. Anne Baude aussprechen. Ihr habt mich all die Jahre auf diesem Weg begleitet und mich in jeder Situation stets unterstützt – sei es im Labor, bei Urlaubsanträgen oder sogar im Standesamt. Auch wenn ihr schon etwas komisch seid, werde ich mich immer gerne an euch und die unzähligen, teils tiefgründigen Gespräche, die Mittagessen und Espresso-Pausen erinnern.

Bedanken möchte ich mich zudem bei Claudia Misiak, Tommy Fuchs, Dr. Bianca Busch und Dr. Markus Glaß, die mir jederzeit bei meiner Arbeit im Labor, den Tierversuchen und der Bioinformatik eine große Hilfe waren. Außerdem danke ich allen anderen Mitarbeitern der AG Hüttelmaier für die unvergesslichen Jahre – Dr. Danny Misiak, Dr. Jean Bertoldo, Dr. Jessica Bell, Hendrik Täuber, Dr. Marcel Köhn, Alexander Rausch, Dr. Rebecca Pötschke, Dr. Jacob Haase, Sven Hagemann, Annekatrin Schott und Alice Wedler.

Selbstverständlich richtet sich mein Dank auch an alle anderen Personen, die maßgeblich an den Veröffentlichungen mitgewirkt haben.

Von ganzem Herzen möchte ich mich bei meiner Familie für die anhaltende mentale Unterstützung bedanken. Meiner Mama und meinen Brüdern Marius, Fabian und Marcus danke ich für das ständige Vertrauen und den Zuspruch.

Zu guter Letzt gilt mein besonderer Dank den wichtigsten Personen in meinem Leben, meiner Frau Daniela und unseren gemeinsamen Kindern Amelie und Maximilian, die in den letzten Jahren viel Geduld aufgebracht und mir den Freiraum für die Anfertigung dieser Dissertation gegeben haben.

Curriculum Vitae

Personal Details

Name:	Simon Müller
Date of birth, birthplace:	21.08.1989, Hannover
Nationality:	German

Education

1995-1999	Grundschule, Wathlingen
1999-2001	Orientierungsstufe Burgstraße, Celle
2001-2010	Gymnasium Ernestinum, Celle – Abitur

Scientific Education

2010-2013	B.Sc. studies in Biochemistry at the Martin-Luther-University Halle-Wittenberg
2013	Bachelor thesis under supervision of Prof. Dr. Frank Bordusa at the Martin-Luther-University Halle Wittenberg; Title: "Expression einer Trypsin-Variante und Validierung eines ELISA-basierten Screening Systems"
2013-2015	M.Sc. studies in Biochemistry at the Martin-Luther-University Halle-Wittenberg
2015	Master thesis under supervision of Prof. Dr. Stefan Hüttelmaier at the Martin-Luther-University Halle-Wittenberg; Title: "Der Einfluss von IGF2BP1 auf die Migration und Invasivität von Ovarialkarzinomzellen"
2015-2021	Doctoral studies in the laboratory of Prof. Dr. Stefan Hüttelmaier at the Martin-Luther-University Halle-Wittenberg